

Dissertation ETH nr. 14333

**The Synthesis, Characterisation, and Reactivity of
Ru(II)-Arene Complexes with MeO-Biphep and Binap**

A dissertation submitted to the
Swiss Federal Institute of Technology Zurich

for the degree of
Doctor of Natural Sciences

presented by
Cornelia Johanna den Reijer
M.Sc., KUN Nijmegen, the Netherlands
born on February 3rd, 1973
Zevenbergen, the Netherlands

accepted on recommendation of
Prof. Dr. P. S. Pregosin, examiner
Prof. Dr. A. Togni, co-examiner

Zurich, 2001

The chemists are a strange class of mortals,
impelled by an almost maniacal impulse to seek
their pleasures amongst smoke and vapour, soot and
flames, poisons and poverty, yet amongst all these
evils I seem to live so sweetly that I would rather die
than change places with the King of Persia.

Johann Joachim Becher, *Physica Subterranea* (1667)

Acknowledgement

It has been my pleasure and honour to have met so many outstanding personalities during my Ph.D. studies who made my graduate period an unforgettable and great experience and who helped this thesis to become what it is.

Dear Professor Pregosin, I have learned a lot from your vision on metals and their interactions, NMR(-spectra) and scientifical research. I respect and appreciate very much your approach towards solving (chemical) problems and handling (unavoidable) setbacks. Thank you very much for the given possibilities and freedom, your critical analysis and infinite stimulating enthusiasm.

Dear Heinz, besides your splendid passion to solve every interesting structure with (the most complicated) NMR-experiments, you were always willing to help me. Your advices and assistance ranged from NMR, chemistry and computers to hikes, (Asian) cooking and interesting geographical places wherever on the globe.

I would like to thank Professor Togni for flexibly taking up this co-examinership and Michael Wörle (ETH) and Professor Albinati (University of Milan) for determining the crystal structures.

Dear Daniela and Massimiliano, I spent the most of the time in B11 with the both of you. I am well educated in the Italian culture, language and mentality now! For sure you know now that Holland is an area in the Netherlands, that is not always raining there and that the Swiss dialect is not similar to the Dutch language at all (anti-aanbaklaag, stropdas). Massimiliano, we have invented terms as discontinuity-point theory, being fox-watched and Dutch ducks during the turbulent but splendid time we shared ‘our office’ downstairs. Daniela, we had many stimulating and sparkling discussions about any topic we could think about. One of the crystal structures in this dissertation is solved by you.

I have learned a lot by supervising two undergraduate students in the lab. Nicola, you put Ticino on my map of Switzerland. Pascal, besides a number of compounds described in this dissertation, you also have synthesised liters of coffee in the lab to get me awake in the morning. I would like to thank also the others with whom I have spent a fruitful time in B11: Tilmann, Daniel, Matthias, Selva, Karin, Nantko, Gerald and all temperory visitors.

I am grateful to all the Ph.D.-fellows, post-docs and permanent staff of the chemistry department for their cooperation, collaboration and kindness. Céline, you had in every situation the right stimulating and friendly words ready. Cube, you kept my German vocabulary up with all our nice and interesting discussions. Sandra, your relaxed approach and everlasting optimism thought me a lot. Torsten, Ingrid and Gilles, thank you for your company during my last year.

De Nederlandse cultuur en humor werden op peil gehouden door een groep vaderlandse chemici in Zürich, met name will ik noemen Aswin en Nicolle. Beste Aswin, bedankt voor je vriendschap! Nicolle, jouw schaterlach en humor zal ik niet gauw vergeten.

Ik wil graag mijn scheikundige collega's en vrienden in Nijmegen en elders (Chiara, good excercise!) bedanken voor hun (wetenschappelijke) discussies, gastvrijheid en support gedurende mijn jaren in Zürich. Dan zijn er nog de vrienden en familie die niets met wetenschap te maken hebben, maar die wel voor een welkome afleiding zorgden. Jullie hebben al die jaren onvermoeibaar en vol belangstelling naar mijn verhalen over moleculen en chemici geluisterd. Tot slot wil ik mijn ouders bedanken voor hun ondersteuning, hun belangstelling en al die kerken dat ik weer in Langeweg neerstreek om van de lage-landelijke weelde te genieten.

Carolien

List of Publications

Protonation and NMR Studies on ^{13}C -Acetate Enriched $\text{Ru}(\text{OAc})_2(\text{Binap})$. Acetate as a Source of Water in P-C bond Splitting, Geldbach, T. J.; den Reijer, C. J.; Wörle, M.; Pregosin, P. S. accepted in *Inorg. Chim. Acta*.

Ru(II)-MeO-Biphep-Arene-Dications: Acetylene Reactions and Unexpected Cyclometallation, den Reijer, C. J.; Drago, D.; Pregosin, P. S. *Organometallics* **2001**, *20*, 2982-2989.

Binap and MeO-Biphep Complexes of Ru(II). Dicationic Ligands as 6e Donors. Unexpected Cyclometallation in Connection with P-C Bond Breaking, den Reijer, C. J.; Dotta P.; Pregosin, P. S.; Albinati, A. *Can. J. Chem.* **2001**, *79*, 693-704.

P-C Bond Splitting Reactions in Ruthenium(II). Complexes of Binap and MeO-Biphep Using $\text{CF}_3\text{SO}_3\text{H}$ and HBF_4 . A Novel Ru-F-H Interaction, den Reijer, C. J.; Wörle, M.; Pregosin, P. S. *Organometallics* **2000**, *19*, 309-316.

Diversity in Complexation of $[\text{RhI}(\text{cod})]^+$ and $[\text{IrI}(\text{cod})]^+$ by Pyridine-Amine-Pyrrole Ligands, de Bruin, A.; Kicken, R. J. N. A. M.; Suos, N. F. A.; Donners, M. P. J.; den Reijer C. J.; Sandee, A. J.; de Gelder, R.; Smits, J. M. M.; Gal, A. W.; Spek, A. L. *Eur. J. Inorg. Chem.* **1999**, 1581-1592.

A New Phosphinite Chelate, $(\text{aryl})_2\text{POBF}_2\text{OH}$, Complexed to Ruthenium(II). HBF_4 -Induced P-C Bond Cleavage in Chiral MeO-Biphep Complexes, den Reijer, C. J.; Rüegger, H.; Pregosin, P. S. *Organometallics* **1998**, *24*, 5213-5215.

Oral Contribution

den Reijer, C. J.; Dotta P.; Drago, D.; Pregosin, P. S. *Netherlands' Catalysis & Chemistry Conference II (NCCII)*, 5-7 March 2001, Noordwijkerhout, the Netherlands.

Table of Contents

Summary

Zusammenfassung

Samenvatting

Chapter 1

General Introduction and Scope

1.1 General introduction	1
1.1.1 Chirality	1
1.1.2 Asymmetric homogeneous catalysis	2
1.1.3 Ligands design	4
1.2 Outline of the thesis	6
1.3 References	7

Chapter 2

MeO-Biphep and Binap as 6e Donor Ligands in Dicationic Ru(II) Arene Complexes: Synthesis, Characterisation, and Reactivity

2.1 Abstract	9
2.2 Introduction	10
2.3 Results and discussion	15
2.3.1 The chloro-precursors	15
2.3.2 η^2 -Compounds from chloro-precursors	18
2.3.3 Hydrides	22
2.3.4 Nitriles and isonitriles	24
2.3.5 ^{13}C -NMR data for the η^6 - <i>p</i> -cymene ligand	26
2.4 Conclusions	28
2.5 Experimental	29

2.5.1 Crystallography	29
2.5.2 Synthesis	33
2.5.3 Selected NMR-data	44
2.6 References	49

Chapter 3

Ru(II)-MeO-Biphep-Arene Dications: Catalysis and Unexpected Cyclo-metallation/Insertion

3.1 Abstract	51
3.2 Introduction	52
3.3 Results and discussion	56
3.3.1 Catalysis and cyclometallation/insertion	56
3.3.2 Solid-state structure of C6	66
3.3.3 Reactions with octyne- <i>d</i> ₁	69
3.3.4 Allenylidene complex C7	70
3.4 Conclusions	72
3.5 Experimental	73
3.5.1 Crystallography	73
3.5.2 Synthesis	80
3.5.3 Selected NMR-data	88
3.6 References	96

Chapter 4

P-C Bond Splitting Induced by CF₃SO₃H, HBF₄ and (Bu₄N)(Ph₃SiF₂)

4.1 Abstract	99
4.2 Introduction	100
4.3 Results and discussion	103
4.3.1 Solid-state structure of precursor	103
4.3.2 P-C bond splitting induced by CF ₃ SO ₃ H	107
4.3.3 P-C bond splitting induced by HBF ₄	117

4.3.4 P-C bond splitting induced by (Bu ₄ N)(Ph ₃ SiF ₂)	125
4.4 Conclusions	127
4.5 Experimental	128
4.5.1 Crystallography	128
4.5.2 Synthesis	151
4.5.3 Selected NMR-data	157
4.6 References	162

Curriculum Vitae

Summary

This thesis describes transition-metal complexes and reactions in which the biaryl phosphine ligands MeO-Biphep and Binap function as 6e donor ligands to Ru(II) by complexing an adjacent biaryl double bond. MeO-Biphep represents 2,2'-Bis(diphenylphosphino)-6,6'-bismethoxy-1,1'-biphenyl and Binap is 2,2'-Bis(diphenylphosphino)-1,1'-binaphthyl.

Chapter 1 gives an introduction.

Chapter 2 deals specifically with the synthesis, characterisation and reactivity of the dicationic $[\text{Ru}(\text{arene})(\text{MeO-Biphep or Binap})](\text{SbF}_6)_2$ (arene = η^6 -benzene or η^6 -*p*-cymene) complexes. Upon reactions of these complexes with methanol, nitriles and isonitriles readily displace the η^2 -olefin bonding mode of these biaryl ligands. The η^6 -*p*-cymene ^{13}C chemical shifts of several of these complexes are discussed.

Chapter 3 describes the catalytic addition of benzoic acid to 1-pentyne and 1-octyne respectively to form enol-ester products using $[\text{Ru}(\text{arene})(\text{MeO-Biphep})](\text{SbF}_6)_2$ as catalysts. Deuterium-labelling experiments show scrambling of the deuterium atom. A new Ru(II)-allenylidene complex was prepared and used in the catalytic reaction. Stoichiometric reactions with acetylenes resulted in cyclometallation/insertion products.

Chapter 4 shows the acid-promoted (stereospecific) P-C bond cleavage and η^6 -arene complexation starting from $[\text{Ru}(\text{OAc})_2(\text{MeO-Biphep or Binap})]$. In the presence of triflic acid plus adventitious water, $[\text{Ru}(\text{OTf})(6'\text{-diphenylphosphino-1'}\text{-(2-dimethoxy)biphenyl})(\text{PPh}_2\text{OH})](\text{OTf})$ and $[\text{Ru}(\text{OTf})(6'\text{-diphenylphosphino-1-naphthyl})(\text{PPh}_2\text{OH})](\text{OTf})$ complexes are obtained. These correspond to the addition of water across the P-C bond. With HBF_4 and adventitious water, $[\text{Ru}(\text{C}_{12}\text{H}_{11}\text{BF}_2\text{O}_2\text{P})(6'\text{-diphenylphosphino-1'}\text{-(2-dimethoxy)biphenyl})](\text{BF}_4)$ and $[\text{Ru}(\text{C}_{12}\text{H}_{11}\text{BF}_2\text{O}_2\text{P})(6'\text{-diphenylphosphino-1-naphthyl})](\text{BF}_4)$ which contain the new chelating phosphinite anion ($\text{C}_{12}\text{H}_{11}\text{BF}_2\text{O}_2\text{P}$) are formed. Novel Ru-F---H and PFPh_2 intermediates were detected. The strained $[\text{Ru}(\text{arene})(\text{MeO-Biphep})](\text{SbF}_6)_2$ complexes readily react with the fluoride source $(\text{Bu}_4\text{N})(\text{Ph}_3\text{SiF}_2)$ to afford the cyclometallated products via P-C bond cleavage and P-F bond formation.

Zusammenfassung

Diese Arbeit beschreibt Übergangsmetallkomplexe und Reaktionen, in denen die Biarylphosphinliganden MeO-Biphep und Binap durch Einbeziehung einer Biaryldoppelbindung als 6e Donorliganden für Ru(II) fungieren. MeO-Biphep steht für 2,2'-Bis(diphenylphosphino)-6,6'-bismethoxy-1,1'-biphenyl und Binap für 2,2'-Bis(diphenylphosphino)-1,1'-binaphthyl.

Kapitel 1 gibt eine Einführung.

Kapitel 2 befasst sich speziell mit der Synthese, Charakterisierung und Reaktivität der dикационischen $[\text{Ru}(\text{aren})(\text{MeO-Biphep oder Binap})](\text{SbF}_6)_2$ (aren = η^6 -Benzen oder η^6 -*p*-Cymen) Komplexe. Bei der Reaktion dieser Komplexe mit Methanol, Nitrilen oder Isonitrilen verdrängen diese die η^2 -Olefinbindung der Biarylliganden. Die ^{13}C chemischen Verschiebungen mehrerer η^6 -*p*-Cymen-Komplexe werden diskutiert.

Kapitel 3 beschreibt die katalytische Addition von Benzoesäure an 1-Pentin bzw. 1-Oktin, die bei Verwendung von $[\text{Ru}(\text{aren})(\text{MeO-Biphep})](\text{SbF}_6)_2$ als Katalysator zur Bildung von Enolestern führt. Deuteriummarkierungsexperimente ergaben eine zufällige Verteilung des Deuteriumatoms. Ein neuer Ru(II)-Allenylidenkomplex wurde hergestellt und in der katalytischen Reaktion benutzt. Stöchiometrische Reaktionen mit Acetylenen erzeugten Cyclometallierung/Insertionsprodukte.

Kapitel 4 beschreibt die, von $[\text{Ru}(\text{OAc})_2(\text{MeO-Biphep oder Binap})]$ ausgehende säureunterstützte (stereospezifische) P-C-Bindungsspaltung unter Komplexierung eines η^6 -Arens. In Gegenwart von Trifluormethansulfonsäure und Wasser wurden die Komplexe $[\text{Ru}(\text{OTf})(6'\text{-diphenylphosphino-1'}\text{-(2-dimethoxy)-biphenyl})(\text{PPh}_2\text{OH})](\text{OTf})$ und $[\text{Ru}(\text{OTf})(6'\text{-diphenylphosphino-1-naphthyl})(\text{PPh}_2\text{OH})](\text{OTf})$ erhalten. Das entspricht einer Addition von Wasser an die P-C-Bindung. Mit HBF_4 und Wasser bilden sich $[\text{Ru}(\text{C}_{12}\text{H}_{11}\text{BF}_2\text{O}_2\text{P})(6'\text{-diphenylphosphino-1'}\text{-(2-dimethoxy)-biphenyl})](\text{BF}_4)$ und $[\text{Ru}(\text{C}_{12}\text{H}_{11}\text{BF}_2\text{O}_2\text{P})(6'\text{-diphenylphosphino-1-naphthyl})](\text{BF}_4)$, die ein neues Phosphinitanion ($\text{C}_{12}\text{H}_{11}\text{BF}_2\text{O}_2\text{P}$) enthalten. Neuartige Ru-F---H und PFPh_2 Intermediate wurden beobachtet. Die sterisch gespannten $[\text{Ru}(\text{aren})(\text{MeO-Biphep})](\text{SbF}_6)_2$ Komplexe reagieren leicht mit der Fluoridquelle $(\text{Bu}_4\text{N})(\text{Ph}_3\text{SiF}_2)$ unter Bildung von cyclometallierten Produkten via eine P-C-Bindungsspaltung und P-F-Bindungsknüpfung.

Samenvatting

Dit proefschrift beschrijft overgangsmetaal-complexen en reacties, waarbij de fosfine biaryl liganden MeO-Biphep en Binap als 6e donor liganden functioneren door complexatie van een biarylsche dubbele binding. MeO-Biphep is de triviale naam voor 2,2'-Bis(difenylfosfino)-6,6'-bismethoxy-1,1'-bifenylen Binap staat voor 2,2'-Bis(difenylfosfino)-1,1'-binaftyl.

Hoofdstuk 1 geeft een inleiding.

Hoofdstuk 2 behandelt de synthese, karakterisatie en reactiviteit van de dikationische $[\text{Ru}(\text{areen})(\text{MeO-Biphep or Binap})](\text{SbF}_6)_2$ (areen = η^6 -benzeen or η^6 -*p*-cymeen) complexen. In deze complexen wordt de η^2 -olefinische binding verbroken door reacties met methanol, nitrillen en isonitrillen. De η^6 -*p*-cymeen ^{13}C chemische verschuivingen van verscheidende complexen worden bediscussieerd.

Hoofdstuk 3 beschrijft de vorming van enol-esters door katalytische additie van bezoëzuur aan 1-pentyn of 1-octyn, waarbij $[\text{Ru}(\text{areen})(\text{MeO-Biphep})](\text{SbF}_6)_2$ complexen als katalysatoren gebruikt worden. Deuterium-labelling experimenten hebben aangetoond dat het deuterium atoom willekeurig wordt ingebouwd. Een nieuw Ru(II)-allenylideen complex is gesynthetiseerd en in de katalytische reactie gebruikt. Stoichiometrische reacties met acetylenen hebben geleid tot cyclometallering/insertie produkten.

Hoofdstuk 4 behandelt de (stereospecifieke) verbreking van een P-C binding en η^6 -areen complexatie in de reactie van $[\text{Ru}(\text{OAc})_2(\text{MeO-Biphep or Binap})]$ met een specifiek sterk zuur. In de aanwezigheid van trifluormethylsulfonzuur en water worden de complexen $[\text{Ru}(\text{OTf})(6'\text{-difenylfosfino-1'}\text{-(2-dimethoxy)-bifenyldiene})(\text{PPh}_2\text{OH})](\text{OTf})$ en $[\text{Ru}(\text{OTf})(6'\text{-difenylfosfino-1-naftyl})(\text{PPh}_2\text{OH})](\text{OTf})$ gevormd: de additie van water aan de P-C binding. Met HBF_4 en water worden de complexen $[\text{Ru}(\text{C}_{12}\text{H}_{11}\text{BF}_2\text{O}_2\text{P})(6'\text{-difenylfosfino-1'}\text{-(2-dimethoxy)-bifenyldiene})](\text{BF}_4)$ en $[\text{Ru}(\text{C}_{12}\text{H}_{11}\text{BF}_2\text{O}_2\text{P})(6'\text{-difenylfosfino-1-naftyl})](\text{BF}_4)$ gevormd, die beide het nieuwe chelerende fosfinit anion ($\text{C}_{12}\text{H}_{11}\text{BF}_2\text{O}_2\text{P}^-$) hebben. Nieuwe Ru-F---H en PFPh_2 intermediairen zijn waargenomen. De gespannen $[\text{Ru}(\text{areen})(\text{MeO-Biphep})](\text{SbF}_6)_2$ complexen reageren snel met de fluoride donor $(\text{Bu}_4\text{N})(\text{Ph}_3\text{SiF}_2)$, resulterend in cyclogemalteerde produkten via de verbreking van de P-C binding en vorming van een nieuwe P-F binding.

Chapter 1

General Introduction and Scope

1.1 General introduction

1.1.1 Chirality

Molecular chirality is an important element in nature and currently plays a key role in science and technology. Life itself depends on chiral recognition, because living systems interact with enantiomers in decisively different ways. A variety of functions responsible for metabolism and numerous biological responses occur because enzymes, receptors and other natural binding sites recognise substrates with specific chirality.¹

The demand for enantiopure compounds is rapidly increasing due to their importance in the development of various new biologically active compounds, such as pharmaceuticals and agrochemicals. For pharmaceuticals or pesticides, usually only one of the enantiomers is responsible for the desired biological activity, while the other is inactive or even causes dangerous side effects. Use of enantiomerically pure agrochemicals minimises their impact on the environment.² Furthermore, flavors, fragrances, chiral polymers, advanced materials with nonlinear optical properties, ferroelectric liquid crystals, etc. all rely on the availability of chiral building blocks.

Most optically pure compounds are produced via one or more of the following methods:

(1) Preferential crystallisation. This is one of the oldest methods for the resolution of racemates and it involves seeding of the racemate solution with pure crystals of the desired enantiomer. This technology is e.g. used in the commercial production of α -methyl-L-dopa.³

(2) Diastereomeric crystallisation. An enantiopure auxilliary compound is added to the racemic mixture of the product to form the corresponding diastereomers which are then separated via crystallisation. For example, (*S*)-naproxen is produced by reacting a chiral amine with the racemic mixture of 2-(6'-methoxy-2'-naphthyl)propionic acid to form the corresponding organoammonium salts of the (*S*)- and (*R*)- isomers followed by crystallisation and reacidification.⁴

(3) Kinetic resolution. This separation process is based on the different rates of transformation of the enantiomers into products under the influence of chiral reagents or catalysts. The enzyme-catalysed enantioselective hydrolysis of chiral esters uses this approach.⁵

(4) Existing chiral compounds as starting material or templates. Natural amino acids have been used extensively for this purpose.⁶ This method is limited by the availability and cost of the existing chiral source.

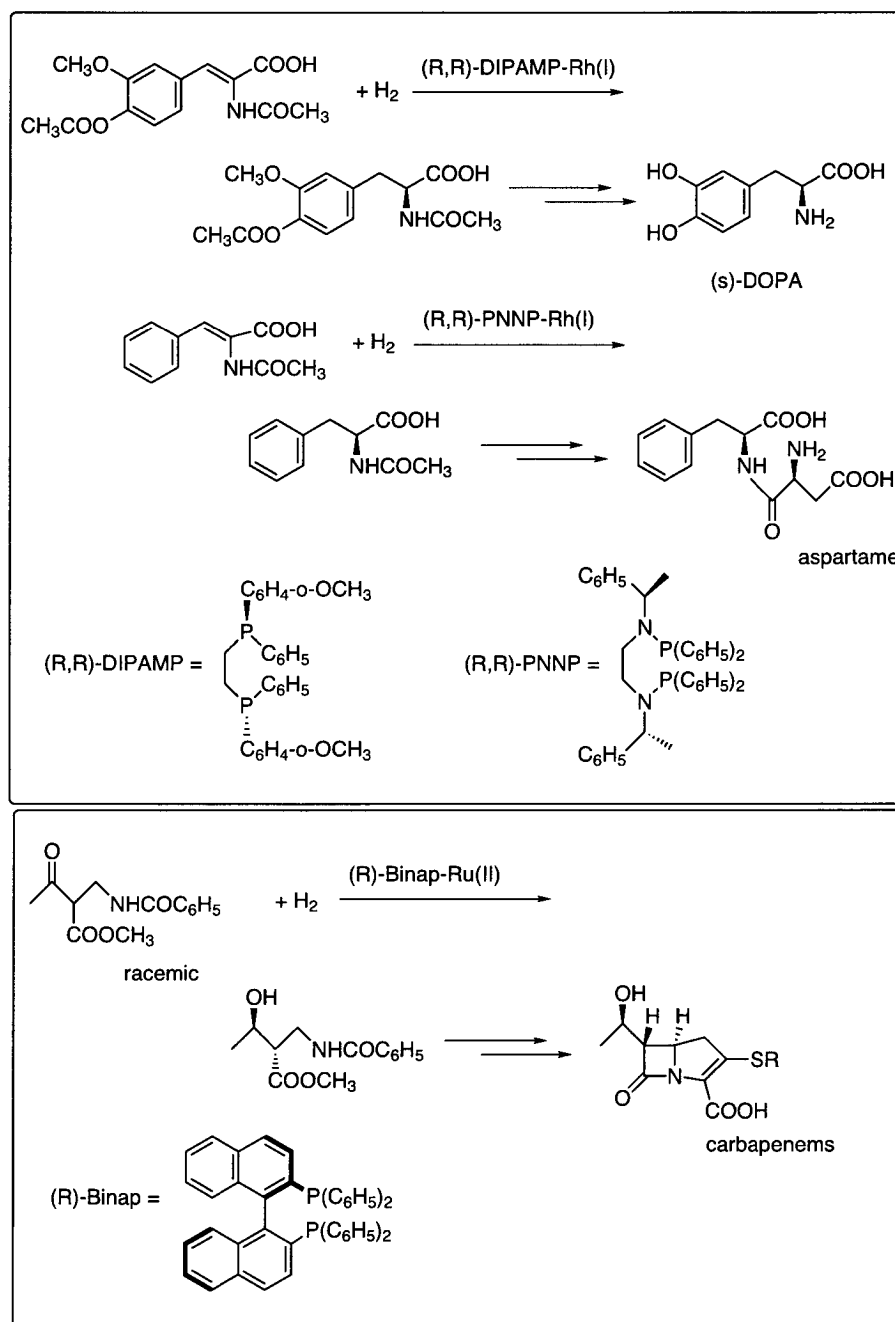
(5) Catalytic asymmetric synthesis. A powerful method for producing enantiopure compounds.⁷ With this technology, a large quantity of a chiral target molecule can be efficiently produced using only a small amount of a chiral catalyst.

1.1.2. Asymmetric homogenous catalysis

Asymmetric homogenous catalysis by means of chiral transition metal complexes has become an important field of current chemical research involving both academia and industry. The advantage of enantioselective catalysis relative to stoichiometric reactions is that the expensive chiral species, often a chiral ligand, is not consumed and needs only to be present in small quantities. Enantioselective catalytic reactions can now be carried out on a large scale with a sufficiently high substrate-to-catalyst ratio.

Scheme 1 illustrates some examples of industrial applications.^{8,9} Rh(I)-catalysed enantioselective hydrogenation has been used for commercial synthesis of (*S*)-DOPA ((*S*)-3-(3,4-dihydroxyphenyl)alanine), an anti-Parkinson amino acid, and (*S*)-phenylalanine which is a component of the sweetener aspartame. Another significant industrial process concerns the Ru(II)-catalysed hydrogenation of a functionalised ketone. This has made

the large scale asymmetric production of a common intermediate of carbapenem antibiotics possible.



Scheme 1. Industrial applications of homogenous asymmetric catalysis.

Although selectivity, particularly in stereochemistry, is a major concern in modern organic synthesis, reactivity and productivity are also important in making reactions effi-

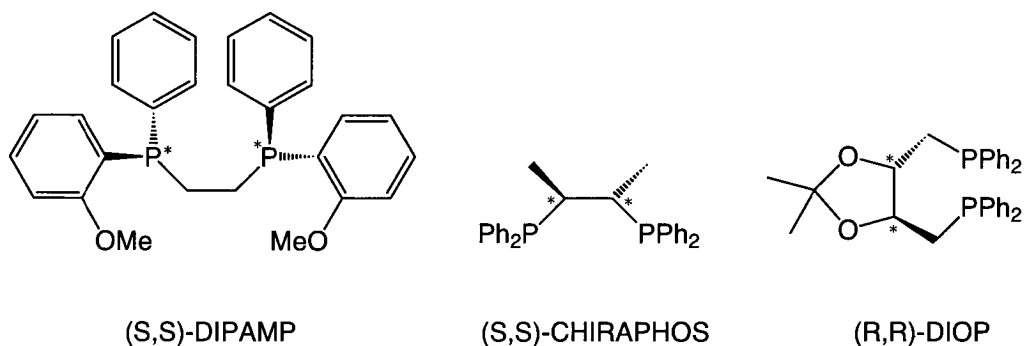
cient and practical. In addition, reactions should be simple, safe and environmentally friendly. These attributes can only be obtained by appropriate combination of metal and chiral ligand, careful molecular design of the chiral ligands, as well as the appropriate selection of reaction conditions.

1.1.3. Ligand design

There are continuing efforts to develop newer and more efficient chiral ligands as the steric and electronic characteristics of such ancillaries have a strong effect on the course of the reactions.¹⁰ The ligands, which modify the intrinsically achiral metal atoms, must be endowed with suitable functionality, configuration and conformational rigidness or flexibility¹¹ to produce the desired stereoselectivity.

Among the variety of ligands in use, organophosphines are the most versatile ones, mainly due to their compatibility with a variety of oxidation states and coordination environments.¹² Moreover, the relative ease with which the substituents at the phosphorus atom can be varied affords a trigger to alter the electronic and steric features. However, oxygen and nitrogen donor atoms have been used in chiral ligands as well.

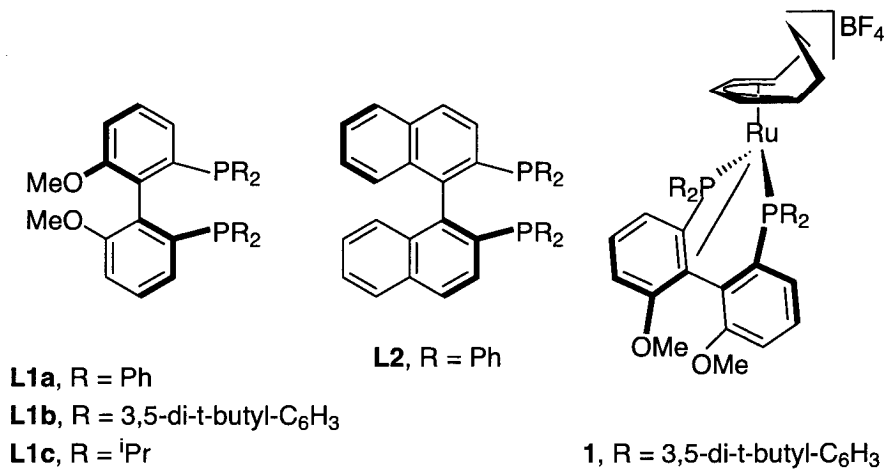
Bidentate phosphines have been widely used. Not only does chelation make the metal complex more stable, but it also has stereochemical consequences. Furthermore, bidentate phosphine ligands undergo slower exchange reactions. During the early developments in asymmetric catalysis, mainly C₂-symmetric biphenyl ligands were used. Scheme 2 shows C₂-symmetric biphenyl ligand (S,S)-DIPAMP which has the stereogenicity on the phosphorus atom and the C₂-symmetric ligands (S,S)-CHIRAPHOS and (R,R)-DIOP having chiral carbons in the backbone.¹³ It was believed that the C₂-symmetry was necessary to gain high enantioselectivities as the number of diastereomeric transition states could be halved. Currently, it has been proven that C₁-symmetric biphenyl ligands can be equally successful in enantioselective catalysis.⁷



Scheme 2. Several important C₂-symmetric chiral biphenyl-based phosphine ligands.

1.2 Outline of the thesis

Among the numerous chiral ligands reported to date, the atropisomeric MeO-Biphep,¹⁴ **L1**, and derivates thereof as well as Binap,¹⁵ **L2**, have attracted continuing attention due to their intrinsic structural features, remarkable chiral recognition ability and broad applicability in transition-metal catalysed reactions such as hydrogenation.⁸



Recently, it has been shown¹⁶ that the biaryl ligands **L1b**, **L1c** and **L2** can act as 6e donor ligands in monocationic Ru(II)-complexes e.g. in **1**. This is a rare and unexpected bonding mode for a bidentate phosphine ligand. The objectives of this thesis are:

- (1) To explore and extend the chemistry of the biaryl ligands **L1** and **L2** with respect to their capability to function as a 6e donor, especially toward dicationic Ru(II)-arene complexes.
- (2) To study the stoichiometric and catalytic reactivity of these compounds.
- (3) To evaluate the importance of this coordination mode in selective transformations.

1.3. References

- (1)Hegstrom, R. A.; Kondepudi, D. K. *Sci. Am.* **1990**, 262, 98; Gardner, M., In *The New Ambidextrous Universe*; W.H. Freeman: New York, 1990.
- (2)Tombo, G. M. R.; Bellus, D. *Angew. Chem., Int. Ed. Engl.* **1991**, 30, 1193.
- (3)Rheinhold, D. F.; Firestone, R. A.; Gaines, W. A.; Chemerda, J. M.; Sletzinger, M. *J. Org. Chem.* **1968**, 33, 1209.
- (4)Harrison, I. T. *J. Med. Chem.* **1970**, 13, 203.
- (5)Kagan, H. B. *Top. Stereochem.* **1988**, 18, 249.
- (6)Coppola, G. M.; Schuster, H. F., In *Asymmetric Synthesis*; John Wiley & Sons: New York, 1987.
- (7)Morrison, J. D., In *Asymmetric Synthesis*; Academic Press: New York, 1985; Ojima, I., In *Asymmetric Catalysis*; VCH Publishers: Weinheim, 1993; Bosnich, B., In *Asymmetric Catalysis*; Martinus Nijhoff: Dordrecht, 1986; Nogradi, M., In *Stereoselective Synthesis*; Verlag Chemie: Weinheim, 1987; Kagan, H. B. In *Comprehensive Organometallic Chemistry*; Wilkinson, G., Stone, F. G. A., Abel, E. W., Eds.; Pergamon Press: Oxford, 1982; Vol. Chapter 53, Vol. 8, Asymmetric Synthesis Using Organometallic Catalysts; Brunner, H. *Top. Stereochem.* **1988**, 18, 129; Brunner, H. *Synthesis* **1988**, 645; Brown, J. M.; Davies, S. G. *Nature* **1989**, 342, 631; Ojima, I.; Clos, N.; Bastos, C. *Tetrahedron* **1989**, 45, 6901; Noyori, R. *Science* **1990**, 248, 1194.
- (8)Noyori, R. *Chem. Soc. Rev.* **1989**, 18, 187.
- (9)Noyori, R.; Takaya, H. *Acc. Chem. Res.* **1990**, 23, 345; Noyori, R. *CHEMTECH* **1992**, 22, 360; Collins, A. N.; Sheldrake, G. N.; Crosby, J., In *Chirality in Industry*; John Wiley & Sons: New York, 1992; Nugent, W. A.; RajanBabu, T. V.; Burk, M. J. *Science* **1993**, 259, 479; Noyori, R. *Science* **1993**, 258, 584; Crosby, J. *Tetrahedron* **1991**, 47, 4789; Sheldon, R. *Chem. Ind.* **1990**, 212; Parshall, G. W.; Nugent, W. A. *CHEMTECH* **1988**, 18, 184, 314 and 376; Kagan, H. B. *Bull. Soc. Chim. Fr.* **1988**, 846.
- (10)Seyden-Penne, J., In *Chiral Auxiliaries and Ligands in Asymmetric Synthesis*; Wiley: Chichester, 1995.
- (11)Noyori, R.; Takaya, H. *Chemica Scripta* **1985**, 25, 83.
- (12)Pignolet, L. H., In *Homogeneous Catalysis with Metal Phosphine Complexes*; Plenum: New York, 1983.
- (13)Vineyard, B. D.; Knowles, W. S.; Sabacky, M. J.; Bachman, G. L.; Weinkauf, D. J. *J. Am. Chem. Soc.* **1977**, 99, 5946; Knowles, W. S.; Sabacky, M. J.; Bachman, G. L.; Weinkauf, D. J. *J. Am. Chem. Soc.* **1975**, 75, 2567; Kagan, H. B.; Dang, T. P. *J. Am. Chem. Soc.* **1972**, 94, 6429; Fryzuk, M. D.; Bosnich, B. *J. Am. Chem. Soc.* **1977**, 99, 6262.
- (14)Schmid, R.; Foricher, J.; Cerrghetti, M.; Schonholzer, P. *Helv. Chim. Acta* **1991**, 74, 370.
- (15)Miyashita, A.; Yasuda, A.; Takaya, H.; Toriumi, K.; Ito, T.; Souchi, T.; Noyori, R. *J. Am. Chem. Soc.* **1980**, 102, 7932.
- (16)Feiken, N.; Pregosin, P. S.; Trabesinger, G.; Albinati, A.; Evoli, G. L. *Organometallics* **1997**, 16, 5756; Feiken, N.; Pregosin, P. S.; Trabesinger, G.; Scalzone, M. *Organometallics* **1997**, 16, 537.

**Seite Leer /
Blank leaf**

Chapter 2

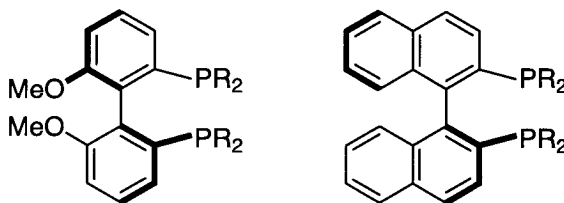
MeO-Biphep and Binap as 6e Donor Ligands in Dicationic Ru(II)-Arene Complexes: Synthesis, Characterisation and Reactivity

2.1 Abstract

The biarylphosphine ligands MeO-Biphep (**L1a**), ⁱPr-MeO-Biphep (**L1c**) and Binap (**L2**) readily complex an adjacent biaryl double bond in dicationic η^6 -*p*-cymene or η^6 -benzene complexes [Ru(**L1a**, **L1c** or **L2**)(arene)](SbF₆)₂ (arene = η^6 -*p*-cymene or η^6 -benzene), **C6-C10**. The precursors [RuCl(**L1a**, **L1c** or **L2**)(arene)]Cl, **C1-C5**, react with 2 equivalents AgSbF₆ for prolonged period of time to afford **C6-C10**. The complexes **C6** and **C9** react easily with MeOH to give the respective hydride complexes [RuH(**L1a**, **L1c** or **L2**)(arene)]SbF₆, **C11** and **C12** respectively, in good yield. Several nitrile complexes, [Ru(nitrile)(**L1a**, **L1c** or **L2**)(arene)](SbF₆)₂, **C13-C18** and isonitrile complexes, [Ru(isonitrile)(**L1a**, **L1c** or **L2**)(arene)](SbF₆)₂, **C19-C21**, were prepared. These substrates readily displace the η^2 -olefinic bonding mode of these biaryl ligands. The η^6 -*p*-cymene ¹³C chemical shifts of complexes **C1**, **C4**, **C15**, **C18-C20** are discussed.

2.2 Introduction

The atropisomeric bidentate phosphine ligands MeO-Biphep (**L1a**), and derivates thereof, 3,5-di-*t*-Bu-MeO-Biphep (**L1b**) and *i*Pr-MeO-Biphep (**L1c**),¹ and Binap (**L2**)² are outstanding in achieving high yields and enantioselectivities in asymmetric hydrogenation when coordinated to ruthenium or rhodium.³



L1a, R = Ph

L1b, R = 3,5-di-*t*-butyl-C₆H₃

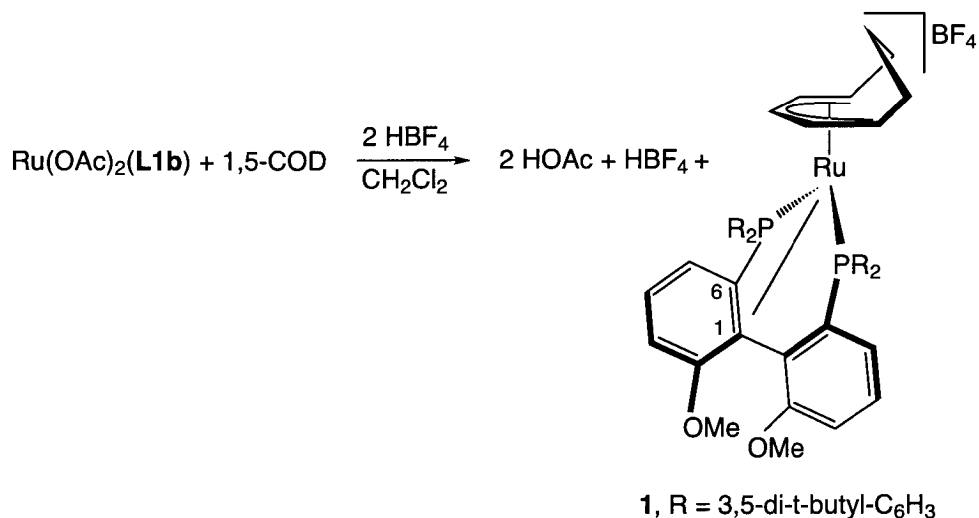
L1c, R = *i*Pr

L2, R = Ph

Prochiral unsaturated substrates including α -(acylamino)acrylic acids,⁴ allylic alcohols,⁵ α,β -unsaturated carboxylic acids,^{6,7} and enamides⁸ are easily reduced to give saturated products in quantitative yields with 90-99% enantioselectivity by using either neutral Ru-MeO-Biphep or/and Ru-Binap dicarboxylato catalyst precursors. Other exocyclic olefinic substrates with aprotic functions as α,β -unsaturated carbonyl compounds, alkylidene lactones, alkenyl esters,⁹ 3-alkylidene-2-piperidones¹⁰ and 2-methylendioxolanes¹¹ have all been hydrogenated with high enantioselectivity using Ru(II)-Binap-arene precatalysts.

Besides their use in asymmetric hydrogenation, the Binap and/or MeO-Biphep ligands have also been used in the Pd-catalysed Heck reaction and allylic alkylation,¹² Rh-catalysed hydroboration¹³ and hydrocyanation, Ru-catalysed hydrosilylation¹⁴ and Diels-Alder reactions.¹⁵

Recently, the reaction of the MeO-Biphep complex $[\text{Ru}(\text{OAc})_2(\text{L1b})]$ (**L1b** = 3,5-di-*t*-Bu-MeO-Biphep) with 1,5-COD (COD = cyclooctadiene) and 2 equivalents of HBF_4 in methylene chloride was shown to afford the monocationic $[\text{Ru}(\eta^5\text{-C}_8\text{H}_{11})(\text{L1b})]\text{BF}_4$, **1**, (Scheme 1).¹⁶ The biaryl 3,5-di-*t*-Bu-MeO-Biphep ligand functions as a 6e donor to Ru(II) via an unexpected coordination of a biaryl double bond using carbons C1 and C6, proximate to a P-donor.



Scheme 1: The protonation reaction resulting in complex **1**. This pentadienyl complex exhibits the additional η^2 -bonding mode of the 3,5-di-*t*-Bu-MeO-Biphep (**L1b**) ligand.

The isopropyl analog $[\text{Ru}(\eta^5\text{-C}_8\text{H}_{11})(\text{L1c})]\text{CF}_3\text{CO}_2$, **2**, (**L1c** = ⁱPr-MeO-Biphep) has been prepared by starting from $[\text{Ru}(\text{CF}_3\text{CO}_2)_2(1,5\text{-COD})]_2$ and reveals the additional η^2 -bonding mode as well. The solid-state structure of the monocationic complex **2** discloses two relatively long Ru-C(1) and Ru-C(6) distances, ca. 2.37 Å and 2.30 Å respectively, thus, suggesting a very weak interaction. However, the ¹³C resonance positions for these coordinated biaryl carbons are a more reliable criterion for recognizing this type of interaction. Specifically, the long-range ¹³C, ¹H correlation NMR-spectrum for **2** (Figure 1) reveals the connectivity between the two non-protonated coordinated carbons, C1 and C6, and the three biphenyl protons, H3, H4 and H5. The four key cross-peaks shown in Figure 2 link the resonances for the coordinated biaryl carbons to several of the biphenyl proton resonances, via ²J(¹³C, ¹H) and ³J(¹³C, ¹H).

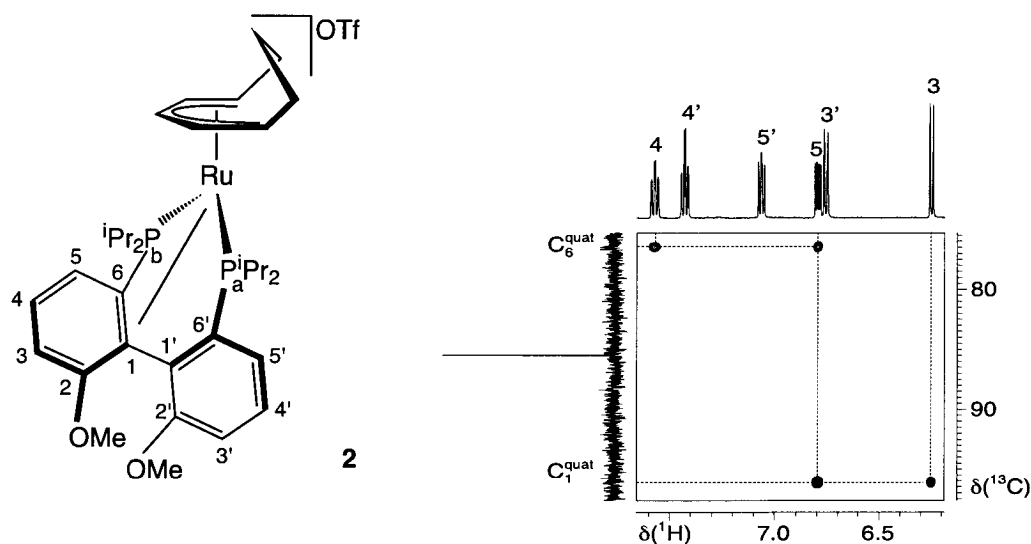


Figure 1. Section of the long-range ^{13}C - ^1H correlation for **2**. The intense signal in the ^{13}C direction stems from one of the five $\eta^5\text{-C}_8\text{H}_{11}$ pentadienyl carbons.

The ^{31}P NMR spectrum for this new η^2 -olefinic bonding mode is informative: the P-atom adjacent to the coordinated C1-C6 aryl bond has a remarkable high field chemical shift. The ^{31}P spectrum of complex **2**, depicted in Figure 2, shows a relative large difference between the two ^{31}P chemical shifts.

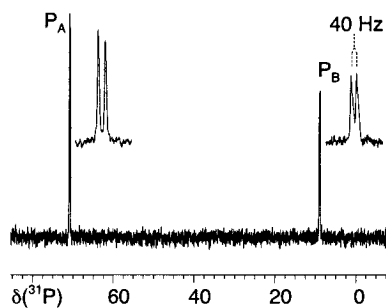
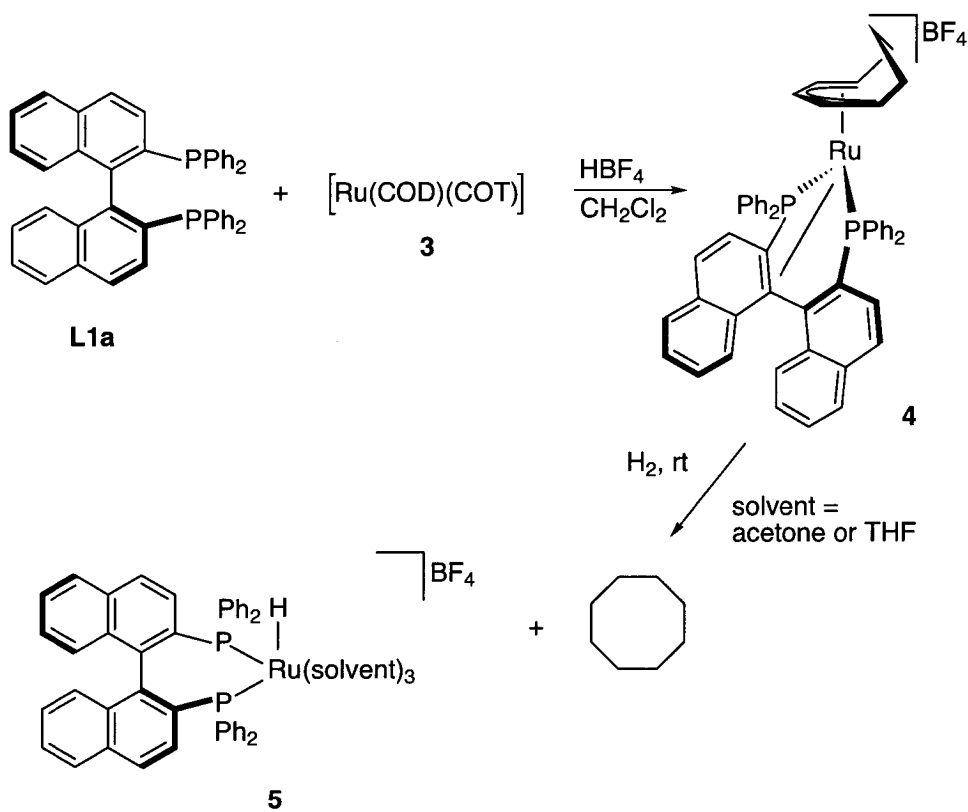


Figure 2. ^{31}P spectrum for **2**.

The additional η^2 -bonding mode of the 3,5-Di-*t*-Bu-MeO-Biphep ligand (**L1b**) has also been recognised in the monocationic complexes $[\text{Ru}(\eta^5\text{-Cp})(\text{L1b})]\text{BF}_4^-$ ($\text{Cp} = \text{C}_5\text{H}_5^-$) and $[\text{Ru}(\eta^5\text{-C}_4\text{H}_4\text{N})(\text{L1b})]\text{BF}_4^-$, as well as in $[\text{Ru}(\eta^6\text{-indole})(\text{L1b})](\text{BF}_4)_2$.¹⁶

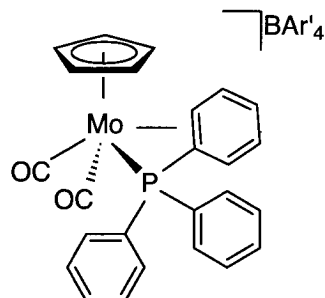
The new bonding mode of Binap (**L2**) in $[\text{Ru}(\eta^5\text{-Cp})(\text{L2})]\text{CF}_3\text{CO}_2$ was recognised from its solid-state structure, i.e. two relative short Ru-C separations ca. 2.26 Å and 2.28 Å.¹⁷ Interestingly, this bonding mode for Binap was not recognised in $[\text{RuCl}_2(\text{L2})]_2$, although one of its P atoms has the characteristic lower frequency ^{31}P chemical shift.¹⁸

Recently, a synthetic route to the active hydrogenation catalyst $[\text{Ru}(\text{L2})(\text{H})(\text{solvent})_3]^+$ (solvent = acetone or THF) (**5**) starting from Binap (**L2**), $[\text{Ru}(\text{COD})(\text{COT})]$ (COD = cyclooctadiene, COT = cyclooctatriene) (**3**) and HBF_4 has been reported (Scheme 2).¹⁹ The main intermediate, **4**, involves Binap as a 6e donor ligand to Ru(II). This η^2 -bond to the binaphthyl backbone in **4** is displaced by an excess MeCN to give $[\text{Ru}(\eta^5\text{-C}_8\text{H}_{11})(\text{L1a})(\text{MeCN})]\text{BF}_4$.



Scheme 2: The reaction resulting in an active catalytic complex **5** via an intermediate with Binap acting as an 6e donor ligand (COD = cyclooctadiene, COT = cyclooctatriene).

We know of only one additional complex, $[\text{Mo}(\eta^5\text{-C}_5\text{H}_5)(\text{CO})_2(\text{PPh}_3)](\text{BAr}'_4)$ ($\text{Ar}' = 3,5\text{-bis}(\text{trifluoromethyl})\text{phenyl}$), **6**, for which a related interaction has been reported.²⁰ This complex contains a PPh_3 which functions as a chelating 4e donor ligand via coordination of the P-atom and the proximate double bond of one of the aryl rings.

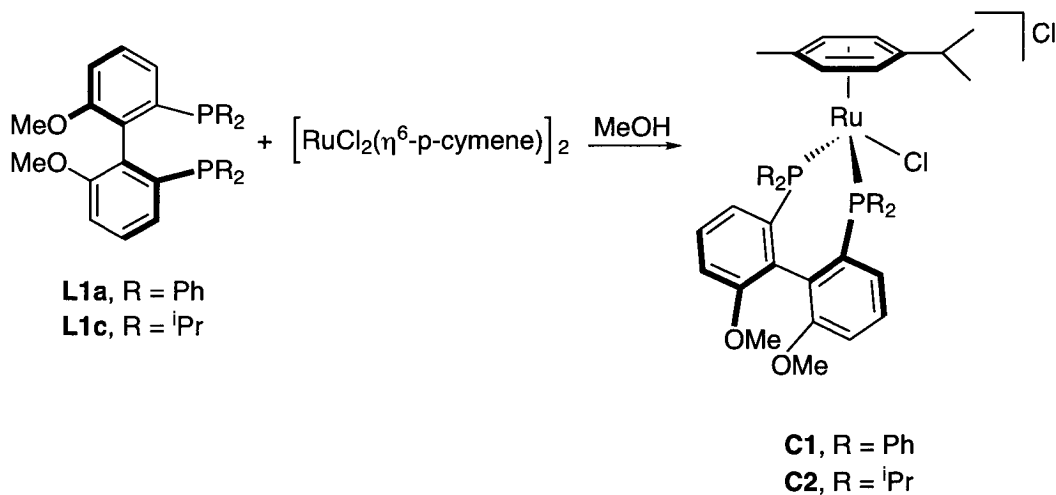


6

2.3 Results and discussion

2.3.1 The chloro-precursors

Given the interest in $[\text{RuCl}(\text{Binap})(\text{arene})]\text{X}$ ($\text{X} = \text{Cl}, \text{Br}, \text{I}$) complexes with respect to asymmetric hydrogenation,^{9,21,22} several MeO-Biphep derivates have been prepared and studied. Treatment of $[\text{RuCl}_2(\eta^6\text{-}p\text{-cymene})]_2$ with 2 equivalents of either MeO-Biphep (**L1a**) or $^i\text{Pr}\text{-MeO-Biphep}$ (**L1c**) dissolved in MeOH at room temperature affords the orange solids of $[\text{RuCl}(\text{L1a or L1c})(\eta^6\text{-}p\text{-cymene})]\text{Cl}$, **C1** and **C2** respectively, in good yields (Scheme 3).



Scheme 3: The reaction resulting in precursors **C1** and **C2**.

The η^6 -benzene derivative of **C1**, $[\text{RuCl}(\text{L1a})(\eta^6\text{-C}_6\text{H}_6)]\text{Cl}$, **C3**, was synthesised starting from the $[\text{RuCl}_2(\eta^6\text{-C}_6\text{H}_6)]_2$ -dimer using a MeOH:toluene mixture. The Binap (**L1a**) analogues $[\text{RuCl}(\text{L1a})(\eta^6\text{-}p\text{-cymene})]\text{Cl}$, **C4**, and $[\text{RuCl}(\text{L1a})(\text{benzene})]\text{Cl}$, **C5**, were prepared according the literature,^{21,23} using MeOH instead of EtOH:CH₂Cl₂ for **4**.

The solid-state structure of $[\text{RuCl}(\text{L1a})(p\text{-cymene})]\text{Cl}$, **C4**, has been determined via X-ray diffraction and a view of the cation is shown in Figure 3. The immediate coordination sphere consists of the two P-donors, the chloride and the six carbon atoms of the $\eta^6\text{-}p\text{-cymene}$ ligand. The six Ru-C(arene) separations fall in the range ca. 2.26–2.32 Å and are

all fairly routine.^{12,24} The two Ru-P distances, Ru-P(1), ca. 2.35 Å, and Ru-P(2), ca. 2.38 Å, are somewhat long but not unusual.^{17,24,25} Both the Ru-Cl bond length, ca. 2.39 Å, and the P(1)-Ru-P(2) angle, ca. 89.5°, are normal. Selected bond lengths and bond angles are given in Table 1 and 2 respectively. The structure of the cation [RuCl(Binap)(η⁶-C₆H₆)]⁺ has been reported previously.^{21,23} Taken together, the X-ray data show a classical "piano-stool" structure with relatively little distortion.

Table 1: Selected Bond Lengths (Å) for the cation in C4.

Ru(1)-C(1L)	2.315(5)	Ru(1)-C(4L)	2.294(5)
Ru(1)-C(2L)	2.258(5)	Ru(1)-C(5L)	2.262(5)
Ru(1)-C(3L)	2.281(5)	Ru(1)-C(6L)	2.280(5)
Ru(1)-P(1)	2.3447(12)	P(1)-C(111) ^a	1.848(5)
Ru(1)-P(1)	2.3803(11)	P(1)-C(121) ^a	1.831(5)
Ru(1)-Cl(1)	2.3942(11)	P(2)-C(211) ^b	1.838(4)
P(1)-C(6)	1.836(5)	P(2)-C(221) ^b	1.840(5)
P(2)-C(6')	1.851(5)		

^a C(111) and C(121) are the ipso-carbons of phenylsubstituents of P1; ^b C(211) and C(221) are the ipso-carbons of phenylsubstituents of P2.

Table 2: Selected Bond Angles (deg) for the Cation in C4.

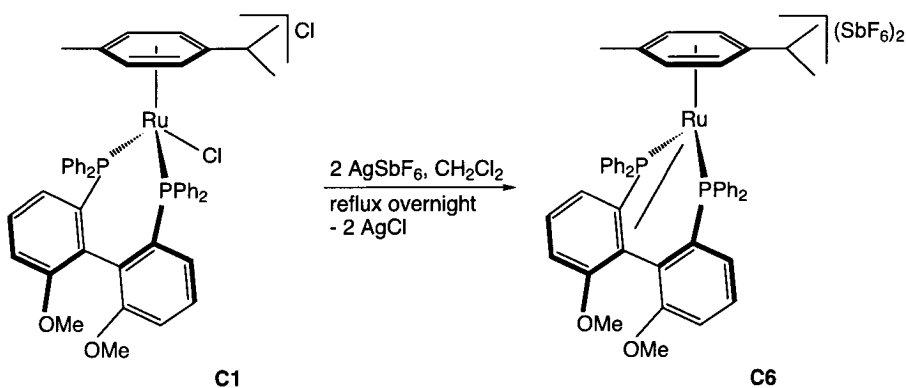
C(1L)-Ru(1)-P(1)	159.02(13)	C(4L)-Ru(1)-P(1)	93.34(13)
C(2L)-Ru(1)-P(1)	122.62(14)	C(5L)-Ru(1)-P(1)	116.94(13)
C(3L)-Ru(1)-P(1)	96.70(13)	C(6L)-Ru(1)-P(1)	153.26(13)
C(1L)-Ru(1)-P(2)	110.94(13)	C(4L)-Ru(1)-P(2)	129.16(13)
C(2L)-Ru(1)-P(2)	146.02(14)	C(5L)-Ru(1)-P(2)	99.79(13)
C(3L)-Ru(1)-P(2)	164.29(13)	C(6L)-Ru(1)-P(2)	92.28(13)
C(1L)-Ru(1)-Cl(1)	89.91(13)	C(4L)-Ru(1)-Cl(1)	139.91(13)
C(2L)-Ru(1)-Cl(1)	82.12(14)	C(5L)-Ru(1)-Cl(1)	155.42(13)
C(3L)-Ru(1)-Cl(1)	103.96(13)	C(6L)-Ru(1)-Cl(1)	121.68(13)
P(1)-Ru(1)-P(2)	89.51(4)		

Table 2: Selected Bond Angles (deg) for the Cation in C4.

C(1L)-Ru(1)-P(1)	159.02(13)	C(4L)-Ru(1)-P(1)	93.34(13)
P(1)-Ru(1)-Cl(1)	84.95(4)		
P(2)-Ru(1)-Cl(1)	90.91(4)		

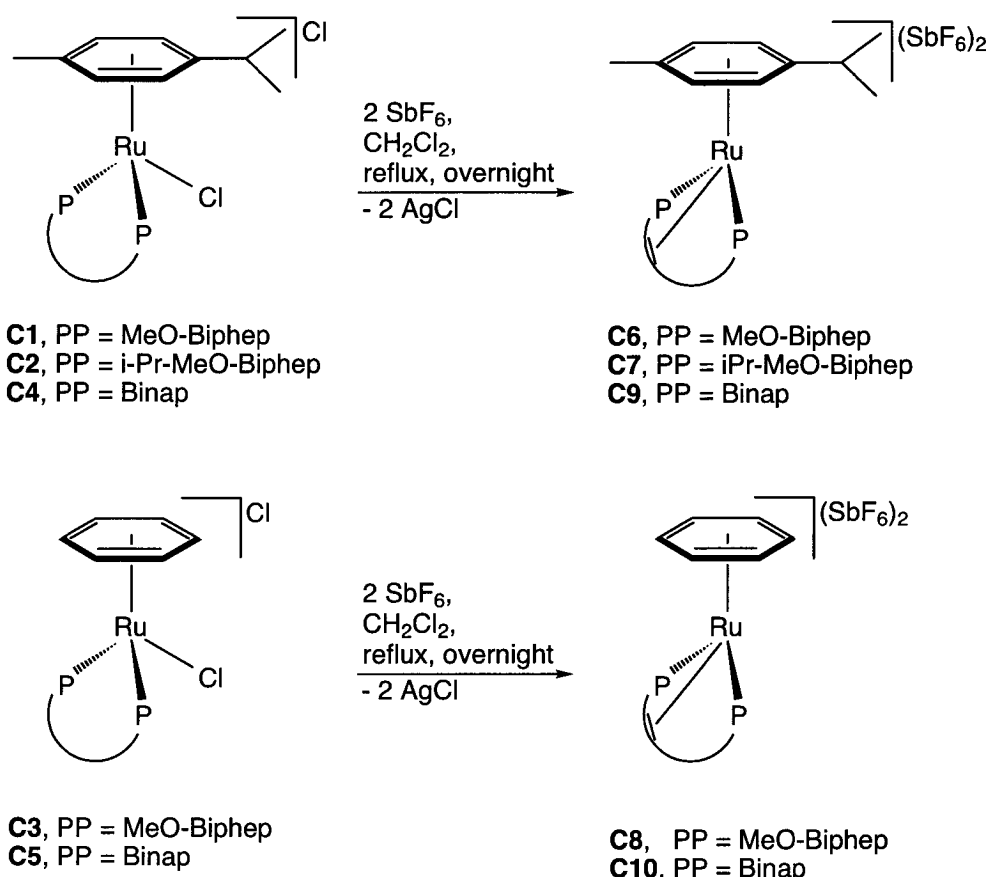
2.3.2 η^2 -Compounds from the chloro-precursors

The chloro-complex $[\text{RuCl}(\text{MeO-Biphep})(\eta^6\text{-}p\text{-cymene})]\text{Cl}$, **C1**, was allowed to react with 2 equivalents AgSbF_6 . This resulted in $[\text{Ru}(\text{MeO-Biphep})(\eta^6\text{-}p\text{-cymene})](\text{SbF}_6)_2$, **C6**, in which the bisphosphino chelating ligand acts as 6e-donors (Scheme 4).



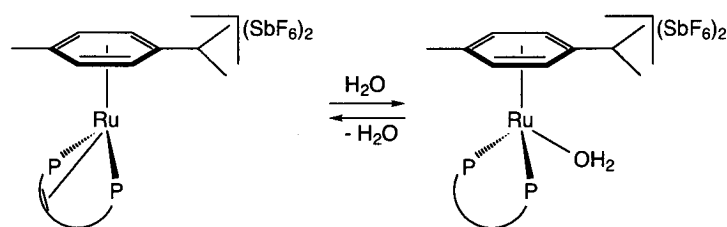
Scheme 4. The preparation of $[\text{Ru}(\text{MeO-Biphep})(p\text{-cymene})](\text{SbF}_6)_2$, **C6**.

The general synthetic pathway is shown in scheme 5. Treatment of the chloro complexes **C1-C5** with two equivalents of AgSbF_6 for prolonged periods affords the compounds **C6-C10**, as η^6 -*p*-cymene and η^6 -benzene derivatives.



Scheme 5. Synthesis of the η^2 -olefin bonding mode complexes **C6-C10**.

The Binap derivatives **C9** and **C10** as well the MeO-Biphep complex, **C7**, containing ⁱPropyl groups on the MeO-Biphep phosphorus donors, could be isolated and afforded satisfactory analytical data. MeO-Biphep analogues **C6** and **C8**, exist in solution together with an aquo-complex (Scheme 6). This latter assignment is based on the observation that addition of water to a solution of **C8** and the presumed aquo-species, results in a marked increase in the concentration of this second species, at the expense of **C8**.



Scheme 6. The equilibrium between an η^2 -olefinic bonding mode complex and its corresponding aquo-complex (PP = Binap or $^1\text{Pr}-\text{MeO}-\text{Biphep}$).

Proof of the coordination mode for **C6-C10** stems from the low frequency ^{13}C coordination chemical shifts for C1 and C6 of the complexed biaryl double bond.²⁶ The chemical shifts of C1 and C6 were determined via their three bond long-range couplings to H4, H5 and H7.²⁷ The proton assignment, necessary in order to be confident with respect to the ^{13}C signals, was made using $(^{31}\text{P}, ^1\text{H})$ and $(^1\text{H}, ^1\text{H})$ correlation spectroscopy. Figure 4 shows a section of the $^{13}\text{C}, ^1\text{H}$ long range NMR spectrum for **C10** and in Table 3 selected NMR-data for **C6-C10** are given. Tables of NMR-data for all of the new dicationic complexes **C6-C10** are given in Section 2.8.

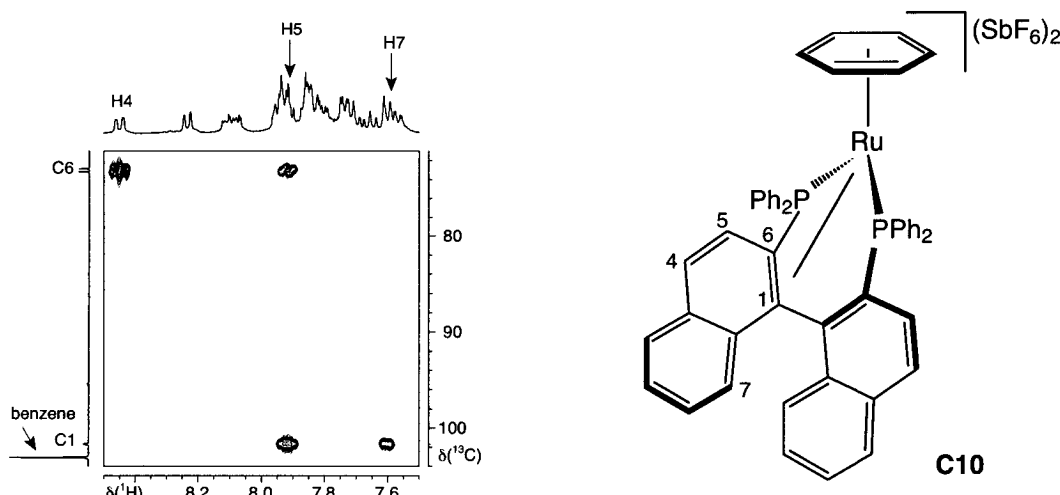
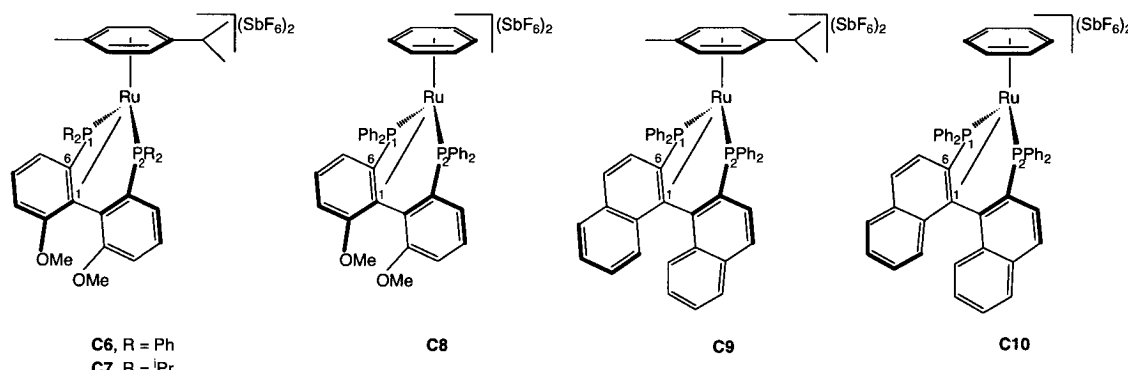


Figure 4. $^{13}\text{C}-^1\text{H}$ long-range correlation for **C10** showing the cross-peaks for two olefinic carbons with the three Binap backbone protons.

It is tempting to use the observed relatively low frequency ^{31}P resonance of P1 (Table 3) as an indication of this bonding mode. This chemical shift empiricism,¹⁶ also noted early on by James et al.,¹⁸ but not explored, is not always a reliable indicator since cyclometalated Ru(II)-complexes can show similar ^{31}P chemical shifts.²⁸ It is interesting that the observed ^{31}P frequencies for complexed MeO-Biphep (**C6-C8**) vs Binap (**C9** and **C10**), do not depend markedly on the structure of the bidentate phosphine. However, the ^{13}C chemical shifts values for C1 and C6 in these dications do vary as a function of the chelate (Table 3).

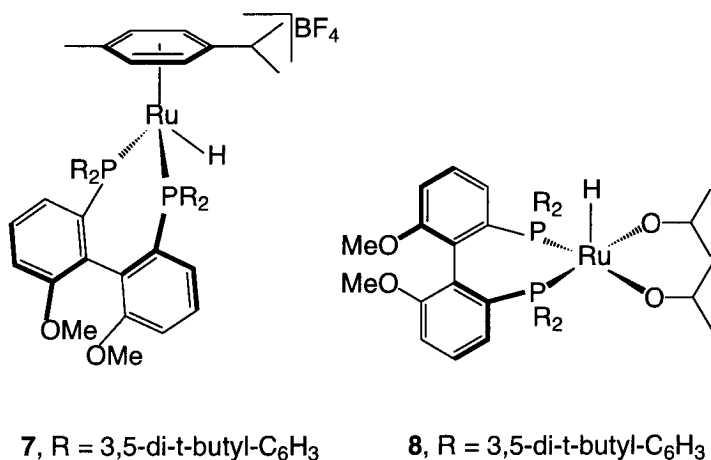
Table 3: Selected NMR chemical shifts for the carbon and phosphorus donors in C6-C10.



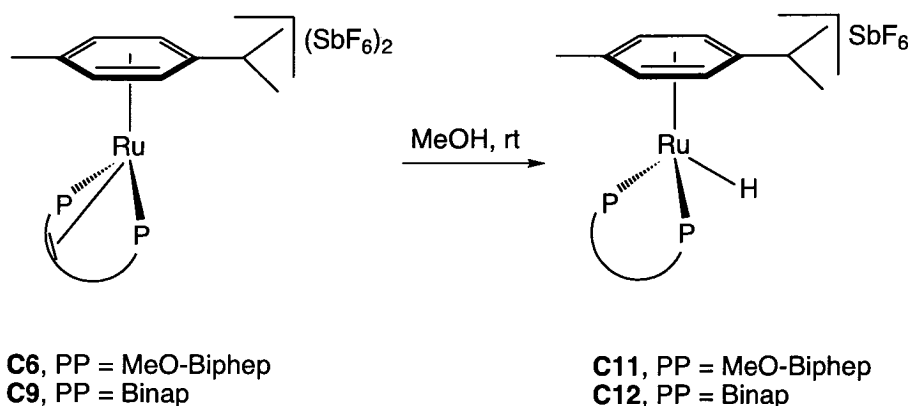
Complex	δ ($^{13}\text{C1}$)	δ ($^{13}\text{C6}$)	δ ($^{31}\text{P1}$)	δ ($^{31}\text{P2}$)
C6	93.0	80.1	7.7	67.1
C7	102.5	79.1	27.3	82.6
C8	90.9	86.0	15.4	64.7
C9	98.0	67.5	3.3	68.7
C10	101.7	73.0	19.0	64.0

2.3.3 Hydrides

There are relatively few well characterised Ru-H complexes of Binap (**L1**) and MeO-Biphep (**L2**) known.^{14,29} A X-ray structure of [RuH(*p*-cymene)(**L2b**)]BF₄, **7**, (**L2b** = 3,5-di-*t*-Bu-MeO-Biphep) has been reported.¹² This hydride compound has been synthesised starting from [Ru(OAc)₂(**L2b**)], *p*-cymene and molecular H₂ in methylene chloride to which HBF₄ was added. Furthermore, a stable cationic five-coordinate hydrido bis-solvento complex, [RuH(ⁱPrOH)₂(**L2b**)]BF₄, **8**, (**L2b** = 3,5-di-*t*-Bu-MeO-Biphep), has been obtained from a hydrogenation mixture.³⁰



The dicationics **C6** (generated *in situ*) and **C9** react smoothly on stirring in MeOH as solvent at room temperature to afford the hydride complexes [RuH(*p*-cymene)(MeO-Biphep)]SbF₆, **C11**, and [RuH(*p*-cymene)(Binap)]SbF₆, **C12** (Scheme 7). No base is necessary and the yields are good. This straightforward approach to hydride synthesis provides an useful alternative to synthetic routes involving molecular hydrogen or boron or aluminium hydrides.



Scheme 7. The straightforward synthesis to hydride-complexes **C11-C12**.

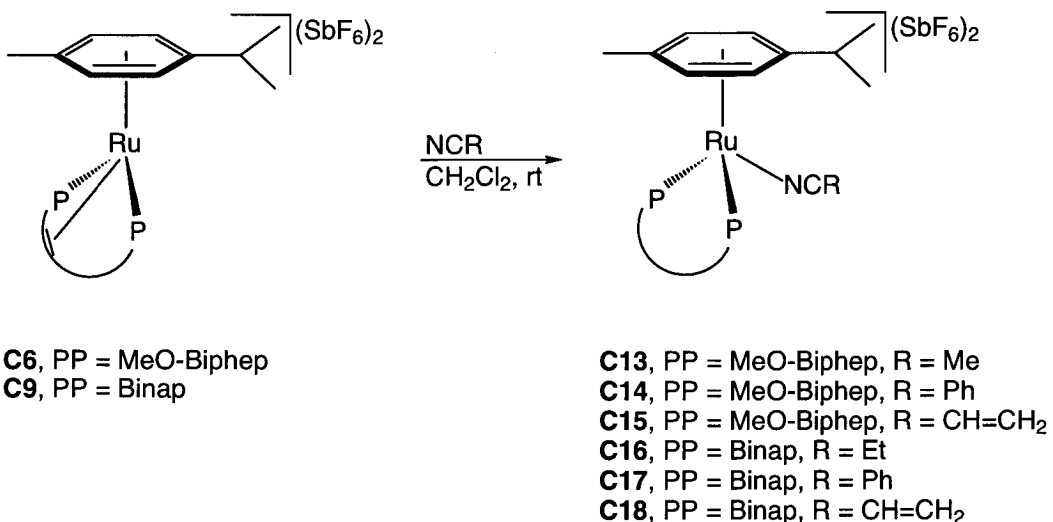
The ^1H spectra for **C11** and **C12** show the hydride resonances as a doublet of doublets at $\delta = -9.79$ and $\delta = -10.10$ for **C11** and **C12**, respectively. The *p*-cymene ^{13}C resonances are shifted to lower frequency and fall in the region $\delta = 91.5\text{-}116.8$. The four CH carbons of the *p*-cymene appear in the narrow range of 91.5-98.3 ppm, exactly where one expects ^{13}C resonances of arenes complexed to Ru(II).²⁶

Interestingly, the MeO-Biphep complex, **C11**, affords product ca 10 times faster than the Binap analogue, **C12**. Similar qualitative observations have been made with respect to relative kinetics in other reactions as well, i.e., MeO-Biphep is generally faster than Binap in our Ru-chemistry.

2.3.4 Nitriles and isonitriles

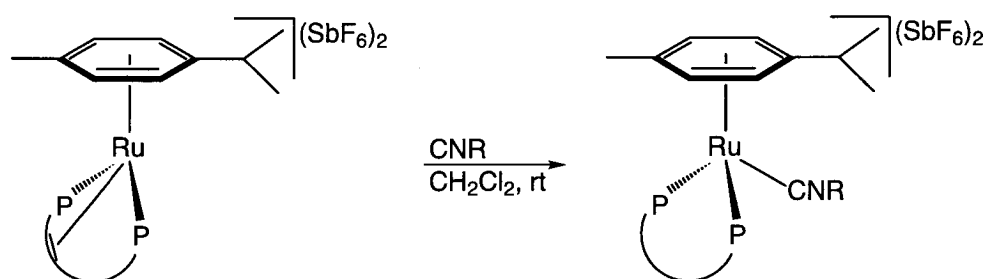
To gain further insight into the reactivity of **C6** (generated *in situ*) and **C9**, these dication were allowed to react with nitriles, i.e. N≡CMe, N≡CEt, N≡CPh and N≡CCH=CH₂, and isonitriles, i.e. C≡NCHCO₂Et and C≡NBu^t.

Treatment of dication **C6** (generated *in situ*) and **C9** with nitriles in methylene chloride readily afforded the nitrile-complexes **C13-C18** as depicted in Scheme 8. These reactions illustrate that the additional η^2 -bond between the biaryl carbons of the biphenyl ligand and Ru(II) is easily displaced by a stronger (donor) ligand. A similar reaction has been reported in the literature.¹⁹



Scheme 8. Reaction of the η^2 -complexes **C6** and **C9** leading to nitriles-complexes **C13-C14**.

The dicationic isonitrile complexes **C19-C21** are smoothly obtained by stirring complexes **C6** (generated *in situ*) and **C9** with the appropriate isonitrile dissolved in methylene chloride at room temperature (Scheme 9).



C6, PP = MeO-Biphep
C9, PP = Binap

C19, PP = MeO-Biphep, R = CH₂CO₂Et
C20, PP = Binap, R = CH₂CO₂Et
C21, PP = Binap, R = ^tBu

Scheme 9. Reaction of the η^2 -complexes **C6** and **C9** with various isonitriles.

As isonitriles are stronger donor ligands than nitriles, it was expected that the additional η^2 -olefin would be substituted by an isonitrile.

2.3.5 ^{13}C -NMR data for the η^6 -*p*-cymene ligand

The ^{13}C chemical shifts for the complexed arenes in e.g., **C1-C21** are readily determined in that they fall in a convenient region, ca 70-110 ppm.²⁶ Having noticed that this NMR parameter varies somewhat for the η^2 -olefin complexes **C6-C10**, we considered it useful to compare the ^{13}C η^6 -*p*-cymene characteristics in several Binap and MeO-Biphep compounds (Figure 5).

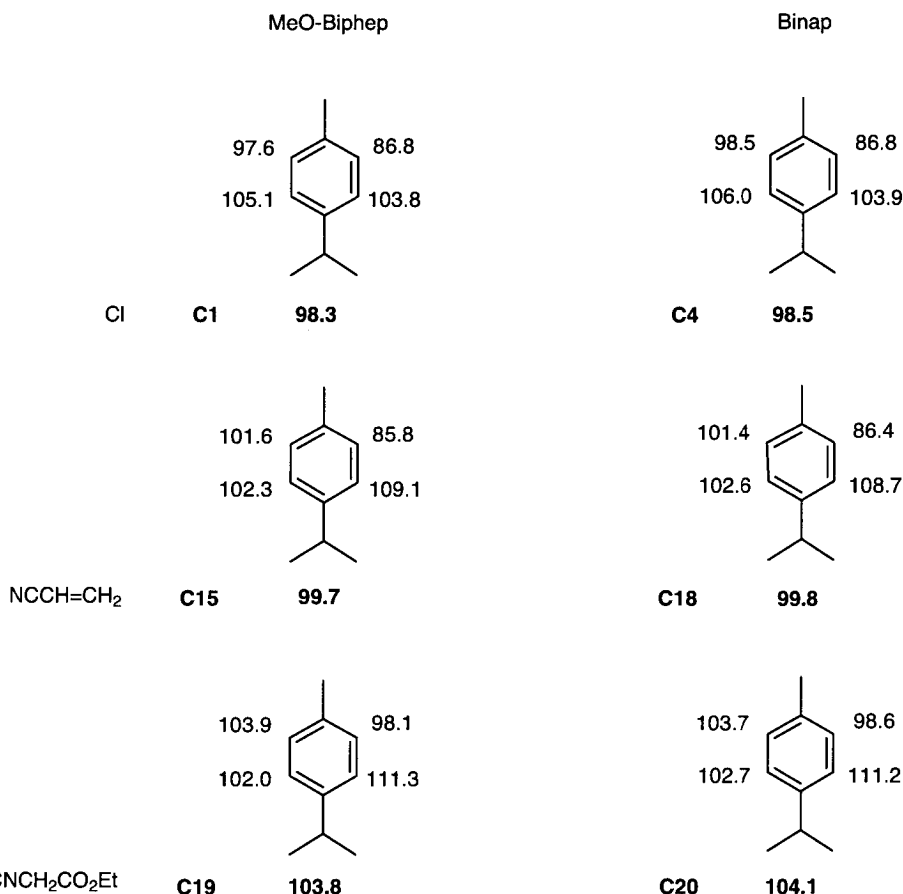
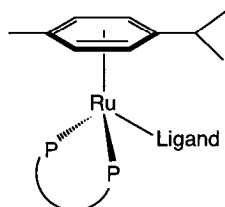


Figure 5. Selected *p*-cymene ^{13}C resonances of selected compounds and their average.

Somewhat unexpectedly, the four unsubstituted ring *p*-cymene ^{13}C signals are well separated suggesting asymmetric bonding for this arene. It is equally interesting that these ^{13}C chemical shifts in **C1**, **C4**, **C15** and **C18** do not vary very much, either as a function of charge on the complex or as a function of the chelate ligand. Moreover, the averages of these four values, 98.3 for **C1**, 98.5 for **C4**, 99.7 for **C15** and 99.8 ppm for **C18**, are quite close. Thus it appears that the total charge on the molecule, i.e., monocationic for

the chloride complexes and dicationic for the acrylonitrile complexes, is of secondary importance in this connection. The nature of the donor is the more important factor as shown by the averages for the isonitriles derivates **C19**, 103.8, and **C20**, 104.1, i.e. ca 4-5 ppm larger than the previous averages. Assuming that a high frequency HC=(cymene) shift arises due to reduced Ru \rightarrow arene d $\rightarrow\pi^*$ back-bonding, this suggests that the ethyl-isocyanoacetate ligand is a better π -acceptor ligand than either the chloride or the acrylonitrile.

Table 4: Averaged CH-arene ^{13}C chemical shifts for in Ru(η^6 -*p*-cymene) complexes.^a



Ligand	MeO-Biphep	Binap
Cl	98.3 (C1)	98.5 (C4)
η^2 -olefin	96.8 (C6)	101.9 (C9)
H	95.8 (C11)	96.0 (C12)
CH_3CN	99.1 (C13)	-
PhCN	99.7 (C14)	99.9 (C17)
$\text{CH}_3\text{CH}_2\text{CN}$	-	99.5 (C16)
$\text{CH}_2=\text{CHCN}$	99.7 (C15)	99.8 (C18)
$\text{EtCO}_2\text{CH}_2\text{NC}$	103.8 (C19)	104.1 (C20)
Bu ^t NC	-	104.2 (C21)

^a As mono- or di- SbF₆ cations.

In Table 4 the averages for these four *p*-cymene signals for a larger data set are shown. The olefin and isonitrile π -acceptor ligands result in higher frequency positions whereas the hydride, due to its stronger sigma-donor character, affords a lower frequency result. For the Binap series, a similar analysis using all six carbons of the *p*-cymene has been carried out. Inclusion of the two fully substituted carbon chemical shifts moves the averaged results to higher frequency by ca 5-6 ppm, but does not change any of the conclusions.

2.4 Conclusions

This chapter shows clearly that several biarylphosphine ligands in **C6-C10** functions as a 6e donor ligand to Ru(II) by complexing an adjacent biaryl double bond. These complexes represent further rare examples of the η^2 -complexation of the double bond of a biaryl phosphine ligand.

Reaction of the complexes **C6** and **C9** with MeOH provides a straightforward synthesis of the corresponding hydride-complexes **C11** and **C12** in good yield. Several nitrile (**C13-C18**) and isonitrile (**C19-C21**) complexes were prepared. These substrates readily displaced the η^2 -olefin bonding mode of these biaryl ligands.

The η^6 -*p*-cymene ^{13}C chemical shifts of complexes **C1**, **C4**, **C15**, **C18-C20** are discussed. Interestingly, they do not depend on the formal positive charge on the cation, but rather on the nature of the donor ligands.

2.5 Experimental

2.5.1 Crystallography

Air stable, orange crystals of compound **C4** were obtained via slow diffusion of diethyl ether into a solution of **C4** in dichloromethane. For the data collection, a prismatic single crystal was mounted on a Bruker SMART CCD diffractometer. The space group was determined from the systematic absences, while the cell constants were refined, at the end of the data collection with the data reduction software SAINT.³² The collected intensities were corrected for Lorentz and polarization factors³² and empirically for absorption using the SADABS program.³³ Selected crystallographic and other relevant data collection and refinement parameters are listed in Tables 5 and 6.

The structure was solved by direct methods and refined by full matrix least squares,³⁴ minimizing the function $[\sum w(F_o^2 - (1/k) F_c^2)^2]$ using anisotropic displacement parameters for all atoms. Toward the end of the refinement a disordered solvent (CH_2Cl_2) molecule was located in a difference Fourier map and successfully refined, allowing two orientations for the Cl atoms (with occupancy factors of 0.75 and 0.25 respectively). After refinement, a second CH_2Cl_2 molecule was located in the difference Fourier map but refined satisfactorily (with isotropic temperature factors) only with partial occupancy of the site (0.5). Upon convergence (maximum parameter shift $\Delta p/\sigma < 0.3$) the final difference Fourier map showed no significant peaks.

The contribution of the hydrogen atoms, in their calculated position ($\text{C-H} = 0.95(\text{\AA})$, $B(\text{H}) = 1.5 \times B(\text{C}_{\text{bonded}})(\text{\AA}^2)$), was included in the refinement using a riding model; the hydrogen atoms bonded to the disordered solvent molecules were not included.

All calculations were carried out by using the PC version of the SHELX-97 programs. The scattering factors used, corrected for the real and imaginary parts of the anomalous dispersion, were taken from the literature.³⁵

Table 5: Crystal data and parameters of the data collection of compound C4.

Empirical formula	C _{55.5} H ₄₉ Cl ₂ P ₂ Ru
Formula weight (g/mol)	1056.26
Crystal size (mm)	0.32 x 0.26 x 0.20
Crystal system	monoclinic
Unit cell dimensions (Å, deg)	<i>a</i> = 12.5980(2) <i>b</i> = 21.8156(1), β = 107.869(2) <i>c</i> = 19.4865(3)
Volume (Å ³)	5097.2(1)
Space group	<i>P</i> 2 ₁
Formula unit pro cell(Z)	4
ρ (calculated) (g cm ⁻³)	1.371
Absorption coefficient μ (mm ⁻¹)	0.507
F(000)	1912
Temperature (K)	200(2)
Data collection	Bruker SMART CCD diffractometer
Monochromator; Wavelength	Graphite-Monochromator; $\lambda(\text{MoK}\alpha)$ = 0.71073 Å
Collection method	Hemisphere, ω -scan
Theta range for data collection	1.94 < θ < 27.47
<i>h</i> (min), <i>h</i> (max); <i>k</i> (max), <i>k</i> (min); <i>l</i> (min, <i>l</i> (max)	-16, 16; -28, 28; -24, 25
Collected reflections	11569
Independent reflections	8741 (<i>R</i> (int) = 0.0567)
Absorption correction	empirical (SADABS)
Structure solution	SHELXS-97 (direct methods)
Structure refinement	SHELXL-97 (full matrix least-square of F^2)
Number of parameters	564
Number of parameters restraints	0
Transmission coefficient (max/min)	0.83/0.93
w <i>R</i> for $ F_o ^2 > 2\sigma(F ^2)$	0.1953
w <i>R</i> for all reflections	0.2264
<i>R</i> for $ F_o ^2 > 2\sigma(F ^2)$	0.0657
<i>R</i> for all reflections	0.0950
Goodness of Fit (<i>GooF</i>) for $ F_o ^2 > 2\sigma(F ^2)$	0.738

Table 6: Final position ($x \times 10^{-4}$) and isotropic equivalent displacement parameters ($\text{\AA}^2 \times 10^3$) for C4·1.5CH₂Cl₂

	x	y	z	U_(eq)
Ru(1)	3969(1)	6792(1)	6284(1)	23(1)
P(1)	5458(1)	7479(1)	6707(1)	24(1)
P(2)	4956(1)	6061(1)	7154(1)	24(1)
Cl(1)	4929(1)	6464(1)	5462(1)	32(1)
Cl(2)	2568(1)	7482(1)	3547(1)	53(1)
C(1L)	2329(4)	6378(2)	5536(3)	34(1)
C(2L)	2571(4)	6946(3)	5250(3)	35(1)
C(3L)	2702(4)	7488(2)	5639(3)	34(1)
C(4L)	2665(4)	7500(2)	6363(3)	34(1)
C(5L)	2465(4)	6942(2)	6666(3)	31(1)
C(6L)	2285(4)	6390(2)	6254(3)	33(1)
C(7L)	2132(5)	5814(3)	5066(3)	44(1)
C(8L)	1956(6)	5225(3)	5439(4)	58(2)
C(9L)	1131(8)	5930(4)	4388(4)	82(3)
C(10L)	2735(5)	8106(3)	6756(3)	46(19)
C(1)	7278(4)	6678(2)	7136(3)	29(1)
C(2)	8139(4)	6311(2)	6993(3)	33(1)
C(3)	8462(3)	8435(3)	6366(3)	40(1)
C(4)	7961(5)	6923(3)	5916(3)	45(1)
C(5)	7131(4)	7261(3)	6043(3)	38(1)
C(6)	6758(4)	7135(2)	6649(2)	30(1)
C(7)	8687(4)	5828(3)	7456(3)	43(1)
C(8)	9491(5)	5476(3)	7294(4)	54(2)
C(9)	9818(5)	5600(3)	6685(4)	52(2)
C(10)	9321(5)	6062(3)	6236(4)	51(2)
C(1')	7072(4)	6589(2)	7852(29)	28(1)
C(2')	7952(4)	6791(2)	8481(3)	31(1)
C(3')	7862(4)	6694(2)	9179(3)	34(1)
C(4')	6911(4)	6391(3)	9243(3)	38(1)
C(5')	6073(4)	6203(2)	8644(2)	32(1)
C(6')	6134(4)	6309(2)	7935(2)	26(1)
C(7')	8937(5)	7097(3)	8431(3)	43(1)
C(8')	9761(5)	7273(3)	9036(4)	55(2)
C(9')	9649(5)	7189(4)	9726(3)	58(2)

Table 6: Final position ($\times 10^{-4}$) and isotropic equivalent displacement parameters ($\text{\AA}^2 \times 10^3$) for C4·1.5CH₂Cl₂

	<i>x</i>	<i>y</i>	<i>z</i>	<i>U_{eq}</i>
C(10')	8725(5)	6900(3)	9797(3)	50(1)
C(111)	5200(4)	8160(2)	6144(3)	30(1)
C(112)	4844(4)	8066(2)	5364(3)	33(1)
C(113)	4528(5)	8560(3)	4893(3)	41(1)
C(114)	4557(5)	9152(3)	5161(3)	48(1)
C(115)	4911(6)	9242(3)	5903(4)	55(2)
C(116)	5211(5)	8755(2)	6381(3)	42(1)
C(121)	5829(4)	7805(2)	7615(2)	30(1)
C(122)	5157(5)	7733(2)	8058(3)	35(1)
C(123)	5437(6)	8002(3)	8736(3)	46(1)
C(124)	7103(5)	8414(3)	8549(3)	49(1)
C(125)	6414(6)	8343(3)	8978(3)	54(2)
C(126)	6821(5)	8144(2)	7866(3)	38(1)
C(211)	5555(4)	5379(2)	6861(3)	29(1)
C(212)	5083(5)	5142(2)	6166(3)	42(1)
C(213)	5475(6)	4579(3)	5979(4)	54(2)
C(214)	6779(6)	4496(3)	7163(4)	57(2)
C(215)	6304(6)	4266(4)	6469(4)	59(2)
C(216)	6387(4)	5050(2)	7368(3)	39(1)
C(221)	3983(4)	5705(2)	7573(2)	28(1)
C(222)	3657(4)	5090(2)	7438(3)	34(1)
C(223)	2851(4)	4844(3)	7717(3)	43(1)
C(224)	2369(4)	5201(3)	8125(3)	45(1)
C(225)	2669(4)	5812(3)	8256(3)	39(1)
C(226)	3472(4)	6063(2)	7979(2)	31(1)
Cl(1S)	-590(3)	8784(2)	7668(2)	104(1)
Cl(2S)	-31(4)	7766(3)	6838(2)	133(2)
C(1CL)	407(13)	8366(8)	7444(9)	103(4)
Cl(3S)	103(9)	8990(5)	6514(6)	89(2)
C(2CL)	130(3)	8913(14)	7316(17)	62(7)
Cl(4S)	1572(12)	5772(7)	9887(8)	166(4)
C(3CL)	540(2)	5632(11)	9324(13)	70(6)
Cl(5S)	242(19)	4849(10)	9113(12)	298(8)

2.5.2 Synthesis

All reactions with air- or moisture-sensitive materials were carried out under Argon using standard Schlenk techniques. The solvents used for synthetic and recrystallisation purposes were of “puriss p.a” quality, purchased from *Fluka AG*, *Riedel-de-Häen* or *Merck*. Methanol was distilled from magnesium. Diethylether was distilled from sodium-benzophenone ketyl. Dichloromethane and pentane were distilled from CaH_2 . Hexane and toluene were distilled from sodium. The deuterated solvent CD_2Cl_2 was purchased from Cambridge Isotope Laboratories. It was distilled and dried over CaH_2 before use.

$[\text{Ru}(\eta^6\text{-C}_6\text{H}_6)\text{Cl}_2]_2$ ³⁶ and $[\text{Ru}(\text{Binap})(\eta^6\text{-C}_6\text{H}_6)\text{Cl}]\text{Cl}$ (**C5**)²³ were prepared according to the literature. $[\text{Ru}(\eta^6\text{-}p\text{-cymene})\text{Cl}_2]_2$ is commercially available at Aldrich, and was purified before use. (*S*)-(6,6'-Dimethoxybiphenyl-2,2'-diyl)bis(diphenylphosphine) ((*S*)-MeO-Biphep, **L1a**) and (*R*)-i-Pr-MeO-Biphep (**L1c**) were provided by F. Hoffmann-La Roche AG. Racemic-2,2'-Bis(diphenylphosphino)-1,1'-binaphthyl (Binap, **L2**) was purchased from Strem Chemicals. All the other chemicals were commercial products used as received.

The routine $^{31}\text{P}\{\text{H}\}$ - , $^{13}\text{C}\{\text{H}\}$ - and ^1H -NMR spectra were measured in CD_2Cl_2 on either a *Brucker AdvanceDPX250* [frequency in MHz: ^{31}P : 101.26, ^{13}C : 62.90, ^1H : 250.14] or *Brucker AdvanceDPX300* [frequency in MHz: ^{31}P : 121.49, ^{13}C : 75.47, ^1H : 300.13] or *Brucker AdvanceDRX400* [frequency in MHz: ^{31}P : 161.98, ^{13}C : 100.61, ^1H : 400.13] or *Brucker AdvanceDRX500* [frequency in MHz: ^{31}P : 202.46, ^{13}C : 125.75, ^1H : 500.13] at room temperature unless stated. The two-dimensional ^1H - ^1H -DQF-COSY, ^{31}P - ^1H -INV-COSY, ^{13}C - ^1H -HMQC, ^{13}C - ^1H -HMBC and ^1H -NOESY experiments were carried out at either *Brucker AdvanceDRX400* or *Brucker AdvanceDRX500*.

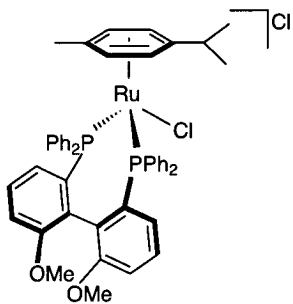
The chemical shifts δ are given in ppm and the coupling constants J are given in Hertz. The multiplicity is denoted by the following abbreviations: s: singlet; d: doublet; t: triplet; m: multiplet; dd: doublet of doublet; ddd: doublet of dd; dt: doublet of triplet; br : broad. Other abbreviations used are bb: backbone of biaryl ligand; cy: aromatic carbon of *p*-cymene ligand; cyH: aromatic proton of *p*-cymene ligand.

Elemental analysis (EA) and EI-MS and FAB-MS spectra were performed by the service of the “Laboratorium für Organische Chemie der ETH Zürich”.

Synthesis of [RuCl((S)-MeO-Biphep)(η^6 -*p*-cymene)]Cl, C1

[Ru(η^6 -*p*-cymene)Cl₂]₂ (151.7 mg, 0.25 mmol) and (*S*)-MeO-Biphep (292.3 mg, 0.50 mmol) were dissolved in 3 ml methanol and then stirred for 3h at room temperature. Then the orange solution was filtered through Celite. The solvent was evaporated i.v. to afford the orange product.

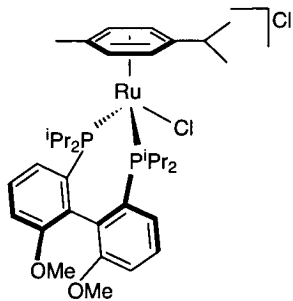
Color: orange. Yield: 410.1 mg (93%). Anal. Calcd for C₄₈H₄₂O₂P₂Cl₂Ru.3MeOH (884.78): C, 62.42; H, 5.49. Found: C, 62.44; H, 5.51. FAB-MS: Calcd: M⁺ 849.4; Found M⁺-Cl-*p*-cymene 679.7. NMR (DRX400, CD₂Cl₂): ³¹P 41.5 (d, 63), 28.3 (d, 63); ¹³C (selected), 105.2 (cy), 103.9 (cy), 97.5 (cy), 86.0 (cy), 55.5 (OCH₃), 55.3 (OCH₃), 30.4 (CH(CH₃)₂), 23.0 (CH(CH₃)₂), 21.6 (CH(CH₃)₂), 19.2 (CH₃); ¹H, 7.97 (br, 1H), 7.75 (t, 8.4, 8.0, 1H), 7.65-7.06 (14H), 7.14-7.06 (2H), 7.00 (dt, 8.6, 8.2, 2.6, 1H), 6.93 (dd, 10.7, 10.5, 1H), 6.70 (m, 1H), 6.52 (d, 6.2, 1H, cyH), 6.43 (d, 8.3, 1H), 5.97 (d, 7.0, 1H, cyH), 4.52 (br d, 6.2, 1H, cyH), 4.38 (d, 7.0, 1H, cyH), 3.45 (s, 3H, OCH₃), 3.38 (s, 3H, OCH₃), 3.09 (m, 1H, CH(CH₃)₂), 1.99 (s, 3H, CH₃), 1.39 (d, 6.9, 3H, CH(CH₃)₂), 1.04 (d, 6.9, 3H, CH(CH₃)₂).



Synthesis of [RuCl((R)-iPropyl-MeO-Biphep)(η^6 -*p*-cymene)]Cl, C2

[Ru(η^6 -*p*-cymene)Cl₂]₂ (65.3 mg, 0.11 mmol) and (*R*)-iPr-MeO-Biphep (95.5 mg, 0.22 mmol) were dissolved in 2 ml methanol and then stirred for 3h at room temperature. Then the orange solution was filtered through Celite and the solvent was evaporated i.v. to afford an orange powder. The product was then washed with 3x1 ml Et₂O and dried i.v.

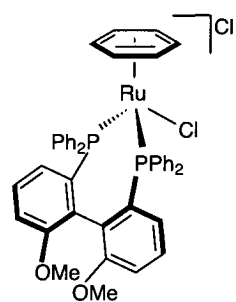
Color: orange. Yield: 130.2 mg (79%). Anal. Calcd for C₃₆H₅₄O₂P₂Cl₂Ru.2MeOH (752.74): C, 55.88; H, 7.59. Found: C, 55.88; H, 7.56. HiResMALDI-MS: Calcd M⁺: 717.3; Found: M⁺-iPr 701.2; M⁺-*p*-cymene 583.1; M⁺-*p*-cymene-Cl 545.2. NMR (DPX300, CD₂Cl₂): ³¹P 41.6 (d, 46), 34.4 (d, 46); ¹H, 7.72 (t, 9.4, 8.3, 1H), 7.62 (t, 8.7, 8.1, 2.8, 1H), 7.40 (t, 9.0, 8.1, 2.6, 1H), 7.22-6.96 (3H), 6.68 (br d, 1H, cyH), 6.06 (d, 5.8, 1H, cyH), 5.60 (br d, 1H, cyH), 3.78 (s, 3H, OCH₃), 3.75 (s, 3H, OCH₃), 2.71 (m, 1H, CH(CH₃)₂), 0.78-1.85 (34H).



Synthesis of [RuCl((S)-MeO-Biphep)(η^6 -C₆H₆)]Cl, C3]

Ru(η^6 -C₆H₆)Cl₂]₂ (122.0 mg, 0.24 mmol) and (*S*)-MeO-Biphep (286.8 mg, 0.49 mmol) were dissolved in 6 ml of a 2:1 mixture of methanol and toluene. Stirring at room temperature for 3h was followed by the filtration through Celite. The solvents were evaporated i.v. and then the yellow powder was washed with 3x1 ml Et₂O and dried i.v.

Color: yellow. Yield: 367.8 mg (90%). Anal. Calcd for C₄₄H₃₈O₂P₂Cl₂Ru

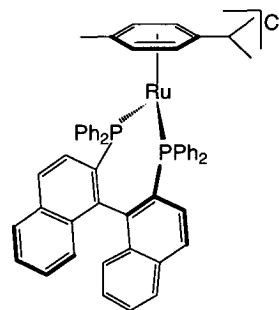


(832.75): C, 63.47; H, 4.60. Found: C, 63.04; H, 5.22. FAB-MS: Calcd M⁺ 832.8; Found M⁺-benzene 718.9; M⁺-benzene-Cl 684.0. NMR (DRX400, CD₂Cl₂): ³¹P, 39.1 (d, 64), 32.3 (d, 64); ¹³C (selected), 159.0 (bb), 158.0 (bb), 130.9 (bb), 129.6 (bb), 129.1 (bb), 127.5 (bb), 127.2 (bb), 126.6 (bb), 126.0 (bb), 125.1 (bb), 133.2 (bb), 113.0 (bb), 97.4 (C₆H₆), 55.6 (OCH₃), 55.5 (OCH₃); ¹H, 7.79-7.10 (22H), 6.95 (dt, 8.8, 8.1, 2.4, 1H), 6.71-6.82 (2H), 6.48 (d, 8.3, 1H), 5.76 (s, 6H, C₆H₆), 3.57 (s, 3H, OCH₃), 3.46 (s, 3H, OCH₃).

Synthesis of [RuCl(Binap)(η⁶-*p*-cymene)]Cl, C4

[Ru(η⁶-*p*-cymene)Cl₂]₂ (60.9 mg, 0.10 mmol) and Binap (130.0 mg, 0.21 mmol) were dissolved in 3 ml methanol and then stirred for 15h at room temperature. The solution was then heated for 8h at 40°C. The reaction mixture was filtered through Celite and then the solvent was evaporated i.v. The resulting orange powder was washed with 2x3 ml Et₂O and 1x2 ml pentane and then dried i.v.

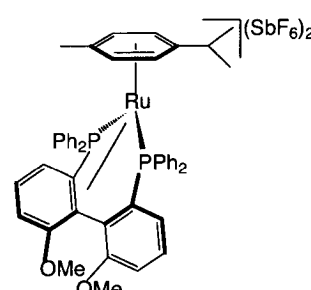
Color: orange. Yield: 62.2 mg (67%). Anal. Calcd for C₅₄H₄₆P₂Cl₂Ru·0.5CH₂Cl₂ (928.1): C, 67.39; H, 4.88. Found: C, 66.67; H, 5.67. FAB-MS: Calcd M⁺ 892.6; Found M⁺-*p*-cymene 758.5; M⁺-Cl: 857.6. NMR (CD₂Cl₂): ³¹P (DPX300), 41.5 (d, 63), 26.7 (d, 63); ¹³C (DRX400), 143.0 (d, 13), 142.9 (d, 13), 138.1, 137.7, 136.5-136.2, 135.7, 135.6, 135.3 (d, 9), 134.7-134.0, 132.0 (d, 2), 131.5 (d, 2), 131.1 (d, 3), 130.3 (d, 2), 130.0-129.8, 129.7, 128.9-128.6, 128.3, 128.1, 128.0 (d, 7), 127.7, 127.4, 126.7, 126.1, 126.0, 125.9, 125.6, 121.6, 121.1, 113.7, 113.6 (cy), 110.8 (cy), 106.0 (cy), 103.9 (cy), 97.1 (cy), 86.8 (cy), 30.6 (CH(CH₃)₂), 23.2 (CH(CH₃)₂), 21.8 (CH(CH₃)₂), 19.4 (CH₃); ¹H (DRX400), 8.10 (br t, 2H), 7.88-7.77 (3H), 7.75-7.58 (10H), 7.53-7.40 (5H), 7.38 (t, 8.5, 7.8, 1H), 7.29 (t, 8.8, 7.3, 1H), 7.21 (t, 8.4, 7.2, 1H), 7.11 (br t, 2H), 7.04-6.83 (5H), 6.50 (d, 3.7, 1H, cyH), 6.41 (d, 8.8, 1H), 6.00 (d, 6.8, 1H, cyH), 5.92 (d, 8.7, 1H), 4.42 (d, 6.8, 1H, cyH), 4.41 (d, 3.7, 1H, cyH), 3.08 (m, 1H, CH(CH₃)₂), 1.99 (s, 3H, CH₃), 1.37 (d, 6.8, 3H, CH(CH₃)₂), 1.03 (d, 6.8, 3H, CH(CH₃)₂).



Synthesis of [Ru((S)-MeO-Biphep)(η⁶-*p*-cymene)](SbF₆)₂, C6

[RuCl((S)-MeO-Biphep)(η⁶-*p*-cymene)]Cl (58.6 mg, 0.07 mmol) and AgSbF₆ (41.6 mg, 0.12 mmol) were dissolved in 1 ml dichloromethane and the resulting suspension was refluxed overnight. Then the precipitate of AgCl was filtered through Celite and the solvent was removed i.v. to afford the product.

Color: red. Yield: 68.2 mg (76%). Anal. Calcd for C₄₈H₄₆F₁₂P₂RuSb₂ (1289.4): C, 44.71; H, 3.60. Found: C, 44.97; H, 3.90. FAB-MS: Calcd M²⁺ 818.0; Found: M²⁺ 818.9; M²⁺-*p*-cymene 683.0. NMR (DRX400, CD₂Cl₂, 243 K): ³¹P, 67.1 (d, 45), 7.7 (d, 45); ¹³C (selected), 172.3 (bb), 157.0 (bb), 141.0 (bb), 134.7 (bb), 132.6 (bb), 123.4 (cy), 121.8

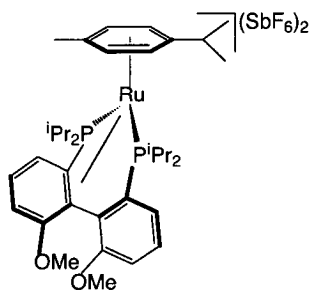


(bb), 121.4 (bb), 115.0 (bb), 108.0 (cy), 107.7 (bb), 103.8 (cy), 103.6 (cy), 100.7 (cy), 93.0 (bb), 92.5 (cy), 80.1 (bb), 57.7 (OCH₃), 56.5 (OCH₃), 29.5 (CH(CH₃)₂), 25.1 (CH(CH₃)₂), 18.6 (CH₃), 17.9 (CH(CH₃)₂); ¹H, 8.22 (t, 9.4, 8.4, 2.4, 1H), 8.10-7.22 (18H), 7.16-6.98 (2H), 6.74-6.50 (5H), 5.95 (d, 6.6, 1H, cyH), 5.57 (d, 6.2, 1H, cyH), 5.17 (d, 6.2, 1H, cyH), 4.29, (d, 6.8, 1H, cyH), 3.92 (s, 3H, OCH₃), 3.58 (s, 3H, OCH₃), 2.16 (s, 3H, CH₃), 1.77 (m, 1H, CH(CH₃)₂), 1.01 (d, 6.8, 3H, CH(CH₃)₂), 0.47 (d, 6.8, 3H, CH(CH₃)₂).

Synthesis of [Ru((R)-iPr-MeO-Biphep)(η⁶-p-cymene)](SbF₆)₂, C7

[RuCl((R)-iPr-MeO-Biphep)(η⁶-p-cymene)]Cl (39.6 mg, 0.05 mmol) and AgSbF₆ (34.1 mg 0.10 mmol) were dissolved in 1 ml dichloromethane and the resulting suspension was refluxed overnight. Then the precipitate of AgCl was removed by filtration through Celite. The evaporation of the solvent i.v. afforded the product.

Color: red. Yield: 42.5 mg (74%). Anal. Calcd for C₃₆H₅₄O₂F₁₂P₂RuSb₂ (1153.4): C, 37.49; H, 4.72. Found: C, 37.51; H, 5.32. FAB-MS: Calcd M²⁺ 681.9; Found M²⁺+SbF₆ 917.7; M²⁺ 682.1; M²⁺-p-cymene 548.0. NMR (DRX400, CD₂Cl₂): ³¹P, 82.6 (d, 39), 27.3 (d, 39); ¹³C (selected), 168.7 (d, 11, bb), 157.8 (d, 18, bb), 138.6 (d, 8, bb), 134.2 (d, 42, bb), 133.3 (d, 8, bb), 132.3 (d, 22, bb), 126.3 (cy), 124.5(bb), 122.7 (bb), 115.4 (d, 2, bb), 107.7 (d, 2, bb), 102.5 (bb), 102.4 (cy), 100.8 (cy), 98.6 (cy), 95.7 (cy), 93.0 (bb), 90.5 (cy), 79.1 (d, 21, bb), 57.0 (OCH₃), 56.0 (OCH₃), 29.1 (CH(CH₃)₂), 24.6 (CH(CH₃)₂), 19.9 (CH(CH₃)₂), 19.7 (CH₃); ¹H, 8.01 (dt, 9.1, 8.3, 1H, bb), 7.61 (2H, bb), 7.24 (d, 7.8, 1H, bb), 7.08 (t, 8.6, 7.8, 1H, bb), 6.95 (d, 8.3, 1H, bb), 6.71 (d, 6.7, 1H, cyH), 5.95 (d, 6.2, 1H, cyH), 5.75 (br, 1H, cyH), 5.06 (d, 6.2, 1H, cyH), 3.78 (s, 3H, OCH₃), 3.54 (s, 3H, OCH₃), 2.40 (s, 3H, CH₃), 2.09-0.86 (34H), 0.72 (3H), 0.31 (m, 1H).



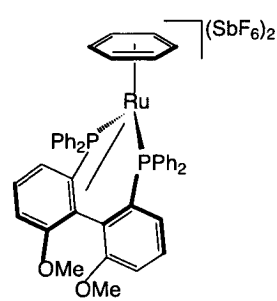
Synthesis of [Ru((S)-MeO-Biphep)(η⁶-C₆H₆)](SbF₆)₂, C8

[RuCl((S)-MeO-Biphep)(η⁶-C₆H₆)]Cl (219.8 mg, 0.26 mmol) and AgSbF₆ (179.2 mg 0.52 mmol) were dissolved in 1 ml dichloromethane and the resulting suspension was refluxed overnight. The precipitate of AgCl was filtered using Celite and the the solvent was removed i.v. to afford the product.

Color: red. Yield: 296.2 mg (92%). Anal. Calcd for C₄₄H₃₈F₁₂P₂RuSb₂ (1233.3): C, 42.85; H, 3.11. Found: C, 42.79; H, 3.61. FAB-MS: Calcd M²⁺:

761.8; Found M²⁺+SbF₆-benzene: 919.3; M²⁺ 761.4; M²⁺-benzene 688.5.

NMR (DRX500, CD₂Cl₂): ³¹P, 64.7 (d, 49), 15.4 (d, 49); ¹³C, 176.6 (bb), 157.6 (bb), 135.6 (bb), 134.2 (bb), 134.1 (bb), 134.0 (bb), 123.0 (bb), 120.9 (bb), 115.4 (bb), 107.6 (bb), 90.9 (bb), 86.0 (bb), 100.8 (C₆H₆), 58.3 (OCH₃), 56.7 (OCH₃); ¹H, 8.15 (1H, bb), 7.38 (1H, bb), 7.27 (1H, bb), 7.26 (1H, bb), 6.99 (1H, bb), 6.75 (1H, bb), 5.68 (s, C₆H₆), 4.16 (s, 3H, OCH₃), 3.78 (s, 3H, OCH₃).

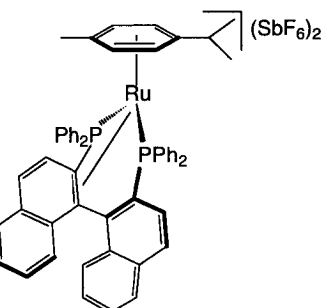


Synthesis of $[\text{Ru}(\text{Binap})(\eta^6\text{-}p\text{-cymene})](\text{SbF}_6)_2$, C9

$[\text{RuCl}(\text{Binap})(\eta^6\text{-}p\text{-cymene})]\text{Cl}$ (185.0 mg, 0.20 mmol) and AgSbF_6 (137.0 mg 0.40 mmol) were dissolved in 6 ml dichloromethane. The resulting suspension was stirred for 24h at 40°C. Then the precipitate of AgCl was filtered and the solvent was removed i.v. to afford the product.

Color: red. Yield: 216.2 mg (87%). Anal. Calcd for $\text{C}_{54}\text{H}_{46}\text{F}_{12}\text{P}_2\text{RuSb}_2\text{H}_2\text{O}$ (1242.6): C, 48.13; H, 3.59. Found: C, 48.10; H, 3.85. FAB-MS: Calcd M^{2+} 857.9; Found M^{2+} + SbF_6 1092.6;

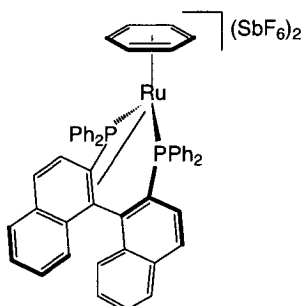
M^{2+} + SbF_6 -*p*-cymene 958.6; M^{2+} 857.9; M^{2+} -*p*-cymene 721.2. NMR (DRX400, CD_2Cl_2 , 253 K): ^{31}P , 68.7 (d, 44), 3.3 (d, 44); ^{13}C (selected), 145.3 (bb), 142.0 (bb), 138.3 (bb), 135.5 (bb), 134.0 (bb), 133.8 (bb), 133.2 (bb), 133.0 (bb), 131.7 (bb), 131.6 (bb), 130.2 (bb), 129.8 (bb), 129.7 (bb), 128.8 (bb), 128.6 (bb), 126.0 (cy), 125.4 (bb), 125.1 (bb), 124.7 (bb), 114.0 (cy), 107.6 (cy), 104.0 (cy), 104.0 (cy), 98.0 (bb), 92.0 (cy), 67.5 (bb), 29.2 ($\text{CH}(\text{CH}_3)_2$), 24.1 ($\text{CH}(\text{CH}_3)_2$), 18.3 ($\text{CH}(\text{CH}_3)_2$), 17.4 (CH_3); ^1H , 8.66 (dd, 9.5, 1.9, 1H, bb), 8.56 (dd, 9.2, 5.2, 1H, bb), 8.31 (d, 8.0, 1H, bb), 8.13-7.51 (24H), 7.44 (t, 8.7, 7.6, 1H, bb), 7.34 (t, 9.6, 8.6, 1H, bb), 7.22 (t, 9.1, 7.7, 1H, bb), 6.74 (t, 8.9, 7.5, 1H, bb), 6.27 (d, 6.8, 1H, cyH), 5.79 (d, 6.1, 1H, cyH), 5.59 (br, 1H, cyH), 5.56 (d, 8.8, 1H, bb), 4.55 (d, 6.7, 1H, cyH), 1.78 (s, 3H, CH_3), 0.71 (d, 6.4, 3H, $\text{CH}(\text{CH}_3)_2$), 0.02 (m, 1H, $\text{CH}(\text{CH}_3)_2$), 0.00 (br, 3H, $\text{CH}(\text{CH}_3)_2$).



Synthesis of $[\text{Ru}(\text{Binap})(\eta^6\text{-C}_6\text{H}_6)](\text{SbF}_6)_2$, C10

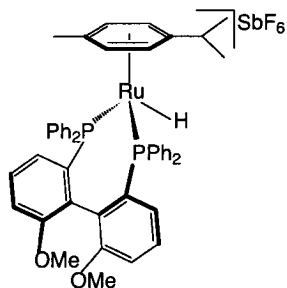
$[\text{RuCl}(\text{Binap})(\eta^6\text{-C}_6\text{H}_6)]\text{Cl}$ (226.9 mg, 0.26 mmol) and AgSbF_6 (178.4 mg 0.52 mmol) were dissolved in 2 ml dichloromethane and the resulting suspension was refluxed overnight. Then the precipitate of AgCl was filtered using Celite and then the solvent was removed i.v. to afford the product.

Color: red. Yield: 285.6 mg (86%). Anal. Calcd for $\text{C}_{50}\text{H}_{38}\text{F}_{12}\text{P}_2\text{RuSb}_2$ (1273.4): C, 47.16; H, 3.01. Found: C, 47.06; H, 3.12. FAB-MS: Calcd M^{2+} 801.9; Found M^{2+} + SbF_6 1036.3; M^{2+} + SbF_6 -benzene 958.2; M^{2+} 801.4; M^{2+} -benzene 730.4. NMR (DPX300, CD_2Cl_2): ^{31}P , 64.0 (d, 46), 19.0 (d, 46); ^{13}C (selected), 146.8 (d, 26, bb), 144.9 (d, 9, bb), 138.3 (d, 8, bb), 136.1 (bb), 133.8 (bb), 133.6 (bb), 133.6 (bb), 133.4 (bb), 131.2 (bb), 130.0 (bb), 129.3 (bb), 126.8 (d, 6, bb), 126.1 (bb), 125.2 (bb), 103.1 (C_6H_6), 101.7 (bb), 73.0 (bb); ^1H , 8.45 (d, 9.4, 1H, bb), 8.23 (d, 8.4, 1H, bb), 8.13-8.06 (2H), 7.97-7.55 (20H), 7.41 (2H, bb), 6.87 (t, 7.9, 7.5, 1H), 6.16 (m, 2H), 5.94 (d, 8.8, 1H, bb), 5.84 (2H), 5.72 (s, C_6H_6).



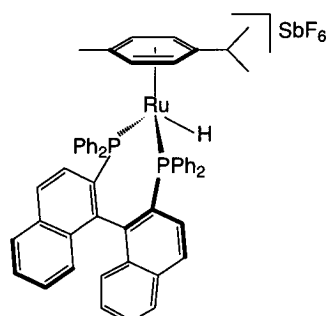
Synthesis of [RuH((S)-MeO-Biphep)(η^6 -*p*-cymene)]SbF₆, C11

[RuCl((*S*)-MeO-Biphep)(η^6 -*p*-cymene)]Cl (156.3 mg, 0.18 mmol) and AgSbF₆ (120.4, 0.35 mmol) were dissolved in 1 ml dichloromethane. The resulting suspension was refluxed overnight. The precipitate of AgCl was filtered using Celite and the solvent was evaporated i.v. 5 ml methanol was added to the remaining powder. The color changed from red to yellow. A ³¹P-NMR spectrum of the sample recorded within 5 minutes, showed complete conversion. The solution was concentrated to 1 ml methanol during which time the yellow product precipitated. After 1h the orange solution was removed by use of a syringe and then the remaining powder was washed with 2x3 ml methanol. The yellow product was dried i.v. Color: yellow. Yield: 158.2 mg (83%). Anal. Calcd for C₄₈H₄₆O₂F₆P₂RuSb₂.MeOH (1053.7): C, 54.26; H, 4.52. Found: C, 54.21; H, 4.66. FAB-MS: Calcd M⁺ 818.0; Found M⁺+SbF₆ 1053.3; M⁺+SbF₆-*p*-cymene 902.2; M⁺ 817.4; M⁺-*p*-cymene-H 683.0. NMR (DRX400, CD₂Cl₂): ³¹P, 51.0 (d, 46), 50.4 (d, 46); ¹³C (selected), 157.3 (bb), 157.0 (bb), 137.2 (bb), 134.2 (bb), 127.0 (bb), 125.7 (bb), 121.0 (bb), 199.2 (bb), 115.7 (cy), 112.4 (cy), 111.2 (bb), 110.6 (bb), 97.8 (cy), 97.5 (cy), 96.3 (cy), 91.5 (cy), 54.7 (OCH₃), 54.6 (OCH₃), 32.2 (CH(CH₃)₂), 23.5 (CH(CH₃)₂), 23.2 (CH(CH₃)₂), 20.4 (CH₃); ¹H, 8.07-6.87 (26H), 7.40 (bb, 1H), 7.12 (1H, bb), 7.07 (1H, bb), 7.03 (1H, bb), 6.30 (d, 5.5, 1H, bb), 6.27 (d, 5.5, 1H, bb), 6.00 (d, 6.6, 1H, cyH), 5.74 (d, 6.6, 1H, cyH), 4.05 (d, 6.6, 1H, cyH), 3.74 (d, 6.6, 1H, cyH), 3.26 (s, 3H, OCH₃), 3.19 (s, 3H, OCH₃), 2.44 (m, 1H, CH(CH₃)₂), 2.12 (s, 3H, CH₃), 1.26 (d, 7.0, 3H, CH(CH₃)₂), 0.92 (d, 7.0, 3H, CH(CH₃)₂), -10.10 (q, 39.7, 31.6, 1H, RuH).



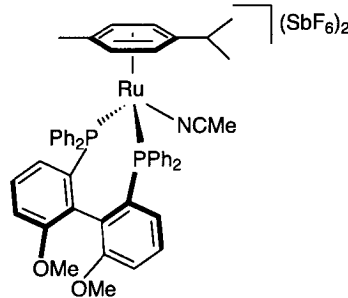
Synthesis of [RuH(Binap)(η^6 -*p*-cymene)]SbF₆, C12

[Ru(Binap)(η^6 -*p*-cymene)](SbF₆)₂ (74.4 mg, 0.06 mmol) was dissolved in 2 ml methanol. The resulting orange solution was then stirred at room temperature. After 15 minutes the yellow product began to precipitate. The suspension was stirred for another 2h after which the orange solution was removed using a syringe. The remaining powder was washed with 2x1 ml methanol. The resulting yellow product was dried i.v. Color: yellow. Yield: 48.4 mg (71%). Anal. Calcd for C₅₄H₄₇F₁₂P₂RuSb₂.H₂O (1132.8): C, 58.28; H, 4.40. Found: C, 57.92; H, 4.80. FAB-MS: Calcd M⁺ 858.5; Found M⁺ 858.4; M⁺-*p*-cymene 722.8. NMR (DRX400, CD₂Cl₂): ³¹P, 52.8 (d, 47), 52.0 (d, 47); ¹³C (selected), 116.8 (br d, cy), 113.0 (cy), 98.3 (cy), 97.3 (d, 5, cy), 96.5 (d, 6, cy), 91.7 (d, 5, cy), 32.3 (CH(CH₃)₂), 23.8 (CH(CH₃)₂), 23.4 (CH(CH₃)₂), 20.5 (CH₃); ¹H, 8.13 (t, 10.2, 8.6, 1H), 7.86 (t, 10.6, 8.9, 1H), 7.77 (d, 8.5, 1H), 7.70 (t, 10.8, 7.9, 1H), 7.66-7.50 (12H), 7.38-7.28 (3H), 7.24 (t, 9.3, 7.5, 1H), 6.92-6.54 (10H), 6.12 (dd, 13.0, 12.4, 2H), 5.97 (d, 5.8, 1H, cyH), 5.71 (d, 5.8, 1H, cyH), 4.08 (d, 5.8, 1H, cyH), 3.84 (d, 5.8, 1H, cyH), 2.41 (m, 1H, CH(CH₃)₂), 2.10 (s, 3H, CH₃), 1.23 (d, 6.6, 3H, CH(CH₃)₂), 0.93 (d, 6.6, 3H, CH(CH₃)₂), -9.79 (q, 40.6, 29.2, 1H, RuH).



Synthesis of [Ru(NCMe)((S)-MeO-Biphep)(η^6 -*p*-cymene)](SbF₆)₂, C13

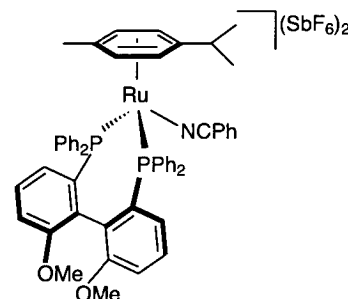
[RuCl((*S*)-MeO-Biphep)(η^6 -*p*-cymene)]Cl (32.1 mg, 0.035 mmol) and AgSbF₆ (24.9, 0.072 mmol) were dissolved in 1 ml dichloromethane. The resulting suspension was refluxed overnight. The precipitate of AgCl was filtrated using Celite. Acetonitrile (6 μ l, 0.11 mmol) was added to the remaining red solution. After the color change from red to yellow, the solvent was evaporated i.v. The remaining powder was washed with 3x1 ml Et₂O and was dried i.v. Color: yellow. Yield: 42.6 mg (92%). Anal. Calcd for C₅₇H₅₁F₁₂NO₂P₂RuSb₂ (1330.4): C, 45.14; H, 3.71; N, 1.05. Found: C, 45.13; H, 3.88; N, 0.94. FAB-MS: Calcd M²⁺ 859.0; Found M²⁺+SbF₆ 1096.1; M²⁺-acetonitrile 818.2. NMR (DPX500, CD₂Cl₂): ³¹P, 43.7 (d, 51), 28.9 (d, 51); ¹³C, 159.9 (d, 13, bb), 158.1 (d, 14, bb), 132.1(CH₃CN), 130.4 (bb), 129.9 (bb), 129.5 (bb), 129.5 (bb), 126.0 (bb), 125.9 (bb), 125.8 (d, 4, bb), 123.9 (d, 7, bb), 117.8 (d, 7, cy), 117.2 (cy), 114.4 (d, 3, bb), 114.0 (d, 3, bb), 108.3 (cy), 101.4 (cy), 101.3 (d, 8, cy), 85.6 (cy), 56.0 (OCH₃), 55.6 (OCH₃), 31.7 (CH(CH₃)₂), 22.6 (CH(CH₃)₂), 22.4 (CH(CH₃)₂), 19.2 (CH₃), 4.7 (CH₃CN); ¹H, 7.91-7.27 (20H), 7.18 (dd, 10.8, 8.1, 1H, bb), 7.08 (dt, 8.6, 8.3, 2.8, 1H, bb), 6.91-6.80 (4H), 6.55 (d, 8.6, 1H, bb), 5.97 (d, 6.4, 1H, cyH), 4.88 (d, 7.0, 1H, cyH), 4.78 (br d, 6.2, 1H, cyH), 3.60 (s, 3H, OCH₃), 3.46 (s, 3H, OCH₃), 3.03 (m, 1H, CH(CH₃)₂), 1.87 (s, 3H, CH₃), 1.72 (s, 3H, CH₃CN), 1.48 (d, 6.8, 3H, CH(CH₃)₂), 1.09 (d, 6.8, 3H, CH(CH₃)₂).



Synthesis of [Ru(NCPh)((S)-MeO-Biphep)(η^6 -*p*-cymene)](SbF₆)₂, C14

[RuCl((*S*)-MeO-Biphep)(η^6 -*p*-cymene)]Cl (67.8 mg, 0.08 mmol) and AgSbF₆ (52.2, 0.15 mmol) were dissolved in 1 ml dichloromethane and the resulting suspension was refluxed overnight. The precipitate of AgCl was filtrated using Celite. Benzonitril (20 μ l, 0.19 mmol) was added to the remaining red solution. The color change from red to yellow and then the solvent was evaporated i.v. The remaining yellow powder was washed with 5x1 ml Et₂O and then dried i.v.

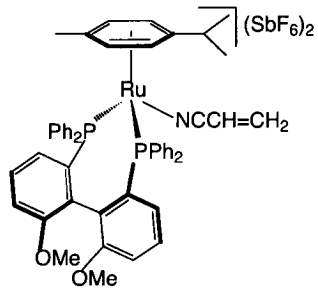
Color: yellow. Yield: 109.2 mg (98%). Anal. Calcd for C₅₅H₅₁F₁₂NO₂P₂RuSb₂ (1392.5): C, 47.44; H, 3.69; N, 1.01. Found: C, 47.56; H, 3.81; N, 1.15. FAB-MS: Calcd M²⁺ 921.0; Found M²⁺+SbF₆ 1158.1; M²⁺-benzonitrile 818.2. NMR (DRX400, CD₂Cl₂): ³¹P, 43.7 (d, 51), 28.8 (d, 51); ¹³C (selected), 159.8 (d, 13, bb), 158.2 (d, 14, bb), 130.2 (bb), 129.8 (bb), 128.9 (bb), 126.1 (bb), 125.8 (bb), 125.1 (bb), 123.7 (bb), 118.4 (cy), 117.9 (d, 7, cy), 114.6 (d, 3, bb), 114.3 (d, 3, bb), 109.4 (cy), 102.3 (cy), 101.3 (d, 8, cy), 85.6 (cy), 56.0 (OCH₃), 55.5 (OCH₃), 32.1(C(CH₃)₂), 23.5 (C(CH₃)₂), 21.3 (C(CH₃)₂), 19.1 (CH₃); ¹H, 7.90-7.24 (23H), 7.08 (2H, bb and cyH), 6.96 (ddd, 11.0, 7.5, 1.4, 1H, bb), 6.84 (ddd, 12.0, 8.2, 0.9, 1H, bb), 6.69-6.52 (5H), 6.01 (d, 6.4, 1H, cyH), 5.12 (d, 7.3, 1H, cyH), 4.80 (br d, 6.4, 1H, cyH), 3.60 (s, 3H, OCH₃), 3.46 (s, 3H, OCH₃), 3.02 (m, 1H, CH(CH₃)₂), 1.89 (s,



3H, CH_3), 1.51 (d, 6.8, 3H, $CH(CH_3)_2$), 1.12 (d, 7.0, 3H, $CH(CH_3)_2$).

Synthesis of $[Ru(NCCH=CH_2)((S)\text{-MeO-Biphep})(\eta^6\text{-}p\text{-cymene})](SbF_6)_2$, C15

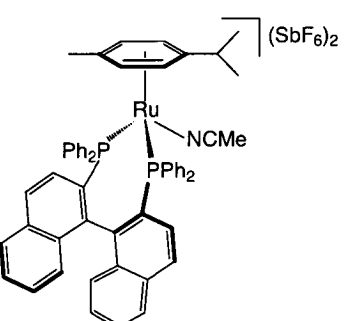
$[RuCl((S)\text{-MeO-Biphep})(\eta^6\text{-}p\text{-cymene})]Cl$ (46.7 mg, 0.05 mmol) and $AgSbF_6$ (35.4, 0.10 mmol) were dissolved in 1 ml dichloromethane. The resulting suspension was refluxed overnight. The precipitate of $AgCl$ was filtrated using Celite. Acrylonitrile (3 μl , 0.08 mmol) was added to the remaining red solution. After the color changed from red to yellow, the solvent was evaporated i.v. The remaining powder was washed with 5x1 ml Et_2O and was dried i.v.



Color: yellow. Yield: 65.4 mg (97%). Anal. Calcd for $C_{51}H_{49}F_{12}NO_2P_2RuSb_2\cdot H_2O$ (1342.5): C, 44.99; H, 3.75; N, 1.03. Found: C, 44.94; H, 3.99; N, 0.94. FAB-MS: Calcd M^{2+} 871.0; Found $M^{2+}\text{+}SbF_6$ 1106.2; M^{2+} -acrylonitrile 818.0. NMR (DPX400, CD_2Cl_2): ^{31}P , 43.8 (d, 50), 28.6 (d, 50); ^{13}C , 160.0 (bb), 158.3 (bb), 143.9 (CH_2CHCN), 130.4 (bb), 130.3 (bb), 130.1 (CH_2CHCN), 129.1 (bb), 126.0 (bb), 125.9 (bb), 125.9 (bb), 125.5 (bb), 123.8 (bb), 118.0 (cy), 117.8 (cy), 114.5 (bb), 144.1 (bb), 109.1 (cy), 106.1 (CH_2CHCN), 102.3 (cy), 101.6 (cy), 85.8 (cy), 56.0 (OCH_3), 55.3 (OCH_3), 32.1 ($CH(CH_3)_2$), 23.2 ($CH(CH_3)_2$), 22.1 ($CH(CH_3)_2$), 19.3 (CH_3); 1H , 7.87-7.24 (20H), 7.19 (dt, 8.3, 8.1, 3.3, 1H, bb), 7.10 (ddd, 10.4, 7.9, 1.1, 1H, bb), 7.07 (td, 8.6, 8.3, 2.8, 1H, bb), 6.94 (d, 7.2, cyH), 6.82 (ddd, 11.9, 8.3, 0.9, 1H, bb), 6.78 (d, 8.4, 1H, bb), 6.54 (d, 8.4, 1H, bb), 6.00 (d, 6.4, 1H, cyH), 5.98 (d, 12, 1H, CH_2CHCN), 5.50 (dd, 17.8, 12.0, 1H, CH_2CHCN), 5.01 (d, 12.0, 1H, CH_2CHCN), 4.95 (d, 7.2, 1H, cyH), 4.77 (d, 6.4, 1H, cyH), 3.58 (s, 3H, OCH_3), 3.46 (s, 3H, OCH_3), 3.00 (m, 1H, $CH(CH_3)_2$), 1.86 (s, 3H, CH_3), 1.49 (d, 6.9, 3H, $CH(CH_3)_2$), 1.10 (d, 6.9, 3H, $CH(CH_3)_2$).

Synthesis of $[Ru(NCEt)(Binap)(\eta^6\text{-}p\text{-cymene})](SbF_6)_2$, C16

Propionitrile (1.7 μl , 0.02 mmol) was added to a solution of $[Ru(Binap)(\eta^6\text{-}p\text{-cymene})](SbF_6)_2$ (31.5 mg, 0.02 mmol) in 1 ml dichloromethane. After the immediate color change from orange to yellow, the solvent was evaporated i.v. The remaining yellow product was dried i.v.



Color: yellow. Yield: 27.7 mg (99%). Anal. Calcd for $C_{57}H_{51}F_{12}NP_2RuSb_2$ (1384.6): C, 49.45; H, 3.71; N, 1.01. Found: C, 49.46; H, 3.91; N, 1.07. FAB-MS: Calcd M^{2+} : 913.1; Found $M^{2+}\text{+}SbF_6$: 1147.5; M^{2+} -propionitrile: 857.7. NMR (DRX300, CD_2Cl_2): ^{31}P , 44.2 (d, 51), 29.4 (d, 51); ^{13}C (selected), 135.5 (CH_3CH_2CN), 118.0 (cy), 118.0 (cy), 108.5 (cy), 102.3 (cy), 100.8 (cy), 86.2 (cy), 31.9 ($CH(CH_3)_2$), 23.1 ($CH(CH_3)_2$), 22.2 ($CH(CH_3)_2$), 19.1 (CH_3), 14.1 (CH_3CH_2CN), 8.4 (CH_3CH_2CN); 1H , 7.96 (dd, 8.9, 1.8, 1H), 7.88 (t, 9.9, 9.3, 2H), 7.83-7.76 (4H), 7.69 (t, 9.5, 8.3, 2H), 7.53-7.40 (4H), 7.38-7.27 (4H), 7.16 (dt, 9.1, 7.9, 1.3, 1H), 7.09-7.02 (2H), 6.87 (d, 6.8, 1H, cyH), 6.87 (d, 6.8, 1H, cyH),

6.64 (d, 8.7, 1H), 5.86 (d, 6.4, 1H, cyH), 5.59 (d, 8.8, 1H), 5.06 (d, 6.8, 1H, cyH), 4.66 (d, 6.4, 1H, cyH), 3.00 (m, 1H, CH(CH₃)₂), 2.52 (m, 1H, CH₃CH₂CN), 1.86 (m, 1H, CH₃CH₂CN), 1.84 (s, 3H, CH₃), 1.49 (d, 6.8, 3H, CH(CH₃)₂), 1.10 (d, 6.8, 3H, CH(CH₃)₂), 0.38 (t, 3H, CH₃CH₂CN).

Synthesis of [Ru(NCPh)(Binap)(η⁶-*p*-cymene)](SbF₆)₂, C17

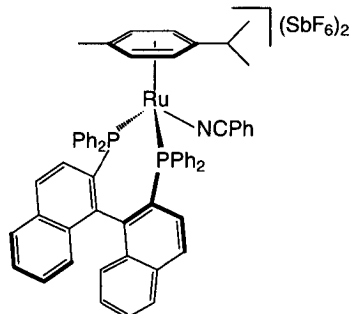
Benzonitrile (3.3 μl, 0.03 mmol) was added to a solution of [Ru(Binap)(η⁶-*p*-cymene)](SbF₆)₂ (39.1 mg, 0.03 mmol) in 1 ml dichloromethane. After an immediate color change from orange to yellow, the solvent was evaporated. The remaining yellow powder was washed with 4x3 ml Et₂O and dried i.v.

Color: yellow. Yield: 34.8 mg (81%). Anal. Calcd for

C₆₁H₅₁F₁₂NP₂RuSb₂H₂O (1432.6): C, 50.50; H, 3.68; N, 0.97.

Found: C, 50.48; H, 3.78; N, 1.09. FAB-MS: Calcd M²⁺ 961.2;

Found M²⁺+SbF₆ 1196.0; M²⁺-benzonitrile 858.1. NMR (DRX400, CD₂Cl₂): ³¹P, 44.5 (d, 51), 29.9 (d, 51); ¹³C (selected), 118.7 (cy), 118.3 (cy), 109.2 (cy), 102.6 (cy), 101.3 (cy), 86.4 (cy), 32.3 (CH(CH₃)₂), 23.7 (CH(CH₃)₂), 21.6 (CH(CH₃)₂), 19.2 (CH₃); ¹H, 8.11-6.90 (35H), 6.67 (d, 8.2, 1H), 6.09 (d, 6.1, 2H), 5.94 (d, 7.0, 2H, 1H = cyH), 5.18 (d, 6.1, 1H, cyH), 4.69 (d, 7.0, 1H, cyH), 3.01 (m, 1H, CH(CH₃)₂), 1.86 (s, 3H, CH₃), 1.48 (d, 6.0, 3H, CH(CH₃)₂), 1.10 (d, 6.0, 3H, CH(CH₃)₂).



Synthesis of [Ru(NCCH=CH₂)(Binap)(η⁶-*p*-cymene)](SbF₆)₂, C18

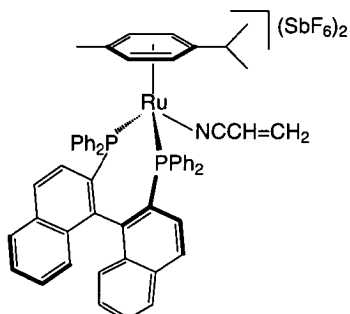
Acrylonitrile (1.6 μl, 0.02 mmol) was added to a solution of [Ru(Binap)(η⁶-*p*-cymene)](SbF₆)₂ (28.3 mg, 0.02 mmol) in 1.5 ml dichloromethane solution. After the immediate color change from orange to yellow, the solvent was evaporated i.v. The yellow remaining powder was washed with 2x3 ml Et₂O and then dried i.v.

Color: yellow. Yield: 15.2 mg (55%). Anal. Calcd for

C₅₇H₄₉F₁₂NP₂RuSb₂ (1382.6): C, 49.52; H, 3.57; N, 1.01. Found: C,

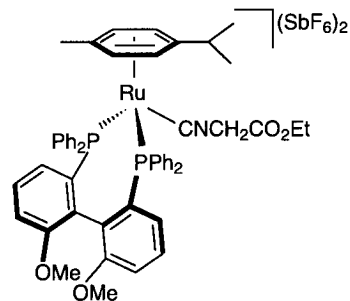
49.38; H, 3.71; N, 1.04. FAB-MS: Calcd M²⁺ 911.1; Found

M²⁺+SbF₆ 1148.1; M²⁺-acrylonitrile 858.1. NMR (DPX400, CD₂Cl₂): ³¹P, 44.3 (d, 50), 29.5 (d, 50); ¹³C (selected), 143.6 (CH₂CHCN), 129.6 (CH₂CHCN), 117.6 (cy), 117.6 (cy), 108.7 (cy), 106.2 (CH₂CHCN), 102.4 (cy), 101.4 (cy), 86.6 (cy), 31.9 (CH(CH₃)₂), 23.0 (CH(CH₃)₂), 22.1 (CH(CH₃)₂), 19.2 (CH₃); ¹H, 7.91-7.64 (10H), 7.56-7.24 ((H), 7.15 (t, 9.2, 7.9, 1H), 7.07 (t, 9.6, 7.6, 2H), 6.95 (d, 6.8, 1H, cyH), 6.63 (d, 8.7, 1H), 5.99 (d, 8.7, 1H), 5.92 (d, 5.9, 1H, cyH), 5.66 (d, 3, 15, 1H, CH₂CHCN), 5.60 (d, 3, 1H, CH₂CHCN), 5.04 (d, 6.8, 1H, cyH), 4.68 (d, 5.9, 1H, cyH), 3.75 (dd, 3, 15, 1H, CH₂CHCN), 3.01 (m, 1H, CH(CH₃)₂), 1.84 (s, 3H, CH₃), 1.47 (d, 6.8, 3H, CH(CH₃)₂), 1.08 (d, 6.8, 3H, CH(CH₃)₂).



Synthesis of [Ru(CNCH₂CO₂Et)((S)-MeO-Biphep)(η⁶-*p*-cymene)](SbF₆)₂, C19

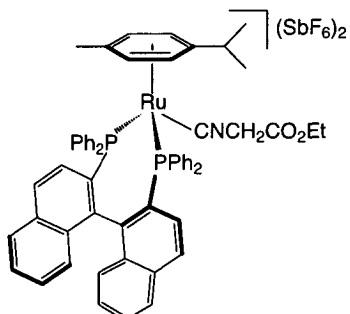
[RuCl((S)-MeO-Biphep)(η⁶-*p*-cymene)]Cl (35.0 mg, 0.04 mmol) and AgSbF₆ (25.3, 0.08 mmol) were dissolved in 1 ml dichloromethane. The resulting suspension was refluxed overnight. The precipitate of AgCl was filtrated using Celite. Ethyl isocyanoacetate (7 μl, 0.06 mmol) was added to the remaining red solution. An immediate color change from red to yellow occurred after which the solvent was evaporated. The remaining powder was washed with 3x1 ml Et₂O and 3x1 ml pentane. The yellow product was dried i.v.



Color: yellow. Yield: 54.1 mg (95%). Anal. Calcd for C₅₃H₅₃F₁₂NO₂P₂RuSb₂ (1402.50): C, 45.39; H, 3.81; N, 1.00. Found: C, 45.11; H, 4.05; N, 1.10. FAB-MS: Calcd M²⁺ 931.0; Found M²⁺+SbF₆ 1165.9. NMR (DRX300, CD₂Cl₂): ³¹P, 44.8 (d, 40), 28.5 (d, 40); ¹³C (selected), 163.7 (CNCH₂CO₂CH₂CH₃), 159.8 (bb), 158.2 (bb), 144.2 (CNCH₂CO₂CH₂CH₃), 131.7 (bb), 130.4 (bb), 129.4 (bb), 129.3 (bb), 126.4 (bb), 125.8 (bb), 125.4 (cy), 125.2 (bb), 122.9 (bb), 122.8 (cy), 114.5 (bb), 114.3 (bb), 111.3 (cy), 103.9 (cy), 102.0 (cy), 98.1 (cy), 63.9 (CNCH₂CO₂CH₂CH₃), 55.8 (OCH₃), 55.6 (OCH₃), 47.1 (CNCH₂CO₂CH₂CH₃), 31.2 (CH(CH₃)₂), 24.1 (CH(CH₃)₂), 20.6 (CH(CH₃)₂), 19.6 (CH₃), 14.1 (CNCH₂CO₂CH₂CH₃); ¹H, 7.87-7.34 (20H), 7.30 (dt, 8.6, 8.2, 3.3, 1H, bb), 7.20-7.05 (3H), 6.92-6.80 (3H), 6.55 (d, 8.4, 1H, bb), 4.87 (d, 6.8, 1H, cyH), 4.68 (d, 7.0, 1H, cyH), 4.45 (m, 2H, CNCH₂CO₂CH₂CH₃), 4.12 (d, 18.9, 1H, CNCH₂CO₂CH₂CH₃), 3.56 (d, 18.9, 1H, CNCH₂CO₂CH₂CH₃), 3.55 (s, 3H, OCH₃), 3.46 (s, 3H, OCH₃), 3.32 (m, 1H, CH(CH₃)₂), 2.00 (s, 3H, CH₃), 1.41 (d, 6.8, 3H, CH(CH₃)₂), 1.40 (t, 3H, CNCH₂CO₂CH₂CH₃), 0.97 (d, 6.8, 3H, CH(CH₃)₂).

Synthesis of [Ru(CNCH₂CO₂Et)(Binap)(η⁶-*p*-cymene)](SbF₆)₂, C20

Ethyl isocyanoacetate (4.5 μl, 0.04 mmol) was added to a solution of [Ru(Binap)(η⁶-*p*-cymene)](SbF₆)₂ (50.3 mg, 0.04 mmol) in 1 ml dichloromethane. An immediate color change from orange to yellow occurred. ³¹P-NMR recorded within 5 minutes after adding the isocyanoacetate, showed complete conversion of the starting material to the product. The solvent was evaporated i.v. and then the remaining powder was washed with 2x3 ml Et₂O. The yellow product was dried i.v.

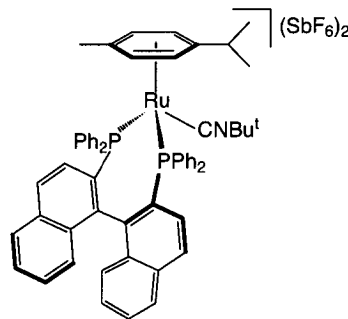


Color: yellow. Anal. Calcd for C₅₉H₅₃F₁₂NO₂P₂RuSb₂ (1442.6): C, 49.12; H, 3.70; N, 0.97. Found: C, 48.39; H, 4.14; N, 1.27. FAB-MS: Calcd M²⁺ 971.1; Found M²⁺ +SbF₆ 1207.9; M²⁺-*p*-cymene 836.9. NMR (DRX300, CD₂Cl₂): ³¹P, 46.0 (d, 40), 29.8 (d, 40); ¹³C (selected), 163.7 (CNCH₂CO₂CH₂CH₃), 142.8 (CNCH₂CO₂CH₂CH₃), 125.7 (cy), 123.2 (cy), 111.2 (cy), 103.7 (cy), 102.7 (cy), 98.6 (cy), 64.3 (CNCH₂CO₂CH₂CH₃), 47.3 (CNCH₂CO₂CH₂CH₃), 31.2 (CH(CH₃)₂), 24.4 (CH(CH₃)₂), 20.5 (CH(CH₃)₂), 19.6 (CH₃), 14.1 (CNCH₂CO₂CH₂CH₃); ¹H, 8.01-7.02 (31H), 6.80 (d, 6.6, 1H, cyH), 6.60

(d, 8.9, 1H), 6.00 (d, 8.9, 1H), 4.77 (d, 6.6, 1H, cyH), 4.75 (d, 6.0, 1H, cyH), 4.41 (m, 2H, CNCH₂CO₂CH₂CH₃), 4.24 (d, 19, 2H, CNCH₂CO₂CH₂CH₃), 3.37 (m, 1H, CH(CH₃)₂), 3.23 (d, 19, 2H, CNCH₂CO₂CH₂CH₃), 1.95 (s, 3H, CH₃), 1.42 (t, 3H, CNCH₂CO₂CH₂CH₃), 1.37 (d, 6.8, 3H, CH(CH₃)₂), 0.94 (d, 6.8, 3H, CH(CH₃)₂).

Synthesis of [Ru(CNBu^t)(Binap)(η⁶-*p*-cymene)](SbF₆)₂, C21

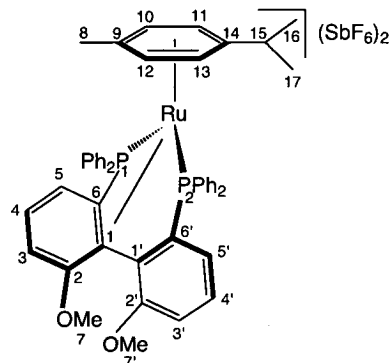
Tert-butyl isocyanide (4.2 μl, 0.04 mmol) was added to a solution of [Ru(Binap)(η⁶-*p*-cymene)](SbF₆)₂ (50.0 mg, 0.04 mmol) in 1 ml dichloromethane. A color change from orange to yellow occurred immediately. A ³¹P-NMR recorded within 5 minutes after adding the tert-butyl isocyanide, showed complete conversion of the starting material to the product. The solvent was evaporated i.v. and then the remaining powder was washed with 3x3 ml Et₂O and 1x2 ml pentane. As ¹H-NMR indicated still free tert-butyl isocyanide, the powder was washed another time with 2x3 ml Et₂O. The yellow product was dried i.v.



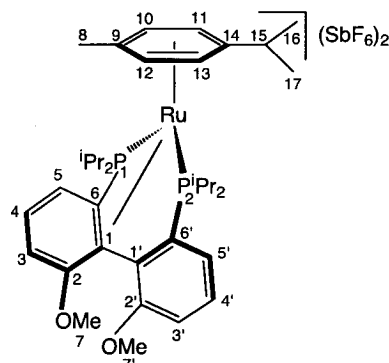
Color: yellow. Anal. Calcd for C₅₉H₅₅F₁₂NP₂RuSb₂ (1412.6): C, 50.17; H, 3.92; N, 0.99. Found: C, 49.93; H, 4.01; N, 1.12. FAB-MS: Calcd M²⁺ 941.1; Found M²⁺+SbF₆ 1176.2; M²⁺-p-cymene 807.1. NMR (DPX400, CD₂Cl₂): ³¹P, 46.3 (d, 42), 30.0 (d, 42); ¹³C, 126.2 (cy), 120.8 (cy), 113.3 (cy), 103.2 (cy), 102.6 (cy), 97.5 (cy), 62.5 (NC(CH₃)₃), 32.0 (CH(CH₃)₂), 29.1 (NC(CH₃)₃), 23.3 (CH(CH₃)₂), 21.8 (CH(CH₃)₂), 19.6 (CH₃); ¹H, 8.07-6.90 (31H), 6.76 (d, 5.8, 1H, cyH), 6.66 (d, 8.7, 1H), 5.78 (d, 8.7, 1H), 4.84 (d, 6.7, 1H, cyH), 4.68 (d, 5.8, 1H, cyH), 2.94 (m, 1H, CH(CH₃)₂), 1.89 (s, 3H, CH₃), 1.48 (d, 6.8, 3H, CH(CH₃)₂), 1.06 (s, 3H, NC(CH₃)₃), 1.03 (d, 6.8, 3H, CH(CH₃)₂).

2.5.3 Selected NMR-data

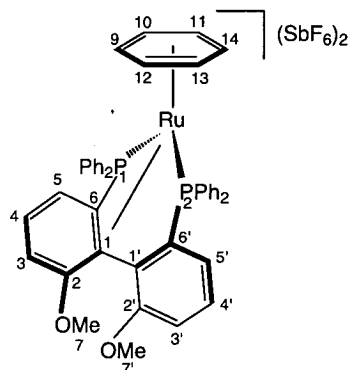
Table 7: Selected NMR-data [Ru((S)-MeO-Biphep)(η^6 -*p*-cymene)](SbF_6)₂, C6



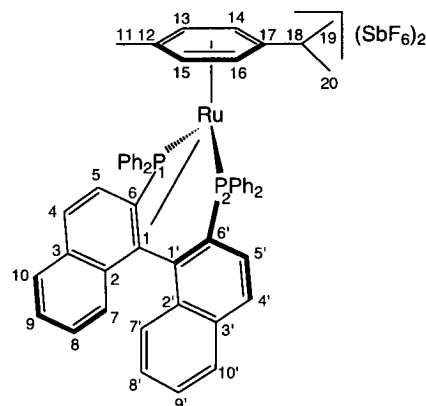
position			position		
	$\delta^{31}\text{P}$				
1	7.7				
2	67.1				
	$\delta^{1}\text{H}$	$\delta^{13}\text{C}$		$\delta^{1}\text{H}$	$\delta^{13}\text{C}$
1	-	93.0	1'	-	
2	-	172.3	2'	-	157.0
3	7.36	107.7	3'	6.56	115.0
4	8.23	141.0	4'	7.04	132.6
5	7.88	121.4	5'	6.57	121.8
6	-	80.1	6'	-	134.7
7	3.92	57.7	7'	3.58	56.5
8	2.16	18.6	13	5.17	100.7
9	-	108.0	14	-	123.4
10	5.57	92.5	15	1.77	29.5
11	4.29	103.6	16	1.01	25.1
12	5.95	103.8	17	0.47	17.9

Table 8: Selected NMR-data [Ru((R)-iPropyl-MeO-Biphep)(η⁶-p-cymene)](SbF₆)₂, C7

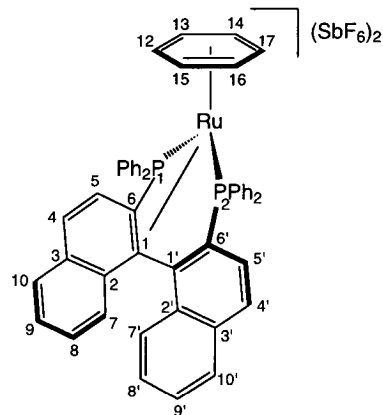
position			position		
	δ ³¹ P				
1	27.3				
2	82.6				
	δ ¹ H	δ ¹³ C		δ ¹ H	δ ¹³ C
1	-	102.5	1'	-	132.3
2	-	168.7	2'	-	157.8
3	7.24	107.7	3'	6.95	115.4
4	8.01	138.6	4'	7.61	133.3
5	7.61	124.5	5'	7.08	122.7
6	-	79.1	6'	-	134.2
7	3.78	57.0	7'	3.54	56.0
8	2.40	19.7	13	5.06	98.6
9	-	100.8	14	-	126.3
10	5.57	95.7	15	1.79	29.1
11	5.95	90.5	16	1.08	24.6
12	6.71	102.4	17	1.21	19.9

Table 9: Selected NMR-data [Ru((S)-MeO-Biphep)(η^6 -C₆H₆)](SbF₆)₂, C8

position					
	δ ³¹ P				
1	15.4				
2	64.7				
	δ ¹ H	δ ¹³ C		δ ¹ H	δ ¹³ C
1	-	90.9	1'	-	134.1
2	-	176.6	2'	-	157.6
3	7.26	107.6	3'	6.99	115.4
4	8.15	134.0	4'	7.27	134.2
5	7.38	120.9	5'	6.57	123.0
6	-	86.4	6'	-	135.6
7	4.16	58.3	7'	3.78	56.7
9-14	5.68	100.8			

Table 10: Selected NMR-data for [Ru(Binap)(η⁶-*p*-cymene)](SbF₆)₂, C9

position			position		
	δ ³¹ P				
1	3.3				
2	68.7				
	δ ¹ H	δ ¹³ C		δ ¹ H	δ ¹³ C
1	-	98.0	1'	-	145.3
2	-	142.0	2'	-	133.2
3	-	130.0	3'	-	135.5
4	8.66	138.3	4'	7.57	133.8
5	8.56	125.4	5'	7.34	124.7
6	-	67.5	6'	-	131.7
7	7.54	128.6	7'	5.56	125.1
8	7.60	133.0	8'	7.59	128.8
9	7.77	134.0	9'	7.44	129.7
10	8.31	131.6	10'	7.22	129.8
11	1.78	17.4	16	5.59	104.0
12	-	114.0	17	-	126.0
13	6.27	104.0	18	0.02	29.2
14	4.55	107.6	19	0.71	24.1
15	5.79	92.0	20	0.00	18.3

Table 11: Selected NMR-data for [Ru(Binap)(η^6 -C₆H₆)](SbF₆)₂, C10

position					
	δ ³¹ P				
1	19.0				
2	64.0				
	δ ¹ H	δ ¹³ C		δ ¹ H	δ ¹³ C
1	-	101.7	1'	-	146.1
2	-	144.9	2'	-	133.8
3	-	133.4	3'	-	136.1
4	8.45	138.3	4'	7.92	133.4
5	7.92	126.8	5'	7.40	126.1
6	-	73.0	6'	-	
7	7.61		7'	5.94	125.7
8	7.71	133.6	8'	7.42	130.0
9	7.85		9'	7.66	
10	8.23	131.2	10'	7.95	129.3
12-17	5.72	103.1			

2.6 References

- (1) Schmid, R.; Foricher, J.; Cereghetti, M.; Schonholzer, P. *Helv. Chim. Acta* **1991**, *74*, 370; Schmid, R.; Cereghetti, M.; Heiser, B.; Schonholzer, P.; Hansen, H. J. *Helv. Chim. Acta* **1988**, *71*, 897.
- (2) Miyashita, A.; Yasuda, A.; Takaya, H.; Toriumi, K.; Ito, T.; Souchi, T.; Noyori, R. *J. Am. Chem. Soc.* **1980**, *102*, 7932.
- (3) Kumobayashi, H. *Recl. Trav. Chim. Pays-Bas.* **1996**, *115*, 381; Akutagawa, S. *Appl. Catal. A, Gen.* **1995**, *128*, 171; Schmid, R.; Broger, E. A.; Cereghetti, M.; Crameri, Y.; Foricher, J.; Lalonde, M.; Muller, R. K.; Scalone, M.; Schoettel, G.; Zutter, U. *Pure Appl. Chem.* **1996**, *68*, 131; Noyori, R. *Asymmetric Catalysis in Organic Synthesis*; John Wiley & Sons: New York, 1994; pp 16-94; Takaya, H.; Ohta, T.; Noyori, R., In *Catalytic Asymmetric Synthesis*; Ojima, I., Ed.; VCH Publishers: New York, 1993; pp 1-39; Noyori, R. *Acta Chem. Scand.* **1996**, *50*, 380.
- (4) Lubell, W. D.; Kitamura, M.; Noyori, R. *Tetrahedron: Asym.* **1991**, *2*, 543.
- (5) Takaya, H.; Ohta, T.; Sayo, N.; Kumobayashi, H.; Akutagawa, S.; Inoue, S.; Kasahara, I.; Noyori, R. *J. Am. Chem. Soc.* **1987**, *109*, 1596.
- (6) Zhang, X. Y.; Uemura, T.; Matsumura, K.; Sayo, N.; Kumobayashi, H.; Takaya, H. *Synlett* **1994**, 501; Genet, J. P.; Pinel, C.; Ratovelomananavidal, V.; Mallart, S.; Pfister, X.; Bischoff, L.; Deandrade, M. C. C.; Darses, S.; Galopin, C.; Laffitte, J. A. *Tetrahedron Asym.* **1994**, *5*, 675; Ashby, M. T.; Halpern, J. *J. Am. Chem. Soc.* **1991**, *113*, 589; Ohta, T.; Takaya, H.; Kitamura, M.; Nagai, K.; Noyori, R. *J. Org. Chem.* **1987**, *52*, 3174.
- (7) Fehr, M. J.; Consiglio, G.; Scalone, M.; Schmid, R. *J. Org. Chem.* **1999**, *64*, 5768; Fehr, M. J.; Consiglio, G.; Scalone, M.; Schmid, R. *New J. Chem.* **1998**, *22*, 1499.
- (8) Kitamura, M.; Hsiao, Y.; Ohta, M.; Tsukamoto, M.; Ohta, T.; Takaya, H.; Noyori, R. *J. Org. Chem.* **1994**, *59*, 297.
- (9) Ohta, T.; Miyake, T.; Seido, N.; Kumobayashi, H.; Takaya, H. *J. Org. Chem.* **1995**, *60*, 357.
- (10) Chung, J. Y. L.; Zhao, D.; Hughes, D. L.; McNamara, J. M.; Grabowski, E. J. J.; Reider, P. J. *Tetrahedron Lett.* **1995**, *36*, 7379.
- (11) LeGendre, P.; Braun, T.; Bruneau, C.; Dixneuf, P. H. *J. Org. Chem.* **1996**, *61*, 8453.
- (12) Trabesinger, G.; Albinati, A.; Feiken, N.; Kunz, R. W.; Pregosin, P. S.; Tschoerner, M. *J. Am. Chem. Soc.* **1997**, *119*, 6315.
- (13) Hayashi, T.; Matsumoto, Y.; Ito, Y. *J. Am. Chem. Soc.* **1989**, *111*, 3426.
- (14) Wiles, J. A.; Lee, C. E.; McDonald, R.; Bergens, S. H. *Organometallics* **1996**, *15*, 3782.
- (15) Faller, J. W.; Grimmond, B. J.; D'Alliessi, D. G. *J. Am. Chem. Soc.* **2001**, *123*, 2525.
- (16) Feiken, N.; Pregosin, P. S.; Trabesinger, G.; Albinati, A.; Evoli, G. L. *Organometallics* **1997**, *16*, 5756; Feiken, N.; Pregosin, P. S.; Trabesinger, G.; Scalone, M. *Organometallics* **1997**, *16*, 537.
- (17) Pathak, D. D.; Adams, H.; Bailey, N. A.; King, P. J.; White, C. *J. Organomet. Chem.* **1994**, *479*, 237.
- (18) Joshi, A. M.; Thorburn, I. S.; Rettig, S. J.; James, B. R. *Inorg. Chim. Acta* **1992**, *200*, 283.

-
- (19)Wiles, J. A.; Bergens, S. H.; Vanhessche, K. P. M.; Dobbs, D. A.; Rautenstrauch, V. *Angew. Chem., Int. Ed.* **2001**, *40*, 914.
- (20)Cheng, T. Y.; Szalda, D. J.; Bullock, R. M. *Chem. Commun.* **1999**, 1629.
- (21)Mashima, K.; Kusano, K. H.; Ohta, T.; Noyori, R.; Takaya, H. *J. Chem. Soc., Chem. Commun.* **1989**, 1208.
- (22)Mashima, K.; Hino, T.; Takaya, H. *J. Chem. Soc., Dalton Trans.* **1992**, 2099; Mashima, K.; Matsumura, Y.; Kusano, K.; Kumobayashi, H.; Sayo, N.; Hori, Y.; Ishizaki, T.; Akutagawa, S.; Takaya, H. *J. Chem. Soc., Chem. Commun.* **1991**, 609.
- (23)Mashima, K.; Kusano, K. H.; Sato, N.; Matsumura, Y.; Nozaki, K.; Kumobayashi, H.; Sayo, N.; Hori, Y.; Ishizaki, T.; Akutagawa, S.; Takaya, H. *J. Org. Chem.* **1994**, *59*, 3064.
- (24)Faller, J. W.; Parr, J. *Organometallics* **2000**, *19*, 1829.
- (25)Faller, J. W.; Patel, B. P.; Albrizzio, M. A.; Curtis, M. *Organometallics* **1999**, *18*, 3096.
- (26)Mann, B. E.; Taylor, B. F. *¹³C NMR Data for Organometallic Compounds*; Academic Press: London, 1981.
- (27)Pregosin, P. S.; Salzmann, R. *Coord. Chem. Rev.* **1996**, *155*, 35; Pregosin, P. S.; Trabesinger, G. *J. Chem. Soc., Dalton Trans.* **1998**, 727; Pregosin, P. S.; Valentini, M. *Enantiomer* **1999**, *4*, 529; Whittlesey, M. K.; Perutz, R. N.; Greener, B.; Moore, M. H. *Chem. Commun.* **1997**, 187.
- (28)Umezawa-Vizzini, K.; Lee, T. R. *Organometallics* **1997**, *16*, 5613.
- (29)Wiles, J. A.; Bergens, S. H. *Organometallics* **1999**, *18*, 3709.
- (30)Currao, A.; Feiken, N.; Macchioni, A.; Nesper, R.; Pregosin, P. S.; Trabesinger, G. *Helv. Chim. Acta* **1996**, *79*, 1587.
- (31)Winter, R. F.; Scheiring, T. Z. *Anorg. Allg. Chem.* **2000**, *626*, 1196.
- (32)SAINT: Area Detector Integration; Bruker Analytical X-ray Systems: Maidison, WI, 1996. Instrumentation.
- 33)Sheldrick, G. M. SADABS. Universität Göttingen, Germany, 1996.
- (34)Sheldrick, G. M. SHELX-97. Structure Solution and Refinement Package; Universitaet Goettingen, 1997.
- (35)Wilson, A. J. C. *International Tables for X-ray Crystallography*; Kluwer Academic Publisher: Dordrecht, The Netherlands, Vol. C., 1992.
- (36)Bennet, M. A.; Smith, A. K. *J. Chem. Soc., Dalton Trans.* **1974**, 233.

Chapter 3

Ru(II)-MeO-Biphep-Arene Dications: Catalysis and Unexpected Cyclometallation/Insertion

3.1 Abstract

Reactions of $[\text{Ru}(\text{arene})(\text{MeO-Biphep})](\text{SbF}_6)_2$ (arene = η^6 -*p*-cymene, **5**, or η^6 -benzene, **6**) with several terminal acetylene compounds, lead to products **C1-C6** derived from cyclometallation of one of the P-phenyl rings, followed by insertion of the acetylene derivative into the new Ru-C bond. The solid-state structure of the η^6 -benzene complex **C6**, derived from phenylacetylene, has been determined by X-ray diffraction. The dicationic complexes **1** and **2** catalyse the reaction of benzoic acid with 1-pentyne or 1-octyne to form enol esters. Using octyne-*d*₁, deuterium-labelling experiments show scrambling of the deuterium atom. A new Ru-allenylidene complex, **C7**, was prepared and used in the catalytic reaction.

3.2 Introduction

Enol esters (Figure 1) have been used in two major areas: polymerisation and acylation. Vinyl acetate, the simplest enol ester, is the key monomer for the production of polyvinyl acetate. Vinyl acetate was industrially prepared by addition of acetic acid to acetylene at 170–250°C in presence of zinc or mercury(II) acetate on activated charcoal. These conditions are not tolerated by optically active acids. Currently, the vinyl acetate production is based on the addition of acetic acid to ethylene in the presence of a palladium(II) catalyst under oxidative conditions.¹ However, this method is not applicable to bulky acids or amino acid derivatives.

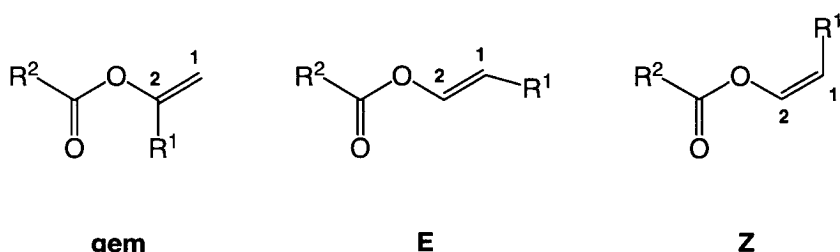
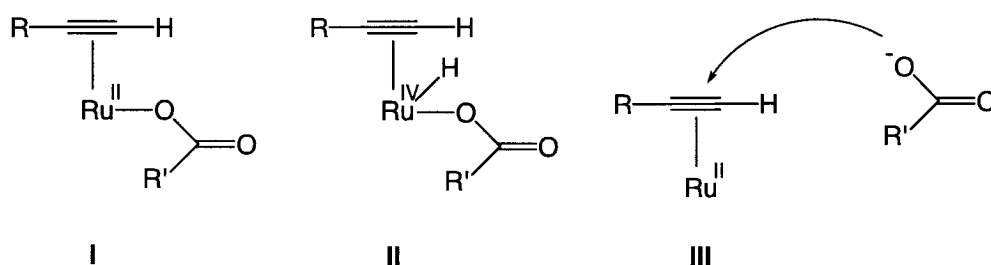


Figure 1. *gem*-, *E*- and *Z*-enol esters.

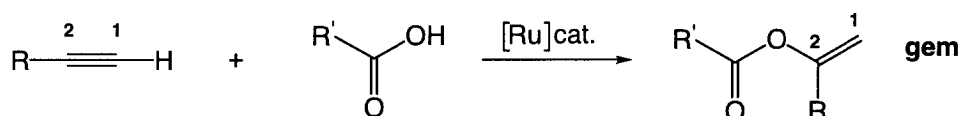
In organic synthesis enol esters can be used as mild and efficient acylating reagents. Mild acylation reagents are especially required to produce biologically and optically active amides from α -amino acids without racemisation² or for the protection of a functional group to enhance the enantioselective hydrogenation of substrates.³ Thus, there is a need for environmentally friendly, mild catalysts for producing enol esters which tolerate a broad class of substrates.

The addition of carboxylic acids to terminal alkynes is known to be catalysed by mercury salts,⁴ strong acids,⁵ or Lewis acids.⁶ Since ruthenium complexes can act as Lewis acids, they can activate the carbon-carbon triple bond of various alkynes upon coordination. Coupling of the alkyne with the carboxylate could occur via three different pathways as suggested in Scheme 1.



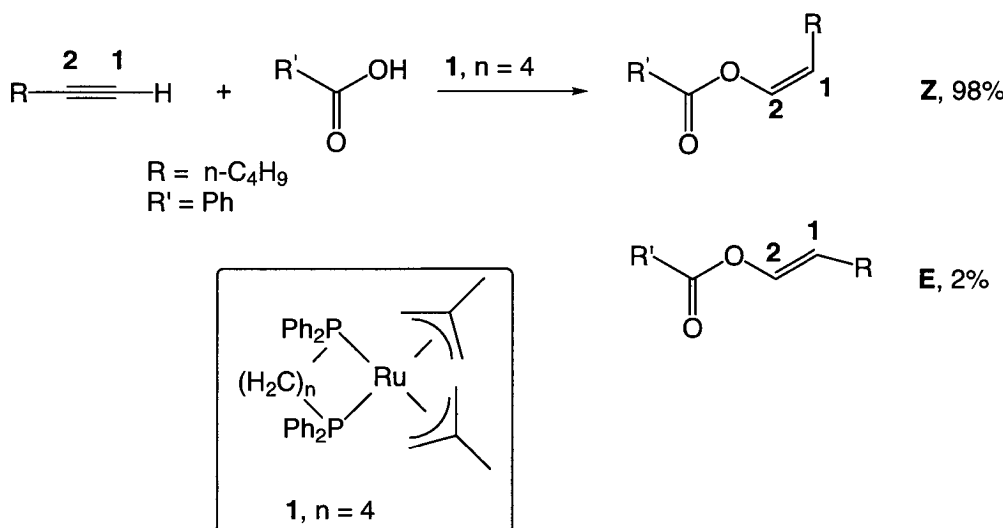
Scheme 1. Three different possibilities for the coupling between the coordinated terminal alkyne and the carboxylic acid.

The first pathway, **I**, involves the insertion of the triple bond into a (carboxylate)O-Ru(II) bond for which two coordination sites at the Ru(II) complex are required. A second pathway, **II**, suggested in the literature,⁷ involves the formation of a hydrido-carboxylate-Ru(IV) complex by oxidative addition of the carboxylic acid to a Ru(II) complex. This process is followed by an insertion of the acetylene into the Ru(IV)-H bond. The reductive elimination could afford the enol esters and regenerate a Ru(II) species. However, such a process is less likely to occur as it would involve a Ru(IV) intermediate. An alternative pathway, **III**, starts with the coordination of the terminal alkyne to Ru(II) followed by an external attack of the nucleophilic carboxylate on the activated alkyne. This pathway utilises one coordination site at Ru(II). Pathway **III** will be explained below in more detail as it is often encountered in the literature.⁸⁻¹⁰



Scheme 2. The Ru-catalysed nucleophilic addition of a carboxylic acid to terminal alkynes resulting in the *gem*-enol ester.

It has been reported that terminal alkynes undergo regioselective nucleophilic addition of carboxylic acids upon heating with various ruthenium complexes such as Ru(COD)₂ (COD = cyclooctadiene),^{7,11} [RuCl₂(η⁶-arene)(PR₃)]^{9,12} and Ru₃(CO)₁₂.¹³ Generally, the nucleophilic attack of the carboxylic acid occurs regioselectively at the C2 position of the alkyne to afford enol esters bearing *gem*-olefins (Scheme 2).



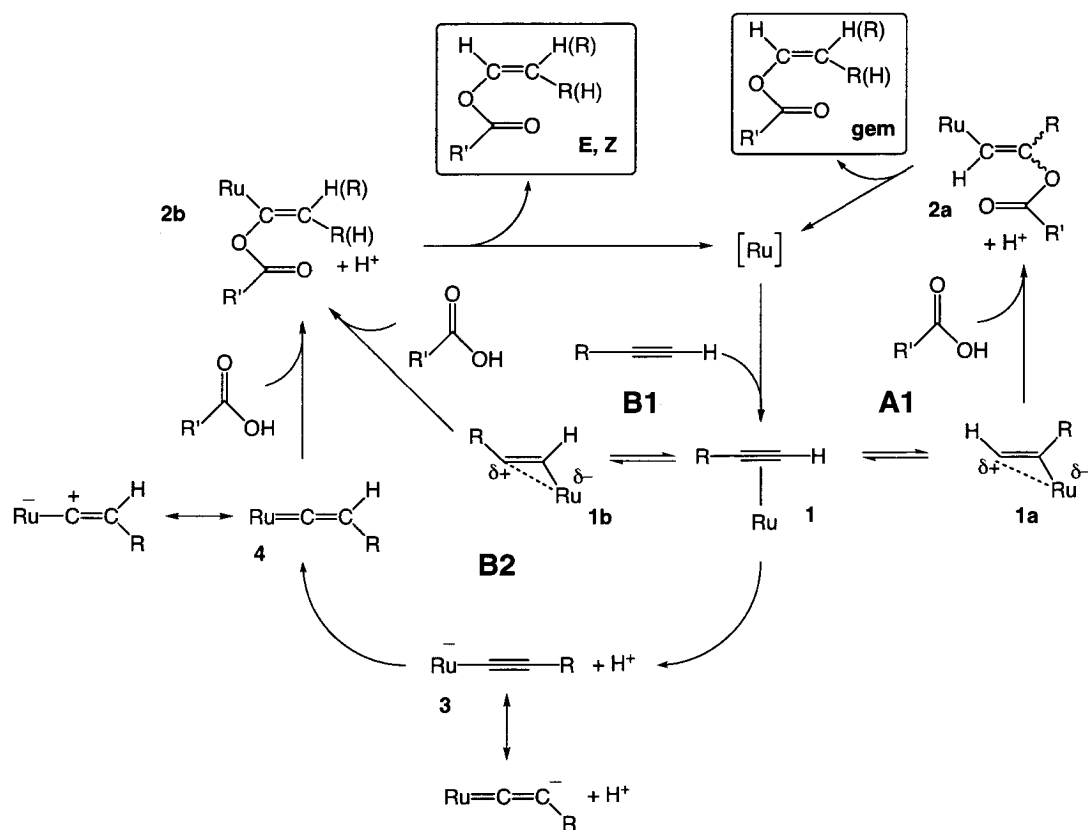
Scheme 3. The $[\text{Ru}(\text{Ph}_2\text{P}(\text{CH}_2)_4\text{PPh}_2)(\eta^3\text{-CH}_2\text{CMe}=\text{CH}_2)_2]$, **1**, catalysed nucleophilic addition of benzoic acid to 1-hexyne resulting in the *Z*- and *E*-enol esters.

However, Dixneuf et al.^{8,10} have recently reported that π -allyl ruthenium complexes bearing alkyldiphosphine ligands $[\text{Ru}(\text{Ph}_2\text{P}(\text{CH}_2)_n\text{PPh}_2)(\eta^3\text{-CH}_2\text{CMe}=\text{CH}_2)_2]$, ($n = 1 - 4$), **1**, catalyse the regioselective attack of carboxylic acids at the C1 position of alkynes producing *Z*- and *E*-enol esters (*anti*-Markovnikov). *Z*-Enol esters can be obtained with high regio- and stereoselectivities upon treatment of terminal alkynes with various carboxylic acids in the presence of **1** ($n = 4$), especially for the reaction between 1-hexyne and benzoic acid as depicted in Scheme 3.

The catalytic cycles **A1**, **A2** and **B2** depicted in Scheme 4 might account for the differences in regioselectivity obtained when using RuCl_3 , $\text{Ru}(\text{COD})_2$ ($\text{COD} = \text{cyclooctadiene}$), $[\text{RuCl}_2(\eta^6\text{-arene})]$ and $\text{Ru}_3(\text{CO})_{12}$ or on the other hand $[\text{Ru}(\text{Ph}_2\text{P}(\text{CH}_2)_4\text{PPh}_2)(\eta^3\text{-CH}_2\text{CMe}=\text{CH}_2)_2]$, **1**, as catalyst precursor. All three possible cycles start with the coordination of the terminal alkyne via its triple bond leading to complex **1** which has two isomeric structures, **1a** and **1b**.

As the positive charge at structure **1a** is located at the less substituted carbon of the coordinated terminal alkyne, the nucleophilic attack of the carboxylate takes place at this carbon affording Ru(II)-acyloxyvinyl **2a**. On subsequent protonolysis of the Ru(II)-C bond in **2a**, the *gem*-enol ester is liberated (catalytic cycle **A1**).

When the partial positive charge is located at the more substituted carbon, structure **1b**, the attack of the carboxylate affords Ru(II)-acyloxyvinyl **2b**. Protonation of complex **2b** produces the *E*- and *Z*-enol esters (catalytic cycle **B1**).



Scheme 4. Possible catalytic cycles **A1**, **B1** and **B2** for the external attack of carboxylic acid to terminal alkyne.

Catalytic cycle **B2** is based on the proton tautomers of **1**, Ru(II)-alkynyl complex **3** which leads to the Ru(II)-vinylidene complex **4**. Nucleophilic attack of the carboxalate at the more positive carbon C2 of the vinylidene affords Ru(II)-acyloxyvinyl complex **2b**. Upon protonolysis the *E*- and *Z*-enol ester are liberated as in cycle **B1**.

The selective formation of the *Z*-isomer when using **1** ($n = 4$) suggests a Ru(II) intermediate of type **2b** in which the carboxylate is trans to Ru(II) due to the steric reasons.¹⁰

3.3 Results and discussion

3.3.1 Catalysis and cyclometallation/insertion

The chelating ligand MeO-Biphep, **L1**, can act as a 6e- donor to Ru(II) with the third pair of electrons stemming from a double bond immediately adjacent to one of the two tertiary phosphine donors. A number of these complexes have been prepared^{14,15} including **5** and **6** as shown in Figure 2. In principle dications **5** and **6** could be catalyst precursors as the biaryl double bond is not strongly coordinated to Ru(II), thus allowing 16e species to be formed.

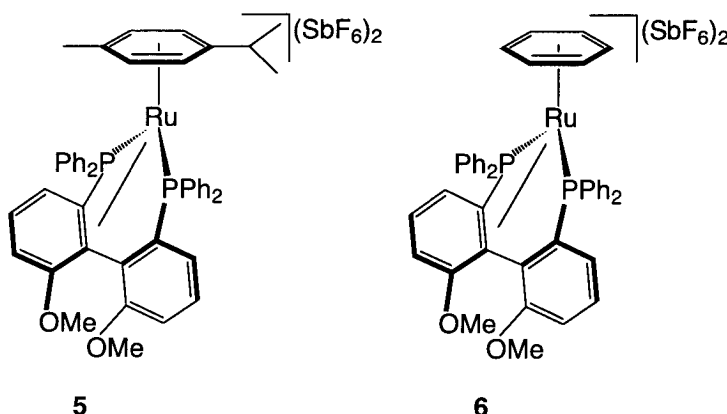
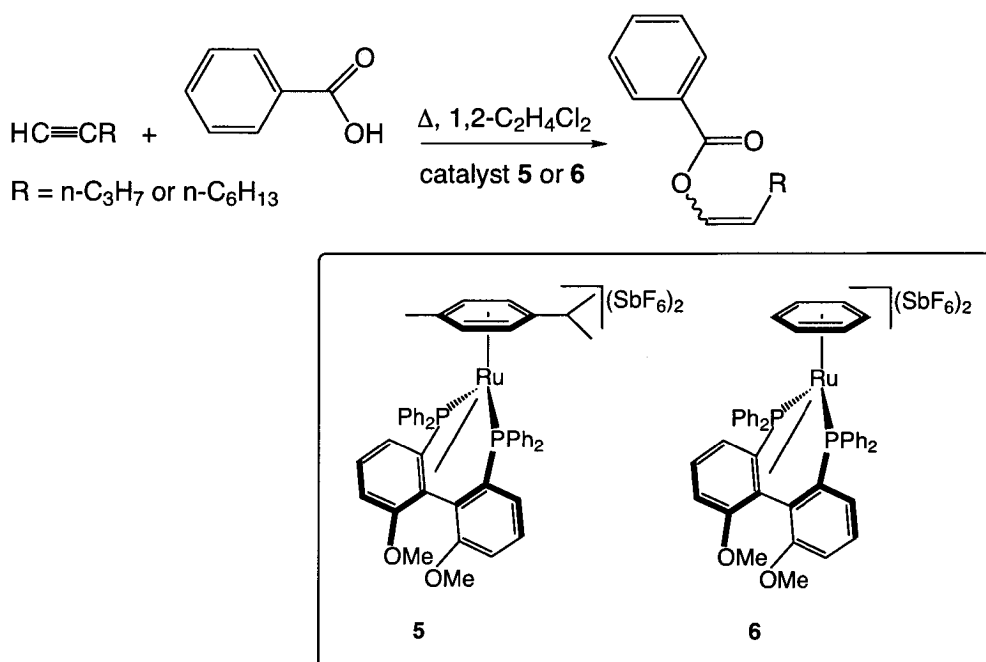


Figure 2. The dicationic Ru(II)-arene complexes **5** and **6** in which the diphosphine ligand MeO-Biphep acts as a 6e donor.

We find that the reaction of 1-pentyne (at 35°C) or 1-octyne (at 60°C) with benzoic acid, catalysed by the Ru(II)- η^6 -arene complexes **5** and **6** (5 mol%), proceeds smoothly, but relatively slowly (96 h and 24 h respectively) as shown in Scheme 5. Little or no trace of the terminal olefin has been found, so that the reaction is highly regioselective. However, both cis and trans internal olefin products are observed in the ratio 7:3. Phenylacetylene did not afford an enol ester and an explanation for this will be suggested later.



Scheme 5. The addition of benzoic acid to the terminal alkynes 1-pentyne and 1-octyne catalysed by Ru(II)- η^6 -arene complexes **5** and **6**.

Using **5** as precursor, a catalytic reaction involving 1-octyne and benzoic acid has been monitored using ^{31}P -NMR. The signals for complex **5** are present at the beginning of the transformation (although its ^{31}P resonances are broad suggesting dynamic behaviour) along with two additional species. One of these, which we have not yet satisfactorily identified,¹⁶ slowly disappears to leave a second complex, **C1a**, as an isolable material. However, if **C1a** is allowed to remain in the catalytic solution, it slowly converts completely to an isomer, **C1b**, which is also isolable and readily identified (see Figure 3). Since the reaction is slow at room temperature we have isolated both **C1a** and **C1b** separately from a reaction with 1-octyne (without added acid).

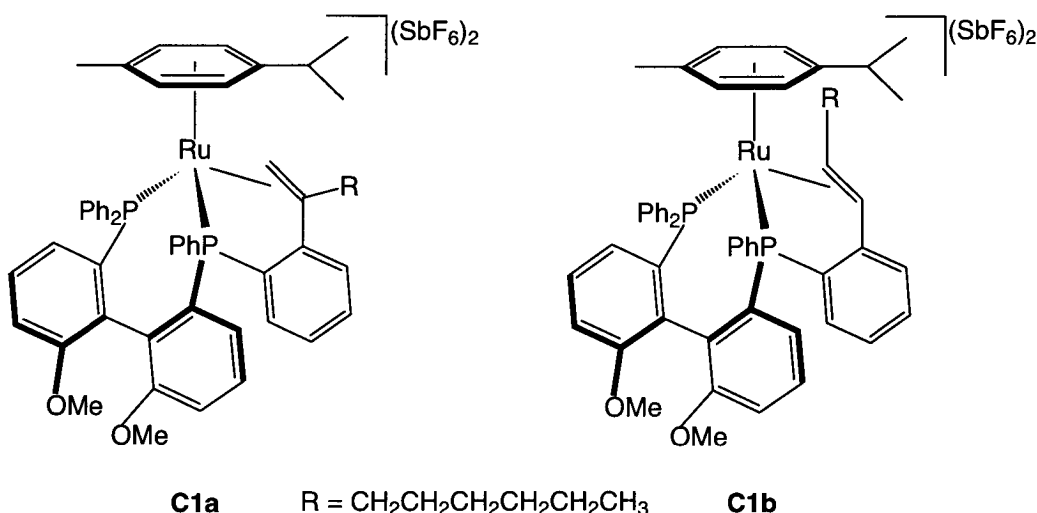


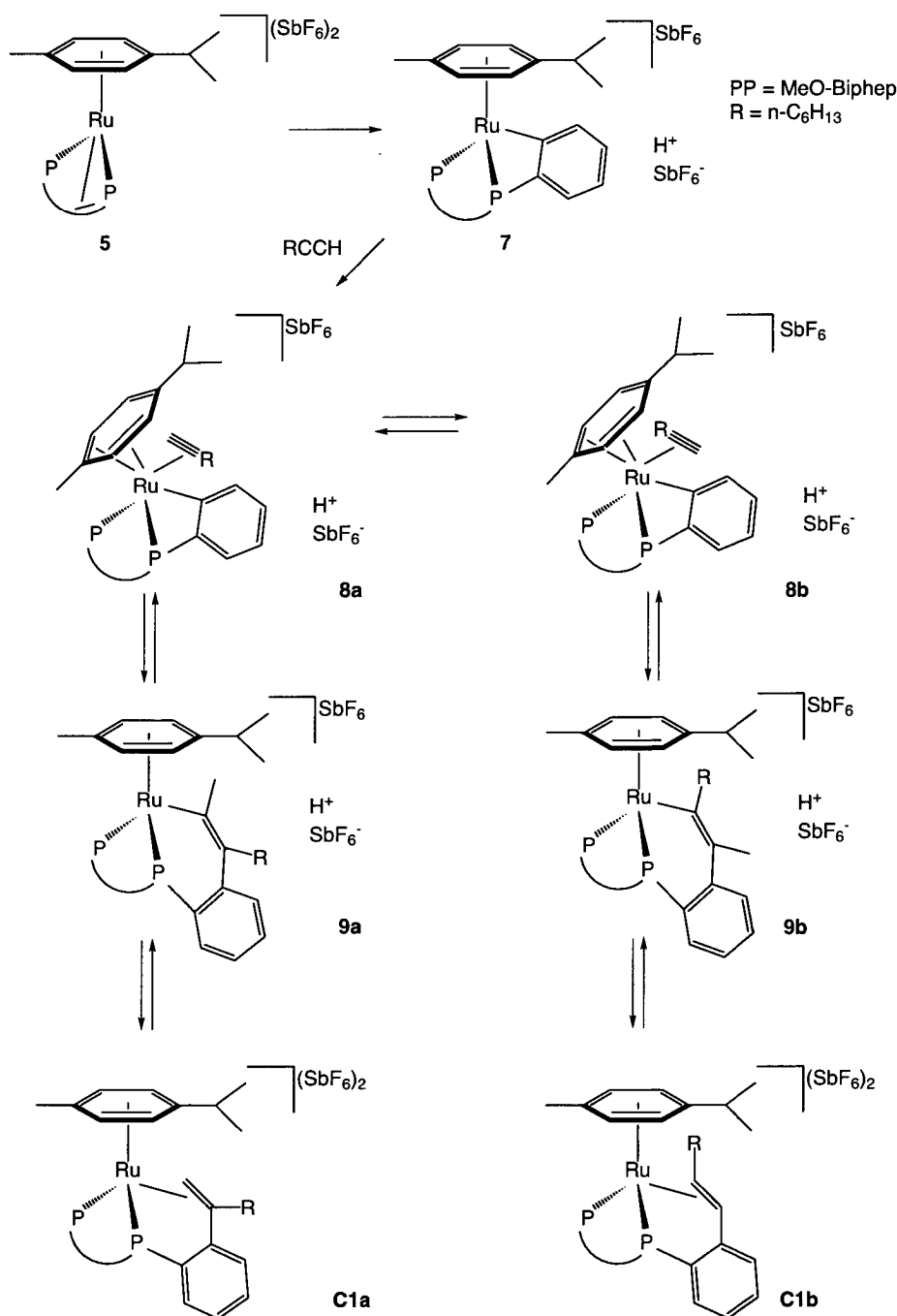
Figure 3. The orthometallation/insertion products **C1a** and **C1b**.

Given the structures for **C1a** and **C1b**, we suggest that these products arise via the mechanism depicted in Scheme 6. After dissociation of the η^2 double bond of one of the P-aryl rings, complex **5** undergoes intramolecular C-H activation which leads to the orthometallated intermediate **7**.^{17,18} This reaction could involve an attack of the electrophilic dicationic Ru(II) center on the C-H bond of the P-aryl as described in the literature for palladium-mediated cyclometallations.^{19,20} Such an electrophilic substitution obviously depends on both the electronic density at the metal and that in the C-H bond that is to be activated.

An η^6 to η^4 isomerisation of the coordinated *p*-cymene in **7** opens a coordination position for either simultaneous or subsequent alkyne coordination affording **8**.²¹ The affinity of alkynes for organometallic Ru(II) species is well documented in the literature.²² The difference in the coordination mode of the terminal alkyne (i.e. **8a** vs **8b**) to Ru(II) might originate from steric factors.¹⁷

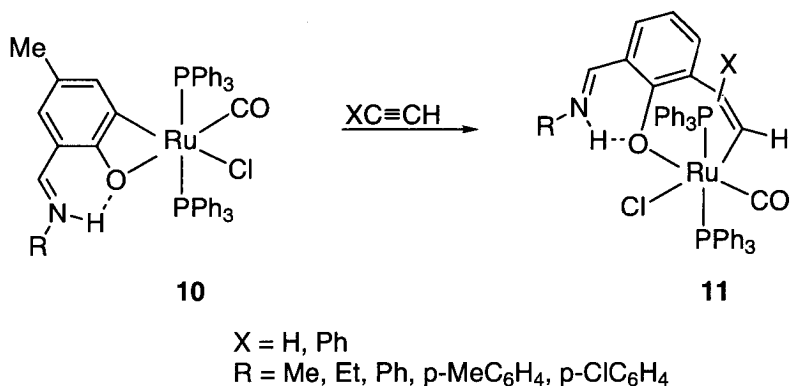
The next step leading to intermediate **9** could occur via the nucleophilic attack of the orthoruthenated carbon at the terminal alkyne (i.e. insertion). This might be a concerted process as well; i.e. the Ru(II) attacks the remaining carbon of the triple bond as has been recently suggested by Pfeffer et al.²³ The attack at the least substituted carbon leads via **8a** to **9a** while attack to the most substituted carbon affords **8b** via **9b**. Protolysis of **9** affords the products **C1a** and **C1b** in which the olefin is π -coordinated to Ru(II).

Although this reaction implies a step from a monocationic Ru(II) complex to a more electrophilic dicationic Ru(II) species, it could be driven by steric reasons. The kinetic product **C1a** bearing a terminal olefin readily isomerises via **9a**, **8a**, **8b**, **8a** to the thermodynamically more stable **C1b** having an internal olefin.



Scheme 6. A possible mechanism leading to orthometallation/insertion products **C1a** and **C1b**.

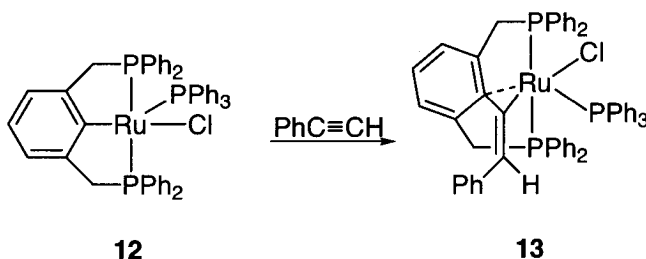
Although the insertion of alkynes into the transition metal-carbon bonds is a rapidly growing area of transition metal chemistry (especially with Pd),²⁰ there are only a few examples described in the literature concerned with alkyne insertion into orthometallated Ru(II) complexes. The most related ones are briefly described below.



Scheme 7. The insertion of acetylene/phenylacetylene into the Ru-C bond of **10** leading to the products **11**.

Chakravorty et al.²⁴ have reported the (regiospecific) insertion of acetylene/phenylacetylene into the Ru-C bond of **10** leading to the products **11**. The hydrogen-bonded zwitter-ionic iminium-phenolato function is retained on going from **10** to **11**, even though the Ru-O bond is believed to be temporarily cleaved during the insertion process to allow initial anchoring of the alkyne (Scheme 7).

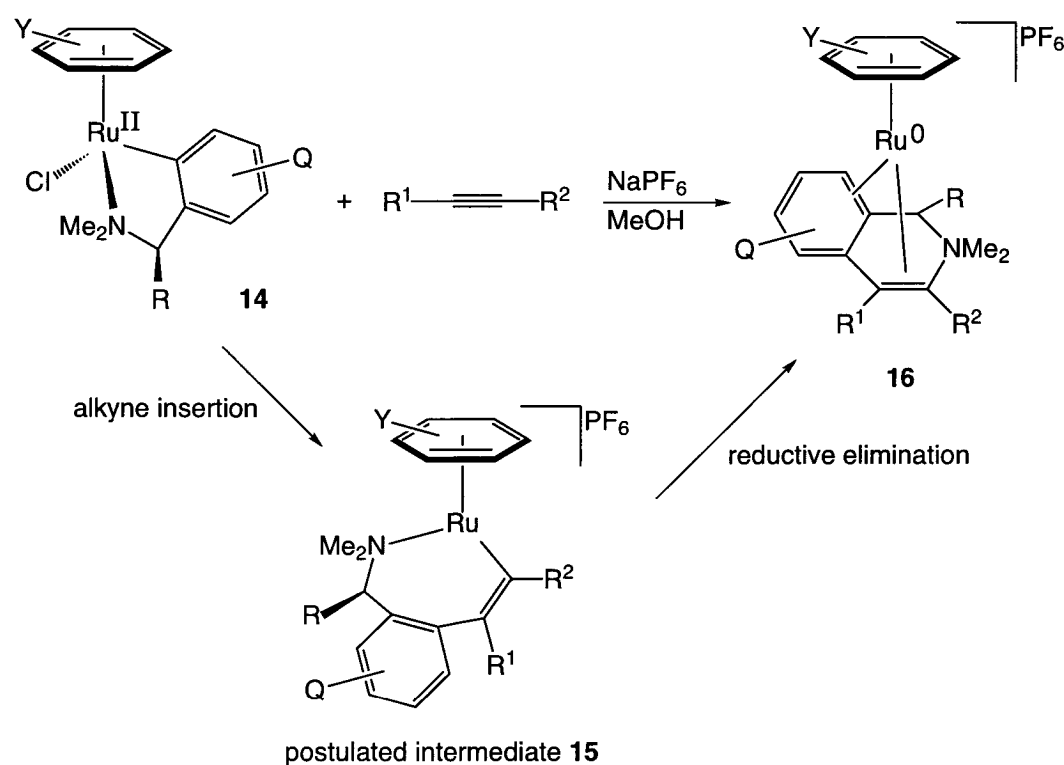
Jia et al.²⁵ have found that the reaction of $[\text{RuCl}(\text{PCP})(\text{PPh}_3)]$, **12**, with phenylacetylene gave the unusual coupling product **13** as shown in Scheme 8. The following mechanism has been proposed.



Scheme 8. The reaction of **12** with phenylacetylene gave the unusual coupling product **13**.

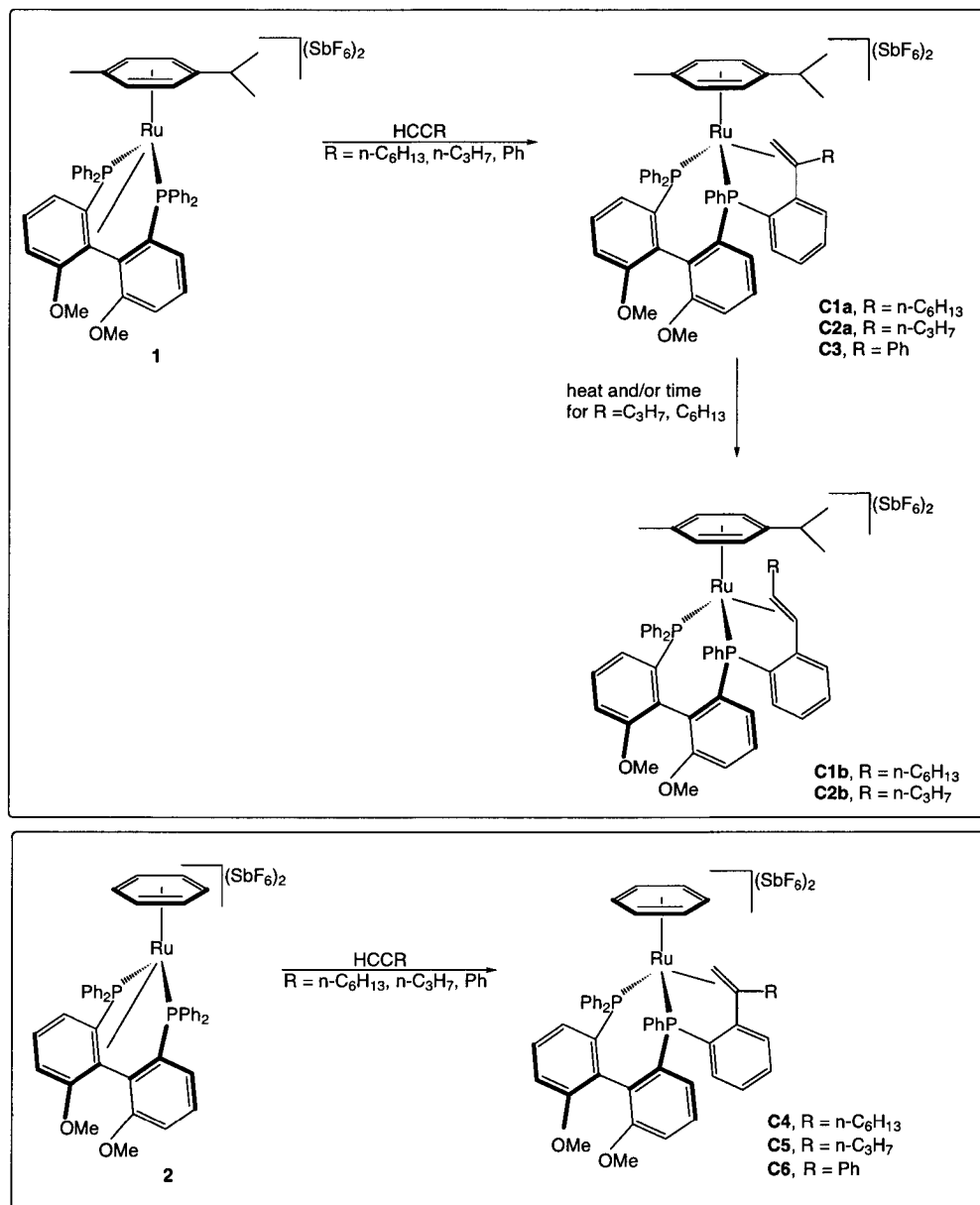
The coordinatively unsaturated complex **12** reacts with phenylacetylene to give initially the η^2 -acetylene complex which then rearranges to form the vinylidene complex $[\text{RuCl}(\text{=C=CHPh})(\text{PPh}_3)(\text{PCP})]$. Migratory insertion of the aryl group of the PCP ligand at the α -carbon of the vinylidene ligand would produce complex **13**.

Pfeffer et al.^{17,23} have shown that the reactions of the cycloruthenated complexes $[\text{RuCl}(\text{C},\text{N})(\text{arene})]$ ($\text{C},\text{N} = \text{C}_6\text{H}_4\text{CH}_2\text{NMe}_2$, $(R)-(+)-\text{C}_6\text{H}_4\text{CH}(\text{Me})\text{NMe}_2$, $\text{C}_6\text{H}_2(\text{OCH}_2\text{O}-2,3)\text{CH}_2\text{NMe}_2$) (arene = η^6 -benzene, η^6 -*p*-cymene), **14**, with internal alkynes lead to the formation of novel Ru(0) sandwich complexes of the type **16** via the postulated intermediate **15** (Scheme 9). The formation of these heterocyclic units occurs with good chemo- and regioselectivity, asymmetric alkynes being incorporated in such a way that the acetylene carbon with the sterically least demanding substituent becomes attached to the nitrogen atom of the arylamine.



Scheme 9. The alkyne insertion reaction of **14** to **16** with the postulated intermediate **15**.

Independent of the catalytic chemistry, we could synthesise and characterise the complexes **C1-C6** via reactions of the Ru(II)-diphosphine η^6 -*p*-cymene complex **5** and the η^6 -benzene analogue **6** with only the appropriate terminal alkyne, as shown in Scheme 10. The isomers differ in that, in one case, a terminal, but in the other an internal olefin has been found.



Scheme 10. Preparation and numbering of orthometalated/insertion compounds **C1-C6**.

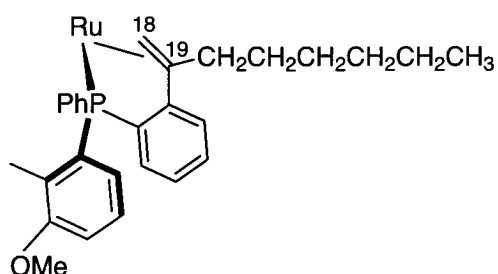


Figure 4. Fragment of compound **C1a**.

The η^6 *p*-cymene complex **C1a** (and related derivatives) could be characterised via multi-dimensional NMR methods.²⁶ The routine one-bond and long-range ^{13}C , ^1H -correlations proved to be the most useful of these NMR methods in that they reveal, for **C1a**, the two olefinic carbons at $\delta = 55.4$ ($^{13}\text{C}18$) and $\delta = 133.0$ ²⁷ ($^{13}\text{C}19$) at relatively low frequency. The important fragment of product **C1a** is shown in Figure 4 and ^{13}C -NMR data for the analogous n-propyl, **C2a**, and phenyl, **C3**, complexes are given in Table 1.

Figure 5 shows a section of the 2D ^{13}C - ^1H -NMR-one-bond-correlation for the crystalline phenyl complex **C3** and shows the two terminal olefinic protons, H18a and H18b, on the terminal olefinic carbon C18. These terminal olefinic protons are somewhat unusual in that a) they do not show a significant $^2J(^1\text{H}, ^1\text{H})$ value and b) only one of the two protons, H18b, is coupled to a single ^{31}P spin.

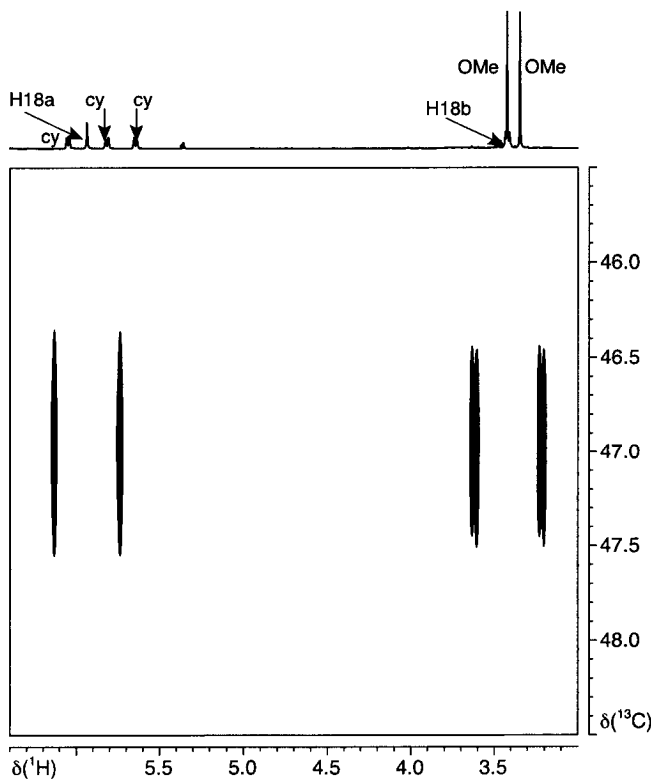


Figure 5. Section of the ^{13}C - ^1H one-bond-correlation of **C3** showing the two terminal olefinic protons, H18a and H18b, on the terminal olefinic carbon C18. Note that H18b and an OMe signal overlap (400 MHz, CD_2Cl_2 , ambient temperature).

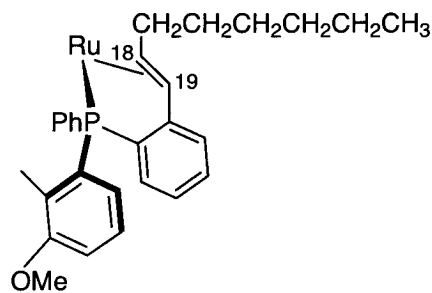
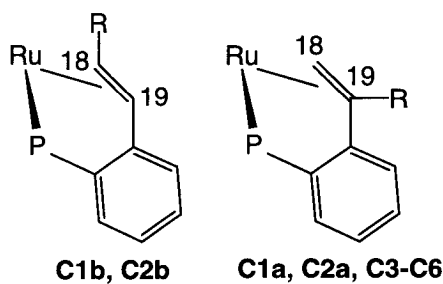


Figure 6. Fragment of compound **C1b**.

The internal olefin isomeric complexes **C1b** and **C2b** are also readily recognised via ^{13}C -NMR; e.g. for **C1b** $\delta = 85.2$ (C18) and $\delta = 89.1$ (C19).²⁸ The assignment of the trans isomer has been made via the relative large 12.6 Hz $^3J(^1\text{H}, ^1\text{H})$ coupling constant²⁹ observed for H19. The important fragment of the structure of **C1b** is shown in Figure 6 and selected NMR-data for these compounds are also given in Table 1.

The analogous reaction of $\text{HC}\equiv\text{CR}$ ($\text{R} = n\text{-C}_6\text{H}_{13}$, $n\text{-C}_3\text{H}_7$ and Ph) with the η^6 -benzene complex **6** afforded exclusively the terminal isomer products, **C4-C6**, **C1a**, **C2a** and **C3**, as well as **C4-C6** which are proposed to be kinetic products. Selected NMR-data for **C4-C6** are given in Table 1 and more extensively in Section 3.8.3. For the phenylacetylene derivative **C6**, a crystal suitable for X-ray diffraction could be obtained.

Table 1: Selected ^{13}C and ^1H chemical shifts for **C1-C6.**



Complex	$^{13}\text{C}18$	$^{13}\text{C}19$	$^1\text{H}18\text{a/b}$	$^1\text{H}19$
η^6 - <i>p</i> -cymene				
C1a , $\text{R} = n\text{-C}_6\text{H}_{13}$	55.4	133.0	5.00/3.75	-
C1b , $\text{R} = n\text{-C}_6\text{H}_{13}$	85.6	89.2	3.11	5.91
C2a , $\text{R} = n\text{-C}_3\text{H}_7$	55.1	^a	5.03/3.73	-
C2b , $\text{R} = n\text{-C}_3\text{H}_7$	85.2	89.1	3.12	5.92
C3 , $\text{R} = \text{Ph}$	47.0	^a	5.93/3.42	-
η^6 -benzene				
C4 , $\text{R} = n\text{-C}_6\text{H}_{13}$	55.1	137.4	5.38/3.31	-
C5 , $\text{R} = n\text{-C}_3\text{H}_7$	55.4	137.0	5.37/3.30	-
C6 , $\text{R} = \text{Ph}$	51.0	^a	6.18/2.98	-

^a Not assignable due to the lack of long-range correlations.

3.3.2 Solid-state structure of C6

The solid state structure of **C6** has been determined by X-ray diffraction methods. An ORTEP view of the cation is shown in Figure 7. The immediate coordination sphere around the Ru(II) consists of the two P-donors, the complexed olefin and the six carbon atoms of the η^6 -benzene ligand. The structure shows a distorted piano-stool arrangement with the olefinic double bond as the third leg. Selected bond lengths are given in Table 2 and the bond angles in Table 3.

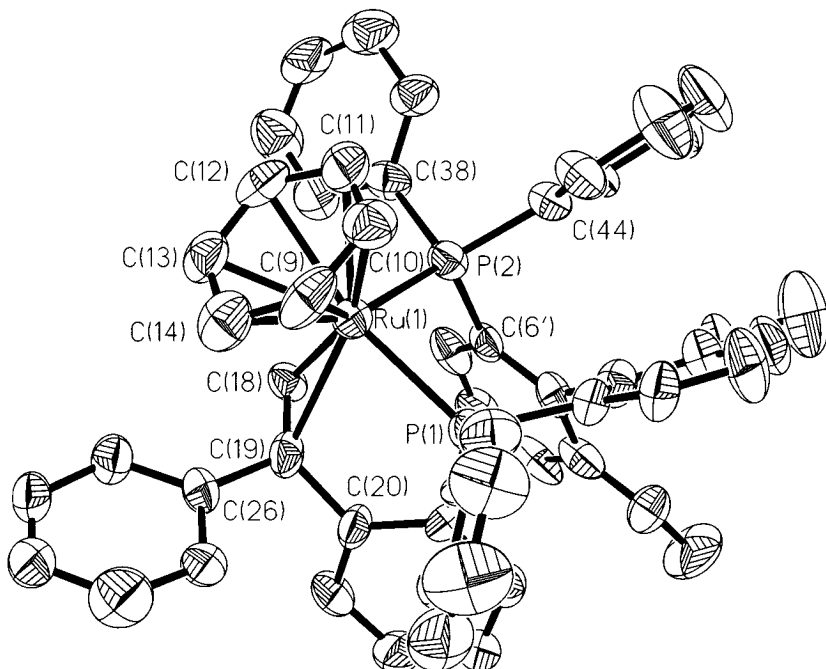


Figure 7. ORTEP view of cation of **C6**, 50% ellipsoid, from one of the two molecules present in the unit cell. Hydrogen atoms are omitted for clarity.

The two Ru-C(olefin) separations are markedly different: 2.413(14) Å for Ru(1)-C(18) and 2.246(12) Å for Ru(1)-C(19). This corresponds to a strongly asymmetric arrangement of the double bond with respect to the Ru(II).^{30,31}

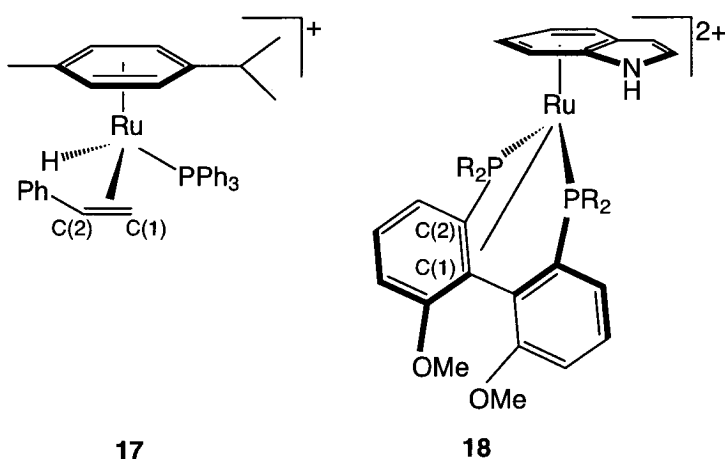


Figure 8. The Ru(II)-arene olefin complexes **17** and **18**.

Faller et al.^{15,32} have reported the structure of **17** as having Ru-C(1) and Ru-C(2) bond distances of 2.195(6) Å and 2.216(6) Å respectively, i.e. relatively short separations. In the arene olefin Ru(II)-complex, **18**, the bond distances between Ru-C(1) and Ru-C(2), 2.34(3) Å and 2.31(3) Å, respectively, are relatively long. The η^2 -bonding distances in $[\text{Ru}\{(\eta^3\text{-1-3}):(\eta^2\text{-5,6})\text{-C}_8\text{H}_{18}\}(\text{CH}_3\text{CN})(\text{Binap})]\text{BF}_4^-$ at ca. 2.40 Å are also quite long.³¹ Taken together with the observed olefinic C(18)-C(19) distance of 1.362(19) Å (which is only slightly longer than a normal uncomplexed double bond, ca. 1.34 Å), it can be concluded that the molecular crowding in **C6** results in a fairly weak Ru(II)-olefin bond. The six Ru-C(arene) separations fall in the range 2.290(14)-2.331(16) Å, with the average ca. 2.30 Å. Inspection of the X-ray literature³³ for η^6 -benzene Ru(II)-complexes suggests that routine Ru-C separations should be of the order of 2.15-2.24 Å, with the average at ca. 2.20 Å. Consequently, these data also suggest some crowding. The Ru(1)-P(1) and Ru(1)-P(2) distances are 2.353(4) Å and 2.361(4) Å, respectively, which are both fairly routine³⁴ as is the P(1)-Ru(1)-P(2) bite angle of ca. 87°.

Table 2: Selected Bond Lengths (Å) for the cation in C6.

Ru(1)-C(18)	2.246(12)	C(18)-C(19)	1.362(19)
Ru(1)-C(19)	2.413(14)	C(19)-C(20)	1.510(19)
Ru(1)-P(1)	2.353(4)	C(19)-C(26)	1.499(19)

Table 2: Selected Bond Lengths (\AA) for the cation in C6.

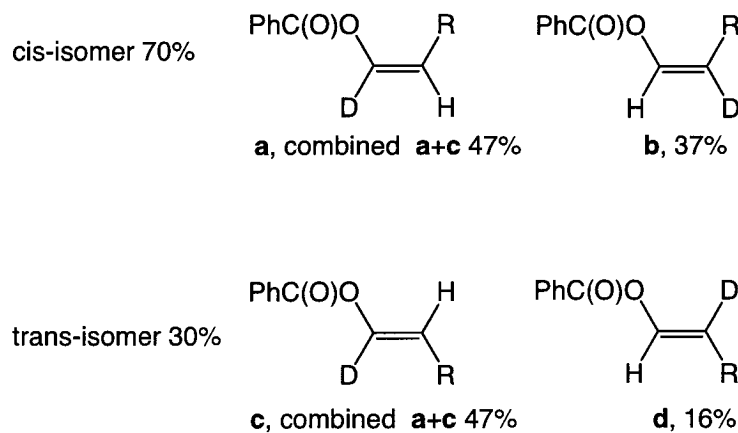
Ru(1)-C(18)	2.246(12)	C(18)-C(19)	1.362(19)
Ru(1)-P(2)	2.361(4)	P(1)-C(6)	1.844(13)
Ru(1)-C(9)	2.286(14)	P(2)-C(6')	1.830(14)
Ru(1)-C(10)	2.290(15)	P(2)-C(38)	1.808(15)
Ru(1)-C(11)	2.297(17)	P(2)-C(44)	1.812(14)
Ru(1)-C(12)	2.330(16)		
Ru(19)-C(13)	2.289(15)		
Ru(1)-C(14)	2.305(15)		

Table 3: Selected Bond Angles (deg) for the Cation in C6.

P(1)-Ru(1)-P(2)	86.67(13)	C(18)-C(19)-C(20)	117.3(12)
P(1)-Ru(1)-C(18)	98.9(4)	C(18)-C(19)-C(26)	123.7(12)
P(1)-Ru(1)-C(19)	77.4(3)	C(20)-C(19)-C(26)	112.8(13)
P(2)-Ru(1)-(C18)	82.4(3)		
P(2)-Ru(1)-C(19)	106.6(3)		
C(18)-Ru(1)-C(19)	33.7(5)		

3.3.1 Reactions with octyne-*d*₁

It was hoped that deuterium labeling might provide mechanistic insight (see Scheme 4 for possible catalytic cycles). However, the catalytic reaction of **5** with C₆H₁₃C≡CD (> 95% D) and benzoic acid resulted in almost random deuterium incorporation, i.e. the four isomers (**a-d**) have been observed as shown in Scheme 11.



Scheme 11. The four isomeric products of the catalytic reaction of C₆H₁₃C≡CD (> 95% D) and benzoic acid catalysed by **5**.

The lack of observed selectivity³⁵ is consistent with H(D) exchange of the complexed alkyne with the acid proton of the benzoic acid. There is no indication of deuterium incorporation into the ortho position of the phenyl groups in **5**.

3.3.4 Allenylidene complex C7

It was conceivable that a carbene complex might be involved in the catalytic reaction. Consequently, the allenylidene compound **C7** was synthesised as shown in Figure 9. Treatment of $[\text{Ru}(\eta^6\text{-}p\text{-cymene})(\text{MeO-Biphep})](\text{SbF}_6)_2$, **5**, with 2-methyl-3-butyn-2-ol in methylene chloride at room temperature leads to complex **C7** within a few hours. The allene carbons of complex **C7** were characterised by using ^{13}C - ^1H -long-range NMR-methods. Carbons C18, C19 and C20 show characteristic ^{13}C -NMR chemical shifts, $\delta = 305.1$, $\delta = 204.0$ and $\delta = 178.2$ respectively.²⁸

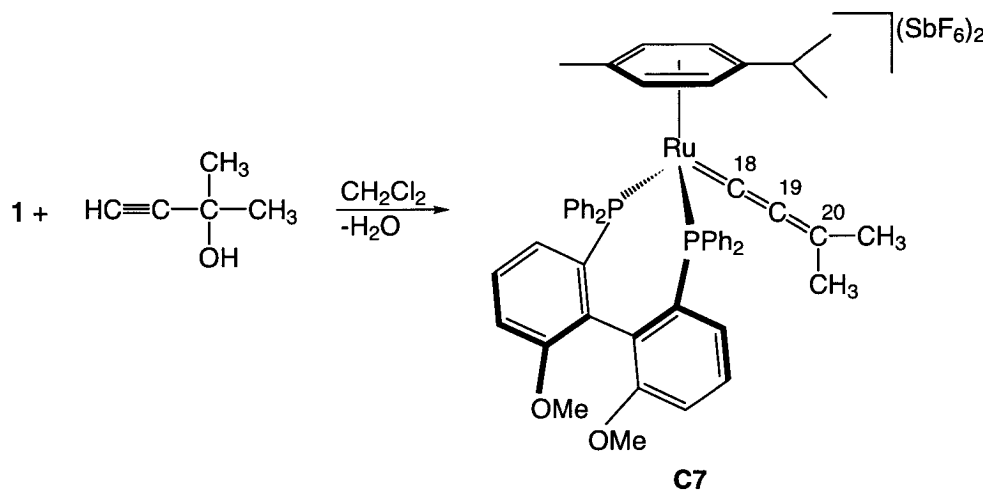


Figure 9. The reaction resulting in compound **C7**.

To the best of our knowledge, **C7** is the first dicationic Ru(II)-arene allenylidene complex described in the literature. However, a few monocationic Ru(II) arene allenylidene complexes are known. Nolan et al.³⁶ have reported the solid state structure of $[\text{Ru}=\text{C}=\text{CPh}_2(\text{IMes})(\text{Cl})(\eta^6\text{-}p\text{-cymene})]\text{PF}_6^-$ ($\text{IMes} = 1,3\text{-bis}(2,4,6\text{-trimethylphenyl})\text{imidazol-2-ylidene}$) complex, **19** (see Figure 10), by treatment of $[\text{Ru}(\text{IMes})(\text{Cl})_2(\eta^6\text{-}p\text{-cymene})]$ with 1,1-diphenylprop-2-ynyl alcohol in the presence of an equivalent of NaPF_6^- . Dixneuf et al.³⁷ have described the synthesis of $[\text{Ru}=\text{C}=\text{CPh}_2(\text{PPh}_3)(\text{Cl})(\eta^6\text{-C}_6\text{Me}_6)]\text{PF}_6^-$, **20** (see Figure 10), and have reported the ^{13}C -NMR chemical shifts for the $\text{Ru}=\text{C}$, $=\text{C}=$ and $=\text{CPh}_2$, $\delta = 288.3$, $\delta = 191.0$ and $\delta = 167.0$ respectively. The chemical shifts of **C7** are in agreement with these values.

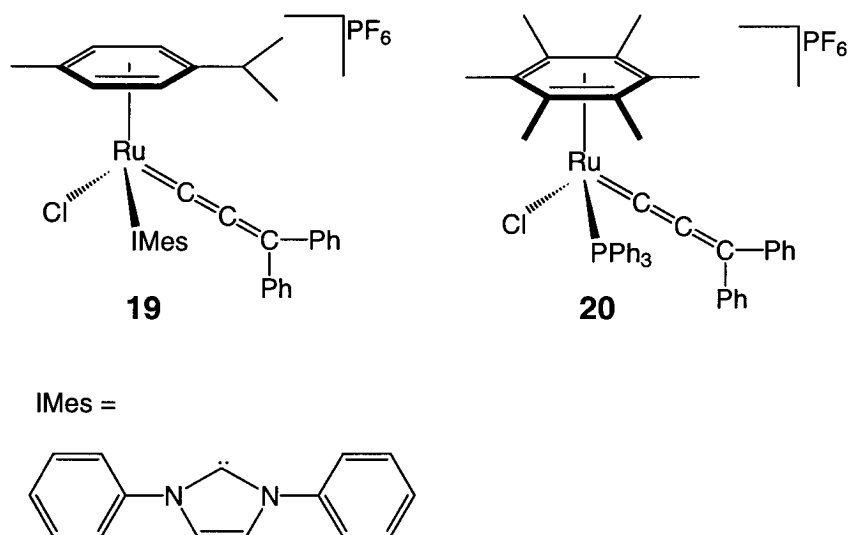


Figure 10. The moncationic Ru(II) η^6 -arene allenylidene complexes **19** and **20**.

The reaction of 1-octyne and benzoic acid catalysed by **C7** gives the cis and trans internal olefin products, detected previously, in the ratio 7:3 in slightly lower yield (60%). During the catalysis with compound **C7** the ^{31}P -NMR spectra indicated several complexes as products from the allenylidene complex. Complex **C7** disappears and the main component was found to be **C1b**. The reaction rate is ca. the same as for **5**. This suggests that the new carbene itself is not responsible for the catalysis.

3.4 Conclusions

The chemistry of Scheme 10 is readily summarised. There would seem to be a not very stable, as yet not detected, cyclometallated species, which reacts with the three alkynes to give **C1-C6**. There is a kinetic, terminal olefin, insertion product, which can be isolated, and in some cases, a more thermodynamically stable trans olefin insertion product, also isolable. The cyclometallation/insertion phenylacetylene products **C3** and **C6** are sufficiently stable such that they do not react further to afford organic product. An indication for this is the stability of **C6** over weeks in solution during crystal growth. On the other hand, the 1-pentyne and 1-octyne reaction products are capable of catalysing the chemistry of Scheme 3. The mechanism of the reaction remains uncertain.

3.5 Experimental

3.5.1 Crystallography

Air stable, orange crystals of C6 were obtained by slow diffusion of pentane into a saturated CH₂Cl₂ solution. A prismatic single crystal was mounted on a glass capillary and a data set were collected on a Siemens SMART platform diffractometer equipped with a CCD detector. Data reduction plus corrections for Lorentz polarization and absorption were performed using the programs SAINT³⁸ and SADABS.³⁹ The structure was solved by direct methods and refined by full-matrix least-squares (versus F²) with the SHELXTL program package.⁴⁰ The SbF₆ molecules are disordered and were described as a rigid group. Crystal data and structure refinements are summarized in Table 4 and 5. Two molecules are present in the unit cell. The bond distances and the conformation are not significantly different.

Table 4: Crystal data and parameters of the data collection of compound C6

Empirical formula	C ₅₂ H ₄₄ F ₁₂ O ₂ P ₂ RuSb ₂
Formula weight (g/mol)	1335.38
Crystal size (mm)	0.64 x 0.08 x 0.02
Crystal system	triclinic
Unit cell dimensions (Å, deg)	$a = 13.976(2)$, $\alpha = 72.619(3)$ $b = 14.859(2)$, $\beta = 66.23(3)$ $c = 15.136(2)$, $\gamma = 78.34$
Volume (Å ³)	2733.2(7)
Space group	P1
Formula unit pro cell (Z)	2
ρ(calculated) (g cm ⁻³)	1.623
Absorption coefficient μ (mm ⁻¹)	1.391
F(000)	1312
Temperature (K)	298(2)
Data collection	Siemens SMART CCD Dectector
Monochromator; Wavelength	Graphite-Monochromator; $\lambda(\text{MoK}\alpha) = 0.71073 \text{ Å}$
Collection method	Hemisphere, ω -scan
Theta range for data collection	1.44 < θ < 23.27
$h(\text{min}), h(\text{max}); k(\text{max}), k(\text{min}); l(\text{min}), l(\text{max})$	-15, 15; -16, 16; -11, 16
Collected reflections	15531
Independent reflections	10624 ($R(\text{int}) = 0.0478$)
Absorption correction	empirical (SADABS)
Structure solution	SHELXS-97 (direct methods)
Structure refinement	SHELXL-97 (full matrix least-square of F^2)
Number of parameters	564
Number of parameters restraints	27
Transmission coefficient (max/min)	0.9727/0.4697
wR for $ F_o ^2 > 2\sigma(F ^2)$	0.1270
wR for all reflections	0.1476
R for $ F_o ^2 > 2\sigma(F ^2)$	0.0477
R for all reflections	0.0672
Goodness of Fit ($GooF$) for $ F_o ^2 > 2\sigma(F ^2)$	1.037

Table 5: Final position ($x \times 10^{-4}$) and isotropic equivalent displacement parameters ($\text{\AA}^2 \times 10^3$) for C6

	<i>x</i>	<i>y</i>	<i>z</i>	<i>U_{eq}</i>
Ru(1)	13291(1)	3525(1)	6961(1)	37(1)
P(1)	12450(3)	5073(2)	6862(3)	37(1)
O(1)	9961(8)	5224(8)	10389(8)	59(3)
C(1)	11100(11)	5243(10)	8775(11)	47(4)
C(1')	10449(10)	4481(10)	8842(10)	43(4)
F(1)	11750(40)	5880(20)	2370(40)	440(30)
Sb(1)	11008(1)	6936(1)	2681(1)	94(1)
Sb(2)	15842(1)	11782(1)	634(1)	96(1)
P(2)	12193(3)	3184(3)	8659(3)	39(1)
O(2)	9080(8)	5733(8)	8902(8)	60(3)
C(2)	10773(12)	5594(11)	9613(12)	54(4)
C(2')	9366(12)	4792(13)	8983(11)	53(4)
F(2)	10420(30)	7242(16)	1772(19)	301(18)
C(3')	8704(12)	4091(15)	9185(11)	62(5)
C(3)	11320(15)	6318(12)	9592(13)	67(5)
F(3)	10029(19)	6144(18)	3394(18)	269(16)
C(4)	12105(15)	6646(13)	8757(15)	76(6)
C(4')	9051(13)	3193(12)	9246(11)	53(4)
F(4)	12110(20)	7600(30)	2100(20)	340(20)
C(5)	12423(13)	6303(10)	7973(12)	55(4)
C(5')	10085(12)	2900(11)	9116(9)	49(4)
F(5)	11480(30)	6677(19)	3664(17)	276(15)
C(6)	11925(10)	5596(9)	7947(10)	39(3)
C(6')	10799(10)	3541(10)	8888(9)	37(3)
F(6)	10250(20)	7910(16)	3150(20)	269(15)
C(7')	7999(14)	6053(16)	9313(19)	97(7)
C(7)	9596(18)	5564(18)	11281(16)	110(9)
F(7)	17249(9)	11629(16)	100(30)	293(18)
F(8)	15680(20)	12055(18)	-558(12)	240(14)
C(9)	14927(11)	3969(12)	5926(14)	63(5)
F(9)	15870(20)	13009(11)	550(20)	270(16)
C(10)	14884(12)	3807(12)	6870(13)	55(4)
F(10)	14429(9)	11970(20)	1200(30)	360(20)

Table 5: Final position ($\times 10^{-4}$) and isotropic equivalent displacement parameters ($\text{\AA}^2 \times 10^3$) for C6

	<i>x</i>	<i>y</i>	<i>z</i>	<i>U_{eq}</i>
C(11)	14655(11)	2909(13)	7510(13)	60(4)
F(11)	15720(20)	11531(18)	1911(11)	224(10)
F(12)	15829(14)	10533(9)	751(16)	189(9)
C(12)	14478(12)	2208(12)	7176(13)	58(4)
C(13)	14500(11)	2424(12)	6229(12)	54(4)
F(13)	6639(18)	15755(15)	6224(11)	197(9)
C(14)	14709(11)	3334(12)	5546(13)	62(5)
F(14)	5813(15)	16244(14)	8686(10)	177(8)
F(15)	5355(13)	15112(12)	7879(16)	180(8)
F(16)	7148(10)	16945(9)	7058(16)	163(8)
F(17)	5284(14)	16922(10)	7076(17)	183(9)
C(18)	12089(11)	2824(9)	6830(10)	36(3)
F(18)	7295(11)	15116(8)	7712(14)	142(6)
C(19)	12216(10)	4582(10)	6033(11)	41(4)
F(19)	14385(8)	10283(8)	6730(9)	94(4)
C(20)	11346(11)	4379(9)	6121(10)	42(3)
F(20)	12497(7)	10530(7)	6718(10)	88(4)
C(21)	11330(10)	5120(9)	6565(10)	39(3)
F(21)	14042(10)	10451(8)	5123(7)	99(4)
C(22)	10498(10)	5811(9)	6688(10)	41(3)
F(22)	14816(7)	8776(8)	5986(11)	110(4)
C(23)	9715(11)	5789(10)	6372(10)	46(4)
F(23)	12836(8)	9024(7)	6037(8)	83(3)
C(24)	9735(12)	5099(11)	5978(12)	54(4)
F(24)	13171(10)	8866(7)	7677(7)	99(4)
C(25)	10562(12)	4394(12)	5809(12)	54(4)
C(26)	12832(12)	3521(11)	4977(10)	49(4)
C(27)	13132(11)	2619(12)	4727(12)	53(4)
C(28)	13685(13)	2612(13)	3731(13)	64(5)
C(29)	13953(13)	3395(12)	3011(13)	60(4)
C(30)	13611(15)	4261(14)	3267(14)	76(6)
C(31)	13020(12)	4329(11)	4209(10)	51(4)
C(32)	13241(10)	5958(9)	5837(10)	41(3)
C(33)	12931(12)	6425(11)	5066(11)	54(4)

Table 5: Final position ($x \times 10^{-4}$) and isotropic equivalent displacement parameters ($\text{\AA}^2 \times 10^3$) for C6

	x	y	z	$U_{(eq)}$
C(34)	13532(16)	7092(12)	4247(14)	79(6)
C(35)	14488(17)	7275(16)	4322(17)	92(7)
C(36)	14747(16)	6834(15)	5046(16)	78(6)
C(37)	14140(13)	6166(11)	5838(13)	60(4)
C(38)	12350(11)	1924(10)	9181(10)	44(4)
C(39)	12809(12)	1605(12)	9882(11)	53(4)
C(40)	12971(14)	613(14)	10311(13)	73(5)
C(41)	12602(15)	9(12)	10038(14)	65(5)
C(42)	12225(16)	269(14)	9331(14)	76(5)
C(43)	12097(14)	1216(10)	8905(12)	58(4)
C(44)	12389(11)	3670(10)	9532(10)	45(3)
C(45)	11704(14)	3479(12)	10481(11)	60(4)
C(46)	11817(19)	3784(16)	11204(14)	91(7)
C(47)	12670(20)	4242(19)	10965(18)	108(8)
C(48)	13334(19)	4464(17)	10045(19)	101(8)
C(49)	13220(14)	4173(12)	9301(13)	62(4)
Ru(1A)	9570(1)	9654(1)	5867(1)	36(1)
Sb(1A)	6265(1)	16027(1)	7442(1)	67(1)
P(1A)	8017(3)	10682(2)	6069(3)	34(1)
C(1A')	9124(10)	12327(9)	4189(9)	34(3)
O(1A)	8492(8)	12936(7)	2638(7)	57(3)
C(1A)	8167(10)	11967(9)	4221(9)	34(3)
Sb(2A)	13642(1)	9622(1)	6376(1)	56(1)
P(2A)	10255(3)	10566(2)	4209(3)	36(1)
C(2A)	7894(11)	12306(10)	3407(11)	47(4)
O(2A)	7995(8)	13763(7)	4294(8)	54(3)
C(2A')	8968(12)	13310(10)	4154(10)	45(4)
C(3A')	9880(13)	13764(10)	4002(10)	51(4)
C(3A)	7009(12)	12025(11)	3345(12)	59(4)
C(4A)	6429(13)	11369(12)	4159(13)	66(5)
C(4A')	10822(11)	13264(11)	3846(10)	47(4)
C(5A')	10916(11)	12333(10)	3901(10)	40(3)
C(5A)	6745(11)	10972(11)	4997(11)	47(4)
C(6A)	7596(9)	11264(9)	5017(10)	36(3)

Table 5: Final position ($\times 10^{-4}$) and isotropic equivalent displacement parameters ($\text{\AA}^2 \times 10^3$) for C6

	<i>x</i>	<i>y</i>	<i>z</i>	<i>U_(eq)</i>
C(6A')	10077(10)	11857(9)	4060(9)	35(3)
C(7A')	7824(15)	14735(12)	4282(14)	72(5)
C(7A)	8283(16)	13280(15)	1729(11)	83(7)
C(9A)	10031(15)	8391(10)	5173(13)	67(6)
C(10A)	10837(14)	8410(11)	5507(15)	58(4)
C(11A)	10570(12)	8380(9)	6482(12)	49(4)
C(12A)	9516(12)	8319(10)	7151(11)	49(4)
C(13A)	8783(12)	8284(9)	6855(12)	48(4)
C(14A)	8996(13)	8344(10)	5821(14)	57(4)
C(18A)	10516(10)	10560(10)	6104(10)	40(3)
C(19A)	9593(11)	10572(9)	6957(11)	41(4)
C(20A)	8888(11)	11442(10)	6941(10)	41(3)
C(21A)	8149(10)	11617(9)	6507(10)	35(3)
C(22A)	7506(10)	12478(10)	6459(10)	42(4)
C(23A)	7606(13)	13127(10)	6896(11)	52(4)
C(24A)	8359(14)	12953(11)	7321(12)	59(5)
C(25A)	8976(14)	12139(11)	7365(12)	57(4)
C(26A)	9500(11)	9982(10)	7996(10)	42(3)
C(27A)	10360(13)	9477(11)	8187(12)	56(4)
C(28A)	10264(16)	8955(12)	9131(14)	71(5)
C(29A)	9200(20)	8952(18)	9839(15)	109(9)
C(30A)	8425(16)	9411(17)	9659(16)	88(7)
C(31A)	8604(13)	9925(13)	8749(11)	60(4)
C(32A)	6875(11)	10125(10)	7084(11)	43(3)
C(33A)	6427(11)	10435(11)	7930(11)	52(4)
C(34A)	5595(12)	9962(13)	8748(12)	65(5)
C(35A)	5269(14)	9207(14)	8657(16)	81(6)
C(36A)	5731(12)	8895(11)	7784(15)	67(5)
C(37A)	6536(11)	9330(10)	7014(12)	53(4)
C(38A)	9708(11)	10498(10)	3297(10)	43(3)
C(39A)	10143(13)	11037(12)	2340(11)	58(4)
C(40A))	9854(16)	11014(14)	1599(13)	73(5)
C(41A)	9100(16)	10415(17)	1826(15)	84(6)
C(42A)	8665(16)	9883(14)	2761(17)	80(6)

Table 5: Final position ($\times 10^{-4}$) and isotropic equivalent displacement parameters ($\text{\AA}^2 \times 10^3$) for C6

	<i>x</i>	<i>y</i>	<i>z</i>	<i>U_(eq)</i>
C(43A)	8929(12)	9930(11)	3513(11)	50(4)
C(44A)	11621(10)	10167(9)	3647(11)	41(3)
C(45A)	11904(12)	9591(11)	2972(11)	51(4)
C(46A)	12914(13)	9237(11)	2545(12)	61(4)
C(47A)	13719(14)	9418(12)	2789(13)	70(5)
C(48A)	13483(11)	9987(12)	3465(12)	58(4)
C(49A)	12419(12)	10294(11)	3927(12)	54(4)

3.5.2 Synthesis

All reactions with air- or moisture-sensitive materials were carried out under Argon using standard Schlenk techniques. The solvents used for synthetic and recrystallisation purposes were of “puriss p.a” quality, purchased from *Fluka AG*, *Riedel-de-Häen* or *Merck*. Methanol was distilled from magnesium. Diethylether was distilled from Na-K-Almagam. Dichloromethane and pentane were distilled from CaH₂. 1,2-Dichloroethane was distilled from P₂O₁₀. The deuterated solvents CDCl₃, CD₂Cl₂ and D₂O were purchased from Cambridge Isotope Laboratories. CD₂Cl₂ was distilled and dried over CaH₂ before use.

[Ru((S)-MeO-Biphep)(η⁶-*p*-cymene)](SbF₆)₂ (**5**) and [Ru((S)-MeO-Biphep)(η⁶-benzene)](SbF₆)₂ (**6**) were prepared according to the literature and references therein.⁴¹ (S)-(2,2'-Bis(diphenylphosphino)-6,6'-bismethoxy-1,1'-biphenyl) ((S)-MeO-Biphep, **L1a**) was provided by F. Hoffmann-La Roche AG. All the other chemicals were commercial products used as received.

The routine ³¹P{¹H}-, ¹³C{¹H}-, ²H- and ¹H-NMR spectra were measured in CD₂Cl₂ on either a *Brucker AdvanceDPX2 50* [frequency in MHz: ³¹P : 101.26, ¹³C : 62.90, ¹H : 250.14] or *Brucker AdvanceDPX300* [frequency in MHz: ³¹P: 121.49, ¹³C : 75.47, ¹H : 300.13] or *Brucker AdvanceDRX400* [frequency in MHz: ³¹P : 161.98, ¹³C : 100.61, ¹H : 400.13] or *Brucker AdvanceDRX500* [frequency in MHz: ³¹P : 202.46, ¹³C : 125.75, ¹H : 500.13] at room temperature unless stated. The two-dimensional ¹H-¹H-DQF-COSY, ³¹P-¹H-INV-COSY, ¹³C-¹H-HMQC, ¹³C-¹H-HMBC and ¹H-NOESY experiments were carried out at either *Brucker AdvanceDRX400* or *Brucker AdvanceDRX500*.

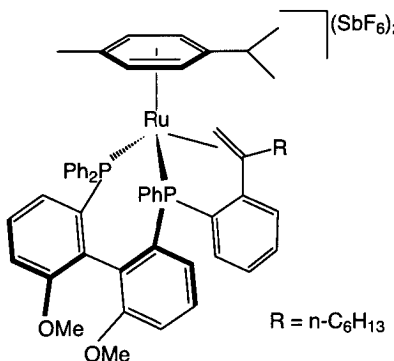
The chemical shifts δ are given in ppm and the coupling constants J are given in Hertz. The multiplicity is denoted by the following abbreviations: s: singlet; d: doublet; t: triplet; m: multiplet; dd: doublet of doublet; ddd: doublet of dd; dt: doublet of triplet; br : broad. Other abbreviations used are bb: backbone of {S}-MeO-Biphep; cy: aromatic carbon of *p*-cymene ligand; cyH: aromatic proton of *p*-cymene ligand.

Elemental analysis (EA) and EI-MS and FAB-MS spectra were performed by the service of the “Laboratorium für Organische Chemie der ETH Zürich”.

Synthesis of C1a

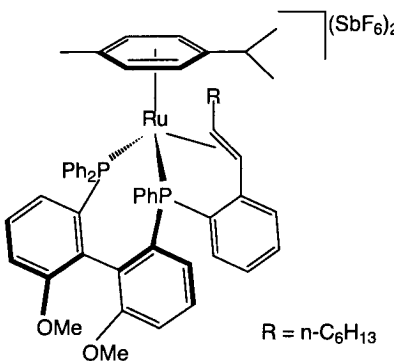
1-Octyne (8 μ l, 0.051 mmol) was added to a solution of $[\text{Ru}((S)\text{-MeO-Biphep})(\eta^6\text{-}p\text{-cymene})](\text{SbF}_6)_2$ (66.2 mg, 0.051 mmol) in 2 ml 1,2-C₂H₄Cl₂. After 2.5 h at room temperature, the ³¹P-NMR spectrum indicated a full conversion to the product. The solvent was evaporated i.v. and the resulting powder was washed with 5x1 ml Et₂O. The orange product was dried i.v. to afford the complex in 93% yield. During the 2D-NMR characterisation the thermodynamically more stable product **C1b** appeared.

Color: orange. Yield: 66.4 mg (93%). Anal. Calcd for C₅₆H₆₀P₂O₂RuSb₂F₁₂·H₂O (1399.7): C, 47.45; H, 4.40. Found: C, 47.09; H, 4.40. FAB-MS: calcd. M²⁺ 928.2; found M²⁺-*p*-cymene-C₈H₁₅+2SbF₆, 1031.0; M²⁺-*p*-cymene-C₈H₁₅+SbF₆, 919.0; M²⁺-*p*-cymene, 792.0; M²⁺-*p*-cymene-C₈H₁₅, 682.9; NMR (DRX400, CD₂Cl₂): ³¹P, 45.6 (d, 48), 38.7 (d, 48); ¹³C, 158.3 (bb), 158.0 (bb), 145.4 (H₂C=CRPh-), 136.0-126.7, 124.9 (bb), 123.3 (bb), 121.7 (cy), 114.7 (bb), 114.6 (bb), 106.3 (cy), 103.3 (cy), 102.5 (cy), 100.8 (cy), 55.4 (H₂C=CRPh-), 55.3 (OCH₃), 55.1 (OCH₃), 46.3 (-CH₂(CH₂)₄CH₃), 32.3 (-CH₂CH₂(CH₂)₃CH₃), 31.8 (-(CH₂)₂CH₂(CH₂)₂CH₃), 31.0 (CH(CH₃)₂), 25.1 (-(CH₂)₃CH₂CH₂CH₃), 22.9 (CH(CH₃)₂), 22.8 (-(CH₂)₄CH₂CH₃), 20.5 (CH(CH₃)₂), 20.0 (CH₃), 14.1 (-(CH₂)₅CH₃); ¹H, 7.10-7.94 (m, 22H), 6.92 (dd, 11.2, 11.6, 1H, H₂C=CRPh-), 6.86 (d, 6.8, 1H, cyH), 6.55 (d, 8.4, 1H, bb), 6.43 (d, 8.4, 1H, bb), 6.18 (d, 6.8, 1H, cyH), 5.97 (d, 6.8, 1H, cyH), 5.88 (d, 6.8, 1H, cyH), 5.00 (s, 1H, H₂C=CRPh-), 3.75 (d, 10.3, 1H, H₂C=CRPh-), 3.44 (s, 3H, OCH₃), 3.25 (s, 3H, OCH₃), 2.35 (m, 1H, CH(CH₃)₂), 2.18 (br s, 3H, CH₃), 1.09-1.68 (m, 10H, -(CH₂)₅CH₃), 0.96 (d, 7.0, 3H, CH(CH₃)₂), 0.89 (t, 7.2, 3H, -(CH₂)₅CH₃), 0.70 (d, 7.0, 3H, CH(CH₃)₂).



Synthesis of C1b

1-Octyne (7 μ l, 0.047 mmol) was added to a solution of $[\text{Ru}((S)\text{-MeO-Biphep})(\eta^6\text{-}p\text{-cymene})](\text{SbF}_6)_2$ (61.0 mg, 0.047 mmol) in 0.5 ml CD₂Cl₂. The resulting orange solution was heated at 35°C for 48h. The solvent was then evaporated i.v. and the resulting powder was washed with 5x1 ml Et₂O and 1x1 ml CH₂Cl₂. The orange product was dried i.v. to afford the product. Color: orange. Yield: 28.3 mg (92%). Anal. Calcd for C₅₆H₆₀P₂O₂RuSb₂F₁₂·H₂O (1399.7): C, 47.45; H, 4.41. Found: C, 47.33; H, 4.46. FAB-MS: Calcd. M²⁺ 928.2; Found M²⁺-*p*-cymene-C₈H₁₄+2SbF₆, 1031.0; M²⁺-*p*-cymene-C₈H₁₄+SbF₆, 919.0; M²⁺-*p*-cymene, 792.0; M²⁺-*p*-cymene-C₈H₁₄, 682.9. NMR (DRX400, CD₂Cl₂): ³¹P, 39.9 (d, 56), 45.5 (d, 56); ¹³C, 159.4 (bb), 158.0 (bb), 144.0 (RHC=CHPh-), 132.0-135.5, 128.1-130.9, 127.6 (bb), 126.6 (bb), 126.1 (cy), 126.0 (bb), 124.9

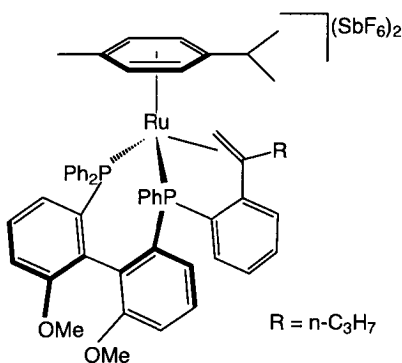


(bb), 123.1 (bb), 115.3 (bb), 114.5 (bb), 108.6 (cy), 106.3 (cy), 103.0 (cy), 95.4 (cy), 89.2 (RHC=CHPh-), 85.6 (RHC=CHPh-), 55.6 (OCH₃), 55.4 (OCH₃), 42.8 (-CH₂(CH₂)₄CH₃), 34.7 (-CH₂CH₂(CH₂)₃CH₃), 32.3 (-CH₂)₂CH₂(CH₂)₂CH₃), 32.2 (CH(CH₃)₂), 29.5 (-CH₂)₃CH₂CH₂CH₃), 25.1 (CH(CH₃)₂), 23.0 (-CH₂)₂CH₂CH₃), 20.2 (CH₃), 18.5 (CH(CH₃)₂), 14.2 (-CH₂)₅CH₃); ¹H, 7.04-8.08 (m, 25H), 6.84 (dd, 7.5, 10.8, 1H, RHC=CHPh-), 6.62 (d, 8.4, 1H, cyH), 6.54 (br s, 1H, bb), 6.11 (d, 6.8, 1H, cyH), 5.91 (d, 12.7, 1H, RHC=CHPh-), 5.10 (d, 6.8, 1H, cyH), 5.01 (br s, 1H, cyH), 3.37 (s, 3H, OCH₃), 3.31 (s, 3H, OCH₃), 3.11 (d, 12.7, 1H, RHC=CHPh-), 2.65 (m, 1H, CH(CH₃)₂), 2.00 (br s, 3H, CH₃), 1.12 (d, 7.0, 3H, CH(CH₃)₂), 0.59 (d, 7.0, 3H, CH(CH₃)₂).

In Situ Preparation and Characterization of C2a

1-Pentyne (6 μ l, 0.061 mmol) was added to a solution of [Ru((S)-MeO-Biphep)(η^6 -*p*-cymene)](SbF₆)₂ (4) (54.2 mg, 0.042 mmol) in 0.5 ml CD₂Cl₂. After 12h at room temperature the ³¹P-NMR spectrum indicated a full conversion to one product which was characterized in situ by 2D-NMR methods (only selected NMR-data for C2a are given). The reaction proceeded to the thermodynamically more stable isomer C2b during these measurements.

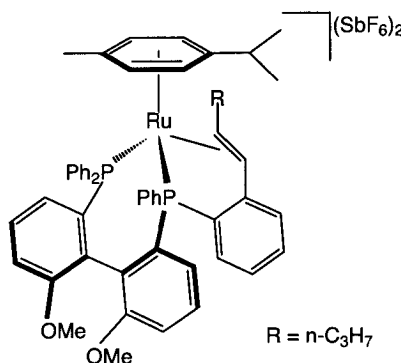
NMR (DRX400, CD₂Cl₂): ³¹P, 39.0 (d, 49), 45.7 (d, 49); ¹³C, 158.3 (bb), 157.9 (bb), 145.2 (H₂C=CRPh-), 136.3 (H₂C=CRPh-), 134.2 (H₂C=CRPh-), 133.8 (cy), 132.4 (H₂C=CRPh-), 130.5 (bb), 129.6 (bb), 129.1 (H₂C=CRPh-), 128.4 (bb), 128.4 (bb), 127.2 (bb), 126.7 (H₂C=CRPh-), 126.4 (bb), 124.9 (bb), 123.4 (bb), 122.1 (cy), 114.6 (bb), 114.5 (bb), 106.7 (cy), 103.5 (cy), 102.3 (cy), 100.1 (cy), 55.4 (OCH₃), 55.1 (H₂C=CRPh-), 55.0 (OCH₃), 48.0 (-CH₂CH₂CH₃), 30.9 (CH(CH₃)₂), 25.6 (-CH₂CH₂CH₃), 23.1 (CH(CH₃)₂), 20.0 (CH₃), 19.8 (CH(CH₃)₂), 13.8 (-CH₂CH₂CH₃); ¹H, 7.64 (bb), 7.40 (H₂C=CRPh-), 7.28 (bb), 7.24 (bb), 7.21 (H₂C=CRPh-), 7.16 (H₂C=CRPh-), 7.12 (bb), 6.91 (H₂C=CRPh-), 6.89 (d, 7.2, 1H, cyH), 6.54 (d, 8.4, 1H, bb), 6.42 (d, 8.4, 1H, bb), 6.14 (d, 7.2, 1H, cyH), 6.04 (d, 7.2, 1H, cyH), 5.97 (d, 7.2, 1H, cyH), 5.03 (s, 1H, H₂C=CRPh-), 3.40 (s, 3H, OCH₃), 3.73 (d, 9.9, 1H, H₂C=CRPh-), 3.24 (s, 3H, OCH₃), 2.47 (m, 1H, -CH₂CH₂CH₃), 2.29 (m, 1H, CH(CH₃)₂), 2.20 (m, 1H, -CH₂CH₂CH₃), 2.09 (br s, 3H, CH₃), 1.50 (m, 1H, -CH₂CH₂CH₃), 1.32 (m, 1H, -CH₂CH₂CH₃), 0.96 (t, 7.4, 3H, -CH₂CH₂CH₃), 0.96 (d, 6.8, 3H, CH(CH₃)₂), 0.66 (d, 6.8, 3H, CH(CH₃)₂).



Synthesis of C2b

4 Equivalents of 1-pentyne ($10 \mu\text{l}$, 0.10 mmol) were added to a solution of $[\text{Ru}((S)\text{-MeO-Biphep})(\eta^6\text{-}p\text{-cymene})](\text{SbF}_6)_2$ (31.6 mg, 0.025 mmol) in 0.5 ml CD_2Cl_2 . The remaining orange solution was heated at 35°C for 48 hours. The solvent was evaporated i.v. and the resulting powder was washed with 5x1 ml Et_2O . The orange product was dried i.v.

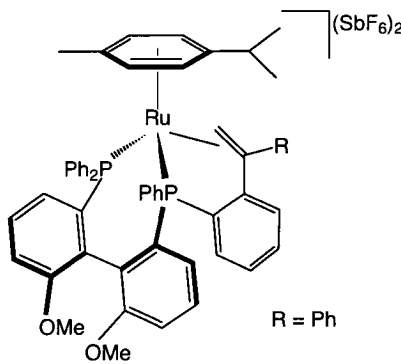
Color: orange. Yield: 29.5 mg (87%). Anal. Calcd for $\text{C}_{53}\text{H}_{54}\text{P}_2\text{O}_2\text{RuSb}_2\text{F}_{12}\cdot\text{Et}_2\text{O}$ (1357.6): C, 47.82; H, 4.51. Found: C, 47.45; H, 4.48. FAB-MS: Calcd. M^{2+} 886.1; Found M^{2+} 887.1; M^{2+} -*p*-cymene, 750.0; M^{2+} -*p*-cymene-C₅H₉, 682.9. NMR (DRX400, CD_2Cl_2): ³¹P, 39.7 (d, 56), 45.4 (d, 56); ¹³C, 159.1 (bb), 157.4 (bb), 144.8, 132.4-134.9, 129.5-131.1, 127.6 (bb), 126.3 (bb), 125.3 (bb), 126.1 (cy), 124.9 (bb), 123.1 (bb), 115.0 (bb), 114.2 (bb), 108.4 (cy), 106.2 (cy), 102.6 (cy), 95.2 (cy), 89.1 (RHC=CHPh-), 85.2 (RHC=CHPh-), 55.5 (OCH₃), 55.3 (OCH₃), 44.4 (-CH₂CH₂CH₃), 31.9 (CH(CH₃)₂), 27.7 (-CH₂CH₂CH₃), 25.1 (CH(CH₃)₂), 20.1 (CH₃), 18.3 (CH(CH₃)₂), 14.0 (-CH₂CH₂CH₃); ¹H, 6.91-8.09 (m, 24H), 6.83 (dd, 1H, H₂C=CPh-), 6.61 (d, 8.1, 1H, bb), 6.53 (d, 8.3, 1H, bb), 6.09 (d, 7.2, 1H, cyH), 5.92 (d, 12.6, 1H, RHC=CHPh-), 5.07 (d, 7.2, 1H, cyH), 5.00 (d, 6.4, 1H, cyH), 3.36 (s, 3H, OCH₃), 3.31 (s, 3H, OCH₃), 3.12 (m, 1H, RHC=CHPh-), 2.79 (m, 1H, -CH₂CH₂CH₃), 2.65 (m, 1H, CH(CH₃)₂), 2.10 (m, 1H, -CH₂CH₂CH₃), 2.00 (br s, 3H, CH₃), 1.92 (m, 1H, -CH₂CH₂CH₃), 1.92 (m, 1H, -CH₂CH₂CH₃), 1.10 (d, 6.9, 3H, CH(CH₃)₂), 1.29 (t, 7.3, 3H, -CH₂CH₂CH₃), 0.59 (d, 6.9, 3H, CH(CH₃)₂).



Synthesis of C3

Phenylacetylene ($5 \mu\text{l}$, 0.046 mmol) was added to a solution of $[\text{Ru}((S)\text{-MeO-Biphep})(\eta^6\text{-}p\text{-cymene})](\text{SbF}_6)_2$ (30.0 mg, 0.023 mmol) in 1 ml 1,2-C₂H₄Cl₂. After 2.5h at room temperature the ³¹P-NMR spectrum showed full conversion to the product. The solvent was evaporated i.v. and the resulting powder was washed with 5x1 ml Et_2O . The orange product was dried i.v.

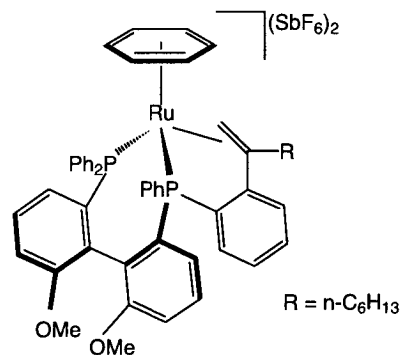
Color: orange. Yield: 30.7 mg (96%). Anal. Calcd for $\text{C}_{56}\text{H}_{52}\text{P}_2\text{O}_2\text{RuSb}_2\text{F}_{12}$ (1391.5): C, 48.34; H, 3.77. Found: C, 48.29; H, 3.72. FAB-MS: Calcd. M^{2+} 920.1; Found M^{2+} , 919.1; M^{2+} -*p*-cymene, 785.0; M^{2+} -*p*-cymene-C₈H₇, 683.0. NMR (DRX400, CD_2Cl_2): ³¹P, 41.4 (d, 54), 45.0 (d, 54); ¹³C, 158.8 (bb), 157.8 (bb), 147.9, 126.0-135.2, 120.9, 120.3, 114.6 (bb), 113.9 (bb), 108.8 (cy), 102.5 (cy), 93.1 (cy), 55.4 (OCH₃), 55.3 (OCH₃), 47.0 (H₂C=CPhPh-), 26.4 (cy), 24.5 (cy), 19.4 (cy), 17.6 (cy); ¹H, 6.92-8.12 (m, 29H), 6.53 (d, 8.3, 1H, bb), 6.44 (d, 8.4, 1H, bb), 6.05 (d, 6.7, 1H, cyH), 5.93 (s, 1H, H₂C=CPhPh-), 5.82 (d, 7.2, 1H, cyH), 5.65 (d, 7.2, 1H, cyH), 3.42 (d, 1.10, 1H, H₂C=CPhPh-), 3.42 (s,



3H, OCH₃), 3.34 (s, 3H, OCH₃), 1.50 (br s, 1H, CH₃), 0.53 (d, 7.0, 1H, CH(CH₃)₂), -0.22 (d, 6.6, 1H, CH(CH₃)₂), -0.41 (m, 1H, CH(CH₃)₂).

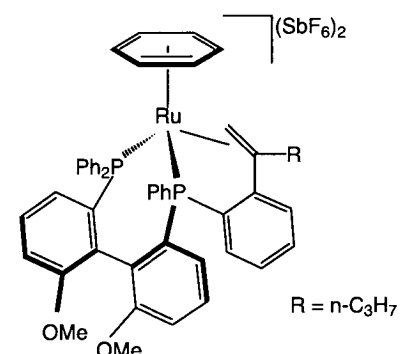
Synthesis of C4

1-Octyne (7 μ l, 0.048 mmol) was added to a solution of [Ru((S)-MeO-Biphep)(η^6 -benzene)](SbF₆)₂ (51.4 mg, 0.042 mmol) in 1 ml CD₂Cl₂. The remaining orange solution was heated at 35°C for 48h. The solvent was evaporated i.v. and the resulting powder was washed with 5x1 ml Et₂O. The orange product was dried i.v. Color: orange. Yield: 61.3 mg (95%). Anal. Calcd for C₅₂H₅₂P₂O₂RuSb₂F₁₂ (1343.5): C, 46.49; H, 3.90. Found: C, 46.83; H, 4.38. FAB-MS: Calcd. M²⁺ 872.1; Found M²⁺-benzene-C₈H₁₅+2SbF₆, 1029.1; M²⁺-benzene-C₈H₁₅+SbF₆, 919.1; M²⁺-benzene, 793.1; M²⁺-benzene-C₈H₁₅, 683.0. NMR (DRX400, CD₂Cl₂): ³¹P, 36.2 (d, 51), 45.8 (d, 51); ¹³C, 158.8 (bb), 157.8 (bb), 146.4 (H₂C=CRPh-), 137.4 (H₂C=CRPh-), 129.4-135.3, 126.9 (bb), 126.4 (bb), 125.9 (bb), 125.6 (bb), 123.1 (bb), 114.7 (bb), 114.3 (bb), 104.3 (C₆H₆), 55.1 (OCH₃), 55.1 (OCH₃), 55.1 (H₂C=CRPh-), 45.5 (-CH₂(CH₂)₄CH₃), 31.7 (-CH₂CH₂(CH₂)₃CH₃), 30.6 (-CH₂)₂CH₂(CH₂)₂CH₃), 29.3 (-CH₂)₃CH₂CH₂CH₃), 22.6 (-CH₂)₄CH₂CH₃), 14.0 (-CH₂)₅CH₃); ¹H, 7.15-7.89 (m, 22H), 6.98 (dd, 7.7, 11.5, 1H), 6.60 (d, 8.6, 1H, bb), 6.43 (d, 8.4, 1H, bb), 6.14 (s, 6H, C₆H₆), 5.38 (s, 1H, H₂C=CRPh-), 3.41 (s, 3H, OCH₃), 3.31 (d, 10.6, 1H, H₂C=CRPh-), 3.24 (s, 3H, OCH₃), 3.24 (m, 1H, -CH₂(CH₂)₄CH₃), 2.09 (m, 1H, -CH₂(CH₂)₄CH₃).



Synthesis of C5

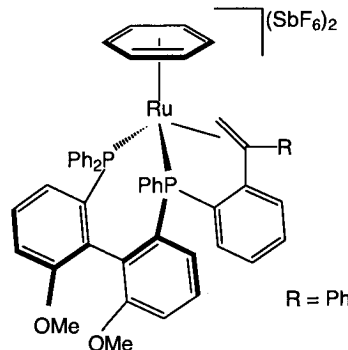
2.5 Equivalents of 1-pentyne (10 μ l, 0.048 mmol) were added to a solution of [Ru((S)-MeO-Biphep)(η^6 -benzene)](SbF₆)₂ (47.4 mg, 0.038 mmol) in 1 ml CD₂Cl₂. The remaining orange solution was heated at 35°C for 48h. The solvent was evaporated i.v. and the resulting powder was washed with 5x1 ml Et₂O. The orange product was dried i.v. Color: orange. Yield: 47.5 mg (96%). Anal. Calcd for C₄₉H₄₆P₂O₂RuSb₂F₁₂·Et₂O (1301.5): C, 46.28; H, 4.11. Found: C, 46.28; H, 4.11. FAB-MS: Calcd. M²⁺ 830.0; Found M²⁺-benzene, 749.0; M²⁺-benzene-C₅H₉, 683.0. NMR (DRX400, CD₂Cl₂): ³¹P, 36.2 (d, 51), 45.7 (d, 51); ¹³C, 158.9 (bb), 157.9 (bb), 146.2 (bb), 137.0 (H₂C=CRPh-), 133.1-134.0, 132.8, 132.2, 129.3-131.1, 126.6 (bb), 132.1 (bb), 114.8 (bb), 114.5 (bb), 104.4 (C₆H₆), 55.4 (H₂C=CRPh-), 55.4 (OCH₃), 55.2 (OCH₃), 47.4 (-CH₂CH₂CH₃), 23.6 (-CH₂CH₂CH₃), 13.8 (-CH₂CH₂CH₃); ¹H, 7.13-7.93 (m, 22H), 6.97 (dd, 8.1, 11.0, 1H), 6.60 (d, 8.5, 1H, bb), 6.43 (d, 8.5, 1H, bb), 6.18 (s, 6H, C₆H₆), 5.37 (s, 1H, H₂C=CRPh-), 3.41 (s, 3H, OCH₃), 3.30 (d, 10.8,



1H, $H_2C=CRPh-$), 3.25 (s, 3H, OCH₃), 3.19 (m, 1H, -CH₂CH₂CH₃), 2.12 (m, 1H, -CH₂CH₂CH₃), 1.33 (m, 1H, -CH₂CH₂CH₃), 0.89 (t, 7.5, 3H, -CH₂CH₂CH₃), 0.77 (m, 1H, -CH₂CH₂CH₃).

Synthesis of C6

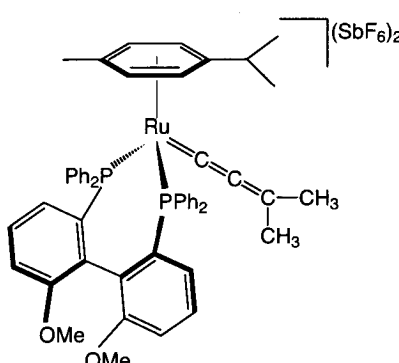
Phenylacetylene (10 μ l, 0.091 mmol) was added to a solution of [Ru((S)-MeO-Biphep)(η^6 -benzene)](SbF₆)₂ (39.5 mg, 0.032 mmol) in 0.5 ml CD₂Cl₂. The remaining orange solution was heated at 35°C for 3h. The solvent was evaporated i.v. and the resulting powder was washed with 5x1 ml Et₂O. The orange product was dried i.v. Color: orange. Yield: 41.5 mg (97%). Anal. Calcd for C₅₂H₄₄P₂O₂RuSb₂F₁₂ (1335.4): C, 47.72; H, 3.86. Found: C, 47.38; H, 3.62. FAB-MS: Calcd. M²⁺ 884.1; Found M²⁺-benzene+SbF₆, 1021.7; M²⁺-benzene, 785.9. NMR (DRX400, CD₂Cl₂): ³¹P, 36.4 (d, 53), 46.0 (d, 53); ¹³C, 159.2 (bb), 158.0 (bb), 147.1 (H₂C=CPhPh-), 129.9-133.4, 126.7(bb), 126.2 (bb), 125.8 (bb), 125.8 (bb), 123.6 (bb), 115.0 (bb), 114.5 (bb), 55.6 (OCH₃), 55.4 (OCH₃), 51.0 (H₂C=CPhPh-); ¹H, 6.42-8.59 (m, 30H), 6.18 (s, 1H, H₂C=CPhPh-), 5.64 (s, 6H, C₆H₆), 3.47 (s, 3H, OCH₃), 3.31 (s, 3H, OCH₃), 2.98 (d, 10.5, 1H, H₂C=CPhPh-).



Synthesis of C7

2-Methyl-3-butyn-2-ol (6 μ l, 0.101 mmol) was added to a solution of [Ru((S)-MeO-Biphep)(η^6 -*p*-cymene)](SbF₆)₂ (61.4 mg, 0.048 mmol) in 1.5 ml CD₂Cl₂. The remaining solution changed color from red to yellow. ³¹P-NMR indicated after 1.5h full conversion to the product. The solvent was evaporated i.v. and the remaining powder was washed with 3x1 ml Et₂O upon which the color changed to purple. The purple powder was dried i.v.

Color: orange. Yield: 58.6 mg (90%). Anal. Calcd for C₅₃H₅₂P₂O₂RuSb₂F₁₂ (1355.49): C, 46.96; H, 3.87. Found: C, 46.80; H, 3.96. FAB-MS: Calcd. M²⁺ 884.1; Found M²⁺ 885.2; M²⁺-*p*-cymene, 749.8; M²⁺-*p*-cymene-C₅H₆, 683.1. NMR (DRX400, CD₂Cl₂): ³¹P, 31.9 (d, 38), 47.7 (d, 38); ¹³C, 305.1 (CCCM₂), 204.0 (CCCM₂), 178.2 (CCCM₂), 159.9 (bb), 158.3 (bb), 129.5-133.3, 126.1, 123.4, 120.1, 120.6, 114.4 (bb), 114.3 (bb), 114.3 (cy), 108.8 (cy), 107.2 (cy), 105.5 (cy), 56.1 (OCH₃), 55.7 (OCH₃), 38.3 (CCCM₂), 32.3 (CH(CH₃)₂), 23.0 (CH(CH₃)₂), 20.2 (CH₃), 21.9 (CH(CH₃)₂); ¹H, 6.81-7.77 (m, 27H), 6.57 (d, 8.6, 1H, bb), 4.87 (d, 6.5, 1H, cyH), 4.72 (d, 7.2, 1H, cyH), 3.61 (s, 3H, OCH₃), 3.44 (s, 3H, OCH₃), 2.90 (m, 1H, CH(CH₃)₂), 2.04 (br s, 3H, CH₃), 1.81 (s, 6H, CCCM₂), 1.49 (d, 7.0, 3H, CH(CH₃)₂), 1.02 (d, 7.0, 3H, CH(CH₃)₂).



Pen-1-en-yl Benzoate (cat 5)

Benzoic acid (105.0 mg, 0.86 mmol), 1-pentyne (85 μ l, 0.86 mmol) and catalyst **5** (55.7 mg, 0.043 mmol) in 1 mL 1,2-C₂H₄Cl₂ were stirred at 35°C for 96h in a closed ampule under inert atmosphere (Ar). The product was purified by preparative TLC (eluent 95% hexane/5% ethyl acetate) to afford 39.3 mg (24%) of the Pen-1-en-yl benzoate (cis:trans, 69%:31%).

Pen-1-en-yl Benzoate (cat 6)

Benzoic acid (104.8 mg, 0.86 mmol), 1-pentyne (85 μ l, 0.86 mmol) and catalyst **6** (55.3 mg, 0.045 mmol) in 1 mL 1,2-C₂H₄Cl₂ were stirred at 35°C for 96h in a closed ampule under inert atmosphere (Ar). The product was purified by preparative TLC (eluent 95% hexane/5% ethyl acetate) to afford 29.4 mg (18%) of the Pen-1-en-yl benzoate (cis:trans, 75%:25%).

Characterisation of Pen-1-en-yl Benzoate

NMR (DPX300, CDCl₃): ¹³C, (major product, Z-product), 164.0 (C=O), 134.7 (CH), 133.8 (CH), 130.0 (CH), 129.9 (CH), 128.9 (CH), 115.1 (CH), 27.1 (CH₂), 22.8 (CH₂), 14.1 (CH₃); (minor product, E-product) 164.3 (C=O), 136.1 (CH), 133.7 (CH), 130.3 (CH), 129.7 (CH), 128.8 (CH), 115.9 (CH), 29.8 (CH₂), 23.1 (CH₂), 14.0 (CH₃); ¹H, 8.08-8.16, 7.57-7.66, 7.44-7.54, 7.34 (m, 12.3), 7.30 (m, 6.4), 5.63 (dt, 12.3, 7.7), 5.04 (dt, 7.4, 6.4), 2.30 (m), 2.08 (m), 1.41-1.57, 0.99 (t, 7.4), 0.97 (t, 7.4).

Oct-1-en-yl Benzoate (cat 5)

Benzoic acid (106.0 mg, 0.87 mmol), 1-octyne (130 μ l, 0.88 mmol) and catalyst **5** (54.6 mg, 0.044 mmol) in 1 mL 1,2-C₂H₄Cl₂ were stirred at 60°C for 24h in a closed ampule under inert atmosphere (Ar). The reaction mixture was washed with aqueous NaHCO₃ solution and dried over MgSO₄. The product was purified by silica gel chromatography (eluent 95% hexane/5% ethyl acetate) to afford 135.7 mg (71%) of the Oct-1-en-yl benzoate (Z:E, 73%:27%).

Oct-1-en-yl Benzoate (cat 6)

Benzoic acid (105.4 mg, 0.86 mmol), 1-octyne (130 μ l, 0.88 mmol) and catalyst **6** (56.0 mg, 0.043 mmol) in 1 mL 1,2-C₂H₄Cl₂ were stirred at 60°C for 24h in a closed ampule under inert atmosphere (Ar). The reaction mixture was washed with aqueous NaHCO₃ solution and dried over MgSO₄. The product was purified by silica gel chromatography (eluent 95% hexane/5% ethyl acetate) to afford 122.4 mg (64%) of the Oct-1-en-yl benzoate (Z:E, 80%:20%).

Oct-1-en-yl Benzoate (cat C7)

Benzoic acid (53.9 mg, 0.44 mmol), 1-octyne (65 μ l, 0.44 mmol) and catalyst **C7** (31.2 mg, 0.023 mmol) in 0.5 mL 1,2-C₂H₄Cl₂ were stirred at 60°C for 24h in a closed ampule under inert atmosphere (Ar). The reaction mixture was washed with aqueous NaHCO₃ solution and dried over MgSO₄. The product was purified by silica gel chromatography (eluent 95% hexane/5% ethyl acetate) to afford 60.6 mg (62%) of the Oct-1-en-yl benzoate (Z:E, 70%:30%).

Characterisation of Oct-1-en-yl Benzoate.

NMR (DPX300, CDCl₃): ¹³C, (major product, Z-product), 164.0 (C=O), 134.6 (CH), 133.8 (CH), 130.3

(CH), 129.9 (CH), 128.9 (CH), 115.3 (CH), 32.7 (CH₂), 29.6 (CH₂), 29.3 (CH₂), 25.0 (CH₂), 23.0 (CH₂), 14.5 (CH₃); (minor isomer, *E*-product) 164.0 (C=O), 136.0 (CH), 133.7 (CH), 129.8 (CH), 128.8 (CH), 116.1 (CH), 32.0 (CH₂), 30.0 (CH₂), 29.2 (CH₂), 27.8 (CH₂), 23.1 (CH₂), 14.5 (CH₃); ¹H, 8.09-8.17, 7.56-7.66, 7.44-7.54, 7.34 (minor isomer, dt, 12.5, 1.5), 7.29 (major isomer, dt, 6.4, 1.5), 5.63 (minor isomer, dt, 12.5, 7.4), 5.03 (major isomer, dt, 7.4, 6.4), 2.32 (major isomer, m), 2.10 (minor isomer, m), 0.81-1.00 (m), 1.20-1.55 (m),

Synthesis of **1-octyne-d₁**

To 1-octyne (1 mL, 6.8 mmol), MeLi (5 mL, 0.1584 M in Et₂O) was slowly added. After 0.5h stirring, the reaction mixture was quenched with 5 mL D₂O. The volume of the reaction mixture was increased by adding 5 mL dried Et₂O. The two liquid layers were separated and the Et₂O layer was dried over MgSO₄. Evaporation of the Et₂O lead to the colorless product. NMR (DPX300): ²H (acetone), 2.23 (br s); ¹H (d₆-acetone), 2.16 (2H, t, 6.6), 1.22-1.57 (8H, m), 0.90 (3H, t, 6.9).

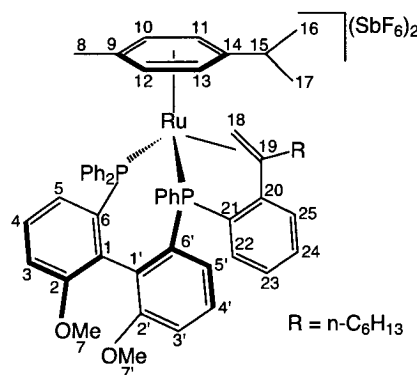
Catalytic reaction with **1-octyne-d₁**

Benzoic acid (105.7 mg, 0.87 mmol), 1-octyne-d₁ (130 μl, 0.88 mmol) and catalyst 5 (54.0 mg, 0.043 mmol) in 1 mL 1,2-C₂H₄Cl₂ were stirred at 60°C for 24 h. The same conditions and work-up as for catalysis with 1-octyne were applied.

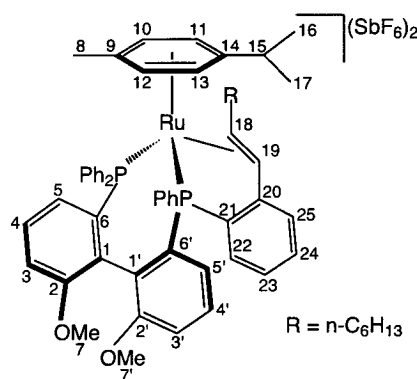
NMR (DPX300): ²H (acetone), 7.31 (37%, br s), 5.70 (16%, br s), 5.09 (47%, br s); ¹H (d₆-acetone), 8.05-8.15, 7.64-7.73, 7.51-7.60, 7.33 (minor isomer, dt, 12.5, 1.5), 7.27 (major isomer, dt, 6.4, 1.5), 5.58 (minor isomer, dt, 12.5, 7.4), 5.08 (major isomer, dt, 7.4, 6.4), 2.32 (major isomer, m), 2.10 (minor isomer, m), 0.80-0.99 (m), 1.21-1.57 (m).

3.5.3. Selected NMR-data

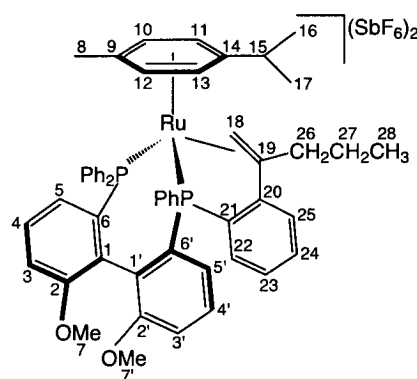
Table 6: Selected NMR-data for C1a



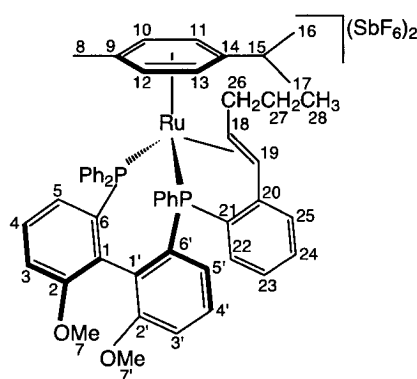
position			position		
	$\delta^{31}\text{P}$				
1	45.6				
2	38.7				
	$\delta^1\text{H}$	$\delta^{13}\text{C}$		$\delta^1\text{H}$	$\delta^{13}\text{C}$
1	-	128.4	1'	-	129.6
2	-	158.0	2'	-	158.3
3	6.43	114.7	3'	6.55	114.6
4	7.25	130.6	4'	7.14	129.7
5	7.63	124.9	5'	7.32	123.3
6	-	128.3	6'	-	126.9
7	3.44	55.3	7'	3.25	55.1
8	2.18	20.0	18(a/b)	5.00/3.75	55.4
9	-	121.7	19	-	133.0
10	6.18	102.5	20	-	145.4
11	5.88	103.3	21	-	136.0
12	6.86	100.8	22	6.92	134.4
13	5.97	106.3	23	7.23	129.1
14	-	134.1	34	7.42	132.5
15	2.35	31.0	25	7.20	126.7
16	0.70	20.5			
17	0.96	22.9			

Table 7: Selected NMR-data for C1b

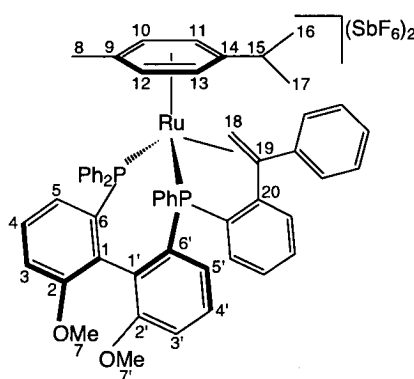
position			position		
	$\delta^{31}\text{P}$				
1	45.5				
2	39.9				
	$\delta^1\text{H}$	$\delta^{13}\text{C}$		$\delta^1\text{H}$	$\delta^{13}\text{C}$
1	-	129.6	1'	-	124.9
2	-	158.0	2'	-	159.4
3	6.54	115.3	3'	6.62	114.5
4	7.13	130.4	4'	7.26	129.8
5	7.37	126.0	5'	7.37	123.1
6	-	126.6	6'	-	128.4
7	3.37	55.6	7'	3.31	55.4
8	2.00	20.2	18	3.11	85.6
9	-	127.6	19	5.91	89.2
10	5.10	103.0	20	-	144.8
11	6.11	108.6	21	-	131.2
12	7.38	95.4	22	6.84	133.9
13	5.01	106.3	23	7.34	128.8
14	-	126.1	34	7.61	133.6
15	2.65	32.2	25	7.54	128.4
16	0.59	18.5			
17	1.12	25.1			

Table 8: Selected NMR-data for C2a

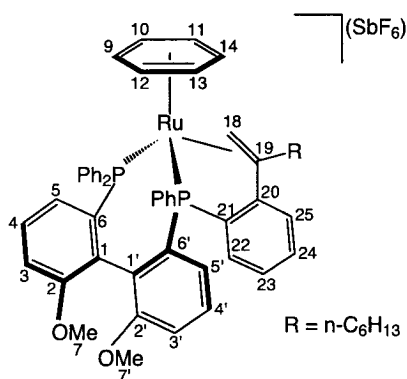
position			position		
	$\delta^{31}\text{P}$				
1	45.7				
2	39.0				
	$\delta^1\text{H}$	$\delta^{13}\text{C}$		$\delta^1\text{H}$	$\delta^{13}\text{C}$
1	-	128.4	1'	-	126.4
2	-	157.9	2'	-	158.3
3	6.42	114.6	3'	6.54	114.5
4	7.24	130.5	4'	7.12	129.6
5	7.64	124.9	5'	7.28	123.4
6	-	128.4	6'	-	127.2
7	3.24	55.0	7'	3.40	55.4
8	2.09	20.0	18(a/b)	5.03/3.73	55.4
9	-	122.1	19	-	
10	6.14	102.3	20	-	145.2
11	5.97	103.5	21	-	136.3
12	6.89	100.1	22	6.91	134.2
13	6.04	106.7	23	7.21	129.1
14	-	133.8	34	7.40	132.4
15	2.29	30.9	25	7.16	126.7
16	0.66	19.8	26	2.20/2.47	48.0
17	0.96	23.1	27	1.32/1.50	25.6
			28	0.96	13.8

Table 9: Selected NMR-data for C2b

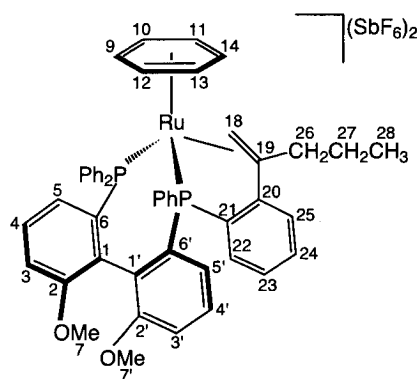
position			position		
	$\delta^{31}\text{P}$				
1	45.4				
2	39.7				
	$\delta^1\text{H}$	$\delta^{13}\text{C}$		$\delta^1\text{H}$	$\delta^{13}\text{C}$
1	-	129.3	1'	-	124.5
2	-	157.4	2'	-	159.1
3	6.53	115.0	3'	6.61	114.2
4	7.12	130.3	4'	7.26	129.7
5	7.37	125.3	5'	7.38	123.1
6	-	126.3	6'	-	127.6
7	3.36	55.5	7'	3.31	55.3
8	2.00	20.1	18	3.12	85.2
9	-	127.7	19	5.92	89.1
10	5.07	102.6	20	-	144.8
11	6.09	108.4	21	-	132.7
12	7.40	95.2	22	6.83	133.8
13	5.00	106.2	23	7.33	128.5
14	-	126.1	24	7.61	133.8
15	2.65	31.9	25	7.54	128.3
16	0.59	18.5	26	2.10/2.79	44.4
17	1.10	25.1	27	1.92/1.92	27.7
			28	1.29	14.0

Table 10: Selected NMR-data for C3

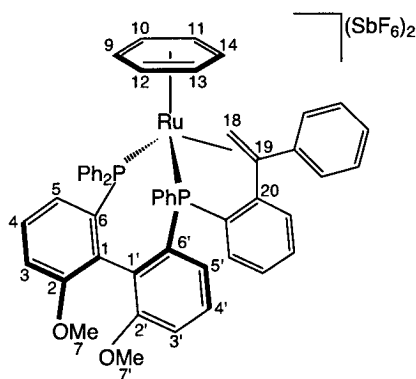
position			position		
	$\delta^{31}\text{P}$				
1	45.0				
2	41.4				
	$\delta^1\text{H}$	$\delta^{13}\text{C}$		$\delta^1\text{H}$	$\delta^{13}\text{C}$
1	-	126.0	1'	-	128.8
2	-	158.8	2'	-	157.8
3	6.53	113.9	3'	6.44	114.6
4	7.12	129.5	4'	7.17	130.6
5	7.17	124.5	5'	7.48	126.0
6	-	129.9	6'	-	130.8
7	3.42	55.4	7'	3.34	55.3
8	1.50	19.4	18(a/b)	5.93/3.42	47.0
9	-	125.2	19	-	
10	5.65	102.5	20	-	147.9
11	6.05	108.0			
12	7.17	93.1			
13	5.82	106.4			
14	-	130.7			
15	-0.41	26.4			
16	0.53	24.5			
17	-0.22	17.6			

Table 11: Selected NMR-data for C4

position			position		
	$\delta^{31}\text{P}$				
1	45.8				
2	32.6				
	$\delta^1\text{H}$	$\delta^{13}\text{C}$		$\delta^1\text{H}$	$\delta^{13}\text{C}$
1	-	128.3	1'	-	125.9
2	-	157.8	2'	-	158.8
3	6.53	114.7	3'	6.44	114.3
4	7.12	130.7	4'	7.17	129.7
5	7.17	125.6	5'	7.48	123.1
6	-	126.4	6'	-	126.9
7	3.42	55.1	7'	3.34	55.1
9-14	6.14	104.3	18(a/b)	5.38/3.31	55.1
			19	-	137.4
			20	-	146.4
			21	-	133.4
			22	6.98	134.9
			23	7.34	129.2
			24	7.58	133.8
			25	7.40	126.2

Table 12: Selected NMR-data for C5

position			position		
	$\delta^{31}\text{P}$				
1	45.7				
2	32.6				
	$\delta^1\text{H}$	$\delta^{13}\text{C}$		$\delta^1\text{H}$	$\delta^{13}\text{C}$
1	-	128.3	1'	-	125.8
2	-	157.9	2'	-	158.9
3	6.43	114.8	3'	6.60	114.5
4	7.23	130.9	4'	7.25	129.9
5	7.59	125.6	5'	7.63	123.1
6	-	126.3	6'	-	126.6
7	3.25	55.2	7'	3.41	55.4
9-14	6.18	104.4	18(a/b)	5.37/3.30	55.4
			19	-	137.0
26	3.19/2.12	47.4	20	-	146.2
27	1.33/0.77	23.6	21	-	133.5
28	0.89	13.8	22	6.97	134.8
			23	7.34	129.2
			24	7.58	133.6
			25	7.40	126.5

Table 13: Selected NMR-data for C6

position			position		
	$\delta^{31}\text{P}$				
1	46.0				
2	36.4				
	$\delta^1\text{H}$	$\delta^{13}\text{C}$		$\delta^1\text{H}$	$\delta^{13}\text{C}$
1	-	128.3	1'	-	128.7
2	-	159.2	2'	-	158.0
3	6.68	114.5	3'	6.49	115.0
4	7.31	133.8	4'	7.25	133.7
5	7.70	123.6	5'	7.65	125.8
6	-	126.7	6'	-	126.2
7	3.47	55.6	7'	3.31	55.4
9-14	5.64	105.3	18	6.12/2.98	51.0
			19	-	
			20	-	147.1

3.6 References

- (1)Colquhoun, H. M.; Holton, J.; Thompson, D. J.; Twigg, M. V. *New Pathways for Organic Synthesis*; Plenum Press: New York, 1984; pp 350.
- (2)Almond, M. R.; Stimmel, J. B.; Thompson, E. A.; Loudon, G. M. *Org. Synth.* **1987**, *66*, 132; Katritzky, A. R.; Urogdi, L.; Mayence, A. *J. Org. Chem.* **1990**, *55*, 2206.
- (3)Kitamura, M.; Noyori, R.; Takaya, H. *Tetrahedron Lett.* **1987**, *28*, 4829.
- (4)Rothman, E. S.; Hecht, S. S.; Pfeffer, P. E.; Silbert, J. L. *J. Org. Chem.* **1972**, *37*, 3551; Larock, R. C.; Oertle, K.; Beatty, K. M. *J. Am. Chem. Soc.* **1980**, *102*, 1966; Kita, Y.; Abkai, N.; Ajimura, N.; Yoshigi, M.; Tsugoshi, T.; Yasuda, H.; Tamura, Y. *J. Org. Chem.* **1986**, *51*, 4150.
- (5)Fahey, R. C.; Lee, D. J. *J. Am. Chem. Soc.* **1966**, *88*, 5555.
- (6)Hudrlik, P. F.; Hudrlik, A. M. *J. Org. Chem.* **1973**, *38*, 4254.
- (7)Mitsudo, T.; Hori, Y.; Watanabe, Y. *J. Org. Chem.* **1985**, *50*, 1566.
- (8)Bruneau, C.; Dixneuf, P. H. *Chem. Commun.* **1997**, 507.
- (9)Bruneau, C.; Neveux, M.; Kabouche, Z.; Ruppin, C.; Dixneuf, P. H. *Synlett* **1991**, 755.
- (10)Doucet, H.; Martinvacá, B.; Bruneau, C.; Dixneuf, P. H. *J. Org. Chem.* **1995**, *60*, 7247.
- (11)Mitsudo, T.; Hori, Y.; Yamakawa, Y.; Watanabe, Y. *Tetrahedron Lett.* **1986**, *27*, 2125; Hori, Y.; Mitsudo, T.; Watanabe, Y. *J. Organomet. Chem.* **1987**, *321*, 397; Mitsudo, T.; Hori, Y.; Yamakawa, Y.; Watanabe, Y. *J. Org. Chem.* **1987**, *52*, 2230.
- (12)Ruppin, C.; Dixneuf, P. H. *Tetrahedron Lett.* **1986**, *27*, 6323; Ruppin, C.; Dixneuf, P. H.; Lecolier, S. *Tetrahedron Lett.* **1988**, *29*, 5365.
- (13)Rotem, M.; Shvo, Y. *Organometallics* **1983**, *2*, 1689.
- (14)Feiken, N.; Pregosin, P. S.; Trabesinger, G.; Albinati, A.; Evoli, G. L. *Organometallics* **1997**, *16*, 5756.
- (15)Feiken, N.; Pregosin, P. S.; Trabesinger, G.; Scalzone, M. *Organometallics* **1997**, *16*, 537.
- (16)The ^{31}P -NMR characteristics are for this species ($\delta = 22.5$ and $\delta = 45.0$) are normal, i. e., within the region observed for the complexes **C1-C6**, but not consistent with a cyclometallated four membered ring (Umeza-Vizzini, K; Lee, T. R.. *Organometallics* **1997**, *16*, 5613). Complex **6** is observed in reactions without benzoic acid. One possibility for this species is an η^2 -acetylene complex.
- (17)Abbenhuis, H. C. L.; Pfeffer, M.; Sutter, J. P.; Decian, A.; Fischer, J.; Ji, H. L.; Nelson, J. H. *Organometallics* **1993**, *12*, 4464.
- (18)Fernandez, S.; Pfeffer, M.; Rotleng, V.; Sirlin, C. *Organometallics* **1999**, *18*, 2390.
- (19)Bruce, M. I.; Goodall, B. L.; Stone, F. G. *J. Chem. Soc., Dalton Trans.* **1978**, 678.
- (20)Ryabov, A. D. *Chem. Rev.* **1990**, *90*, 403.
- (21)Davies, R.; Kane-Maguire, L. A. P. *Comprehensive Organometallic Chemistry*; Pergamon Press: Oxford, New York, 1982; Vol. 3; pp 953-1077.
- (22)Koelle, U.; Rietmann, C.; Tjoe, J.; Wagner, T.; Englert, U. *Organometallics* **1995**, *14*, 703.
- (23)Ferstl, W.; Sakodinskaya, I. K.; BeydounSutter, N.; LeBorgne, G.; Pfeffer, M.; Ryabov, A. D. *Organometallics* **1995**, *14*, 703.

-
- metallics* **1997**, *16*, 411.
- (24)Ghosh, K.; Chattopadhyay, S.; Pattanayak, S.; Chakravorty, A. *Organometallics* **2001**, *20*, 1419; Ghosh, K.; Pattanayak, S.; Chakravorty, A. *Organometallics* **1998**, *17*, 1956.
- (25)Lee, H. M.; Yao, J. Z.; Jia, G. C. *Organometallics* **1997**, *16*, 3927.
- (26)Pregosin, P. S.; Valentini, M. *Enantiomer* **1999**, *4*, 529; Pregosin, P. S.; Trabesinger, G. *J. Chem. Soc., Dalton Trans.* **1998**, 727; Pregosin, P. S.; Salzmann, R. *Coord. Chem. Rev.* **1996**, *155*, 35.
- (27)The estimated ^{13}C -NMR chemical shifts of the uncomplexed olefin carbons of $\text{CH}_2=\text{C}(\text{Ph})\text{C}_6\text{H}_{13}$ are 112.6 ppm and 148.1 ppm, for the terminal and interanl olefinic carbons, respectively. Consequently, 133.0 ppm represents, a coordination chemical shift of ca. 15 ppm for the internal olefinic carbon.
- (28)Mann, B. E.; Taylor, B. F. ^{13}C NMR Data for Organometallics Compounds; Academic Press: London, 1981.
- (29)Verkade, J. G.; Mosbo, J. A. In Stereospecificity in ^1J Coupling to Metals; Verka, J. G., Mosbo, J. A., Eds.; VCH: Deerfield Beach, FL, 1987; Vol. 8, pp 425-463.
- (30)delosRios, I.; Tenorio, M. J.; Padilla, J.; Puerta, M. C.; Valerga, P. *Organometallics* **1996**, *15*, 4565; Sustmann, R.; Patzke, B.; Boese, R. *J. Organomet. Chem.* **1994**, *470*, 191.
- (31)Wiles, J. A.; Lee, C. E.; McDonald, R.; Bergens, S. H. *Organometallics* **1996**, *15*, 3782.
- (32)Faller, J. W.; Chase, K. J. *Organometallics* **1995**, *14*, 1592.
- (33)Hansen, H. D.; Maitra, K.; Nelson, J. H. *Inorg. Chem.* **1999**, *38*, 2150; Asano, H.; Katayama, K.; Kurosawa, H. *Inorg. Chem.* **1996**, *35*, 5760; Brunner, H.; Oeschey, R.; Nuber, B. *Organometallics* **1996**, *15*, 3616; Beck, U.; Hummel, W.; Burgi, H. B.; Ludi, A. *Organometallics* **1987**, *6*, 20.
- (34)Jones, N. D.; MacFarlane, K. S.; Smith, M. B.; Schutte, R. P.; Rettig, S. J.; James, B. R. *Inorg. Chem.* **1999**, *38*, 3956; Pathak, D. D.; Adams, H.; Bailey, N. A.; King, P. J.; White, C. J. *J. Organomet. Chem.* **1994**, *479*, 237.
- (35)We cannot exclude the presence of doubly deuterated and fully protonated olefinic compounds. Both carbene and acetylene mechanisms could involve exchange of the terminal-D and the benzoic acid-H.
- (36)Jafarpour, L.; Huang, J.; Stevens, E. D.; Nolan, S. P. *Organometallics* **1999**, *18*, 3760.
- (37)Pilette, D.; Ouzzine, K.; Le Bozec, H.; Dixneuf, P. H.; Rickard, C. E. F.; Roper, W. R. *Organometallics* **1992**, *11*, 809.
- (38)SAINT, Version 4; Siemens Analytical X-ray Systems, Inc., Madison, WI, 1994-1996.
- (39)Sheldrick, G. SADABS; Göttingen, Germany, 1997.
- (40)SHELXL program package, version 5.1; Bruker AXS, Inc., Madison, WI, 1997.
- (41)den Reijer, C. J.; Dotta, P.; Pregosin, P. S.; Albinati, A. *Can. J. Chem.* **2001**, *79*, 693.

Seite Leer /
Blank leaf

Chapter 4

P-C Bond Splitting: Induced by $\text{CF}_3\text{SO}_3\text{H}$, HBF_4 and $(\text{Bu}_4\text{N})(\text{Ph}_3\text{SiF}_2)$

4.1 Abstract

The solid-state structures of the precursors $[\text{Ru}(\text{OAc})_2((S)\text{-L1a})]$ or $[\text{Ru}(\text{OAc})_2((R)\text{-L1b})]$ ($(S)\text{-L1a}$ = (S) -MeO-Biphep and $(R)\text{-L1b}$ = (R) -3,5-di-*t*-Bu-MeO-Biphep) respectively **9a** and **9b** are reported.

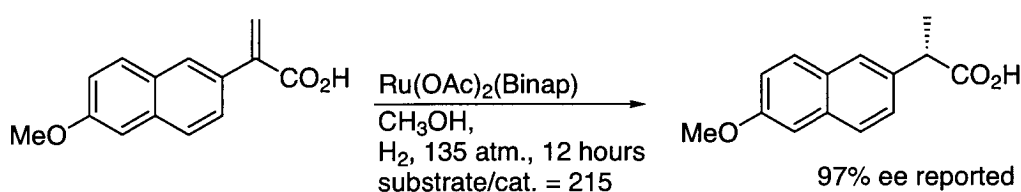
Reaction of $[\text{Ru}(\text{OAc})_2(\text{L1a}$ or **L2**)] (**L2** = Binap), respectively **9a** and **10**, with wet $\text{CF}_3\text{SO}_3\text{H}$ (= HOTf) in 1,2-dichloroethane at 90°C results in stereospecific P-C bond breaking to afford the cationic triflates $[\text{Ru}(\text{OTf})(6'\text{-diphenylphosphino-1'}\text{-(2-dimethoxy)-biphenyl})(\text{PPh}_2\text{OH})](\text{OTf})$, **C1**, and $[\text{Ru}(\text{OTf})(6'\text{-diphenylphosphino-1-naphthyl})(\text{PPh}_2\text{OH})](\text{OTf})$, **C2**. Formally, the H^+ protonates the acetate and water adds stereospecifically across the P-C bond with the resulting arene ring complexed η^6 to the Ru(II). The solid-state structures of **C1** and **C2** are reported.

A related reaction of $[\text{Ru}(\text{OAc})_2(\text{L1a}, \text{L1b}$ or **L2**)] with HBF_4 gives P-C bond cleavage with the formation of compounds, **C3-C5**, which contains the new phosphinite anion ($\text{C}_{12}\text{H}_{11}\text{BF}_2\text{O}_2\text{P}$), derived from hydrolysis of the BF_4^- anion. The solid-state structure of **C4** is reported. NMR studies at -60°C on the reaction mixture derived from $\text{Ru}(\text{OAc})_2(\text{L2})$ and HBF_4 show an HF addition product, **C6**, containing a Ru-F---H moiety with ${}^1J({}^{19}\text{F}, {}^1\text{H}) = 66$ Hz. Warming of this mixture to 0°C give P-C bond breaking and isolable complexes, **C7a** and **C7b**, containing the fluorophosphine, Ph_2PF . Complex **C8**, a Ru-Cl-analog of **C7** with complexed Ph_2PF , has also been isolated.

Reaction of $[\text{Ru}(\text{L2})(\text{arene})](\text{SbF}_6)_2$ (arene = η^6 -*p*-cymene, **26**, or η^6 -benzene, **27**) with $(\text{Bu}_4\text{N})(\text{Ph}_3\text{SiF}_2)$ leads to cyclometallated products **C9** and **C10** which arises via P-C bond breaking and P-F bond making.

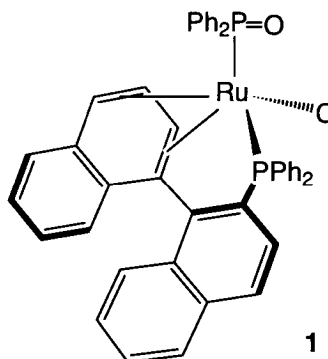
4.2 Introduction

Since naproxen and many other chiral 2-acrylpropionic acids represent high-value pharmaceutical products, there has been significant interest in the development of a practical process based on the efficient asymmetric hydrogenation of the 2-arylacrylic acids. An important breakthrough using [Ru(OAc)₂(Binap)] as a catalyst precursor was achieved by Noyori et al. (Scheme 1).¹



Scheme 1. The asymmetric hydrogenation of 2-(6'-methoxy-2'-naphthyl)acrylic acid using [Ru(OAc)₂(Binap)] as catalyst precursor.

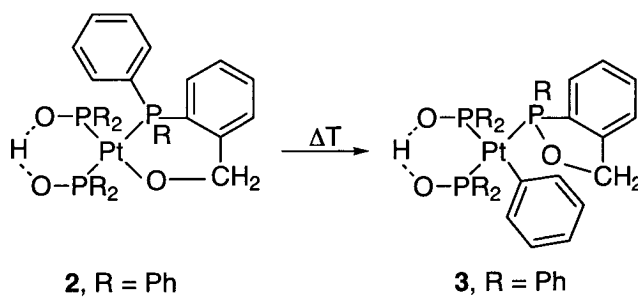
Monsanto² has reported attempts to optimise the preparation of the [Ru(OAc)₂(Binap)] catalyst which is derived from the reaction between NaOAc and Ru₂(Binap)₂Cl₄(NEt₃).³ The latter is obtained from the reaction of [Ru(COD)Cl₂]_n (COD = 1,5-cyclooctadiene) with Binap in presence of an excess triethylamine. The mixture of chloro-ruthenium-Binap complexes obtained from the one-pot reaction carried out in the absence of NaOAc, catalyses the asymmetric hydrogenation of 2-(6'-methoxy-2'-naphthyl)acrylic acid with excellent rates and enantioselectivities. However, complex **1** in which one of the phosphorus-naphthyl bonds in the Binap ligand was cleaved, was found to be inactive.



Since **1** accounted for a large portion of the mixed complexes (ca. 50%), it was obvious that the catalytic activity of the mixed species would be substantially increased if the formation of **1** could be avoided.

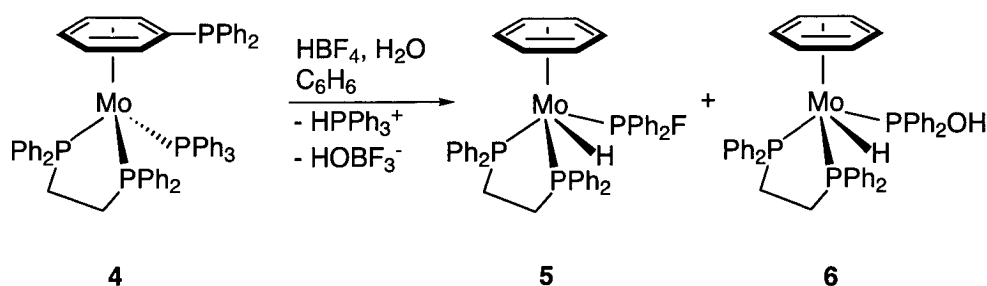
Clearly, P-C bond cleavage can represent an undesirable (but interesting) side reaction in homogeneous catalysis. It is of importance to understand the mechanisms of these reactions in order to improve our understanding of catalytic relevant mechanistic processes.

Interesting new metal complexes derived from P-C bond cleavage have been described in the literature.^{4,5} For example, van Leeuwen et al.⁶ have described the rearrangement of the cyclic platinum alkoxide **2** to **3** as shown in Scheme 2. Alkoxide complexes are intermediates in industrial processes such as the conversion of syngas to methanol or ethylene glycol. Complex **2** is believed to rearrange via a nucleophilic attack at the coordinated phosphorus center by the alkoxy group, followed by a shift of a phenyl group from the phosphorus to platinum. Possibly, this type of P-C bond splitting reaction is related to the decomposition of arylphosphines in syngas reactions with late transition-metal catalysts.



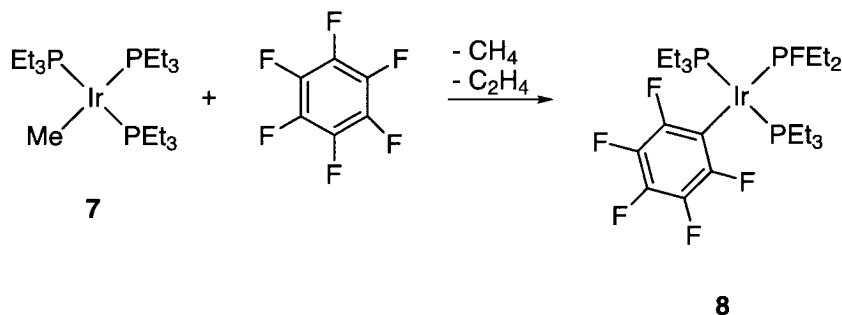
Scheme 2. The P-C bond cleavage in cyclic platinum complex **2** resulting in complex **3**.

Protonation of organometallic compounds is a well-established means of generating-metal-bound hydrides. However, it can also result in undesired P-C bond cleavage. Although examples are scarce, Morris et al.⁷ have recently reported on a P-C bond cleavage induced by HBF₄ in the Mo-arene complexes (Scheme 3). Addition of HBF₄ to [Mo(η^6 -PhPPh₂)(dppe)(PPh₃)] (dppe = Ph₂PCH₂CH₂PPh₂), **4**, in benzene leads to complex **5** in which a new P-F bond is generated, and to hydroxyphosphine complex **6**



Scheme 3. P-C bond cleavage induced by protonation of complex **4** resulting in **5** and **6**.

Another P-C bond cleavage along with C-F bond activation has been reported by Milstein et al.⁸ Upon reaction of $[\text{IrMe}(\text{PEt}_3)_3]$, **7**, with hexafluorobenzene at 60°C in benzene, complex **8** together with methane and ethylene were generated.

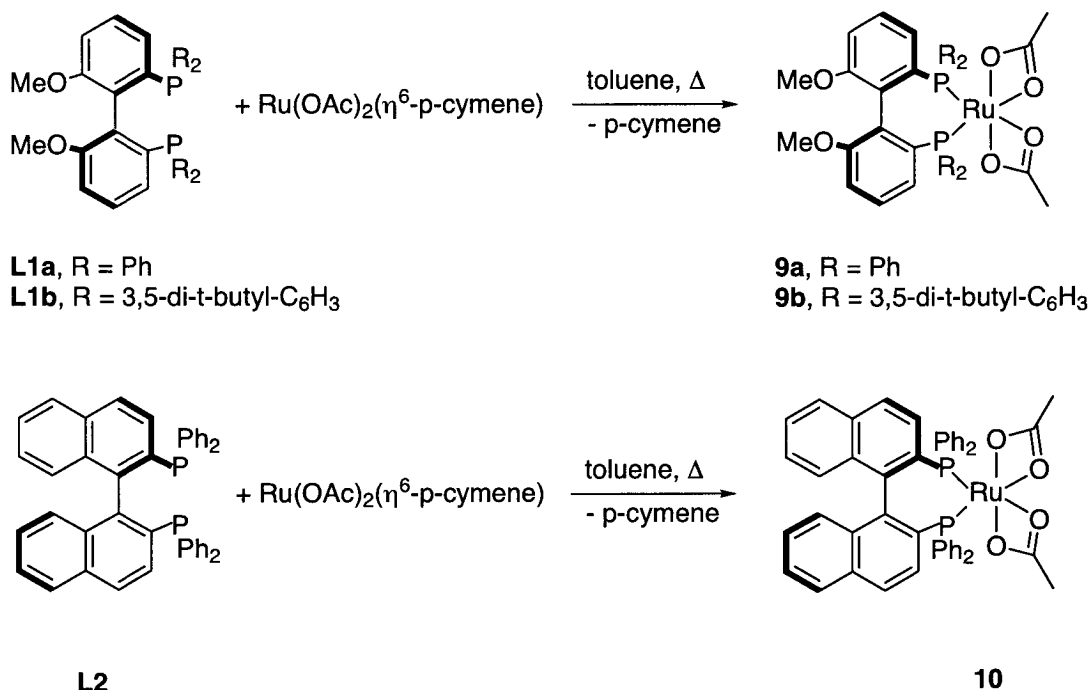


Scheme 4. P-C bond splitting in Ir(I)-complex **7** resulting in fluoro-phosphine Ir(1)-complex **8**.

4.3 Results and discussion

4.3.1 Solid-state structures of precursor

Given the interest in asymmetric hydrogenation,⁹ several [Ru(OAc)₂(biphosphine)]^{10,11} complexes have been prepared and studied. Treatment of [Ru(OAc)₂(η^6 -*p*-cymene)] with (*S*)-MeO-Biphep¹² ((*S*)-**L1a**), (*R*)-3,5-di-*t*-Bu-MeO-Biphep¹² ((*R*)-**L1c**) or Binap¹³ (**L2**) in toluene affords the yellow solids of [Ru(OAc)₂((*S*)-**L1a**)], (*R*)-**L1c** or **L2**, respectively **9a**, **9b** and **10**, in good yields (Scheme 5). Suitable crystals of **9a** and **9b** for X-ray diffraction could be obtained from a saturated toluene solution. The syntheses of these complexes^{3,14} has been described in the literature, however, no solid-state structures for **9a** and **9b** have been reported so far.



Scheme 5. Preparation of complexes **9a**, **9b** and **10**.

The structures of **9a** and **9b** were determined by X-ray diffraction and views of the cations are shown in Figures 1 and 2, respectively. The immediate coordination spheres of both cations contain two anionic bidentate acetate ligands and two phosphorus donors of the biarylphosphine ligand. The structures show a distorted octahedral coordination geometry around Ru(II). Table 1 shows a list of selected bond lengths and bond angles for **9a** and **9b**.

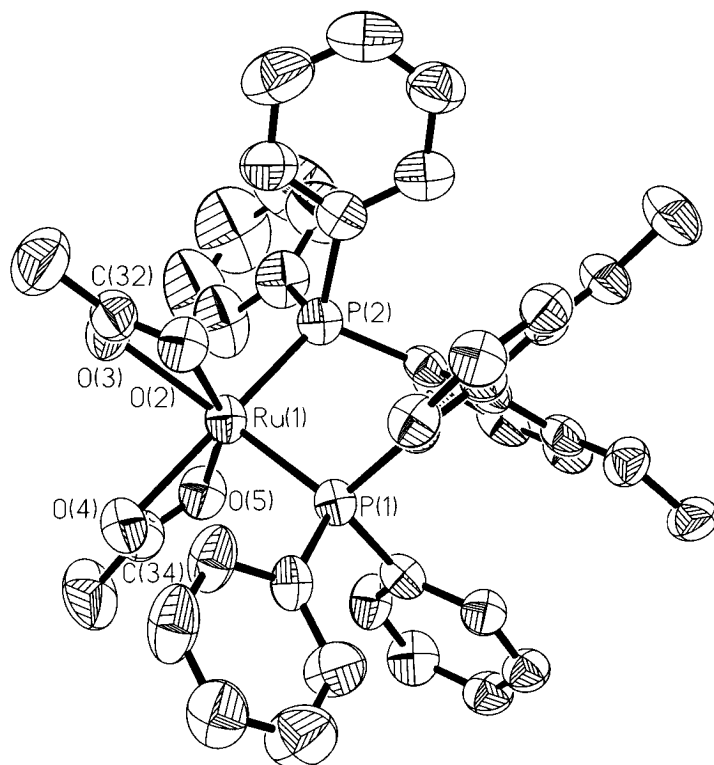


Figure 1. View of the structure of the cation of **9a**, 50% ellipsoids. The oxygen atoms attached to P(1) and P(2) are clearly visible as well as the atropisomeric MeO-Biphep ligand (**L1a**).

The bond distances of Ru-O trans to the phosphorus atoms are both ca. 2.21 Å for **9a** and ca. 2.22-2.23 Å for **9b**. These are considerably longer than the Ru-O separations trans to the oxygen atoms, ca. 2.11-2.12 Å for **9a** and 2.10-2.13 Å for **9b**. This difference is consistent with the high trans influence of the strongly σ-donating phosphorus ligand atom. Noyori et al.¹⁵ have reported the solid-state structure of [Ru(OAc)₂(Binap)], **10**, as having an average Ru-O separations (trans to phosphorus) of ca. 2.20 Å and the average Ru-O separations (trans to oxygen) of 2.13 Å. The Ru-O separations of ca. 2.20 Å (trans to phosphorus) and ca. 2.12 Å (trans to oxygen) in

$[\text{Ru}(\text{O}_2\text{CCMe}=\text{CHMe})_2(\text{Binap})]^{11}$ are consistent with the observed averages for **9a** and **9b**.

The Ru(1)-P(1) and Ru(1)-P(2) separations are ca. 2.24 Å for **9a** and 2.22 Å for **9b**. The bond angles P(1)-Ru(1)-P(2) are ca. 92° for both complexes. Again these are consistent with the values reported in the literature for these types of complexes.^{11,15}

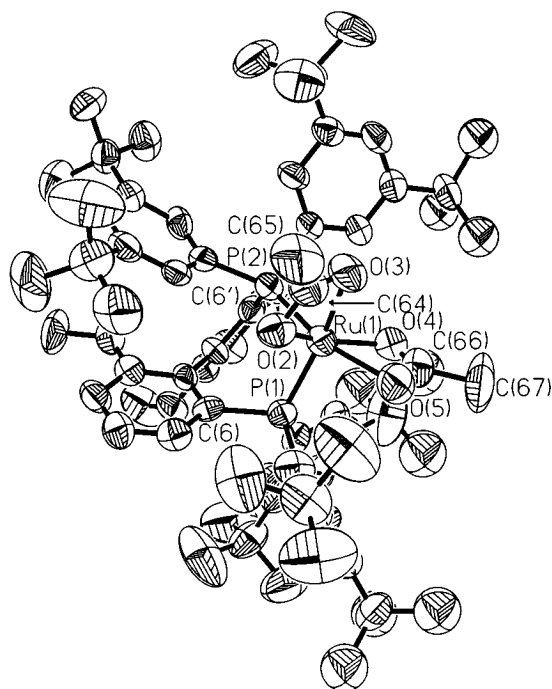


Figure 2. View of the structure of the cation of **9b**, 50% ellipsoids.

Table 1: Selected bond lengths (Å) and bond angles (deg) for **9a** and **9b**.

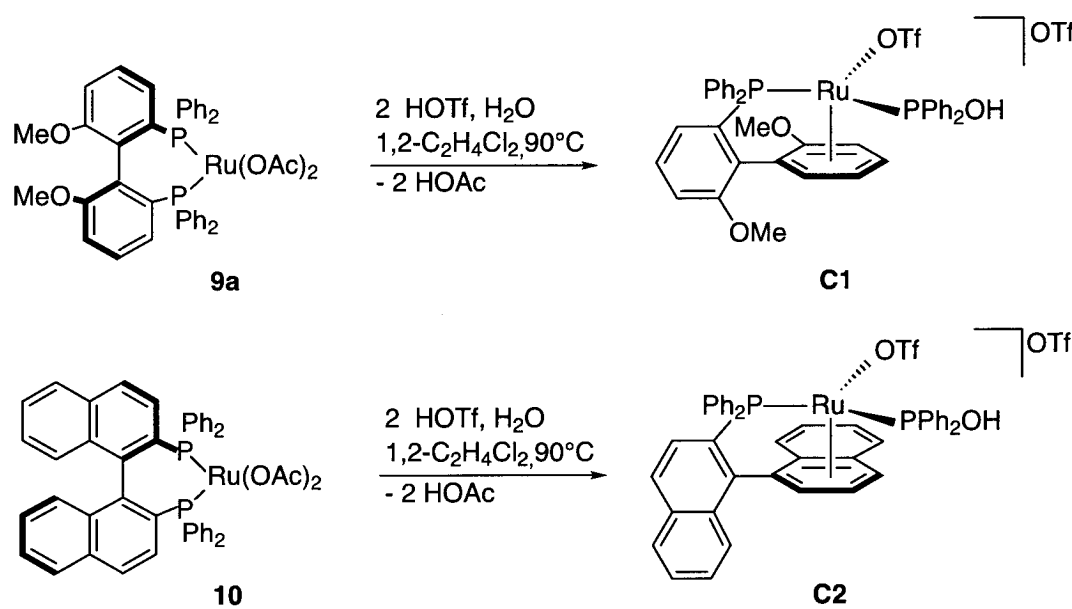
	9a	9b
Ru(1)-P(1)	2.2356(14)	2.225(2)
Ru(1)-P(2)	2.2355(15)	2.223(3)
Ru(1)-O(2)	2.208(4)	2.132(7)
Ru(1)-O(3)	2.111(4)	2.231(7)
Ru(1)-O(4)	2.208(4)	2.097(8)
Ru(1)-O(5)	2.119(4)	2.213(8)
O(2)-C(32)/C(64)	1.247(8)	1.296(13)
O(3)-C(32)/C(64)	1.265(7)	1.253(13)

Table 1: Selected bond lengths (Å) and bond angles (deg) for 9a and 9b.

	9a	9b
O(4)-C(34)/C(66)	1.254(8)	1.273(19)
O(5)-C(34)/C(66)	1.283(8)	1.206(19)
P(1)-Ru(1)-P(2)	92.73(5)	92.44(10)
O(2)-C(32)/C(64)-O(3)	120.0(6)	119.5(11)
O(4)-C(34)/C(66)-O(5)	118.7(6)	122.5(14)

4.3.2 P-C bond splitting induced by $\text{CF}_3\text{SO}_3\text{H}$

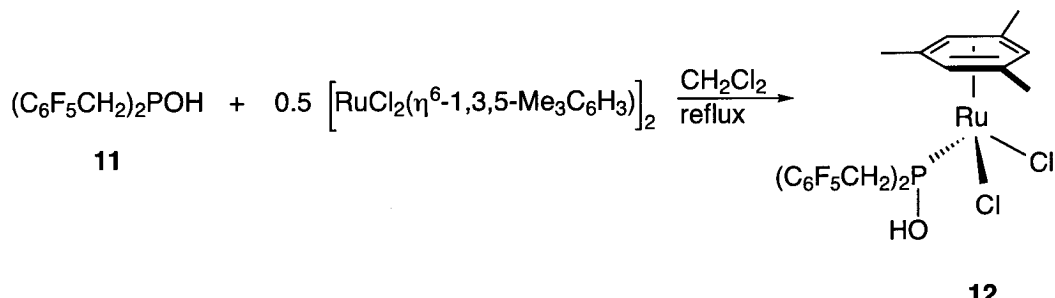
As part of our study on structural properties of the biarylphosphine ligands MeO-Biphep and Binap,^{14,16,17} $[\text{Ru}(\text{OAc})_2(\text{L1a or L2})]$ (**L1a** = MeO-Biphep and **L2** = Binap), **9a** and **10** respectively, were allowed to react with slightly more than two equivalents of wet $\text{CF}_3\text{SO}_3\text{H}$ (= HOTf) in 1,2-dichloroethane at 90°C. These conditions resulted in stereospecific (*vide infra*) P-C bond breaking to afford the products **C1** and **C2** in a few hours in good yield (Scheme 6). A new chiral center has been created on the Ru(II)-atom. The complexes **C1** and **C2** contain a hydroxyphosphine ligand (PPh_2OH), a coordinated triflate and an asymmetric η^6 -complexation of one of the aryl rings of the new $\text{P}(\text{biaryl})\text{Ph}_2$ ligand. Formally, the H^+ protonates the acetate and the water adds across the P-C bond.



Scheme 6. The preparation of complexes **C1** and **C2**.

Several related reactions leading to hydroxyphosphines and complexes thereof are known in the literature, e.g. the synthesis of $(\text{C}_6\text{F}_5\text{CH}_2)_2\text{POH}$, **11**, and its complexation to Ru(II) as shown in Scheme 7.¹⁸ The ligand **11** was prepared by reacting bis(pentafluorop-

robenzyl)bromophosphine with lithium aluminium hydride in diethylether. The reaction of ligand **11** with half an equivalent of $[\text{RuCl}_2(\eta^6\text{-1,3,5-Me}_3\text{C}_6\text{H}_3)]_2$ in dichloromethane affords Ru(II)-hydroxyphosphine complex **12**.



Scheme 7. The reaction leading to hydroxyphosphine Ru(II)-complex **12**.

Recently, the treatment of $[\text{Os}(\eta^5\text{-C}_5\text{H}_5)\text{Cl}(\text{Ph}_2\text{PH})(\text{P}^i\text{Pr}_3)]$, **13**, with TiPF_6 in wet acetone affording the cationic hydridophosphine complex $[\text{OsH}_2(\eta^5\text{-C}_5\text{H}_5)(\text{Ph}_2\text{POH})(\text{P}^i\text{Pr}_3)]\text{PF}_6$ has been reported.¹⁹ D_2O experiments have indicated that this reaction proceeds via hydride-phosphido intermediate, $[\text{OsH}(\eta^5\text{-C}_5\text{H}_5)(\text{PPh}_2)(\text{P}^i\text{Pr}_3)]^+$, which is generated by intramolecular P-H oxidative addition of the unsaturated $[\text{Os}(\eta^5\text{-C}_5\text{H}_5)(\text{PHPh}_2)(\text{P}^i\text{Pr}_3)]^+$. Once the hydrido-phosphide species is formed, the HO-H addition to the Os-phosphido bond affords **13**. However, the P-C bond splitting mechanism as described above, is unlikely to be the case for our Ru-chemistry as it involves oxidative addition leading to a Ru(IV) species.

The solution structures for the new P(OH)Ph₂ complexes **C1** and **C2** were confirmed by multinuclear, multidimensional NMR spectroscopy.²⁰ Their ³¹P spectra show the expected AX pattern, with the complexed Ph₂POH ligand appearing at higher frequency ($\delta = 104.1$ in **C1** and 114.5 in **C2**). Their ¹³C spectrum show six, and their ¹H spectra, four (**C1**) or three (**C2**) resonances from the coordinated ring, all strongly shifted to lower frequencies, due to the complexation.^{21,22} The complexed arene protons were connected to their corresponding ¹³C signals via a 2-D ¹³C,¹H correlation. A section of the spectrum for **C1** is shown in Figure 3. It depicts the cross-peaks for the four ¹³C and ¹H resonances of the complexed η^6 -ring. The chemical shifts appear at relatively low frequency, indicative of complexation.

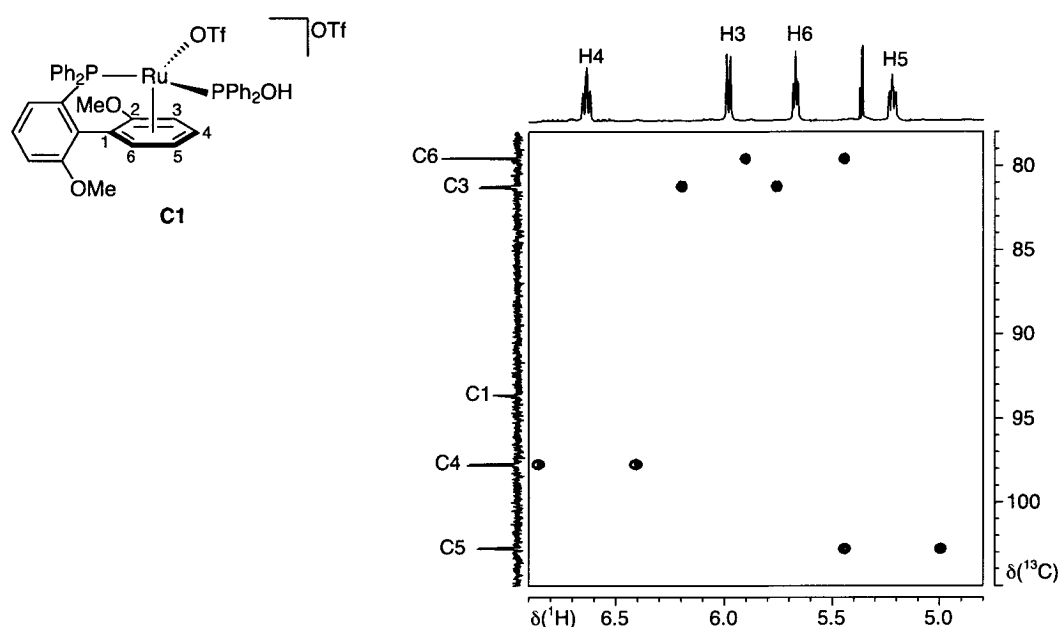


Figure 3. A section of the ^{13}C - ^1H correlation for **C1** (400 MHz, CD_2Cl_2 , ambient temperature).

The PPh_2OH hydroxy-proton for **C1** and **C2** are observed at $\delta = 9.66$, and 10.02, respectively. For **C2**, the OH-proton can be correlated to its ^{31}P signal, P1, via a 2D-NMR ^{31}P - ^1H correlation. Figure 4 shows a section of this spectrum in which the correlation to the OH-proton is clear, as are the two strong sets of cross-peaks due to the two sets of ortho P-phenyl protons. There are weak correlations to the meta protons and one of the protons of the complexed ring. The high frequency position of the OH-proton combined with its relatively slow exchange observed with water in the solvent (based on 2-D exchange spectroscopy) suggests that the OH is hydrogen bonded.

The ^{19}F spectrum for **C1** and **C2** reveals two separate triflate absorptions for each complex. A ^{19}F , ^1H -HOESY experiment shows a close contact between the uncomplexed OTf and the OH-proton. ^{19}F - and ^1H -diffusion measurements²³ have confirmed the H-bonding of the uncomplexed triflate for **C2** in solution.²⁴ Table 12 (Section 4.5.3) shows a selection of ^1H , ^{13}C , ^{19}F and ^{31}P NMR data for **C1** and **C2**.

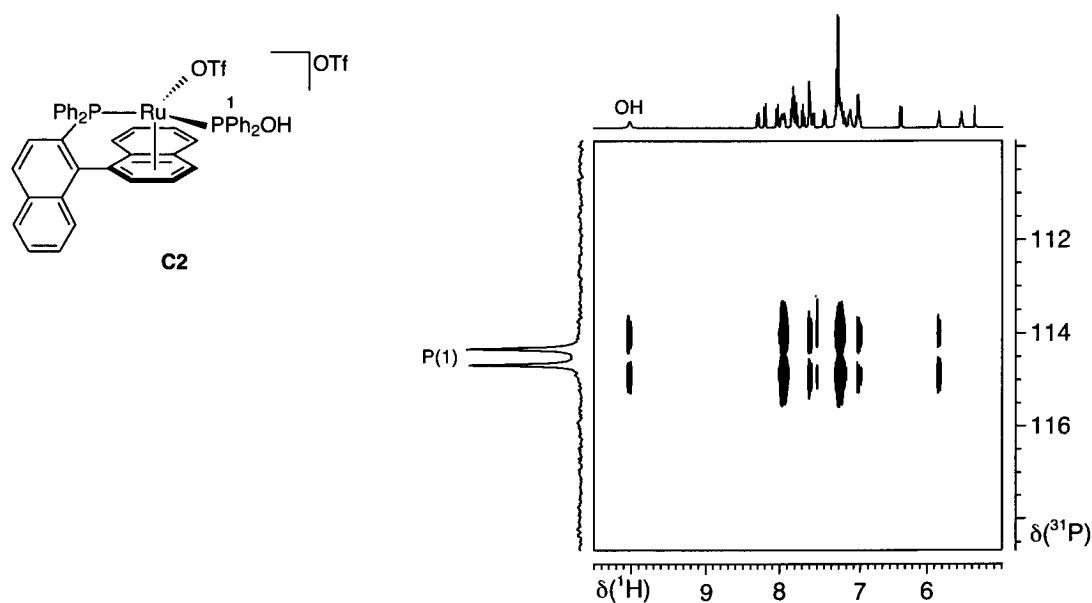


Figure 4. Section of the ^{31}P - ^1H correlation for compound **C2** (400 MHz, CD_2Cl_2 , ambient temperature).

The observation of a single diasteromer in the NMR spectra of **C1** and **C2** is thought to be due to kinetic control of the P-C bond splitting. Starting from e.g., racemic MeO-Biphep, the new phosphorus ligand moves from the position indicated by the arrows in Figure 5 to the stereogenic Ru(II)-atom such that either the (*R,R*)- or (*S,S*)-diasteromer, or (*R,S*)- or (*S,R*)-diastereomers, is formed. Solution NMR measurements show that these complexes do not epimerize rapidly on the NMR time scale at ambient temperature.

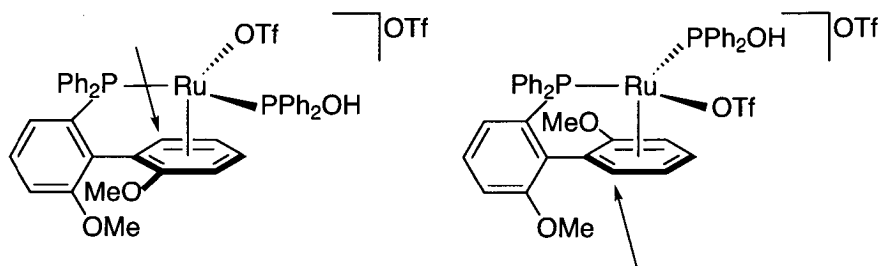
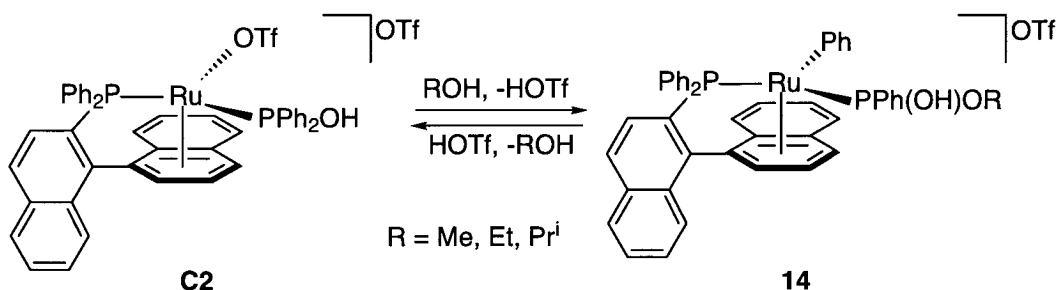


Figure 5. The kinetic controlled P-C bond splitting.

Another stereospecific P-C bond splitting reaction starting from **C1** and **C2** has been described recently.⁵ Complexes **C1** and **C2** undergo rapid stereospecific alcoholysis to afford complexes of type **14** as depicted in Scheme 8 for **C2**. A new chiral center has been created on the P-atom. A dicationic solvent complex which starts to dissociate in the transition state has been suggested. At the same time the phenyl bridges the Ru and P atoms and nearby H-bonded solvent begins to form the new P-O bond. Protonation of these Ru-phenyl complexes using an excess of HOTf in dichloromethane affords a reaction in which the Ru-phenyl group migrates from the metal back to the P atom without loss of stereogenicity at the Ru atom.



Scheme 8. The stereospecific reaction of **C2** leading in complex **14**.

The structures of **C1** and **C2** were determined by X-ray diffraction. The immediate coordination spheres both contain an asymmetric η^6 -arene, one oxygen of the triflate anion and two phosphorus donors: one from the new monodentate $\text{P}(\text{OH})\text{Ph}_2$ ligand and the second from the $\text{P}(\text{biaryl})\text{Ph}_2$ ligand. The oxygen-atoms attached to the P(1) donors are clearly visible. Table 2 shows a list of selected bond lengths and bond angles for these complexes. The views of the cations are shown in Figures 6 and 7.

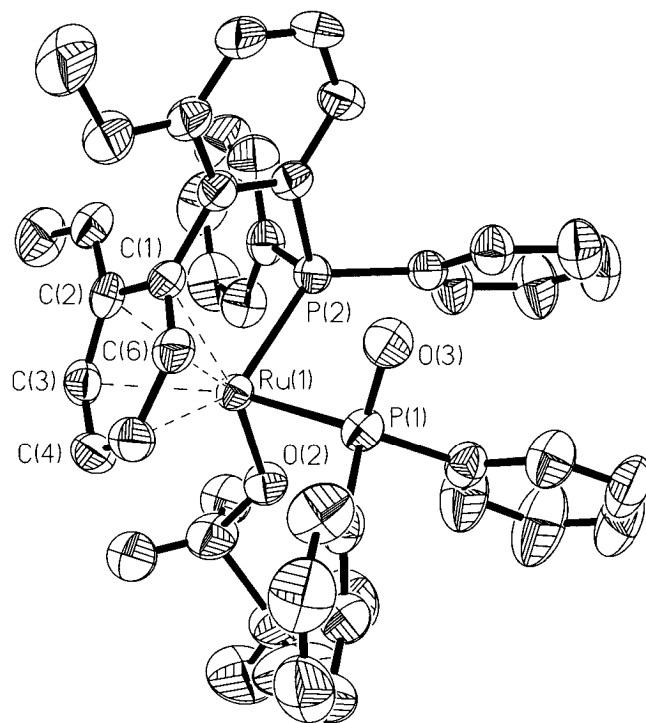


Figure 6. View of the structure of the cation of **C1**, 50% ellipsoids. The oxygen attached to P(1) is clearly visible, and the η^6 -complexation is indicated by dotted lines.

Table 2: Selected Bond Lengths (Å) and Bond Angles (deg) for the Cations C1 and C2.

	C1	C2
Ru(1)-P(1)	2.3105(16)	2.2865(14)
Ru(1)-P(2)	2.3529(16)	2.3389(14)
Ru(1)-O(2)	2.178(4)	2.155(4)
Ru(1)-C(1)	2.136(5)	2.135(5)
Ru(1)-C(6)	2.153(6)	2.161(5)
Ru(1)-C(4)	2.306(6)	2.321(5)
Ru(1)-C(5)	2.290(6)	2.300(5)
Ru(1)-C(2)	2.408(6)	2.480(5)
Ru(1)-C(3)	2.347(6)	2.477(5)
P(1)-OH	1.583(4)	1.591(4)
P(1)-Ru(1)-P(2)	89.59(6)	91.76(5)
P(1)-Ru(1)-O(2)	93.31(12)	94.64(11)
P(2)-Ru(1)-P(2)	96.87(13)	94.73(11)

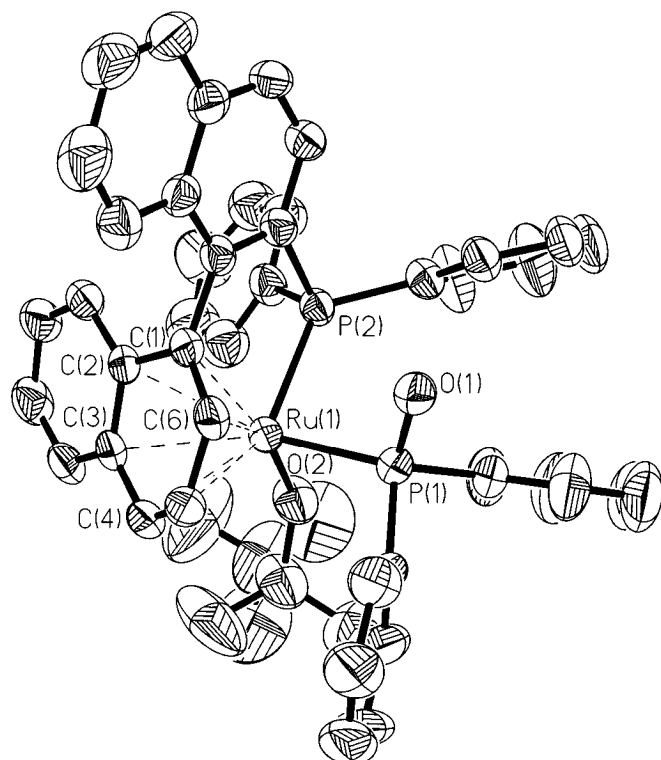


Figure 7. View of the structure of the cation of **C2**, 50% ellipsoids. The oxygen attached to P(1) is clearly visible, and the η^6 -complexation is indicated by dotted lines.

There are relatively few structurally characterised ruthenium triflate complexes known in the literature. The Ru-O bond length of ca. 2.30 Å in *trans*-[Ru(OTf)(C≡NH)(dppe)₂]OTf (dppe = Ph₂PCH₂CH₂PPh₂), **15**, is relatively large,²⁵ especially when compared with the complexes [Ru(dppe)(CO)₂(OTf)₂], **16**, and [Ru(dppe)(CO)(H₂O)(OTf)₂], **17**.²⁶ The Ru-O(OTf) bond lengths in these complexes are ca. 2.18-2.20 Å for **16** and ca. 2.20 Å for **17**. Thus, the Ru(1)-O(2) bond lengths for **C1** and **C2**, 2.178(4) Å and 2.155(4) Å, respectively, fall at the lower end of the known range (ca 2.12-2.30 Å) for this bond.^{25,27}

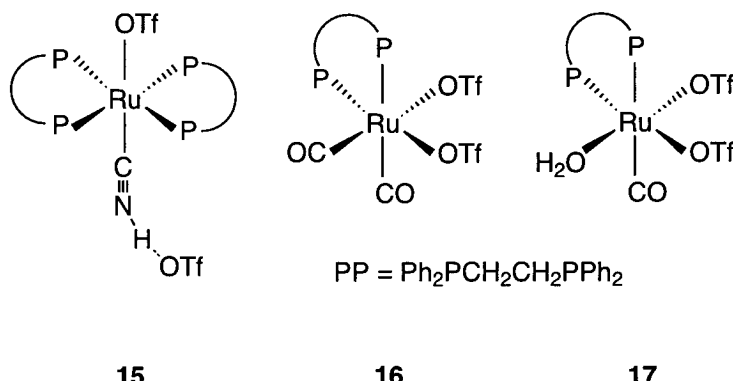


Figure 8. Ru(II)-complexes **15**, **16**, and **17** bearing OTf-ligands.

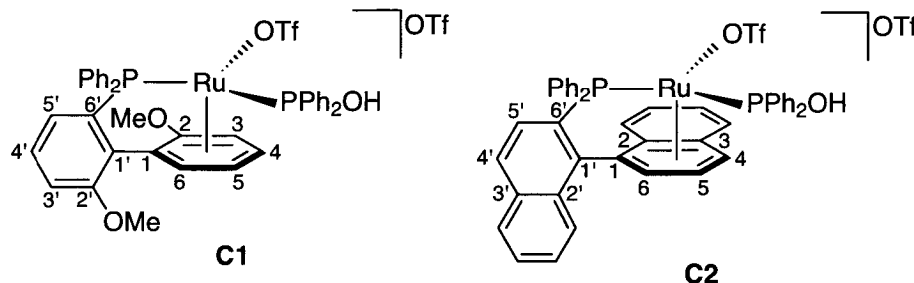
No evidence has been found for an intramolecular H-bond between the P(OH) and an oxygen of the complexed triflate. However, a short separation of 1.8 Å for **C1** has been found between the assigned position of the hydroxyl-H and an oxygen of the uncomplexed triflate. This H-bond also exists in solution as proven by NMR experiments described above.

The Ru(1)-P separations, ca. 2.31 Å and 2.35 Å for **C1** and ca. 2.29 Å and 2.34 Å for **C2**, are routine. However, the six Ru(1)-C arene bond lengths in both **C1** and **C2** are very different and seem to exist in three groups of two. Two distances are relatively short, Ru-C(1) and Ru-C(6), ca 2.13-2.16 Å, but fairly normal.^{21,28} Two are slightly longer, Ru(1)-C(4) and Ru(1)-C(5), 2.29-2.32 Å and two are quite long, Ru(1)-C(2) and Ru(1)-C(3), ca 2.35-2.48 Å.

Inspection of the X-ray literature for arene complexes of Ru(II) suggests that routine Ru-C separations in a variety of substituted and simple Ru-arene complexes should be of the order of 2.15-2.28 Å with the average at ca 2.23 Å.²⁹ Specifically, the observed values at 2.480(5) Å and 2.477(5) Å for C(2) and C(3) in **C2** suggest a weak interaction. These differences might be related to steric effects, in that the longer distances involve the two sterically hindered fully substituted arene carbons.

Moreover, in **C2** modest intra-molecular ^{13}C coordination chemical shifts, $\Delta\delta$, 14.9 ppm and 24.6 ppm, for the complexed arene carbons C2 and C3, relative to the 41.4 ppm and 62.7 ppm values of $\Delta\delta$ found for C1 and C6 (Table 3) have been found. These data supporting a weak interaction between Ru-C2 and Ru-C3. For **C2** it is probably correct to consider the arene bonding as closer to η^4 than to η^6 .

Table 3: ^{13}C coordination chemical shifts, $\Delta\delta$, for **C1** and **C2**.



	$\Delta\delta$ ^{13}C C1	$\Delta\delta$ ^{13}C C2
1'-1	33.3	41.1
6'-6	64.4	62.7
4'-4	34.2	32.0
5'-5	22.9	20.3
2'-2	12.2	14.9
3'-3	33.6	24.6

It is interesting that Ru-C1 and Ru-C6 are relatively short, as these were the two arene carbons involved in the η^2 -olefin bonding shown in e.g., **19** and **20**. This suggests that the metal does not release C1 and C6 during the change from the η^2 -mode to the η^6 -mode, but has simply slipped across the face of the arene. Also the η^6 bonding mode in **C1** and **C2** is not completely unexpected as the η^6 -mode has also been found in the Ru(II)-dialkyl complexes **21**. The molecule achieves this structure by dissociating one tertiary phosphine donor.

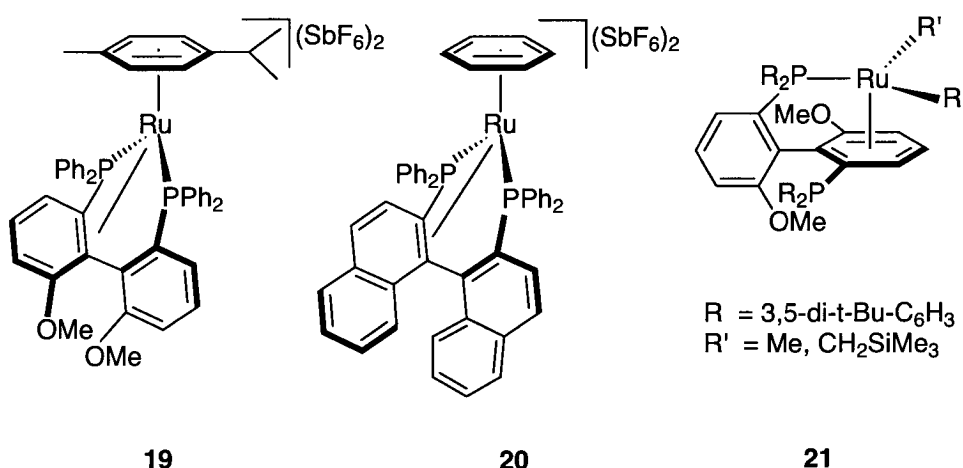
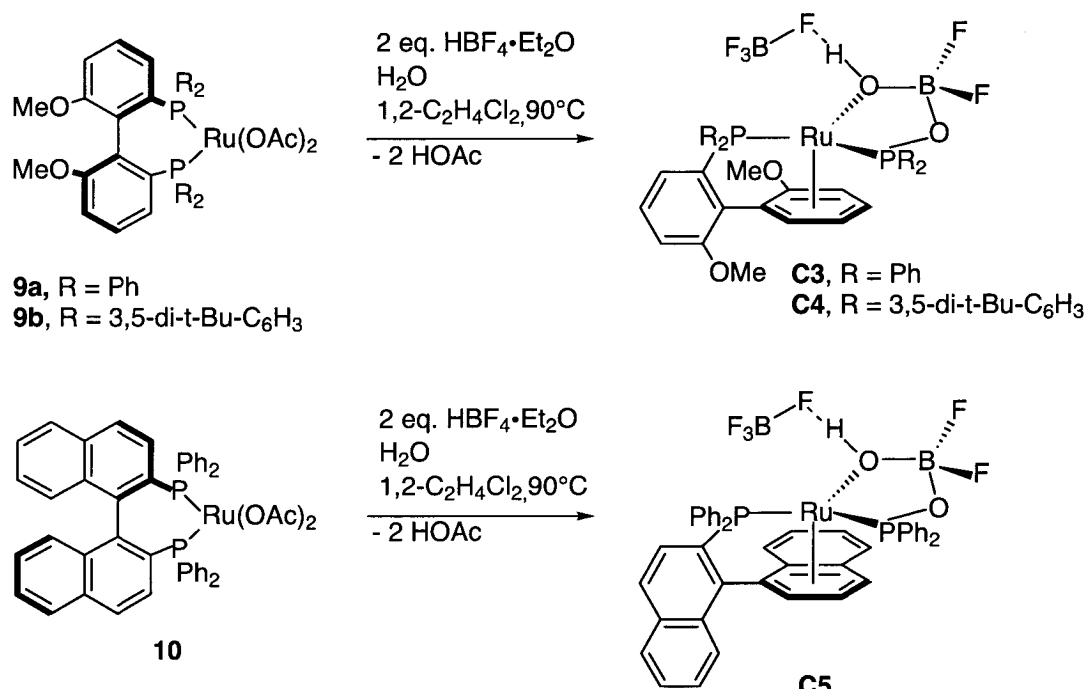


Figure 9. The biaryl biphenyl ligands MeO-Biphep and Binap as 6e (**19** and **20**) respectively 8e (**21**) donor ligands.

Taking the NMR- and X-ray data together with the stereospecificity of the reaction, we propose a mechanism for the formation of **C1** and **C2** which involves an intermediate bearing the additional coordination of one of the biaryl double bonds of the biphenyl ligand. To further our mechanistic understanding, and to extend this chemistry to another strong acid, HBF₄ was allowed to react with **9a**, **9b** and **10**.

4.3.3 P-C bond splitting induced by HBF_4

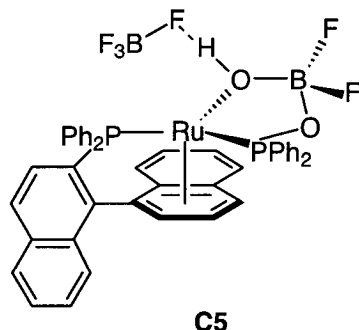
Reaction of complexes $[\text{Ru}(\text{OAc})_2(\text{L1a, L1b or L2})]$, **9a**, **9b** and **10**, (**L1a** = MeO-Biphep, **L1b** = 3,5-di-*t*-Bu-MeO-Biphep and **L2** = Binap) with $\text{HBF}_4/\text{H}_2\text{O}$ in 1,2-dichloroethane at 90 °C affords the products **C3-C5** respectively, after ca. 6 hours (Scheme 9). Initially, the reactions were done in an NMR-tube containing adventitious water. Under these conditions, the formation of the products was slow and diastereomers were observed since the Ru-atom represents a stereogenic center. The slow kinetics are thought to be responsible for ligand dissociation during the hydrolysis, i.e. epimerisation (*vide infra*).



Scheme 9. The preparation of complexes **C3-C5**.

The rather unusual complexes **C3-C5** contain new P-O and B-O bonds in addition to an η^6 -arene interaction with Ru(II). This η^6 -arene stems from complexation of the biaryl ring previously connected to the P-donor. The bis-phosphine bidentate has been cleaved to afford two different chelating ligands. Formally, **C3-C5** contain the phosphinite anion, ($\text{C}_{12}\text{H}_{11}\text{BF}_2\text{O}_2\text{P}$) which, to our knowledge, is as yet unknown. This ligand arises via a hydrolysis reaction of BF_4^- . The second BF_4^- is held close to ($\text{C}_{12}\text{H}_{11}\text{BF}_2\text{O}_2\text{P}$) via a hydrogen-bond as shown by $^{19}\text{F}-^1\text{H}$ HOESY and diffusion measurements.^{23,24}

Several examples of related ligands are known, e.g. complex [PtCl((OP(OMe)₂)₂BF₂)(PEt₃)] which is prepared by treating [PtCl((OP(OMe)₂)₂H)(PEt₃)] with BF₃·Et₂O.³⁰



The major features of the structure of **C3-C5** were determined via one and two-dimensional multinuclear NMR spectroscopy.²⁰ Specifically:

- i) **C5** shows an AX ³¹P NMR spectrum with one unexpectedly high frequency ³¹P signal, $\delta = 116.6$ ($^2J(^{31}\text{P}, ^{31}\text{P}) = 52$ Hz). This ³¹P chemical shift is consistent with a complexed P-O phosphinite.³¹ Normally these kinds of Ru(II) complexes have their ³¹P signals in the region 30-70 ppm.
- ii) The boron decoupled ¹⁹F NMR spectrum reveals an ABX spin system (X = ³¹P) for the two nonequivalent fluorine signals of the BF₂ (without decoupling these signals are quite broad) plus the BF₄⁻ anion. The presence of ³¹P coupling to the ¹⁹F signals is consistent with the proposed new-phosphinite fragment. Figure 10 shows ¹⁹F and ³¹P resonances for (in this case) the two diastereomers of **C5**.

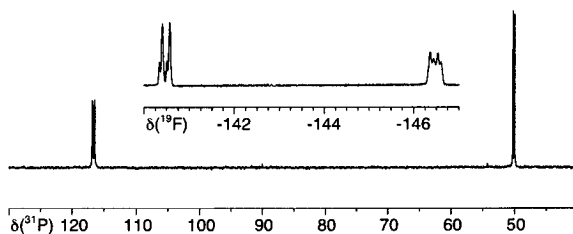


Figure 10. ¹⁹F- and ³¹P-NMR spectra for **C5** (400 MHz, CD₂Cl₂, ambient temperature). Top: BF₂ region showing two sets of ¹⁹F resonances for each of the nonequivalent F atoms of the BF₂. Bottom: The nonequivalent ³¹P resonances. When expanded, one can see the second set of ³¹P signals.

- iii) The ^{11}B spectrum shows the signals for the new ligand plus the uncomplexed BF_4^- .
 iv) In both the ^1H and ^{13}C spectra one observes three relatively low frequency absorptions, due to the three CH-types in the η^6 -arene moiety. For **C5** these three carbon signals appear at 73.3, 95.1 and 105.7 ppm exactly where one expects ^{13}C resonances for arenes complexed to Ru(II).²² Table 13 (Section 4.5.3) shows a selection of ^1H , ^{13}C , ^{19}F and ^{31}P NMR data for **C3** and **C5**.

A rather poor crystal of **C3**, R = Ph, was obtained. However, it was adequate to confirm the solid-state structure (see Figure 11). The data are just sufficient for a qualitative analysis. The view shows the aryl η^6 -arene bonding as well as the new phosphinite.

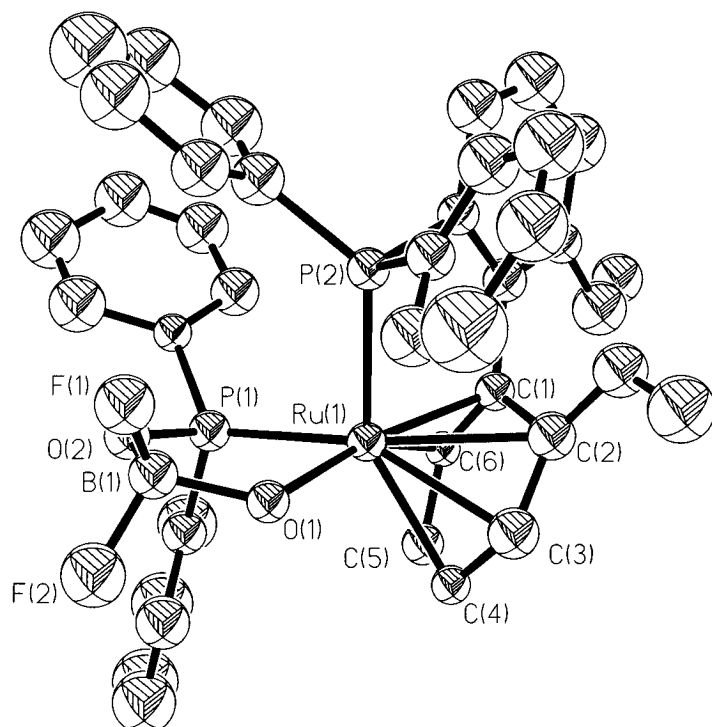
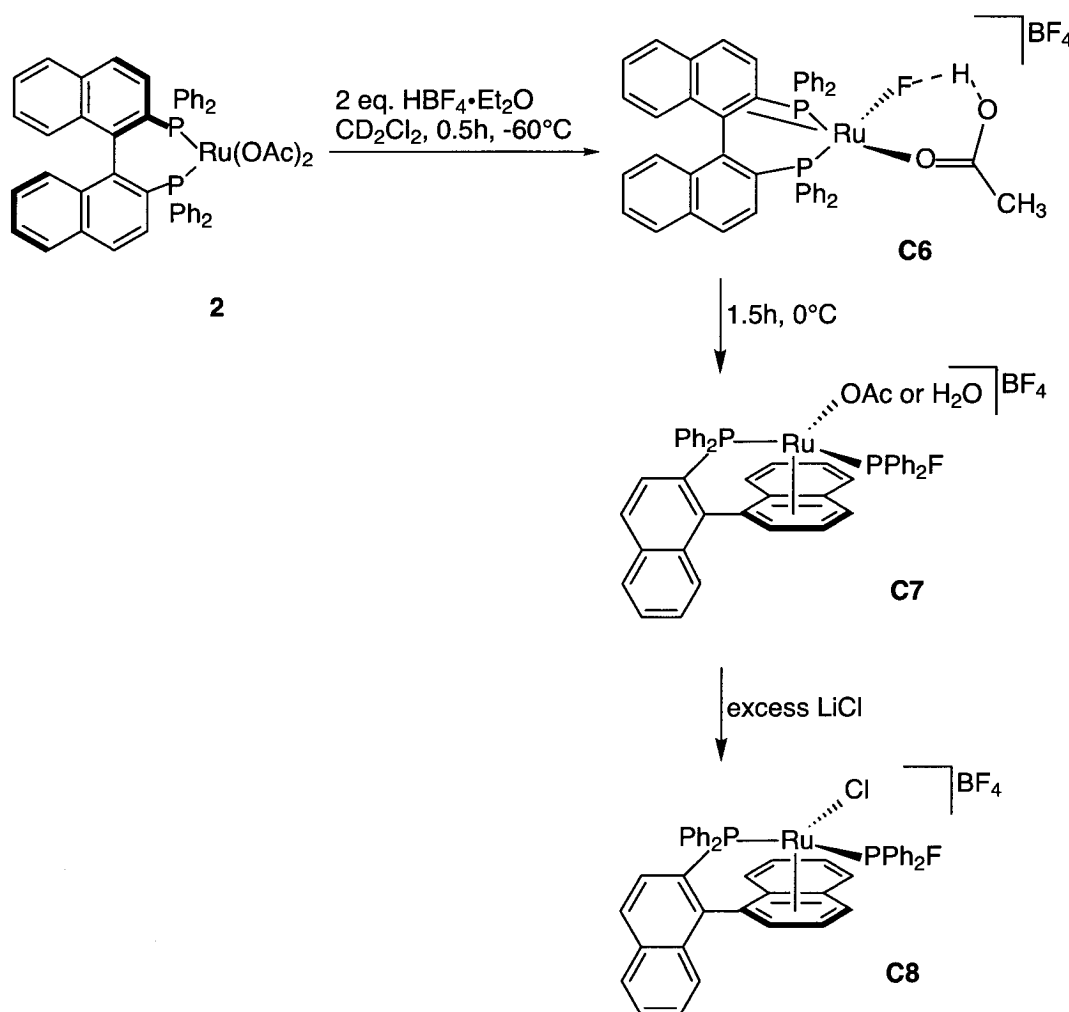


Figure 11. View of one of the two independent molecules of **C3**. It readily displays the coordinated η^6 -arene as well as the new phosphinite.

With the goal of identifying intermediates in the P-C bond splitting reaction, a set of NMR spectra of mixed solutions of $[\text{Ru}(\text{OAc})_2(\text{Binap})]$ with 2.2 equivalents of $\text{HBF}_4 \cdot \text{Et}_2\text{O}$ were measured at low temperature. Several species in solutions have been observed (Scheme 10).



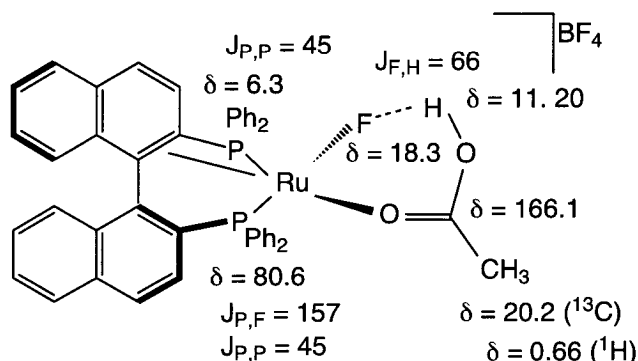
Scheme 10. Chemistry of [Ru(OAc)₂(Binap)] with HBF₄.

The first major component (ca 8 times more abundant than the others), can be assigned to **C6**, a structure in which Binap functions as a 6e donor^{14,16,32} based on the observed very low frequency ³¹P chemical shift, $\delta = 6.3$, of the ³¹P spin adjacent to the complexed olefin. The second phosphorus signal appears at its normal position $\delta = 80.6$, $^2J(^{31}\text{P}, ^{31}\text{P}) = 45$ Hz. This represents yet another, albeit rare, example of the complexation of the adjacent biaryl double bond.

The BF₄⁻ anion has been cleaved to afford a Ru-F--H interaction plus Et₂O•BF₃ whose identity has been confirmed via comparison with an independent sample.³³ Complex **C6**

shows a ^{19}F signal at $\delta = 18.3$, with a coupling to the proton of 66 Hz and a second spin-spin coupling to only one of the two ^{31}P signals, 157 Hz.³⁴

There is a ^1H signal³⁵ at $\delta = 11.20$, with $^1J(^{19}\text{F}, ^1\text{H}) = 66$ Hz. The complexed acetate methyl signal is found at relatively low frequency, $\delta = 0.66$, due to the anisotropy of a proximate P-Phenyl ring. However, its ^{13}C chemical shift is routine, $\delta = 20.2$ ($\delta ^{13}\text{CO} = 166.1$). These NMR data for **C6** are summarized below.

**C6**

There are very few M-F-H complexes,^{36,37} although some M-F---H-F derivatives are known.³⁸ These latter can be considered as examples of intermolecular hydrogen bonding involving a metal fluoride complex and an outer sphere HF. In the compound $[\text{RuH}(\text{HF}_2)(\text{dmpe})]$ (dmpe = $\text{Me}_2\text{PCH}_2\text{CH}_2\text{PMe}_2$), **22**, two different $^1J(^{19}\text{F}, ^1\text{H})$ values, one large, 274 Hz for the strong H-F interaction, and a much smaller one, <30 Hz, for the H---F moiety are observed (Figure 12).³⁹

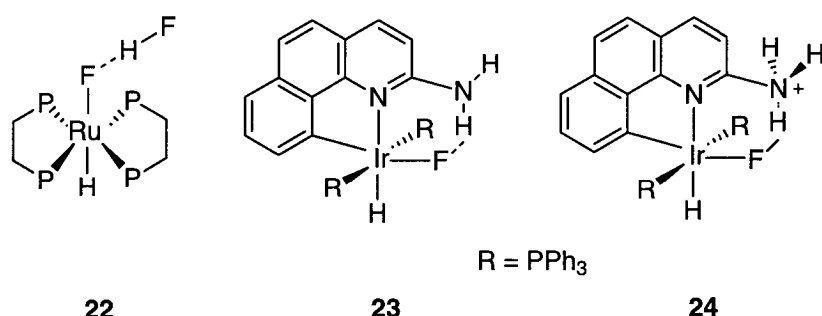
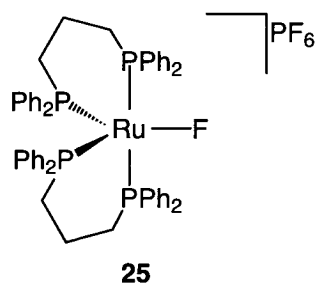
**22****23****24**

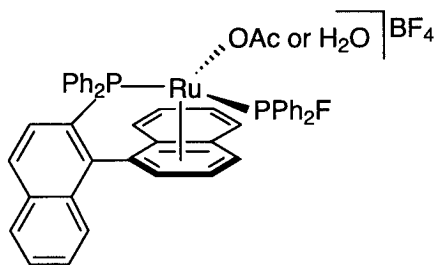
Figure 12. The Ru(II)-F complexes **22**, **23** and **24**.

Crabtree et al.³⁶ have reported the effect of a pendant group on the stabilisation of a MFH complex. A $^1J(^{19}\text{F}, ^1\text{H})$ value of 52 Hz has been observed for complex **23**, while for the protonated derivative **24**, a much larger value, 440 Hz, has been found. The latter observation is consistent with **24** being a N---H-F complex, rather than having a hydrogen-bonded N-H---F system as in complex **23**. Consequently, given the value of 66 Hz, the HF bond in **C6** is weak, and the complex can be considered as possessing a stabilised Ru-F complex.

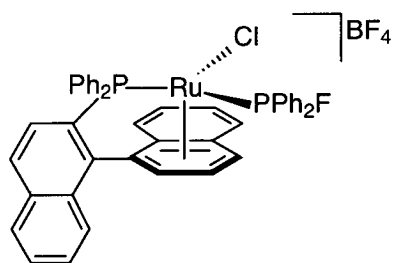
Models for **C6** suggest that if the acetate was bound in a bidentate mode, the observed methyl ^1H chemical shift would be incorrect. However, H-bonding of the acetate oxygen to the hydrogen of the HF places the methyl group correctly. The possibility that water is involved in the H-bond network and/or that it functions as a sixth ligand cannot be excluded.

Most of the reported complexes combining fluoride and phosphine ligands contain strong π -acceptor CO-ligands, e.g. $[\text{RuF}_2(\text{CO})_2(\text{PEtPh}_2)_2]$.⁴⁰ The CO-ligands are *trans* to the fluoride ligands and thus create push-pull interactions. Although five-coordinate electronically unsaturated fluoro complexes are exceedingly rare,⁴¹ it has been shown that fluoride can be used to stabilise 16e species of relatively soft metals ions such as Ru(II), e.g. in complex $[\text{RuF}(\text{dppp})_2]\text{PF}_6$ (dppp = Ph₂PCH₂CH₂CH₂PPh₂), **25**, which has adopted a distorted trigonal-bipyramidal geometries in order to optimise the π -donation of the F atom to the metal.⁴²



**C7a and C7b**

Warming the solution containing **C6** to 0 °C affords the fluoro-phosphine complexes **C7a** and **C7b**. Formally, the proton of the HF (or one from proximate water) cleaves the P-C bond while forming the new P-F bond. The fluoro-phosphine complexes **C7** exist as a mixture of two components, **C7a** and **C7b**, and show the characteristic very large $^1J(^{31}\text{P}, ^{19}\text{F})$ values, ca 948 Hz⁴³ (and 956 Hz) as well as $^2J(^{31}\text{P}, ^{31}\text{P})$ values, 54 Hz (and 52 Hz). The η^6 -arene bonding is supported by the ^1H and ^{13}C data which reveal the expected low frequencies shifts (Table 14, Section 4.5.3).

**C8**

Reaction of the mixture containing **C7a** and **C7b** with an excess of LiCl afforded the chloro, fluoro-phosphine complex **C8** as a single product, in which only the oxygen donor ligand has been substituted. This observation supports the idea that only one diastereomer is formed if the reaction proceeds quickly. Chloro-compound **C8** could be isolated in 74% yield and its structure proof followed in analogy to **C7**. Figure 13 shows the ^{19}F and ^{31}P resonances for **C8** with their characteristic large one-bond spin-spin interactions. Table 14 (Section 4.5.3) shows a selection of ^1H , ^{13}C , ^{19}F and ^{31}P NMR data for **C7** and **C8**.

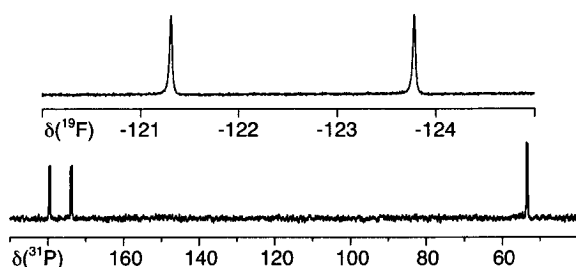


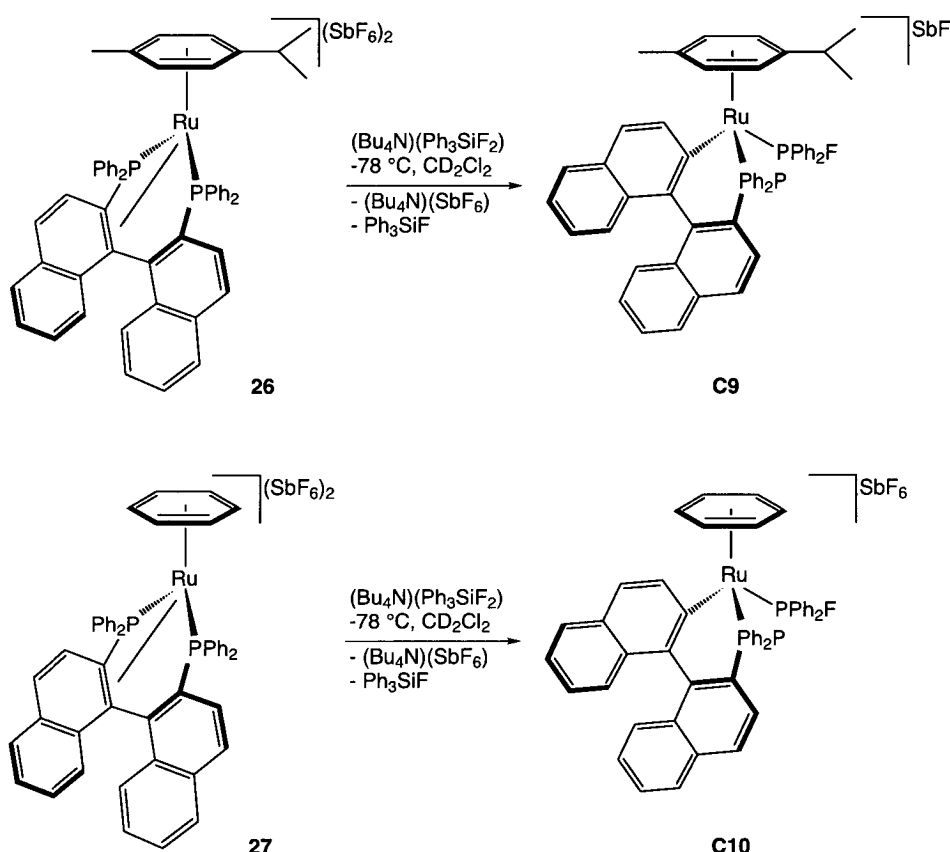
Figure 13. ^{19}F - and ^{31}P -NMR spectra for **C8** (400 MHz, CD_2Cl_2 , ambient temperature). Top: ^{19}F -NMR spectrum showing the large $^1J(^{31}\text{P}, ^{19}\text{F})$ for the complexed $\text{Ph}_2\text{P}-\text{F}$ ligand. Bottom: ^{31}P -NMR spectrum showing the $^1J(^{31}\text{P}, ^{19}\text{F})$ coupling and if expanded also the $^2J(^{31}\text{P}, ^{31}\text{P})$ coupling.

Another case of phosphorus fluorination by HBF_4 has been reported by Kündig et al.⁴⁴ Treatment of $[\text{Cr}(\eta^6\text{-naphthalene})(\text{P}(\text{OMe})_3)]$ with an excess of HBF_4 did not result in the expected protonated metal complexes but in the fluoro-phosphine complex $[\text{Cr}(\eta^6\text{-naphthalene})((\text{OMe})_2\text{PF})]$.

In summary, once the proximate double bond of biaryl phosphine ligand complexes to Ru(II), it is relatively easy to cleave the P-C bond with the metal attaining an 18e configuration by sliding from the η^2 -mode to the η^6 -arene.

4.3.4 P-C bond splitting induced by $(\text{Bu}_4\text{N})(\text{Ph}_3\text{SiF}_2)$

The Ru-F complex **C6** is an intermediate in the P-C bond reaction induced by HBF_4 as described in the previous section. The products **C3-C5** contain a complexed diphenyl-fluoro-phosphine ligand with the BF_4^- anion functioning as the source of the fluoride. It seemed of interest to attempt the preparation of a Ru-F species via an independent route, as the fluoride is transferred initially to the metal and only later to the P-atom. To this end $(\text{Bu}_4\text{N})(\text{Ph}_3\text{SiF}_2)$,⁴⁵ a soluble fluoride source, was allowed to react with the Binap (**L2**) dication $[\text{Ru}(\text{L2})(\text{arene})](\text{SbF}_6)_2$ (arene = η^6 -*p*-cymene, **26**, or η^6 -benzene, **27**) as depicted in Scheme 11.



Scheme 11. The reaction of the Ru(II) complexes $[\text{Ru}(\text{Binap})(\text{arene})](\text{SbF}_6)_2$ (arene = η^6 -*p*-cymene, **26**, or η^6 -benzene, **27**) with $(\text{Bu}_4\text{N})(\text{Ph}_3\text{SiF}_2)$ leading to the orthometallated products **C9** and **C10**.

As shown in Scheme 11 the products **C9** and **C10** are the cyclometallated fluorophosphine derivatives. Obviously the complexed P-donor is sufficiently electrophilic to accept the fluoride anion with resulting cleavage of the P-C bond. In **C9** and **C10** the Ru(II) coordinates the (formally) negative charged carbon, whereas in the chemistry of HBF₄/H₂O, one observes protonation.

Compounds **C9** and **C10** were identified by ¹H, ¹³C, ¹⁹F and ³¹P NMR spectroscopy. The PFPh₂ ligand is readily identified via its large ¹J(³¹P, ¹⁹F) value (936 Hz (**C9**), 951 Hz (**C10**)) and its high frequency ³¹P chemical shift (181.7 ppm (**C9**), 180.4 ppm (**C10**)).⁴³ The cyclometallated carbons are observed at 147.0 ppm and 145.6 for **C9** and **C10**, respectively. Figure 14 shows the ¹⁹F and ³¹P NMR-spectra of the cation of compound **C10**.

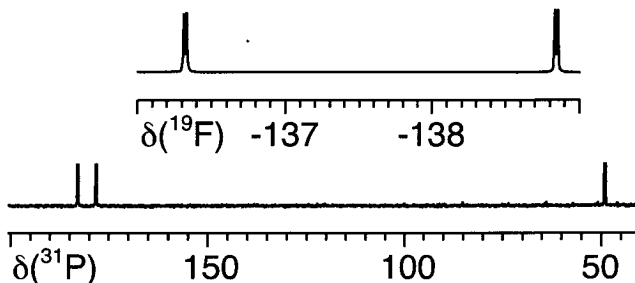


Figure 14. ¹⁹F and ³¹P NMR spectra of the cation of **C10**. Top: PFPh₂ region showing the ¹⁹F NMR resonance for the F atom of the new PFPh₂-ligand with a large ¹J(³¹P, ¹⁹F) coupling constant and the smaller ³J(³¹P, ¹⁹F) coupling constant. Bottom: the nonequivalent ³¹P NMR resonances. The high frequency signal show the large ¹J(³¹P, ¹⁹F) if expanded also the ²J(³¹P, ³¹P) coupling constant.

Since the biaryl phosphine ligand Binap (**L2**) readily complexes an adjacent biaryl double bond, this coordination introduces some strain in the complexes **26** and **27**. Reaction with (Bu₄N)(Ph₃SiF₂) readily leads to P-C bond cleavage (which releases the strain) and the formation of cyclometallated complexes **C9** and **C10**.

4.4 Conclusions

This chapter introduces a number of new and relatively unusual complexes. Many of the reactions discussed are unprecedented. The results described above clearly show that, in the absence of suitable ligands, acid-promoted stereospecific P-C bond cleavage and η^6 -arene complexation can be facile in Ru(II)-complexes of both **9** and **10**. In the presence of triflic acid plus adventitious water, complexed diphenyl hydroxy-phosphine (Ph_2POH) is produced, **C1** and **C2**. With water and HBF_4 , the complexes **C3-C5** (which contain the new phosphinite anion ($\text{C}_{12}\text{H}_{11}\text{BF}_2\text{O}_2\text{P}$) derived from hydrolysis of the BF_4^- anion) were synthesised. The epimerisation of **C3-C5** using adventitious water can now be rationalized in terms of slow hydrolysis thereby allowing sufficient time for ligand dissociation.

In the HBF_4 chemistry with Binap, a novel Ru-F---H, **C6**, intermediate was detected at -60°C in which the Binap acts as a 6e donor, using both phosphorus atoms and one double bond of the adjacent biaryl ring. Once the proximate double bond complexes to Ru(II), it is relatively easy to cleave the P-C bond, with the metal attaining an 18e configuration by sliding from the η^2 -mode to the η^6 -arene. This precoordination mode in **C6** causes stereoselective P-C bond splitting on warming to 0°C , giving fluorophosphine complexes, **C7a** and **C7b**. Complex **C8**, a Ru-Cl-analog of **C7** with complexed Ph_2PF , has also been isolated.

The strained Ru(II)-complexes **26** and **27** readily react with the fluoride source ($\text{Bu}_4\text{N}(\text{Ph}_3\text{SiF}_2)$) to afford the cyclometallated products **C9** and **C10** via P-C bond breaking and P-F bond making.

4.5 Experimental

4.5.1 Crystallography

Crystals of **9a**, **9b**, **C1**, **C2** and **C4** were mounted on glass capillaries and data sets covering a hemisphere were collected on a Siemens SMART platform diffractometer equipped with a CCD detector (ω -scans with 0.3° step width). Data reduction, corrections for Lorentz polarisation and absorption were performed using the programs SAINT⁴⁶ and SADABS.⁴⁷ The structures were solved by direct methods and refined by full-matrix least squares (versus F^2) with the SHELXTL program package.⁴⁸ All non-hydrogen atoms except the atoms belonging to disordered groups or solvent molecules were refined with anisotropic, all hydrogen atoms at calculated positions with common isotropic thermal parameters for each group.

In **9b** many atoms showed a considerably strong positional disorder. Wherever possible, a split model was applied. Crystallographic data and details of the structure determinations for **9a** and **9b** are given in Tables 4, 7 and 8.

In **C1** one triflate anion is strongly disordered. Initially, the observed electron density was described with several partially occupied fluorine atom positions. Later, on a more illustrative description of the disorder, consisting of two partially occupied anion positions has been selected. The occupation factors refined to values of 0.533(4) and 0.467(4), respectively. To achieve a stable refinement, the geometry of the affected anion had to be fixed by different constraints and the thermal displacement factors were assumed to be equal for all atoms belonging to this anion. The same geometric constraints were applied for both possible anion positions and a common isotropic displacement parameter was used for the affected atoms. The somewhat larger R -values are certainly acceptable considering that there is now a model for the observed disorder available. Crystallographic data and details of the structure determinations are given in Tables 5 and 9.

In **C2**, all the triflate anions, one phenyl group and a not further specified solvent molecule showed a considerably strong positional disorder. Wherever possible, a split model was applied. The solvent molecule was described with partially occupied C atom positions with a common isotropic displacement parameter. Unfortunately, in **C2** there are electron density peaks (C(1L) to C(3L)) located in a large void of the structure which could not be interpreted in terms of a clearly identified solvent. These peaks were included in the refinement, the effect of neglecting them on the R -value is relatively small (improvement of R1 of about 0.4%). Crystallographic data and details of the structure determinations are given in Tables 5 and 10. For **C4** all selected crystals showed very broad reflections, which made indexing and integration very difficult and affected the quality of the results. This is reflected by the relatively high R -values. Also as a consequence, an anisotropic refinement of the thermal displacement parameters was not possible, and all atoms had to be refined isotropically. All hydrogen atoms were placed on calculated positions and refined according to the riding model. One BF₄⁻ anion showed strong positional disorder and had to be refined as a rigid group. Crystallographic data and details of the structure determinations are given in Tables 6 and 11.

Table 4: Crystal data and parameters of the dat collection of compounds **9a and **9b**.**

Emperical formula	$C_{42}H_{38}O_6P_2Ru$ (9a)	$C_{74}H_{102}O_6P_2Ru$ (9b)
Formula weight (g/mol)	801.76	1250.61
Crystal size (mm)	0.80 x 0.20 x 0.10	0.58 x 0.40 x 0.08
Crystal system	orthorhombic	monoclinic
Unit cell dimensions (Å, deg)	$a = 17.822(3)$ $b = 19.508(3)$ $c = 25.881(4)$	$a = 15.644(2)$ $b = 25.702(4), \beta = 99.36(3)$ $c = 20.410(3)$
Volume (Å ³)	8998(2)	8097(2)
Space group	$P2_12_12_1$	$P2_1$
Formula unit pro cell (Z)	8	4
ρ (calculated) (g cm ⁻³)	1.184	1.026
Absorption coefficient μ (mm ⁻¹)	0.459	0.275
F(000)	3296	2672
Temperature (K)	293(2)	293(2)
Data collection	Siemens SMART CCD diffractometer	Siemens SMART CCD diffractometer
Monochromator; Wavelength	Graphite-Monochromator; $\lambda(MoK\alpha) = 0.71073$ Å	Graphite-Monochromator; $\lambda(MoK\alpha) = 0.71073$ Å
Detector distance; Collection method	d = 30 mm; Hemisphere, ω -scan	d = 60 mm; Hemisphere, ω -scan
Theta range for data collection	1.31 < θ < 24.74	1.28 < θ < 20.83
$h(\min), h(\max); k(\max), k(\min); l(\min), l(\max)$	-15, 20; -19, 22; -29, 30	-15, 15; -25, 15; -20, 20
Collected reflections	58299	26120
Independent reflections	15364 ($R(int) = 0.0791$)	26120 ($R(int) = 0.0455$)
Absorption correction	empirical (SADABS)	empirical (SADABS)
Structure solution	SHELXS-96 (direct methods)	SHELXS-96 (direct methods)
Structure refinement	SHELXL-96 (full matrix least-square of F^2)	SHELXL-96 (full matrix least-square of F^2)
Number of parameters	920	1457
Number of parameters restraints	0	13
Transmission coefficient (max/min)	0.9555/0.7103	0.9783/0.8567
wR for $ F_o ^2 > 2\sigma(F ^2)$	0.1110	0.1465
wR for all reflections	0.1252	0.1605
R for $ F_o ^2 > 2\sigma(F ^2)$	0.0419	0.0584
R for all reflections	0.0704	0.0788
Goodness of Fit ($GooF$) for $ F_o ^2 > 2\sigma(F ^2)$	1.062	1.023

Table 5: Crystal data and parameters of the data collection of compounds C1 and C2.

Empirical formula	C ₄₀ H ₃₄ F ₆ O ₉ P ₂ RuS ₂ (C1)	C _{46.83} H ₃₄ F ₆ O ₇ P ₂ RuS ₂ (C2)
Formula weight (g/mol)	999.80	1049.83
Crystal size (mm)	0.36 x 0.32 x 0.22	0.50 x 0.18 x 0.08
Crystal system	monoclinic	triclinic
Unit cell dimensions (Å, deg)	<i>a</i> = 21.020(3) <i>b</i> = 10.2942(15), β = 117.16(3) <i>c</i> = 21.626(3)	<i>a</i> = 15.099(2), α = 108.20(3) <i>b</i> = 16.131(2), β = 103.14(3) <i>c</i> = 19.817(3), γ = 94.34(3)
Volume (Å ³)	4163.4(11)	4408.7(12)
Space group	<i>P</i> 2 ₁ / <i>c</i>	<i>P</i> 1
Formula unit pro cell (Z)	4	4
ρ (calculated) (g cm ⁻³)	1.595	1.582
Absorption coefficient μ (mm ⁻¹)	0.639	0.601
F(000)	2024	2124
Temperature (K)	293(2)	293(2)
Data collection	Siemens SMART CCD diffractometer	Siemens SMART CCD diffractometer
Monochromator; Wavelength	Graphite-Monochromator; $\lambda(\text{MoK}\alpha)$ = 0.71073 Å	Graphite-Monochromator; $\lambda(\text{MoK}\alpha)$ = 0.71073 Å
Detector distance; Collection method	d = 30 mm; Hemisphere, ω -scan	d = 40 mm; Hemisphere, ω -scan
Theta range for data collection	1.89 < θ < 26.40	1.12 < θ < 24.74
<i>h</i> (min), <i>h</i> (max); <i>k</i> (max), <i>k</i> (min); <i>l</i> (min), <i>l</i> (max)	-25, 26; -8, 12; -27, 27	-17, 17; -18, 18; -23, 23
Collected reflections	25182	24430
Independent reflections	8492 (<i>R</i> (int) = 0.0545)	14887 (<i>R</i> (int) = 0.0486)
Absorption correction	empirical (SADABS)	empirical (SADABS)
Structure solution	SHELXS-96 (direct methods)	SHELXS-96 (direct methods)
Structure refinement	SHELXL-96 (full matrix least-square of F^2)	SHELXL-96 (full matrix least-square of F^2)
Number of parameters	512	1156
Number of parameters restraints	0	0
Transmission coefficient (max/min)	0.8627/0.7888	0.9535/0.7535
w <i>R</i> for $ F_o ^2 > 2\sigma(F ^2)$	0.1664	0.1245
w <i>R</i> for all reflections	0.1911	0.1483
<i>R</i> for $ F_o ^2 > 2\sigma(F ^2)$	0.0647	0.0504
<i>R</i> for all reflections	0.1022	0.0890
Goodness of Fit (GooF) for $ F_o ^2 > 2\sigma(F ^2)$	1.038	0.976

Table 6: Crystal data and parameters of the data collection of compound C4.

Empirical formula	C ₃₈ H ₃₃ B ₂ F ₆ O ₄ P ₂ Ru
Formula weight (g/mol)	1302.26
Crystal size (mm)	1.10 x 0.60 x 0.16
Crystal system	monoclinic
Unit cell dimensions (Å, deg)	$a = 10.326(2)$ $b = 20.068(4)$, $\beta = 94.858(4)$ $c = 19.624(4)$
Volume (Å ³)	4052.2(14)
Space group	P2 ₁
Formula unit pro cell (Z)	4
ρ (calculated) (g cm ⁻³)	1.397
Absorption coefficient μ (mm ⁻¹)	0.530
F(000)	1724
Temperature (K)	293
Data collection	Siemens SMART CCD diffractometer
Monochromator; Wavelength	Graphite-Monochromator; $\lambda(\text{MoK}\alpha) = 0.71073$ Å
Detector distance; Collection method	d = 50 mm; Hemisphere, ω -scan
Theta range for data collection	1.04 < θ < 20.82
$h(\text{min}), h(\text{max}); k(\text{max}), k(\text{min});$ $l(\text{min}), l(\text{max})$	-9, 10; -19, 20; -19, 19
Collected reflections	13617
Independent reflections	8061 ($R(\text{int}) = 0.0870$)
Absorption correction	empirical (SADABS)
Structure solution	SHELXS-96 (direct methods)
Structure refinement	SHELXL-96 (full matrix least-square of F^2)
Number of parameters	436
Number of parameters restraints	20
Transmission coefficient (max/min)	0.9200/0.5932
wR for $ F_o ^2 > 2\sigma(F ^2)$	0.3423
wR for all reflections	0.3649
R for $ F_o ^2 > 2\sigma(F ^2)$	0.1442
R for all reflections	0.1702
Goodness of Fit (<i>GooF</i>) for $ F_o ^2 > 2\sigma(F ^2)$	1.312

Table 7: Final position ($\times 10^{-4}$) and isotropic equivalent displacement parameters ($\text{\AA}^2 \times 10^3$) for 9a.

	<i>x</i>	<i>y</i>	<i>z</i>	<i>U(eq)</i>
Ru(1)	7630(1)	13729(1)	7397(1)	44(1)
P(1)	7583(1)	13321(1)	6591(1)	41(1)
P(2)	7697(1)	12680(1)	7741(1)	49(1)
O(1)	6768(2)	10802(2)	6850(2)	58(1)
O(2)	7253(3)	14243(2)	8111(2)	61(1)
O(3)	6473(2)	13889(2)	7523(2)	55(1)
O(4)	7940(3)	14780(2)	7164(2)	61(1)
O(5)	8772(2)	14032(2)	7418(2)	61(1)
O(1')	7963(2)	11123(2)	6124(2)	56(1)
C(1)	7080(3)	11952(3)	6710(2)	42(1)
C(2)	6545(3)	11434(3)	6689(2)	45(1)
C(3)	5817(3)	11578(2)	6519(2)	53(2)
C(4)	5632(3)	12245(3)	6362(2)	56(2)
C(5)	6168(3)	12756(3)	6375(2)	50(2)
C(1')	7860(3)	11771(3)	6879(2)	41(1)
C(2')	8307(3)	11347(3)	6559(2)	46(1)
C(3')	9032(3)	11197(3)	6680(3)	57(2)
C(4')	9327(4)	11467(3)	7129(3)	61(2)
C(5')	8926(3)	11869(3)	7453(3)	52(2)
C(6')	8174(3)	12036(3)	7329(2)	44(1)
C(7')	8417(4)	10805(3)	5738(2)	62(2)
C(6)	6899(3)	12621(3)	6549(2)	40(1)
C(7)	6238(4)	10255(3)	6844(3)	85(2)
C(8)	7188(3)	13963(3)	6143(2)	46(1)
C(9)	6682(4)	14436(3)	6328(3)	64(2)
C(10)	6378(4)	14921(4)	5991(3)	77(2)
C(11)	6561(4)	14930(4)	5480(3)	75(2)
C(12)	7037(5)	14452(4)	5279(3)	92(3)
C(13)	7358(4)	13969(3)	5619(2)	73(2)
C(14)	8413(3)	13021(39)	6232(2)	44(1)
C(15)	9119(3)	13231(3)	6379(3)	55(2)
C(16)	9736(3)	13066(3)	6092(3)	63(2)
C(17)	9668(3)	12690(3)	5652(2)	56(2)

Table 7: Final position ($x \times 10^{-4}$) and isotropic equivalent displacement parameters ($\text{\AA}^2 \times 10^3$) for 9a.

	<i>x</i>	<i>y</i>	<i>z</i>	<i>U(eq)</i>
C(18)	8969(3)	12459(3)	5504(2)	50(2)
C(19)	8357(3)	12626(3)	5789(2)	47(1)
C(20)	8268(4)	12661(4)	8338(3)	72(2)
C(21)	8265(6)	12087(5)	8659(3)	104(3)
C(22)	8723(8)	12075(7)	9093(5)	160(5)
C(23)	9194(9)	12642(7)	9201(5)	167(6)
C(24)	9203(7)	13197(5)	8880(4)	146(5)
C(25)	8754(5)	13201(4)	8441(3)	99(3)
C(26)	6868(4)	12260(3)	8007(2)	57(2)
C(27)	6662(4)	11580(4)	7934(3)	67(2)
C(28)	6070(4)	11280(4)	8195(39)	74(2)
C(29)	5667(5)	11643(5)	8530(3)	88(2)
C(30)	5860(5)	12332(5)	8618(3)	101(3)
C(31)	6457(5)	12633(4)	8352(3)	84(2)
C(32)	6602(4)	14216(3)	7935(3)	57(2)
C(33)	5978(5)	14570(4)	8192(3)	95(3)
C(34)	8606(4)	14646(4)	7282(3)	62(2)
C(35)	9220(5)	15181(4)	7276(4)	110(3)
Ru(1A)	7285(1)	7659(1)	9059(1)	37(1)
P(1A)	7061(1)	8636(1)	8638(1)	42(1)
P(2A)	7620(1)	7102(1)	8344(1)	39(1)
O(1A)	6991(3)	7803(2)	6767(2)	74(1)
O(2A)	7127(2)	6695(2)	9497(1)	51(1)
O(3A)	6204(2)	7215(2)	9108(1)	46(1)
O(4A)	7343(2)	8174(2)	9823(1)	48(1)
O(5A)	8340(2)	7944(2)	9360(2)	47(1)
O(1'A)	7825(3)	9048(2)	7023(2)	72(1)
C(1A)	6967(3)	8230(3)	7606(2)	47(1)
C(2A)	6565(4)	8073(3)	7160(2)	57(2)
C(3A)	5792(4)	8171(4)	7136(3)	76(2)
C(4A)	5424(4)	8416(4)	7543(3)	75(2)
C(5A)	5791(3)	8594(3)	7981(3)	57(2)
C(6A)	6566(3)	8494(3)	8021(2)	45(1)
C(1'A)	7796(3)	8137(3)	7609(2)	48(1)

Table 7: Final position (x 10⁻⁴) and isotropic equivalent displacement parameters (Å² x 10³) for 9a.

	<i>x</i>	<i>y</i>	<i>z</i>	<i>U(eq)</i>
C(2'A)	8232(4)	8577(3)	7298(2)	57(2)
C(3'A)	9004(4)	8523(4)	7274(3)	66(2)
C(4'A)	9360(4)	8021(3)	7576(3)	69(2)
C(5'A)	8952(3)	7575(39)	7877(2)	54(2)
C(6'A)	8174(3)	7632(3)	7898(2)	43(1)
C(7'A)	8250(5)	9495(4)	6693(4)	111(3)
C(7A)	6613(6)	7607(6)	6304(3)	125(4)
C(8A)	6433(3)	9155(3)	9036(2)	51(2)
C(9A)	5812(4)	8834(3)	9259(3)	64(2)
C(10A)	5324(4)	9188(5)	9585(3)	86(2)
C(11A)	5455(6)	9874(5)	9698(3)	94(3)
C(12A)	6086(6)	10191(4)	9486(3)	101(3)
C(13A)	6565(4)	9832(3)	9146(3)	77(2)
C(14A)	8471(4)	9256(3)	8693(3)	74(2)
C(15A)	9016(4)	9754(4)	8580(4)	99(3)
C(16A)	8828(5)	10258(4)	8228(4)	89(3)
C(17A)	8160(4)	10271(3)	7983(3)	76(2)
C(18A)	7632(4)	9772(39)	8095(2)	62(2)
C(19A)	7775(3)	9259(3)	8461(2)	51(2)
C(20A)	8220(3)	6393(3)	8550(2)	42(1)
C(21A)	8050(4)	5716(3)	8468(3)	60(2)
C(22A)	8478(4)	5193(3)	8686(3)	76(2)
C(23A)	9092(4)	5350(3)	8996(3)	67(2)
C(24A)	9270(3)	6032(3)	9092(3)	58(2)
C(25A)	8833(3)	6545(3)	8877(29)	49(2)
C(26A)	6978(3)	6686(3)	7892(2)	45(1)
C(27A)	7252(4)	6346(3)	7467(2)	59(2)
C(28A)	6797(4)	6036(4)	7122(3)	74(2)
C(29A)	6017(4)	6070(4)	7191(3)	74(2)
C(30A)	5718(4)	6420(3)	7603(2)	65(2)
C(31A)	6197(3)	6718(3)	7953(2)	53(2)
C(32A)	6453(4)	6726(3)	9383(2)	50(2)
C(33A)	5911(4)	6175(3)	9569(3)	76(2)
C(34A)	8040(4)	8171(3)	9773(2)	49(2)

Table 7: Final position ($\times 10^{-4}$) and isotropic equivalent displacement parameters ($\text{\AA}^2 \times 10^3$) for 9a.

	<i>x</i>	<i>y</i>	<i>z</i>	<i>U(eq)</i>
C(35A)	8563(4)	8430(4)	10188(3)	87(2)

Table 8: Final position ($\times 10^{-4}$) and isotropic equivalent displacement parameters ($\text{\AA}^2 \times 10^3$) for 9b.

	<i>x</i>	<i>y</i>	<i>z</i>	<i>U(eq)</i>
Ru(1)	2371(1)	3020(3)	7762(1)	66(1)
P(1)	2903(2)	3061(3)	8840(1)	54(1)
P(2)	1547(2)	2338(3)	7901(1)	58(1)
O(1)	667(4)	1989(4)	9867(3)	74(2)
O(2)	1345(4)	3574(4)	7673(4)	75(2)
O(3)	1629(6)	3202(5)	6761(4)	96(3)
O(4)	3466(5)	2677(5)	7469(4)	92(2)
O(5)	3368(7)	3520(5)	7427(5)	104(3)
O(1')	2476(4)	1799(4)	10354(3)	69(2)
C(1)	1709(6)	2513(5)	9455(4)	50(2)
C(2)	1019(6)	2478(5)	9810(5)	60(3)
C(3)	704(7)	2914(6)	10091(5)	73(3)
C(4)	1075(7)	3401(6)	10003(5)	75(3)
C(5)	1720(6)	3429(5)	9632(5)	67(3)
C(6)	2055(5)	3003(5)	9356(4)	49(2)
C(7)	-1(8)	1929(6)	10258(7)	113(5)
C(1')	2045(6)	2007(5)	9221(5)	55(3)
C(2')	2427(6)	1644(5)	9715(5)	60(3)
C(3')	2735(7)	1173(5)	9533(6)	76(3)
C(4')	2655(7)	1045(5)	8870(6)	78(3)
C(5')	2301(7)	1389(5)	8371(5)	69(3)
C(6')	1990(6)	1867(5)	8543(5)	52(2)
C(7')	2403(10)	1398(5)	10825(6)	115(5)
C(8)	3754(6)	2626(5)	9278(5)	57(3)
C(9)	4175(7)	2296(5)	8933(6)	75(3)
C(10)	4827(8)	1972(6)	9256(8)	98(4)
C(11)	5324(8)	1592(4)	8876(8)	173(8)
C(12)	5077(17)	1601(12)	8104(8)	168(6)
C(12X)	4735(16)	1239(8)	8370(13)	168(6)

Table 8: Final position ($\times 10^{-4}$) and isotropic equivalent displacement parameters ($\text{\AA}^2 \times 10^3$) for **9b**.

	<i>x</i>	<i>y</i>	<i>z</i>	<i>U(eq)</i>
C(13)	6330(10)	1639(12)	9045(14)	168(6)
C(13X)	5780(18)	1987(8)	8467(15)	168(6)
C(14)	5070(20)	1044(7)	9116(15)	168(6)
C(14X)	6043(16)	1238(8)	9264(14)	168(8)
C(15)	5030(7)	2011(6)	9926(8)	90(4)
C(16)	4604(7)	2354(5)	10293(6)	71(3)
C(17)	4883(7)	2384(6)	11037(7)	100(4)
C(18)	4879(12)	1809(7)	11355(8)	175(8)
C(19)	5851(9)	2557(7)	11196(8)	157(7)
C(20)	4314812)	2726(9)	11365(7)	202(11)
C(21)	3957(6)	2657(5)	9966(5)	61(3)
C(22)	3388(6)	3715(5)	8998(4)	53(2)
C(23)	4241(6)	3796(5)	9282(5)	59(3)
C(24)	4614(7)	4281(6)	9305(5)	70(3)
C(25)	5567(7)	4367(6)	9618(7)	93(4)
C(26)	6080(20)	4530(14)	9049(17)	136(5)
C(26X)	5840(20)	4923(14)	9532(17)	136(5)
C(27)	6060(20)	3913(14)	9952(17)	136(5)
C(27X)	6110(20)	3971(14)	9223(16)	136(5)
C(28)	5600(20)	4816(14)	10167(17)	136(5)
C(28X)	5680(20)	4210(14)	10335(18)	136(5)
C(29)	4108(8)	4693(5)	9018(6)	78(3)
C(30)	3258(8)	4631(5)	8731(5)	74(3)
C(31)	2646(10)	5082(6)	8382(7)	107(5)
C(32)	3022(13)	5608(6)	8546(10)	185(8)
C(33)	1731(10)	5068(7)	8604(8)	149(7)
C(34)	2493(14)	4991(7)	7639(8)	178(8)
C(35)	2913(7)	4143(5)	8712(5)	74(3)
C(36)	432(6)	2374(5)	8060(4)	58(3)
C(37)	22(6)	2850(5)	8149(4)	53(3)
C(38)	-850(8)	2845(5)	8233(5)	69(3)
C(39)	-1331(8)	3368(6)	8318(7)	96(4)
C(40)	-738(10)	3832(6)	8397(8)	125(5)
C(41)	-1689(10)	3327(7)	8998(8)	158(7)

Table 8: Final position ($\times 10^{-4}$) and isotropic equivalent displacement parameters ($\text{\AA}^2 \times 10^3$) for 9b.

	<i>x</i>	<i>y</i>	<i>z</i>	<i>U(eq)</i>
C(42)	-2067(11)	3405(7)	7743(8)	187(9)
C(43)	-1288(6)	2383(6)	8236(5)	70(3)
C(44)	-902(6)	1900(5)	8149(4)	57(3)
C(45)	-1420(7)	1398(5)	8146(5)	70(3)
C(46)	-932(8)	914(5)	7913(6)	89(4)
C(47)	-2292(7)	1451(6)	7674(6)	102(4)
C(48)	-1592(8)	1288(6)	8859(6)	112(4)
C(49)	-19(6)	1909(5)	8080(4)	59(3)
C(50)	1424(6)	1991(5)	7100(4)	61(3)
C(51)	605(7)	1962(5)	6697(5)	64(3)
C(52)	526(7)	1778(5)	6051(5)	61(3)
C(53)	-396(7)	1767(5)	5631(5)	76(3)
C(54)	-741(9)	2329(6)	5526(7)	1178(5)
C(55)	-1006(8)	1447(7)	5965(7)	126(5)
C(56)	-390(10)	1550(7)	4929(6)	130(6)
C(57)	1257(8)	1607(5)	5829(5)	68(3)
C(58)	2076(7)	1639(5)	6206(5)	68(3)
C(59)	2895(8)	1475(6)	5929(5)	84(3)
C(60)	3494(17)	1973(11)	5969(14)	106(3)
C(60X)	3069(17)	1905(11)	5417(14)	106(3)
C(61)	2620(17)	1305(11)	5184(14)	106(3)
C(61X)	2803(17)	917(11)	5604(14)	106(3)
C(62)	3359(18)	1054(12)	6363(14)	106(3)
C(62X)	3737(18)	1421(12)	6470(14)	106(3)
C(63)	2147(7)	1833(5)	6855(5)	71(3)
C(64)	1180(8)	3513(6)	7035(7)	84(4)
C(65)	496(9)	3824(7)	6668(7)	142(6)
C(66)	3719(11)	3122(10)	7305(7)	123(6)
C(67)	4611(10)	3128(8)	7012(9)	193(9)
Ru(1A)	72(1)	3394(3)	2438(1)	54(1)
P(1A)	797(2)	4106(3)	2817(1)	50(1)
O(1A)	-410(5)	4598(4)	4944(3)	77(2)
C(1'A)	551(6)	3941(5)	4297(5)	58(3)
O(1'A)	1442(5)	4525(4)	5002(3)	90(2)

Table 8: Final position (x 10⁻⁴) and isotropic equivalent displacement parameters (Å² x 10³) for 9b.

	<i>x</i>	<i>y</i>	<i>z</i>	<i>U(eq)</i>
C(1A)	128(6)	4410(5)	3955(5)	55(2)
P(2A)	-497(2)	3313(3)	3367(1)	52(1)
O(2A)	-1052(4)	3705(4)	1820(3)	70(2)
C(2A)	-344(7)	4739(5)	4298(5)	68(3)
C(2'A)	1241(7)	4016(6)	4853(5)	66(3)
O(3A)	-840(5)	2860(5)	1806(4)	88(3)
C(3A')	1610(7)	3586(6)	5208(5)	76(3)
C(3A)	-735(7)	5177(5)	4010(6)	78(3)
O(4A)	835(5)	3275(4)	1636(3)	78(2)
C(4A)	-657(7)	5315(5)	3361(6)	73(3)
C(4'A)	1355(7)	3101(6)	5030(5)	83(3)
O(5A)	1159(4)	2886(4)	2600(3)	64(2)
C(5'A)	721(6)	3016(5)	4483(5)	66(3)
C(5A)	-197(6)	5006(5)	3017(5)	56(3)
C(6'A)	301(5)	3437(5)	4112(4)	48(2)
C(6A)	203(6)	4548(5)	3291(5)	51(2)
C(7A)	-442(11)	4997(6)	5408(6)	127(6)
C(7'A)	2061(11)	4612(7)	5586(7)	151(7)
C(8A)	1876(6)	4116(5)	3333(4)	51(2)
C(9A)	2249(6)	4592(5)	3539(5)	61(3)
C(10A)	3104(7)	4612(5)	3890(5)	73(3)
C(11A)	3522(7)	5166(5)	4074(6)	92(4)
C(12A)	2811(18)	5588(11)	4105(15)	117(4)
C(13A)	4139(19)	5311(11)	3523(13)	117(4)
C(14A)	4089(17)	5135(10)	4801(14)	117(4)
C(12Y)	3610(30)	5464(14)	3387(18)	117(4)
C(13Y)	4500(20)	5102(13)	4419(18)	117(4)
C(14Y)	2940(20)	5485(14)	4530(20)	117(4)
C(15A)	3541(7)	4151(6)	4027(5)	70(3)
C(16A)	3189(7)	3679(6)	3849(5)	72(3)
C(17A)	3696(8)	3184(6)	4016(7)	102(4)
C(18A)	4452(9)	3185(6)	3598(8)	145(6)
C(19A)	4076(9)	3173(6)	4774(7)	142(6)
C(20A)	3163(10)	2694(6)	3864(9)	151(6)

Table 8: Final position ($x \times 10^{-4}$) and isotropic equivalent displacement parameters ($\text{\AA}^2 \times 10^3$) for 9b.

	x	y	z	$U(eq)$
C(21A)	2342(6)	3670(5)	3493(5)	61(3)
C(22A)	993(6)	4451(4)	2058(4)	51(2)
C(23A)	1829(6)	4480(4)	1919(4)	51(2)
C(24A)	1981(6)	4647(4)	1295(5)	52(2)
C(25A)	2925(6)	4638(5)	1153(5)	63(3)
C(26A)	2997(8)	4880(6)	476(6)	104(4)
C(27A)	3531(17)	4957(5)	1692(6)	93(4)
C(28A)	3256(7)	4082(6)	1178(6)	96(4)
C(29A)	1264(7)	4791(5)	823(5)	61(3)
C(30A)	414(6)	4751(5)	953(5)	55(2)
C(31A)	-368(7)	4892(5)	437(5)	75(3)
C(32A)	-698(17)	5430(11)	598(13)	95(6)
C(32Y)	-1028(17)	5195(11)	763(12)	95(6)
C(33A)	-1008(19)	4405(12)	352(15)	112(7)
C(33Y)	-687(19)	4405(12)	76(15)	112(7)
C(34A)	-99(19)	4901(12)	-318(14)	104(6)
C(34Y)	-43(18)	5190(12)	-213(14)	104(6)
C(35A)	287(6)	4570(4)	1572(5)	55(3)
C(36A)	-1433(6)	3667(5)	3550(5)	54(2)
C(37A)	-1660(6)	3672(5)	4202(5)	64(3)
C(38A)	-2397(6)	3894(5)	4345(5)	71(3)
C(39A)	-2634(7)	3876(7)	5028(6)	99(4)
C(40A)	-1922(9)	3699(8)	5549(6)	149(7)
C(41A)	-2820(16)	4438(11)	5222(9)	275(18)
C(42A)	-3375(13)	3534(13)	5014(8)	309(19)
C(43A)	-2929(7)	4125(6)	3834(6)	84(3)
C(44A)	-2743(7)	4152(5)	3178(5)	69(3)
C(45A)	-3375(9)	4401(7)	2614(7)	103(4)
C(46A)	-4134(13)	4664(11)	2847(12)	259(13)
C(47A)	-3864(13)	4022(9)	2192(9)	203(10)
C(48A)	-2922(13)	4719(11)	2193(14)	330(20)
C(49A)	-1982(6)	3923(5)	3059(5)	63(3)
C(50A)	-846(6)	2631(5)	3409(4)	53(2)
C(51A)	-314(7)	2260(5)	3227(5)	61(3)

Table 8: Final position ($\times 10^{-4}$) and isotropic equivalent displacement parameters ($\text{\AA}^2 \times 10^3$) for 9b.

	<i>x</i>	<i>y</i>	<i>z</i>	<i>U(eq)</i>
C(52A)	-561(8)	1725(5)	3150(5)	68(3)
C(53A)	85(9)	1335(5)	2936(7)	89(4)
C(54A)	983(10)	1404(7)	3351(11)	182(9)
C(55A)	-193(11)	774(7)	3026(8)	153(6)
C(56A)	93(18)	1412(8)	2217(9)	239(14)
C(57A)	-1381(8)	1605(5)	3262(5)	67(3)
C(58A)	-1939(7)	1967(5)	3441(4)	60(3)
C(59A)	-2863(7)	1817(6)	3556(6)	89(4)
C(60A)	-3076(19)	2152(13)	4200(15)	118(4)
C(60Y)	-2871(19)	1778(13)	4278(15)	118(4)
C(61A)	-2891(18)	1254(12)	3830(14)	118(4)
C(61Y)	-3304(19)	1535(13)	2899(15)	118(4)
C(62A)	-3461(19)	2021(13)	3000(16)	118(4)
C(62Y)	-3471(19)	2306(12)	3472(16)	118(4)
C(63A)	-1667(6)	2478(5)	3515(4)	54(3)
C(64A)	-1251(8)	3248(7)	1572(6)	81(4)
C(65A)	-1992(7)	3180(6)	1010(6)	127(6)
C(66A)	1298(7)	2971(6)	2012(6)	72(3)
C(67A)	2080(8)	2678(6)	1799(7)	119(5)

Table 9: Final position ($\times 10^{-4}$) and isotropic equivalent displacement parameters ($\text{\AA}^2 \times 10^3$) for C1.

	<i>x</i>	<i>y</i>	<i>z</i>	<i>U(eq)</i>
Ru(1)	2686(1)	6700(1)	250(1)	32(1)
S(1)	1373(1)	8812(2)	-652(1)	63(1)
P(1)	2881(1)	6716(2)	1391(1)	38(1)
P(2)	2170(1)	4624(1)	107(1)	36(1)
O(1)	2925(2)	4965(4)	-1001(2)	50(1)
O(2)	1696(2)	7802(4)	-116(2)	46(1)
O(3)	3378(2)	5506(4)	1760(2)	51(2)
O(4A)	667(8)	8197(11)	-1215(6)	74(2)
O(4B)	926(8)	8396(11)	-1330(6)	74(2)
O(5A)	1767(7)	9476(12)	-879(7)	64(2)
O(5B)	1936(7)	9830(12)	-609(7)	64(2)

Table 9: Final position ($x \times 10^{-4}$) and isotropic equivalent displacement parameters ($\text{\AA}^2 \times 10^3$) for C1.

	<i>x</i>	<i>y</i>	<i>z</i>	<i>U(eq)</i>
O(1')	4707(2)	4108(5)	528(3)	64(1)
F(1)	1377(4)	10329(6)	302(4)	143(3)
F(2)	460(3)	9146(6)	-175(4)	135(3)
F(3)	568(3)	10754(5)	-726(4)	125(2)
C(1)	3490(3)	5535(5)	178(3)	38(1)
C(2)	3113(3)	5924(6)	-544(3)	40(1)
C(3)	2917(3)	7229(6)	-686(3)	45(1)
C(4)	3228(4)	8179(6)	-158(4)	51(2)
C(5)	3709(3)	7849(6)	501(3)	46(1)
C(6)	3832(3)	6503(5)	688(3)	41(1)
C(7)	2528(5)	5272(8)	-1730(4)	76(2)
C(1')	3538(3)	4133(5)	372(3)	38(1)
C(2')	4165(4)	3425(6)	553(3)	50(2)
C(3')	4189(4)	2150(7)	746(4)	63(2)
C(4')	3606(4)	1571(6)	757(4)	63(2)
C(5')	2972(4)	2254(6)	561(4)	53(2)
C(6')	2945(3)	3561(5)	376(3)	39(1)
C(7')	5350(5)	3427(9)	659(5)	98(3)
C(8)	1667(3)	3999(5)	545(3)	41(1)
C(9)	923(4)	3971(7)	193(4)	61(2)
C(10)	543(4)	3528(9)	528(4)	77(2)
C(11)	886(5)	3094(8)	1204(4)	79(2)
C(12)	1621(5)	3093(8)	1545(4)	68(2)
C(13)	2009(4)	3540(6)	1221(3)	50(2)
C(13)	2009(4)	3540(6)	1221(3)	50(2)
C(14)	1588(3)	4231(6)	-805(3)	45(1)
C(15)	1619(4)	3028(7)	-1085(4)	64(2)
C(16)	1152(5)	2761(10)	-1773(4)	81(3)
C(17)	673(5)	3674(10)	-2184(4)	83(3)
C(18)	640(4)	4860(9)	-1913(4)	74(2)
C(19)	1100(4)	5138(7)	-1229(3)	56(2)
C(20)	3389(3)	8128(6)	1868(3)	46(2)
C(21)	4128(4)	8059(8)	2266(4)	68(2)
C(22)	4510(5)	9140(10)	2616(4)	82(3)

Table 9: Final position ($\times 10^{-4}$) and isotropic equivalent displacement parameters ($\text{\AA}^2 \times 10^3$) for C1.

	<i>x</i>	<i>y</i>	<i>z</i>	<i>U(eq)</i>
C(23)	4171(6)	10295(9)	2559(4)	83(3)
C(24)	3447(6)	10372(8)	2180(5)	79(3)
C(25)	3052(4)	9305(7)	1818(4)	59(2)
C(26)	2156(3)	6690(6)	1632(3)	45(1)
C(27)	1478(4)	7074(10)	1190(4)	83(3)
C(28)	950(5)	7114(13)	1410(6)	112(4)
C(29)	1102(5)	6731(10)	2064(5)	89(3)
C(30)	1760(5)	6284(9)	2496(4)	76(2)
C(31)	2297(4)	6286(8)	2292(4)	62(2)
C(32)	914(5)	9812(8)	-300(6)	81(3)
S(1B)	4211(2)	10911(3)	-1591(2)	101(1)
Q(1)	4051(5)	9674(8)	-1833(4)	160(2)
Q(2)	3806(5)	12587(11)	-1002(5)	160(2)
Q(3)	4658(8)	11751(12)	-1617(7)	160(2)
Q(4)	3246(8)	10733(13)	-1160(6)	160(2)
Q(5)	3630(12)	11460(30)	-1172(10)	160(2)
Q(6)	3089(8)	11854(13)	-1946(8)	160(2)
Q(7)	4891(9)	10698(15)	-825(9)	160(2)
Q(8)	3579(10)	11659(15)	-2287(9)	160(2)
Q(9)	4037(9)	10587(15)	-580(9)	160(2)

Table 10: Final position ($\times 10^{-4}$) and isotropic equivalent displacement parameters ($\text{\AA}^2 \times 10^3$) for C2.

	<i>x</i>	<i>y</i>	<i>z</i>	<i>U(eq)</i>
Ru(1)	4541(1)	1267(1)	7730(1)	35(1)
P(1)	3419(1)	1663(1)	8317(1)	39(1)
P(2)	3922(1)	1861(1)	6822(1)	37(1)
C(1)	4065(3)	82(3)	6797(3)	36(1)
C(2)	5021(3)	159(3)	6751(3)	36(1)
C(3)	5738(4)	359(3)	7420(3)	41(1)
C(4)	5481(4)	312(3)	8069(3)	43(1)
C(5)	4606(4)	12(3)	8047(3)	46(1)
C(6)	3857(4)	-76(3)	7415(3)	40(1)
C(7)	5265(4)	119(4)	6099(3)	48(1)
C(8)	6162(4)	303(4)	6115(3)	60(2)

Table 10: Final position ($x \times 10^{-4}$) and isotropic equivalent displacement parameters ($\text{\AA}^2 \times 10^3$) for C2.

	<i>x</i>	<i>y</i>	<i>z</i>	<i>U(eq)</i>
C(9)	6870(4)	551(4)	6774(3)	59(2)
C(10)	6651(4)	574(4)	7410(3)	50(1)
C(1')	3330(3)	90(3)	6156(3)	37(1)
C(2')	2729(3)	-706(3)	5619(3)	41(1)
C(3')	2172(4)	-652(4)	4975(3)	47(1)
C(4')	2095(4)	186(4)	4913(3)	49(1)
C(5')	2583(4)	942(4)	5450(3)	48(1)
C(6')	3213(3)	897(3)	6078(3)	39(1)
C(7')	2824(4)	-1543(4)	5706(3)	58(2)
C(8')	2267(5)	-2277(4)	5184(4)	75(2)
C(9')	1692(5)	-2215(5)	4544(4)	73(2)
C(10')	1644(4)	-1428(4)	4444(3)	60(2)
C(11)	3292(4)	2809(4)	8707(3)	50(1)
C(12)	2530(5)	2968(5)	8985(4)	82(2)
C(13)	2400(6)	3837(6)	9304(5)	106(3)
C(14)	3037(7)	4527(5)	9341(5)	100(3)
C(15)	3788(6)	4365(5)	9089(5)	100(3)
C(16)	3904(5)	3506(4)	8755(4)	72(2)
C(17)	3580(4)	1292(4)	9100(3)	45(1)
C(18)	4317(4)	1728(5)	9708(3)	66(2)
C(19)	4544(5)	1358(6)	10262(3)	86(2)
C(20)	4050(6)	600(7)	10219(4)	87(3)
C(21)	3324(5)	181(5)	9637(4)	77(2)
C(22)	3076(4)	520(4)	9069(3)	59(2)
C(23)	3184(4)	2713(3)	6898(3)	44(1)
C(24)	2277(4)	2524(4)	6898(3)	49(1)
C(25)	1728(4)	3172(4)	6989(3)	60(2)
C(26)	2078(5)	4017(5)	7081(4)	79(2)
C(27)	2964(6)	4207(4)	7051(5)	100(3)
C(28)	3528(5)	3559(4)	6974(4)	80(2)
C(29)	4832(4)	2265(4)	6474(3)	49(1)
C(30C)	5761(11)	2363(11)	6849(8)	69(3)
C(30D)	5593(10)	2818(10)	6985(7)	69(3)
(C31C)	6454(14)	2690(13)	6581(11)	95(4)

Table 10: Final position ($\times 10^{-4}$) and isotropic equivalent displacement parameters ($\text{\AA}^2 \times 10^3$) for C2.

	<i>x</i>	<i>y</i>	<i>z</i>	<i>U(eq)</i>
C(31D)	6315(12)	3146(12)	6762(10)	95(4)
C(32)	6235(6)	2925(6)	5991(5)	100(3)
C(33C)	5348(11)	2970(10)	5681(8)	77(3)
C(33D)	5486(10)	2226(10)	5460(8)	77(3)
C(34C)	4637(9)	2599(9)	5921(7)	63(2)
C(34D)	4754(9)	1918(8)	5685(7)	63(2)
C(35)	7123(6)	3368(8)	8893(6)	126(4)
S(1)	6275(1)	2675(1)	9088(1)	84(1)
O(1)	2451(2)	1143(2)	7772(2)	48(1)
F(1)	7400(4)	2868(5)	8346(4)	201(4)
F(2)	7849(4)	3667(5)	9485(4)	188(3)
F(3)	6815(5)	4025(4)	8765(4)	158(3)
O(2)	5522(3)	2436(2)	8407(2)	60(1)
O(3)	6049(4)	3274(4)	9716(3)	109(2)
O(4)	6688(5)	1954(4)	9189(4)	161(3)
Ru(1B)	8025(1)	-2517(1)	6977(1)	37(1)
P(1B)	9482(1)	-2640(1)	6857(1)	40(1)
P(2B)	8239(1)	-3136(1)	7916(1)	46(1)
O(1B)	10191(2)	-2198(2)	7644(2)	45(1)
C(1B)	7985(3)	-1399(3)	7901(3)	37(1)
C(2B)	6981(3)	-1648(3)	7608(3)	37(1)
C(3B)	6602(4)	-1840(3)	6837(3)	44(1)
C(4B)	7203(4)	-1665(4)	6404(3)	47(1)
C(5B)	8090(4)	-1225(3)	6731(3)	44(1)
C(6B)	8506(4)	-1113(3)	7480(3)	39(1)
C(7B)	6391(4)	-1783(3)	8033(3)	45(1)
C(8B)	5483(4)	-2078(4)	7716(3)	59(2)
C(9B)	5110(4)	-2302(4)	6957(4)	65(2)
C(10B)	5658(4)	-2191(4)	6525(3)	60(2)
C(1*)	8417(3)	-1386(3)	8663(3)	40(1)
C(2*)	8570(3)	-597(4)	9279(3)	44(1)
C(3*)	8940(4)	-630(4)	9996(3)	53(2)
C(4*)	9143(4)	-1454(5)	10059(3)	69(2)
C(5*)	8985(4)	-2193(4)	9465(3)	60(2)

Table 10: Final position ($\times 10^{-4}$) and isotropic equivalent displacement parameters ($\text{\AA}^2 \times 10^3$) for C2.

	<i>x</i>	<i>y</i>	<i>z</i>	<i>U(eq)</i>
C(6*)	8615(4)	-2172(4)	8750(3)	47(1)
C(7*)	8380(4)	220(4)	9210(3)	54(2)
C(8*)	8525(4)	962(4)	9818(4)	65(2)
C(9*)	8885(4)	913(5)	10515(4)	74(2)
C(10*)	9089(4)	146(5)	10602(3)	67(2)
C(11B)	7136(4)	-3633(4)	7961(3)	53(2)
C(12B)	6447(4)	-4084(4)	7335(4)	69(2)
C(13B)	5618(5)	-4471(5)	7363(5)	88(2)
C(14B)	5467(5)	-4405(5)	8033(5)	90(2)
C(15B)	6128(6)	-3950(6)	8676(5)	97(3)
C(16B)	6966(5)	-3572(5)	8634(4)	82(2)
C(17B)	8987(4)	-3939(4)	8045(4)	67(2)
C(18B)	8623(6)	-4824(5)	7807(6)	114(3)
C(19B)	9180(8)	-5453(6)	7858(8)	174(6)
C(20B)	10105(8)	-5189(7)	8169(8)	161(5)
C(21B)	10495(6)	-4320(7)	8413(6)	125(4)
C(22B)	9926(5)	-3685(5)	8345(4)	79(2)
C(23B)	9798(4)	-2017(4)	6301(3)	45(1)
C(24B)	9370(4)	-2312(4)	5547(3)	59(2)
C(25B)	9565(6)	-1780(6)	5134(4)	80(2)
C(26B)	10158(6)	-1015(6)	5464(6)	93(3)
C(27B)	10580(5)	-728(5)	6190(5)	81(2)
C(28B)	10399(4)	-1229(4)	6616(4)	60(2)
C(29B)	9788(4)	-3712(4)	6445(3)	51(2)
C(30B)	9258(5)	-4490(4)	6326(4)	82(2)
C(31B)	9579(7)	-5288(5)	6031(5)	117(4)
C(32B)	10403(7)	-5274(6)	5864(4)	106(3)
C(33B)	10925(6)	-4514(6)	5984(4)	94(3)
C(34B)	10630(5)	-3725(4)	6262(3)	68(2)
C(35B)	6581(9)	-5121(8)	5026(6)	138(5)
S(1B)	7008(1)	-3947(1)	5316(1)	81(1)
O(2B)	7431(3)	-3753(2)	6112(2)	56(1)
O(3BA)	5952(13)	-3788(12)	5395(10)	97(2)
O(3BB)	6371(6)	-3484(5)	5104(4)	97(2)

Table 10: Final position (x 10⁻⁴) and isotropic equivalent displacement parameters (Å² x 10³) for C2.

	<i>x</i>	<i>y</i>	<i>z</i>	<i>U(eq)</i>
O(4BA)	7428(14)	-3611(13)	4873(10)	98(2)
O(4BB)	7780(6)	-4107(6)	491184)	98(2)
F(1B)	5965(7)	-5196(6)	5376(5)	229(5)
F(2B)	6127(5)	-5382(4)	4317(3)	172(3)
F(3B)	7191(7)	-5543(4)	5165(5)	236(5)
S(1)	10005(1)	1202(1)	7518(1)	62(1)
O(5)	10298(5)	1535(5)	6984(4)	132(3)
O(6)	9241(3)	563(3)	7162(4)	120(2)
O(7)	10758(3)	1076(4)	8016(3)	97(2)
C(36)	9577(6)	2127(6)	8060(5)	92(3)
F(4)	10199(5)	2783(4)	8440(5)	216(5)
F(5)	9214(6)	1890(5)	8522(4)	177(3)
F(6)	8924(4)	2368(3)	7659(3)	131(2)
S(2B)	12808(1)	-2177(1)	7780(1)	64(1)
O(5B)	12819(4)	-2603(5)	7042(39)	140(3)
O(6B)	11955(3)	-1897(4)	7853(3)	103(2)
O(7B)	13603(3)	-1553(3)	8225(3)	90(2)
C(36B)	12879(7)	-3032(6)	8182(7)	108(3)
C(36B)	12879(7)	-3032(6)	8182(7)	108(3)
F(4B)	12779(6)	-2703(6)	8859(4)	200(4)
F(5B)	13616(5)	-3324(4)	8216(5)	212(4)
F(6B)	12178(4)	-3691(3)	7792(4)	160(2)
C(1L)	110(30)	4260(20)	9913(19)	241(9)
C(2L)	-1040(30)	4260(20)	9913(19)	241(9)
C(3L)	810(20)	4664(18)	10362(16)	241(9)

Table 11: Final position (x 10⁻⁴) and isotropic equivalent displacement parameters (Å² x 10³) for C4.

	<i>x</i>	<i>y</i>	<i>z</i>	<i>U(eq)</i>
Ru(1)	3455(2)	6320(3)	3865(1)	28(1)
P(1)	4445(6)	7186(4)	4476(3)	32(2)
P(2)	3845(6)	5523(4)	4758(3)	31(2)
F(1)	1712(15)	6904(9)	5487(8)	57(4)
F(2)	1336(16)	7815(10)	4795(8)	68(3)

Table 11: Final position ($x \times 10^{-4}$) and isotropic equivalent displacement parameters ($\text{\AA}^2 \times 10^3$) for C4.

	<i>x</i>	<i>y</i>	<i>z</i>	<i>U(eq)</i>
C(2)	3140(30)	5371(15)	3099(13)	42(7)
O(1)	1882(15)	6784(9)	4308(7)	30(4)
O(2)	3487(16)	7413(9)	5004(8)	38(4)
O(3)	2980(18)	4719(11)	3204(9)	52(5)
C(1)	4490(20)	5610(13)	3326(11)	29(6)
C(3)	2290(30)	5897(16)	2907(13)	46(7)
C(4)	2700(20)	6518(13)	2787(11)	28(6)
C(5)	4020(20)	6678(15)	2846(12)	34(6)
C(6)	4880(20)	6221(13)	3141(10)	25(6)
C(7)	1690(30)	4470(20)	3022(16)	75(10)
C(1')	5370(20)	5124(14)	3760(13)	37(7)
C(2')	6380(20)	4771(14)	3502(12)	35(6)
C(3')	7080(30)	4277(19)	3897(16)	71(10)
O(3')	6640(20)	4933(12)	2846(10)	62(6)
C(4')	6730(30)	4161(19)	4530(16)	68(9)
C(5')	5790(30)	4487(17)	4824(15)	57(8)
C(6')	5080(20)	4998(14)	4421(12)	32(6)
C(7')	7940(30)	4824(17)	2655(14)	57(8)
C(8)	4700(20)	7918(14)	3944(12)	39(7)
C(9)	3600(30)	8282(17)	3736(14)	56(8)
C(10)	3760(40)	8880(20)	3297(17)	82(11)
C(11)	4870(40)	9030(30)	3170(20)	95(13)
C(11)	4870(40)	9030(30)	3170(20)	95(13)
C(12)	5970(40)	8720(20)	3353(18)	85(12)
C(13)	5840(40)	8100(20)	3756(16)	75(10)
C(14)	6010(20)	7128(13)	4956(11)	29(6)
C(15)	6220(30)	7484(18)	5556(15)	65(9)
C(16)	7430(30)	7489(19)	5893(16)	73(10)
C(17)	8410(30)	7069(19)	5636(16)	68(10)
C(18)	8200(30)	6777(18)	5086(15)	58(9)
C(19)	7030(30)	6771(16)	4724(14)	49(8)
C(20)	2470(20)	4998(14)	4802(12)	38(7)
C(21)	2580(30)	4352(17)	5009(14)	58(9)
C(22)	1490(30)	3910(20)	5048(15)	69(10)

Table 11: Final position ($\times 10^{-4}$) and isotropic equivalent displacement parameters ($\text{\AA}^2 \times 10^3$) for C4.

	<i>x</i>	<i>y</i>	<i>z</i>	<i>U(eq)</i>
C(23)	230(30)	4175(19)	4957(16)	68(9)
C(24)	30(50)	4850(30)	4760(20)	103(14)
C(25)	1190(30)	5261(18)	4711(14)	57(9)
C(26)	4370(30)	5679(16)	5658(14)	48(8)
C(27)	3440(30)	5749(16)	6100(14)	54(8)
C(28)	3820(40)	5850(20)	6782(18)	77(10)
C(29)	5050(40)	5940(20)	6990(20)	102(13)
C(30)	6030(40)	5860(20)	6572(17)	80(11)
C(31)	5700(30)	5734(18)	5872(16)	67(9)
B(2)	-1020(30)	6604(17)	3125(15)	37(8)
B(1)	2100(30)	7203(18)	4925(15)	40(8)
F(3)	-84(18)	7073(11)	3356(9)	76(5)
F(4)	-2161(16)	6892(10)	3082(8)	65(5)
F(5)	-713(18)	6369(12)	2492(9)	82(5)
F(6)	-940(20)	6079(12)	3584(10)	94(7)
Ru(1A)	2606(2)	7666(3)	9522(1)	40(1)
P(1A)	3440(7)	8499(5)	8889(4)	39(2)
P(2A)	2986(7)	8226(5)	10565(3)	39(2)
F(1A)	677(18)	9363(11)	9487(9)	80(6)
F(2A)	245(16)	9046(10)	8389(8)	64(5)
O(1A)	904(18)	8234(10)	9201(9)	49(5)
O(2A)	2382(16)	9069(10)	8861(8)	39(1)
O(3A)	2248(17)	6549(10)	10842(8)	46(5)
B(1A)	1020(40)	8970(20)	8944(18)	54(10)
C(1A)	3780(30)	6919(15)	10106(13)	41(7)
C(2A)	2480(30)	6621(16)	10208(14)	47(7)
C(3A)	1590(30)	6604(17)	9623(15)	61(9)
C(4A)	1940(30)	6719(17)	8948(15)	58(9)
C(5A)	3300(30)	6852(16)	8865(14)	47(8)
C(6A)	4170(20)	6970(14)	9428(11)	33(6)
C(7A)	910(30)	6260(20)	10957(15)	66(9)
C(1'A)	4620(30)	7174(15)	10670(12)	41(7)
C(2'A)	5630(30)	6767(18)	10961(15)	59(9)
C(3'A)	6470(30)	7028(16)	11542(14)	54(8)

Table 11: Final position ($x \times 10^{-4}$) and isotropic equivalent displacement parameters ($\text{\AA}^2 \times 10^3$) for C4.

	<i>x</i>	<i>y</i>	<i>z</i>	<i>U(eq)</i>
O(3'A)	5850(20)	6191(13)	10640(10)	72(6)
C(4'A)	6130(30)	7568(17)	11828(14)	56(8)
C(5'A)	5090(30)	7988(18)	11553(15)	60(9)
C(6'A)	4350(20)	7752(15)	10964(11)	32(6)
C(7'A)	7080(40)	5840(20)	10764(19)	92(12)
C(8'A)	4980(20)	8893(13)	9088(12)	30(6)
C(9A)	6030(30)	8554(18)	9409(14)	57(8)
C(10A)	7200(30)	8883(18)	9506(15)	64(9)
C(11A)	7410(40)	9500(20)	9277(17)	77(11)
C(12A)	6360(40)	9810(30)	8950(20)	98(13)
C(13A)	5170(30)	9529(19)	8869(15)	67(9)
C(14A)	3550(30)	8193(16)	8028(13)	48(8)
C(15A)	2420(30)	8026(16)	7647(14)	52(8)
C(16A)	2480(30)	7720(20)	6994(16)	76(10)
C(17A)	3620(30)	7600(20)	6759(18)	84(11)
C(18A)	4700(40)	7780(20)	7131(17)	80(10)
C(19A)	4690(30)	8043(19)	7798(16)	71(10)
C(20A)	3420(30)	9057(18)	10708(14)	56(8)
C(21A)	4680(20)	9377(13)	10681(11)	28(6)
C(22A)	4970(50)	10040(30)	10800(20)	107(14)
C(23A)	3950(50)	10450(30)	10970(20)	111(15)
C(24A)	2790(50)	10240(20)	11000(20)	102(14)
C(25A)	2370(30)	9490(20)	10880(16)	73(10)
C(26A)	1630(30)	8104(15)	11123(12)	41(7)
C(27A)	1870(30)	8140(15)	11846(12)	40(7)
C(28A)	850(40)	8080(20)	12238(19)	85(11)
C(29A)	-420(30)	7997(16)	11920(14)	54(8)
C(30A)	-660(30)	7976(17)	11243(15)	60(9)
C(31A)	350(30)	8049(18)	10828(17)	67(9)
B(2A)	-1881(19)	7078(10)	8891(9)	140(20)
F(3A)	-3092(17)	7071(13)	8641(11)	129(9)
F(4AA)	-1220(30)	7550(30)	8580(30)	174(11)
F(4BA)	-1400(40)	7694(13)	8910(60)	174(11)
F(5AA)	-1310(30)	6491(15)	8820(40)	174(11)

Table 11: Final position ($\times 10^{-4}$) and isotropic equivalent displacement parameters ($\text{\AA}^2 \times 10^3$) for C4.

	<i>x</i>	<i>y</i>	<i>z</i>	<i>U(eq)</i>
F(5BA)	-1160(30)	6700(50)	8490(40)	174(11)
F(6AA)	-1820(30)	7230(40)	9563(12)	174(11)
F(6BA)	-1760(40)	6820(60)	9520(30)	174(11)

4.5.2 Synthesis

All reactions with air- or moisture-sensitive materials were carried out under Argon using standard Schlenk techniques. The solvents used for synthetic and recrystallisation purposes were of “puriss p.a” quality, purchased from *Fluka AG*, *Riedel-de-Haen* or *Merck*. Diethylether was distilled from sodium-benzophenone ketyl. Hexane was distilled from sodium. Dichloromethane was distilled from CaH₂. 1,2-Dichloroethane was distilled from P₂O₁₀. The deuterated solvent CD₂Cl₂ was purchased from Cambridge Isotope Laboratories. It was distilled and dried over CaH₂ before use.

Racemic-2,2'-Bis(diphenylphosphino)-1,1'-binaphthyl (Binap) was purchased from Strem Chemicals. Racemic-(6,6'-Dimethoxybiphenyl-2,2'-diyl)bis(diphenylphosphine oxide), (*S*)-(6,6'-Dimethoxybiphenyl-2,2'-diyl)bis(diphenylphosphine) ((*S*)-MeO-Biphep) and (*R*)-3,5-di-*tert*-Bu-MeO-Biphep were given by F. Hoffmann-La Roche AG. The reduction of this diphosphine oxide by reported methods gave the ligand (rac)-(6,6'-Dimethoxybiphenyl-2,2'-diyl)bis(diphenylphosphine) (MeO-Biphep). [Ru(OAc)₂(MeO-Biphep)], **9a**, [Ru(OAc)₂((*R*)-3,5-di-*tert*-Bu-MeO-Biphep)], **9b**, [Ru(OAc)₂(Binap)], **10**, [Ru(Binap)(η⁶-benzene)](SbF₆)₂, **26**, and [Ru(Binap)(η⁶-*p*-cymene)](SbF₆)₂, **27**, were prepared according methods reported in the literature.^{16,49} All the other chemicals were commercial products used as received.

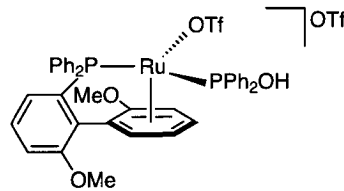
The routine ³¹P{¹H}-, ¹³C{¹H}-, ²H- and ¹H-NMR spectra were measured in CD₂Cl₂ on either a *Brucker AdvanceDPX250* [frequency in MHz: ³¹P : 101.26, ¹³C : 62.90, ¹H : 250.14] or *Brucker AdvanceDPX300* [frequency in MHz: ³¹P: 121.49, ¹⁹F : 282.39, ¹³C : 75.47, ¹H : 300.13] or *Brucker AdvanceDRX400* [frequency in MHz: ³¹P : 161.98, ¹⁹F : 376.46, ¹³C : 100.61, ¹H : 400.13] or *Brucker AdvanceDRX500* [frequency in MHz: ³¹P : 202.46, ¹³C : 125.75, ¹H : 500.13] at room temperature unless stated. The two-dimensional ¹H-¹H-DQF-COSY, ³¹P-¹H-INV-COSY, ¹³C-¹H-HMQC, ¹³C-¹H-HMBC, ¹⁹F-¹H-NOESY and ¹H-NOESY experiments were carried out at either *Brucker AdvanceDRX400* or *Brucker AdvanceDRX500*.

The chemical shifts δ are given in ppm and the coupling constants J are given in Hertz. The multiplicity is denoted by the following abbreviations: s: singlet; d: doublet; t: triplet; m: multiplet; dd: doublet of doublet; ddd: doublet of dd; dt: doublet of triplet; br : broad.

Elemental analysis (EA) and EI-MS and FAB-MS spectra were performed by the service of the “Laboratorium für Organische Chemie der ETH Zürich”.

Synthesis of C1

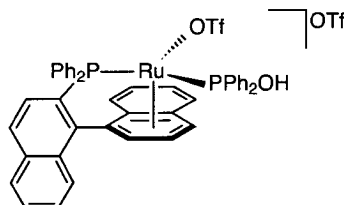
[Ru(OAc)₂(MeO-Biphep)] (60.8 mg, 0.08 mmol) was dissolved in 2 mL of 1,2-dichloroethane and 2.1 equivalents of trifluoromethanesulfonic acid (14 mL, 0.16 mmol) added. The solution color turned immediately from yellow to orange. After heating for 1 h at 90° C, the reaction mixture was filtered using a glass filter. The 1,2-dichloroethane was evaporated under high vacuum. The crude reaction mixture was stirred and washed three times with 1 mL of Et₂O. The complex was recrystallized from dichloromethane-Et₂O. A suitable crystal for X-ray diffraction was obtained form the same mixture of solvents.



Color: orange. Yield: 59.2 mg (78%). Anal. Calcd for C₄₀H₃₄O₉F₆P₂S₂Ru (999.84): C, 48.05; H, 3.43. Found: C, 48.00; H, 3.56. FAB-MS: calcd M⁺-OTf 701.7; found 701.3; NMR (DRX400, CD₂Cl₂): ³¹P, 104.1 (d, 63), 50.2 (d, 63); ¹⁹F, -77.8 (s), -79.3 (s); ¹³C, 158.7 (d, 17), 146.4 (d, 6), 143.9 (d, 62), 143.9 (d, 48), 134.2 (d, 11), 133.8 (d, 10), 133.1, 133.2, 132.1 (d, 3), 131.8 (d, 3), 131.1 (br s), 131.0, 130.8, 130.7, 129.4-128.8, 128.3, 128.2, 127.8, 125.6 (d, 1), 115.0 (d, 2), 102.7 (d, 6), 97.6 (d, 6), 93.7 (d, 4), 81.4 (d, 8), 79.6, 56.9, 56.4; ¹H, 9.66 (br s, 1H), 7.81-7.96 (4H), 7.68 (dt, 8.0, 3.4, 0.5, 1H), 7.64-7.49 (6H), 7.25-7.10 (8H), 7.02 (dt, 8.8, 7.8, 2.7, 1H), 6.94 (dt, 8.8, 7.9, 3.1, 2H), 6.63 (dd, 7.0, 6.6, 2.1, 1.4, 1H), 5.98 (dd, 7.0, 1.5, 0.7, 1H), 5.67 (dd, 5.2, 3.7, 1.4, 1H), 5.22 (td, 6.6, 2.2, 2.1, 0.7, 1H), 3.94 (s, 3H), 2.99 (s, 3H).

Synthesis of C2

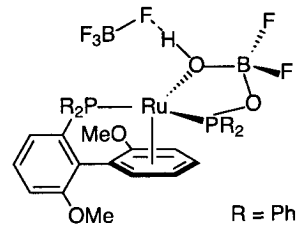
[Ru(OAc)₂(Binap)] (65.0 mg, 0.08 mmol) was dissolved in 2 mL of 1,2-dichloroethane and 2.4 equivalents of trifluoromethanesulfonic acid (16 mL, 0.18 mmol) added. The solution color turned immediately from yellow to orange. After heating for 1h at 90° C, the reaction mixture was filtered using a glass filter. The 1,2-dichloroethane was evaporated under high vacuum. The crude reaction mixture was stirred and washed three times with 1 mL of Et₂O. The complex was recrystallized from dichloromethane-Et₂O. A suitable crystal for X-ray diffraction was obtained form the same mixture of solvents.



Color: orange. Yield: 59.6 mg (74%). Anal. Calcd for C₄₆H₃₄O₇F₆P₂S₂Ru (1039.94): C, 53.13; H, 3.30. Found: C, 53.01; H, 3.44. FAB-MS: calcd M⁺ 890.9; found 891.1; NMR (DRX400, CD₂Cl₂): ³¹P, 114.5 (d, 56), 53.4 (d, 56); ¹⁹F, -78.2 (s), -79.5 (s); ¹³C, 142.6 (d, 60), 141.0 (d, 19), 140.7 (d, 56), 135.4 (d, 2), 135.2, 134.9, 134.9, 134.8, 132.9, 132.8, 132.2-131.8, 131.7, 131.6, 131.5 (d, 3), 131.2 (d, 3), 129.8, 129.6 (d, 2), 129.5 (d, 2), 129.3, 129.2, 129.1, 129.0, 128.8, 128.6, 128.2, 128.1, 127.7 (d, 2), 127.4, 125.1, 116.9 (d, 7), 110.6 (dd, 6, 2), 107.6 (d, 6), 100.0 (d, 8), 99.6 (d, 4), 77.9; ¹H, 10.02 (br s, 1H), 8.30 (dd, 8.5, 2.3, 1H), 8.20 (d, 8.3, 1H), 8.03 (d, 8.1, 1H), 7.95 (m, 1H), 7.86-7.75 (4H), 7.68 (m, 1H), 7.62-7.57 (3H), 7.54 (dd, 7.3, 2.1, 1H), 7.40 (m, 1H), 7.26-7.10 (11H), 7.04 (dt, 9.3, 7.7, 2H), 6.97-6.89 (3H), 6.34 (d, 8.6, 1H), 5.84 (t, 5.3, 4.3, 1H), 5.54 (ddd, 7.3, 5.3, 2.3, 1H).

Synthesis of C3

Method I: A solution of $[\text{Ru}(\text{OAc})_2((S)\text{-MeO-Biphep})]$ (68.5 mg, 0.09 mmol) in 1 mL of CD_2Cl_2 in an NMR tube was treated with 2.1 equivalents of tetrafluoroboric acid (24 μL , 7.3 M in Et_2O). After 28 days the reaction mixture was transferred to a Schlenk tube and the solvent was distilled under high vacuum. The remaining yellow powder was three times washed with 2 mL of Et_2O . Drying under vacuum afforded a pale yellow powder in 61.2 mg (85%) yield. A yellow crystal was grown by slow diffusion of diethyl ether into a CH_2Cl_2 solution of the product.

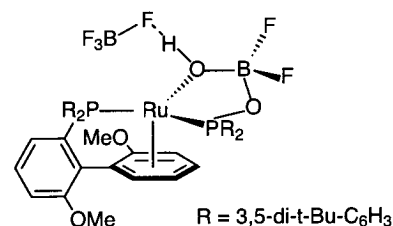


Method II: $[\text{Ru}(\text{OAc})_2(\text{MeO-Biphep})]$ (120.4 mg, 0.15 mmol) was dissolved in 5 ml 1,2-dichloroethane. After addition of tetrafluoroboric acid (30 μL , 7.3 M in Et_2O), distilled water (10 μL) was added to the resulting solution. The ^{31}P -NMR showed full conversion to the product after heating the solution for ca 6 h at 90° C. The solvent was removed in vacuo and the remaining residue was washed three times with pentane.

Anal. Calcd for $\text{C}_{38}\text{H}_{34}\text{O}_4\text{B}_2\text{F}_6\text{P}_2\text{Ru}\cdot\text{H}_2\text{O}$ (853.31): C, 52.33; H, 4.13. Found: C, 52.04; H, 4.48. FAB-MS: calcd M^+ 766.3; found 766.9, 701.0 (100%, $\text{M}^+ + \text{BF}_2\text{OH}$). NMR (DRX400, CD_2Cl_2): ^{31}P , 114.1 (br d, 55), 46.5 (d, 55); ^{19}F , -141.1 (d, 66), -141.1 (d, 66), -143.5 (d, 66), -143.6 (d, 66), -151.5 (25%, s), -151.6 (75%, s); ^{13}C (DPX300), 159.0 (d, 17), 147.4 (d, 7), 144.5 (d, 54), 144.4 (d, 57), 133.6, 133.5, 133.4 (d, 4), 133.2 (d, 4), 132.9 (d, 7), 132.9 (d, 3), 132.2 (d, 3), 131.8 (d, 3), 131.4 (d, 3), 130.1 (d, 3), 130.0, 129.9, 129.6-129.1, 128.8 (d, 24), 128.0 (d, 11), 126.6 (d, 49), 126.0, 114.8, 101.2 (d, 7), 96.4 (d, 7), 92.7 (d, 4), 80.6 (d, 8), 75.4 (d, 5), 57.0, 56.5; 1H, 7.93 (m, 2H), 7.73 (dt, 8.7, 8.3, 3.2, 1H), 7.58-7.44 (9H), 7.36 (t, 8.7, 7.9, 1H), 7.31 (d, 8.3, 1H), 7.21 (m, 1H), 7.17 (m, 2H), 7.01-6.83 (6H), 6.49 (d, 6.7, 1H), 6.35 (t, 7.0, 6.7, 1H), 5.43 (t, 5.8, 3.9, 1H), 5.10 (br s, 1H), 4.54 (t, 7.0, 5.8, 1H), 3.96 (s, 3H), 2.96 (s, 3H).

Synthesis of C4

Method I: A solution of $[\text{Ru}(\text{OAc})_2((R)\text{-3,5-Di-}t\text{-Bu-MeO-Biphep})]$ (42.3 mg, 0.034 mmol) in 2 mL of CD_2Cl_2 in an NMR tube was treated with 2.1 equivalents of tetrafluoroboric acid (10 μL , 7.3 M in Et_2O). After 18 days at 30° C the reaction mixture was transferred to a Schlenk tube. Washing three times with 5 mL of water and drying over MgSO_4 was followed by evaporation to dryness. Drying under vacuum afforded a pale yellow powder in 78% yield.

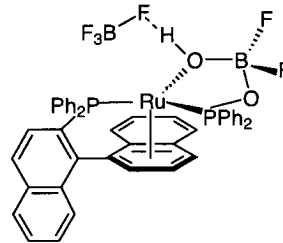


Method II: $[\text{Ru}(\text{OAc})_2((R)\text{-3,5-Di-}t\text{-Bu-MeO-Biphep})]$ (106.0 mg, 0.09 mmol) was dissolved in 1 ml 1,2-dichloroethane. After addition of tetrafluoroboric acid (25 μL , 7.3 M in Et_2O), distilled water (10 μL) was added to the resulting solution. The ^{31}P -NMR showed full conversion to the product after heating the solution for ca 6 h at 90° C. The solvent was removed in vacuo and the remaining residue was washed three times with pentane.

Anal. Calcd for C₇₀H₉₈O₄B₂F₆P₂Ru·H₂O (1302.26): C, 63.68; H, 7.64. Found: C, 63.62; H, 8.14. FAB-MS: calcd M⁺ 1215.5; found 1215.5, 1149.4 (100%, M+·BF₂OH). NMR (DRX400, CD₂Cl₂): ³¹P, 119.9 (d, 57), 46.3 (d, 57); ¹⁹F, -138.1 (d, 64), -138.2 (d, 64), -143.4 (d, 64), -143.5 (d, 64), -151.0 (25%, s), -151.1 (75%, s); ¹³C, 159.5 (d, 17), 151.6 (d, 10), 150.1 (d, 11), 147.0 (d, 8), 147.0 (d, 58), 146.1 (d, 53), 133.7 (d, 73), 133.0 (d, 44), 132.1 (d, 9), 129.5 (d, 11), 129.2 (d, 23), 127.4, 127.3, 127.0, 126.8, 126.3, 126.2, 126.2, 125.0, 124.9, 123.7, 114.0, 102.6 (d, 7), 96.1 (d, 7), 92.1 (d, 4), 79.8 (d, 9), 75.7, 56.5, 56.2, 35.5, 35.3, 35.2, 35.2, 31.4, 31.4, 31.3, 31.3; ¹H, 7.78 (d, 11, 1H), 7.70 (dt, 8.5, 8.1, 3.0, 1H), 7.61 (m, 2H), 7.45 (m, 1H), 7.27 (m, 2H), 7.24 (t, 8.1, 7.8, 1H), 7.06 (dd, 12.9, 1.7, 2H), 6.34 (7.3, 6.4, 1H), 6.23 (d, 6.8, 1H), 5.60 (s, 1H), 5.33 (t, 5.0, 4.1, 1H), 4.20 (t, 6.7, 5.9, 1H), 3.96 (s, 3H), 2.66 (s, 3H), 1.34 (s, 18H), 1.24 (s, 18H), 1.12 (s, 18H), 1.02 (s, 18H).

Synthesis of C5

Method I: [Ru(OAc)₂(Binap)] (77.7 mg, 0.09 mmol) was dissolved in 2 mL 1,2-dichloroethane. After addition of tetrafluoroboric acid (25 μ L, 7.3 M in Et₂O), distilled water (10 μ L) was added to the resulting solution. The ³¹P-NMR showed full conversion to the product after heating the solution for 3.5 h at 90° C. The solvent was removed in vacuo and the remaining residue was washed three times with pentane.



Method II: [Ru(OAc)₂(Binap)] (40.0 mg, 0.05 mmol) was dissolved in 2 mL 1,2-dichloroethane. This was followed by addition of 2.3 equivalents of tetrafluoroboric acid (15 μ L, 7.3 M in Et₂O). After ca. 48h at 65° C the resulting mixture was filtered using a glass filter and the 1,2-dichloroethane was distilled under high vacuum. The crude reaction mixture was washed three times with 1 mL hexane. The product was recrystallized from a dichloromethane-ether mixture to afford 36.8 mg (87%) of yellow product.

Anal. Calcd for C₄₄H₃₄O₂B₂F₆P₂Ru (893.38): C, 59.16; H, 3.84. Found: C, 59.07; H, 3.90. FAB-MS: calcd M⁺ 805.6; found 805.8. NMR (DRX400, CD₂Cl₂): ³¹P, 116.6 (d, 52), 50.1 (d, 52); ¹⁹F, -140.4 (d, 62), -140.5 (d, 62), -146.5 (d, 62), -146.6 (d, 62), -150.8 (25%, s), -150.8 (75%, s); ¹³C, 142.3 (d, 53), 141.5 (d, 22), 135.1, 134.4, 134.4, 132.9, 132.8, 132.6, 132.1, 131.2, 130.6, 130.1, 130.0, 129.8, 129.5, 128.8, 128.7, 128.4, 128.4, 127.7, 125.4, 113.6 (d, 9), 110.0 (d, 6), 105.7 (d, 6), 102.4 (d, 4), 95.1 (d, 9), 73.3; ¹H, 8.43 (d, 8.3, 1H), 8.28 (dd, 8.8, 2.0, 1H), 8.24 (dd, 8.8, 2.0, 1H), 7.95 (d, 8.2, 1H), 7.92 (t, 8.2, 7.8, 1H), 7.84 (ddd, 8.3, 6.9, 1.2, 1H), 7.77 (dd, 8.9, 6.9, 1H), 7.71 (ddd, 8.3, 6.9, 1.2, 1H), 7.64-7.49 (5H), 7.30 (br d, 7.0, 2.1), 7.29-7.15 (4H), 7.10-7.00 (3H), 6.95 (dd, 8.8, 7.8, 1H), 6.90-6.79 (3H), 6.26 (br d, 8.6, 1H), 5.93 (br d, 1H), 5.84 (dd, 4.7, 2.7, 1H), 5.15 (ddd, 7.0, 4.7, 2.3, 1H).

Preparation and/or Isolation products of low temperature NMR, C6-C8

[Ru(OAc)₂(Binap)] (41.1 mg, 0.05 mmol) was dissolved in 2 mL of CD₂Cl₂. The solution was cooled to -78° C before 2.2 equivalents of tetrafluoroboric acid (15 µL, 7.3 M in Et₂O) was added. The reaction was then immediately monitored by NMR at -60° C. After 30 min, intermediate **C6** was observed as the main product. The mixture was then warmed to 0° C for 1.5 h to afford intermediates **C7a** and **C7b**. The reaction mixture was then cooled to -60° C (to stabilize these intermediates), and **C7a** and **C7b** were characterised via NMR methods (see selected data below for two isomers).

Major isomer: NMR (DRX400, -60° C, CD₂Cl₂): ³¹P, 181.8 (dd, 948, 54), 51.5 (dd, 54, 11); ¹⁹F, -121.7 (dd, 948, 11); ¹³C, 106.3, 101.8, 77.7; ¹H, 6.56 (d, 7.2, 1H), 6.07 (ddd, 7.2, 5.3, 2.7, 1H), 5.69 (dd, 5.3, 4.2, 1H).

Minor isomer: NMR (DRX400, -60° C, CD₂Cl₂): ³¹P, 183.6 (dd, 956, 52), 41.4 (dd, 52, 13); ¹⁹F, -115.5 (dd, 956, 13); ¹³C, 108.8, 103.8, 78.4; ¹H, 6.55 (br d, 7.3, 1H), 5.82 (ddd, 7.3, 5.2, 2.3, 1H), 5.60 (dd, 5.2, 4.2, 1H).

At -60° C, 23.6 mg (0.56 mmol) of LiCl was added to the yellow reaction mixture. The mixture became immediately red in color. After stirring overnight, the reaction mixture was filtered through Celite. The solvent was evaporated in vacuo and the product **C8** was recrystallized from dichloromethane-ether to afford 32.3 (74%) of a red solid.

Anal. Calcd for C₄₄H₃₃BF₅ClP₂Ru.H₂O (866.02): C, 59.16; H, 3.84. Found: C, 59.07; H, 3.90. FAB-MS: calcd M⁺ 780.26; found 780.89. NMR (DRX400, CD₂Cl₂): ³¹P, 176.7 (dd, 932, 59), 53.5 (d, 59); ¹⁹F, -122.5 (d, 932), -153.5 (25%, s), -153.6 (75%, s); ¹³C, 144.2, 136.4, 135.0, 133.9, 133.8, 133.7, 132.9, 132.1, 131.5, 130.2, 130.0, 129.8, 129.6-127.6, 125.5, 113.2 (d, 6), 113.0 (d, 7), 109.0 (br d), 108.7 (br d), 101.4 (d, 11), 81.8; ¹H, 8.24 (dd, 8.7, 2.3, 1H), 8.20 (d, 8.3, 1H), 8.03-7.80 (6H), 7.73 (t, 9.4, 7.4, 1H), 7.67-7.57 (4H), 7.53-7.42 (3H), 7.40-7.11 (7H), 6.89-7.09 (7H), 5.97 (br s), 5.95 (br s).

Reaction of [Ru(Binap)(η⁶-p-cymene)](SbF₆)₂ with (Bu₄N)(Ph₃SiF₂), product **C9**

[Ru(Binap)(η⁶-p-cymene)](SbF₆)₂ (18.8 mg, 0.014 mmol)

was dissolved in 1 ml CD₂Cl₂ in an NMR-tube. The resulting

red solution was cooled to -78° C before (Bu₄N)(Ph₃SiF₂)

(7.9 mg, 0.014 mmol), under a continuous Ar flow, was added.

The color of the solution changed from red to yellow. A ³¹P

NMR-spectrum of the cooled solution, measured immedi-

ately, showed complete conversion of the starting Ru-com-

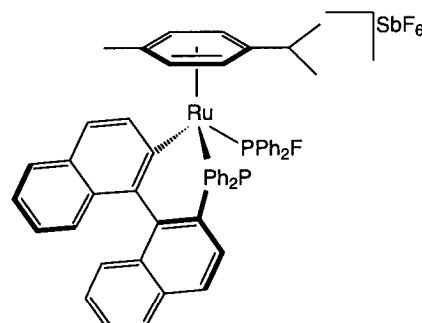
ponent to a single new Ru-complex, **C9**. The solution was

allowed to come to room temperature and the complex **C9** was characterised by NMR spectroscopic meth-

ods (see selected data below). Then the solvent was evaporated i.v. and washed 3x3 ml Et₂O. The yellow

powder was dried i.v. This solid did not afford satisfactory microanalytic data. ¹H-NMR indicated still

(Bu₄N)(SbF₆) and FSiPh₃.



FAB-MS: calcd M⁺ 877.0; found 877.3, M⁺-p-cymene 743.3; NMR (DRX400, CD₂Cl₂): ³¹P, 181.7 (dd, 936, 50), 50.9 (dd, 50, 13); ¹⁹F, -139.1 (dd, 936, 13); ¹³C, 147.7, 147.0, 144.1, 140.3, 140.3, 134.8, 134.3, 133.3, 132.3, 131.9, 129.3, 128.0, 127.6, 127.3, 127.2, 126.2, 125.9, 125.0, 124.9, 124.2, 114.1, 103.8, 102.3, 99.4, 31.0, 23.8, 20.1, 17.4; ¹H, 8.39 (d, 8.4, 1H), 7.76 (br d, 8.3, 1H), 7.70 (1H), 7.48 (1H), 7.33 (1H), 7.32 (1H), 7.30 (1H), 7.19 (1H), 6.79 (1H), 6.33 (d, 8.7, 1H), 6.67 (ddd, 8.8, 7.8, 1.2, 1H), 6.12 (br d, 6.9, 1H), 6.09 (br d, 6.5, 1H), 5.84 (br d, 6.7, 1H), 5.71 (d, 8.8, 1H), 5.56 (br d, 6.5, 1H), 2.56 (m, 1H), 1.67 (s, 3H), 1.03 (d, 6.9, 3H), 0.13 (d, 6.9, 1H).

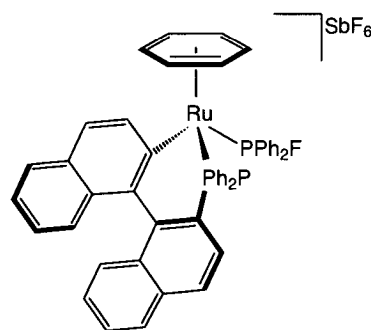
Reaction of [Ru(Binap)(η₆-benzene)](SbF₆)₂ with (Bu₄N)(Ph₃SiF₂), product C10

[Ru(Binap)(η₆-benzene)](SbF₆)₂ (33.5 mg, 0.03 mmol) was dissolved in 1 ml CD₂Cl₂ in an NMR-tube. The resulting red solution was cooled to -78° C before (Bu₄N)(Ph₃SiF₂) (13.9 mg, 0.03 mmol), under a continuous Ar flow, was added. The color of the solution changed immediately from red to yellow. A ³¹P NMR-spectrum of the cooled solution, measured immediately, showed complete conversion of the starting Ru-compound to a single new Ru-complex, C10. The solution was allowed to come to room temperature and the complex C10 was characterised by NMR spectroscopic methods (see selected data below).

NMR (DRX400, CD₂Cl₂): ³¹P, 180.4 (dd, 950, 48), 49.0 (dd, 48, 7); ¹⁹F, -137.2 (dd, 950, 7); ¹³C, 146.8, 145.6, 144.2, 140.3, 134.7, 134.2, 133.2, 131.9, 128.9, 128.6, 128.1, 127.3, 127.2, 126.6, 125.7, 124.3, 124.3, 102.1; ¹H, 8.53 (d, 8.6, 1H), 7.91 (dd, 8.6, 2.4, 1H), 7.83 (br d, 8.4, 1.5, 1H), 7.71 (1H), 7.64 (br d, 8.3, 1.5, 1H), 7.54 (1H), 7.33 (ddd, 8.4, 7.5, 1.1, 1H), 6.60 (ddd, 8.8, 7.6, 1.3, 1H), 6.56 (ddd, 8.8, 7.7, 1.5, 1H), 5.68 (br d, 8.8, 1.1, 1H).

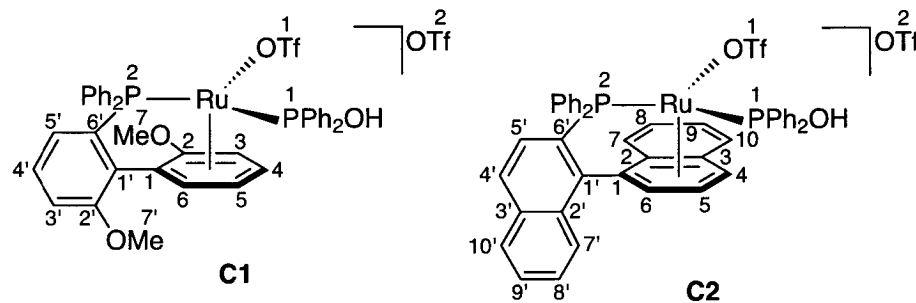
In an attempt to separate the metal complex from (Bu₄N)(SbF₆) and FSiPh₃, a second reaction was carried on a 2.5-fold larger scale following the same procedure described previously but using dichloromethane at room temperature. After five minutes the solvent was evaporated i.v. The resulting yellow powder was washed with 3x1 ml Et₂O. Slow diffusion of Et₂O into a dichloromethane solution resulted in two crystalline materials (i.e. yellow and white crystals). X-ray diffraction measurements on the yellow crystals failed to give a structure. An attempt was made to separate the two species on basis of the color of the crystals. However, this solid did not afford satisfactory microanalytic data. The isolated yellow product is stable under Ar and affords the same ³¹P, ¹⁹F and ¹H-NMR characteristics described above. However, in solution it decomposes over a short period of time.

FAB-MS: calcd M⁺ 820.9; found 820.2, M⁺-benzene 742.8, M⁺-PPh₂F 614.0.

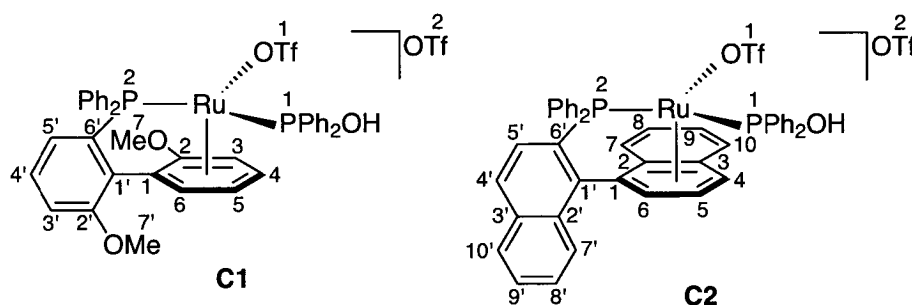


4.5.3 Selected NMR data

Table 12: Selected NMR data for the complexes C1 and C2^a

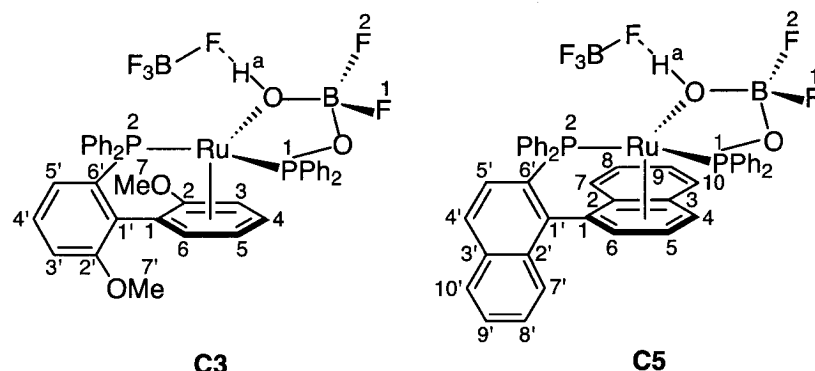


position	C1		C2	
	$\delta^{31}\text{P}$	$\delta^{19}\text{F}$	$\delta^{31}\text{P}$	$\delta^{19}\text{F}^{\text{e}}$
1	104.1	-77.8	114.5	-78.2
2	50.2	-79.3	53.4	-79.5
	$\delta^{1}\text{H}^{\text{b,c}}$	$\delta^{13}\text{C}$	$\delta^{1}\text{H}^{\text{d}}$	$\delta^{13}\text{C}$
1		93.7		99.6
2		146.4		116.9
3	5.98	81.4		110.6
4	6.63	97.6	7.54	100.0
5	5.22	102.7	5.54	107.6
6	5.67	79.6	5.84	77.9
7	2.99	56.9	6.34	127.4
8			6.94	135.4
9			7.78	134.8
10			8.03	131.8
1'		127.8		141.0
2'		158.7		131.7
3'	7.25	115.0		135.2
4'	7.68	131.8	8.30	132.0
5'	7.15	125.6	7.81	127.9
6'		143.9		140.7
7'	3.94	56.4	7.81	129.1
8'			7.68	129.2

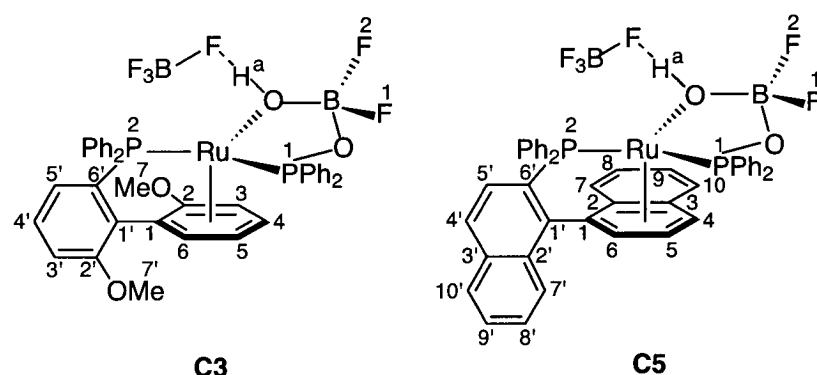
Table 12: Selected NMR data for the complexes C1 and C2^a

position	C1		C2	
9'			7.82	127.7
10'			8.20	129.1
OH	9.66		10.02	

^a 400 MHz, CD₂Cl₂ ambient temperature. ^b Exchange between OH and water. ^c Correlation between P1 and OH. ^d Exchange between OH and water. ^e No or slow exchange between OTf groups. ^f **C1:** H3, 5.98, *J*(H,H) = 7.0, 0.7, ³*J*(P,H) = 1.5; **H4**, 6.63, *J*(H,H) = 7.0, 6.6, and 1.4, ³*J*(P,H) = 2.1; **H5**, 5.22, *J*(H,H) = 6.6, 5.2, and 0.7, ³*J*(P,H) = 2.1; **H6**, 5.67, *J*(H,H) = 5.2 and 1.4, ³*J*(P,H) = 3.7. **C2:** **H4**, 7.54, ³*J*(H,H) = 7.3, ³*J*(P,H) = 2.1; **H5**, 5.54, ³*J*(H,H) = 7.3 and 5.3, ³*J*(P,H) = 2.3; **H6**, 5.84 *J*(H,H) = 5.3, ³*J*(P,H) = 4.3.

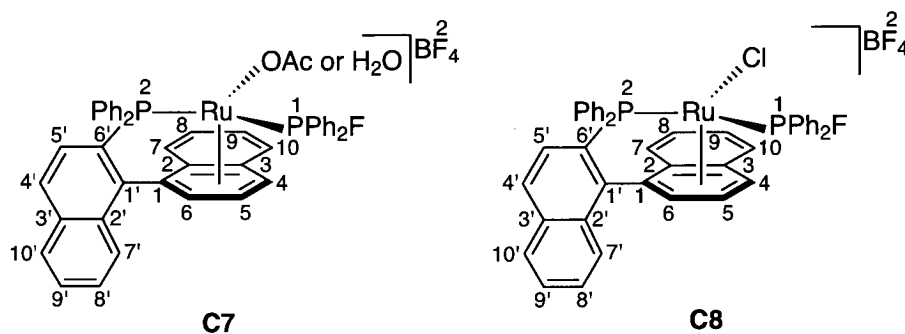
Table 13: Selected NMR data for the complexes C3 and C5^a

position	C3		C5	
	$\delta^{31}\text{P}$	$\delta^{19}\text{F}$	$\delta^{31}\text{P}$	$\delta^{19}\text{F}^e$
1	114.1	-143.5 (-143.6)	116.6	-146.5 (-146.6)
2	46.5	-141.1 (-141.1)	50.1	-140.4 (-140.5)
	$\delta^{1}\text{H}$	$\delta^{13}\text{C}$	$\delta^{1}\text{H}$	$\delta^{13}\text{C}$
1		92.7		102.7
2		147.4		113.6
3	6.49	80.6		110.0
4	6.35	96.4	7.30	95.1
5	4.54	101.2	5.15	105.7
6	5.43	75.4	5.85	73.3
7	2.96	57.0	6.26	127.7
8			6.95	134.8
9			7.92	136.3
10			8.43	130.3
1'		128.8		134.8
2'		159.0		131.4
3'	7.31	114.8		141.5
4'	7.73	132.9	8.24	131.7
5'	7.36	126.6	7.77	128.4
6'		144.4		142.3
7'	3.96	56.0	7.95	125.4
8'			7.84	129.9

Table 13: Selected NMR data for the complexes C3 and C5^a

position	C3		C5	
9'			7.71	128.4
10'			8.20	129.1
Ha	5.10		5.95	

^a 400 MHz, CD₂Cl₂ ambient temperature.

Table 14: Selected NMR-data for the complexes C7a, C7b and C8

position	C7a			C8	
	$\delta^{31}\text{P}$	$\delta^{19}\text{F}$		$\delta^{31}\text{P}$	$\delta^{19}\text{F}$
1	181.8	-127.7	1	176.7	-122.5
2	51.5		2	53.5	
	$\delta^1\text{H}$	$\delta^{13}\text{C}$		$\delta^1\text{H}$	$\delta^{13}\text{C}$
4	5.69	106.3	1		109.0
5	6.07	77.7	2		113.2
6	6.56	101.8	3		113.0
			4	5.95	108.7
			5	5.97	81.8
			6	6.93	101.4
			7	7.92	129.3
	C7b		8	7.98	136.4
	$\delta^{31}\text{P}$	$\delta^{19}\text{F}$	9	7.16	132.1
1	183.6	-115.5	10	6.57	128.7
2	41.4		2'		131.5
	$\delta^1\text{H}$	$\delta^{13}\text{C}$	3'		135.0
4	5.60	108.8	4'	8.24	132.1
5	5.82	78.4	5'	7.61	128.0
6	6.55	103.8	6'		144.2
			7'	7.94	129.0
			8'	7.84	130.0
			9'	7.73	129.6
			10'	8.20	125.5

^a 400 MHz, CD₂Cl₂. ^b Major isomer, -60 °C, assignment based on the observations of **C8**. ^c Minor isomer, -60 °C, assignment based on the observations for **C8**. ^d Ambient temperature. ^e **C7a**: H4, 5.69, ³J(H,H) = 5.3, ³J(P,H) = 4.2; H5, 6.07, ³J(H,H) = 7.2 and 5.3, ³J(P,H) = 2.7; H6, 6.56, ³J(H,H) = 7.2. **C7b**: H4, 5.60, ³J(H,H) = 5.2, ³J(P,H) = 4.2; H5, 6.07, ³J(H,H) = 7.3 and 5.2, ³J(P,H) = 2.3; H6, 6.55, br d, ³J(H,H) = 7.3

4.6 References

- (1) Noyori, R.; Takaya, H. *J. Org. Chem.* **1987**, *52*, 3174.
- (2) Chan, A. S. C.; Laneman, S. A.; Miller, R. E. In *Selectivity in Catalysis*; ACS Symposium Series 517; American Chemical Society: Washington, DC, 1993; p 27.
- (3) Ikariya, T.; Ishii, Y.; Kawano, H.; Arai, T.; Saburi, M.; Yoshikawa, S.; Akutagawa, S. *J. Chem. Soc., Chem. Commun.* **1985**, *13*, 922.
- (4) Bender, R.; Bouaoud, S. E.; Braunstein, P.; Dusausoy, Y.; Merabet, N.; Raya, J.; Rouag, D. *J. Chem. Soc., Dalton Trans.* **1999**, 735; Goodson, F. E.; Wallow, T. I.; Novak, B. M. *J. Am. Chem. Soc.* **1997**, *119*, 12441; Sakamoto, M.; Shimizu, I.; Yamamoto, A. *Chem. Lett.* **1995**, 1101; Morita, D. K.; Stille, J. K.; Norton, J. R. *J. Am. Chem. Soc.* **1995**, *117*, 8576; Kong, K. C.; Cheng, C. H. *J. Am. Chem. Soc.* **1991**, *113*, 6313; Vierling, P.; Riess, J. G.; Grand, A. *Inorg. Chem.* **1986**, *25*, 4144; Garrou, P. E. *Chem. Rev.* **1985**, *85*, 171; Abatjoglou, A. G.; Billig, E.; Bryant, D. R. *Organometallics* **1984**, *3*, 923; Dogan, J.; Schulte, J. B.; Swiegers, G. F.; Wild, S. B. *J. Org. Chem.* **2000**, *65*, 951; Hermann, W. A.; Thiel, W. R.; Brossmer, C.; Oefele, K.; Priermeier, T.; Scherer, W. *J. Organomet. Chem.* **1994**, *461*, 51.
- (5) Geldbach, T. J.; Drago, D.; Pregosin, P. S. *Chem. Comm.* **2000**, 1629; Geldbach, T. J.; Pregosin, P. S.; Bassetti, M. *Organometallics* **2001**, *20*, 2990.
- (6) van Leeuwen, P.; Roobek, C. F.; Orpen, A. G. *Organometallics* **1990**, *9*, 2179.
- (7) Morris, R. H.; Sawyer, J. F.; Schweitzer, C. T.; Sella, A. *Organometallics* **1989**, *8*, 2099.
- (8) Blum, O.; Frolov, F.; Milstein, D. *J. Chem. Soc., Chem. Comm.* **1991**, 258.
- (9) Noyori, R. *Asymmetric Catalysis in Organic Synthesis*; John Wiley & Sons: New York, 1994; pp 16-94; Noyori, R. *Acta Chem. Scand.* **1996**, *50*, 380; Takaya, H.; Ohta, T.; Noyori, R., In *Catalytic Asymmetric Synthesis*; Ojima, I., Ed.; VCH Publishers: New York, 1993; pp 1-39; Schmid, R.; Broger, E. A.; Cereghetti, M.; Crameri, Y.; Foricher, J.; Lalonde, M.; Muller, R. K.; Scalzone, M.; Schoettel, G.; Zutter, U. *Pure Appl. Chem.* **1996**, *68*, 131.
- (10) Ohta, T.; Takaya, H.; Noyori, R. *Inorg. Chem.* **1988**, *27*, 566.
- (11) Ashby, M. T.; Khan, M. A.; Halpern, J. *Organometallics* **1991**, *10*, 2011.
- (12) Schmid, R.; Foricher, J.; Cereghetti, M.; Schonholzer, P. *Helv. Chim. Acta* **1991**, *74*, 370.
- (13) Miyashita, A.; Yasuda, A.; Takaya, H.; Toriumi, K.; Ito, T.; Souchi, T.; Noyori, R. *J. Am. Chem. Soc.* **1980**, *102*, 7932.
- (14) Feiken, N.; Pregosin, P. S.; Trabesinger, G.; Scalzone, M. *Organometallics* **1997**, *16*, 537.
- (15) Ohta, T.; Takaya, H.; Noyori, R. *Inorg. Chem.* **1988**, *27*, 566.
- (16) Feiken, N.; Pregosin, P. S.; Trabesinger, G.; Albinati, A.; Evoli, G. L. *Organometallics* **1997**, *16*, 5756.
- (17) Feiken, N.; Pregosin, P. S.; Trabesinger, G. *Organometallics* **1997**, *16*, 3735.
- (18) Krafczyk, R.; Thonnissen, H.; Jones, P. G.; Schmutzler, R. *J. Fluor. Chem.* **1997**, *83*, 159.
- (19) Esteruelas, M. A.; Lopez, A. M.; Tolosa, J. I.; Vela, N. *Organometallics* **2000**, *19*, 4650.
- (20) Pregosin, P. S.; Valentini, M. *Enantiomer* **1999**, *4*, 529-539; Pregosin, P. S.; Trabesinger, G. *J. Chem.*

- Soc., Dalton Trans.* **1998**, 727; Pregosin, P. S.; Salzmann, R. *Coord. Chem. Rev.* **1996**, 155, 35.
- (21)Roethlisberger, M. S.; Salzer, A.; Beurgi, H. B.; Ludi, A. *Organometallics* **1986**, 5, 298.
- (22)Bennett, M. A.; McMahon, I. J.; Pelling, S.; Brookhart, M.; Lincoln, D. M. *Organometallics* **1992**, 11, 127; Faller, J. W.; Chase, K. J. *Organometallics* **1995**, 14, 592.
- (23)Valentini, M.; Pregosin, P. S.; Ruegger, H. *Organometallics* **2000**, 19, 2551.
- (24)Valentini, M.; Pregosin, P. S.; Ruegger, H. *J. Chem. Soc., Dalton Trans.* **2000**, 4507.
- (25)Fong, T. P.; Lough, A. J.; Morris, R. H.; Mezzetti, A.; Rocchini, E.; Rigo, P. *J. Chem. Soc., Dalton Trans.* **1998**, 2111.
- (26)Mahon, M. F.; Whittlesey, M. K.; Wood, P. T. *Organometallics* **1999**, 18, 4068.
- (27)Burns, R. M.; Hubbard, J. L. *J. Am. Chem. Soc.* **1994**, 116, 9514; Blosser, P. W.; Gallucci, J. C.; Wojcicki, A. *Inorg. Chem.* **1992**, 31, 2376; Abbenhuis, R. A. T. M.; Del Rio, I.; Bergshoef, M.; Boersma, J.; Veldman, N.; Spek, A. L.; van Koten, G. *Inorg. Chem.* **1998**, 37, 1749.
- (28)Yamamoto, A.; Sato, R.; Matsuo, F.; Sudoh, C.; Igoshi, T. *Inorg. Chem.* **1996**, 35, 2329; Brunner, H.; Oeschey, R.; Nuber, B. *Organometallics* **1996**, 15, 3616; Bhambri, S.; Tocher, D. A. *Polyhedron* **1996**, 15, 2763.
- (29)Orpen, A. G.; Brammer, L.; Allen, F. H.; Kennard, O.; Watson, P. G.; Taylor, R. *J. Chem. Soc., Dalton Trans.* **1989**, 1.
- (30)Beaulieu, W. B.; Rauchfuss, T. B.; Roundhill, D. M. *Inorg. Chem.* **1975**, 14, 1732; Roundhill, S. G. N.; Roundhill, D. M. *Acta Cryst.*, **1982**, 38 Sect. B, 2479.
- (31)Roucoux, A.; Thieffry, L.; Carpentier, J. F.; Devocelle, M.; Meliet, C.; Agbossou, F.; Mortreux, A. *Organometallics* **1996**, 15, 2440; Agbossou, F.; Carpentier, J. F.; Hatat, C.; Kokel, N.; Mortreux, A.; Betz, P.; Goddard, R.; Kruger, C. *Organometallics* **1995**, 14, 2480; Roucoux, A.; Devocelle, M.; Carpentier, J. F.; Agbossou, F.; Mortreux, A. *Synlett* **1995**, 358.
- (32)Pathak, D. D.; Adams, H.; Bailey, N. A.; King, P. J.; White, C. *J. Organomet. Chem.* **1994**, 479, 237.
- (33)Observed for an independent sample of BF₃·Et₂O: δ = 4.23 (q, 2H) and δ = 1.38 (t, 3H). In-situ measurements on **C6** show δ = 4.23 (q, 2H) and δ = 1.40 (t, 3H), both under the same conditions (CD₂Cl₂, 400 MHz, 0°C).
- (34)We are not certain of the source of this selectivity. It might arise from the well-known geometric dependence of ²J(³¹P, X, X = ¹H, ¹³C, ³¹P, ..., etc., with trans larger than cis. If the structure were indeed five-coordinate, the high-frequency ³¹P spin would occupy a pseudo-trans position relative to the ¹⁹F spin. Since both the ¹⁹F and ³¹P lines are broad, couplings smaller than 5 Hz would not be observed.
- (35)We also find a very weak proton signal at δ = 9.92, as a doublet with ¹J(¹⁹F, ¹H) = 267 Hz, as well as a broad singlet at δ = 13.09. These are assigned to solvated HF (a slight excess of HBF₄, 2.2 equivalent, is present) and HOAc, respectively. The 267 Hz value is similar to that found by Whittlesey, M.K.; Perutz, R.N.; Greener, B.; Moore, M.H. *Chem Comm.* **1997**, 187.
- (36)Lee, D. H.; Kwon, H. J.; Patel, P. P.; Liable-Sands, L. M.; Rheingold, A. L.; Crabtree, R. H. *Organometallics* **1999**, 18, 1615.

-
- (37)Mazej, Z.; Borrmann, H.; Lutar, K.; Zemva, B. *Inorg. Chem.* **1998**, *37*, 5912.
- (38)Murphy, V. J.; Hascall, T.; Chen, J. Y.; Parkin, G. *J. Am. Chem. Soc.* **1996**, *118*, 7428.
- (39)Whittlesey, M. K.; Perutz, R. N.; Greener, B.; Moore, M. H. *Chem. Comm.* **1997**, 187.
- (40)Brewer, S. A.; Coleman, K. S.; Fawcett, J.; Holloway, J. H.; Hope, E. G.; Russell, D. R.; Watson, P. G. *J. Chem. Soc., Dalton Trans.* **1995**, 1073; Coleman, K. S.; Fawcett, J.; Holloway, J. H.; Hope, E.; Russell, D. R. *J. Chem. Soc., Dalton Trans.* **1997**, 3557-3562.
- (41)Poulton, J. T.; Sigalas, M. P.; Folting, K.; Streib, W. E.; Eisenstein, O.; Caulton, K. G. *Inorg. Chem.* **1994**, *33*, 1476; Caulton, K. G. *New J. Chem.* **1994**, *18*, 25.
- (42)Barthazy, P.; Stoop, R. M.; Worle, M.; Togni, A.; Mezzetti, A. *Organometallics* **2000**, *19*, 2844; Barthazy, P.; Hintermann, L.; Stoop, R. M.; Wörle, M.; Mezzetti, A.; Togni, A. *Helv. Chim. Acta* **1999**, *82*, 2448.
- (43)Verkade, J. G.; Mosbo, J. A. In *Stereospecificity in ¹J Coupling to Metals*; Verkade, J. G., Mosbo, J. A., Eds.; VCH: Deerfield Beach, FL, 1987; Vol. 8, pp 425-463.
- (44)Desobry, V.; Kündig, E. P. *Helv. Chim. Acta* **1981**, *64*, 1288.
- (45)Pilcher, A. S.; Ammon, H. L.; DeShong, P. *J. Am. Chem. Soc.* **1995**, *117*, 5166.
- (46)SAINT, Version 4; Siemens Analytical X-ray Systems, Inc.: Madison, WI.
- (47)Sheldrick, G. *SADABS*; Göttingen, Germany, 1997.
- (48)*SHELXTL* program package, Version 5.1; Bruker AXS, Inc.: Madison, WI.
- (49)Bennett, M. A.; Smith, M. B. *J. Chem. Soc., Dalton Trans.* **1974**, 233.

Curriculum Vitae

Carolien J. den Reijer was born in Zevenbergen, the Netherlands, on February 3rd, 1973. In 1991 she received her grammar school (VWO) diploma from ‘Thomas More College’ in Oudenbosch. In September of the same year she started her undergraduate education in Chemistry at the University of Nijmegen. During her studies she carried out research-projects in Inorganic Chemistry under supervision of Prof. Dr. A. W. Gal and Solid State Chemistry under supervision of Prof. Dr. P. Bennema. During 6 months in 1996, she performed an Erasmus project at the Nottingham Trent University in the United Kingdom under supervision of Dr. K. Moss. After receiving her M.Sc. in Chemistry in 1997, she moved to the Swiss Federal Institute of Technology (ETH) in Zurich to carry out her Ph.D. studies under supervision of Prof. Dr. P. S. Pregosin. During this time, she supervised two undergraduate students and was the NMR-assistent of the Laboratories of Inorganic Chemistry.